DESIGN, SYNTHESIS AND BINDING STUDIES OF CALIX(4)PYRROLE BASED RECEPTORS SUITABLE FOR ION-PAIR COMPLEXATION AND N-OXIDE RECOGNITION. SYNTHESIS OF RESORCIN(4) ARENE DERIVATIVES AS POTENTIAL LIGANDS FOR SUPRAMOLECULAR CATALYSIS

Moira Ciardi

Dipòsit Legal: T.1298-2012

Moira Ciardi

Design, Synthesis and Binding Studies of Calix[4]pyrrole Based Receptors suitable for Ion-Pair Complexation and *N*-oxide Recognition. Synthesis of Resorcin[4]arene Derivatives as Potential Ligands for Supramolecular Catalysis

PhD Thesis

Supervised by Prof. Pablo Ballester Balaguer

Institute of Chemical Research of Catalonia (ICIQ) and Catalan Institution for Research and Advanced Studies (ICREA)

UNIVERSITAT ROVIRA I VIRGILI

Tarragona

2012

UNIVERSITAT ROVIRA I VIRGILI

Av. Països Catalans, 16
43007 Tarragona
Tel +34 977 920 200
Fax +34 977 920 224

Prof. Pablo Ballester Balaguer, Group Leader of the Institute of Chemical Research of Catalonia (ICIQ) and Research Professor of the Catalan Institution for Research and Advanced Studies (ICREA),

CERTIFIES that the present research work entitled "Design, Synthesis and Binding Studies of Calix[4]pyrrole Based Receptors suitable for Ion-Pair Complexation and *N*-oxide Recognition. Synthesis of Resorcin[4]arene Derivatives as Potential Ligands for Supramolecular Catalysis" that Moira Ciardi presents to obtain the PhD degree in Chemistry, has been carried out under my supervision in the ICIQ and fulfils all the requirements to be awarded with the "Doctor" Mention.

Tarragona, July 2012

PhD Thesis supervisor

Prof. Pablo Ballester Balaguer

…Y a mí enterradme sin duelo entre la playa y el cielo...
en la ladera de un monte, más alto que el horizonte…
Cerca del mar…
Porque yo nací en el Mediterráneo.

Joan Manuel *Serrat*

Acknowledgements

THIS IS YOUR LIFE.

Do what you LOVE, and do it OFTEN.

If you DON'T LIKE something, CHANGE IT.

If you DON'T LIKE your job, QUIT.

If you DON'T have enough TIME, STOP watching TV.

If you are looking for the love of your life, STOP. They will be waiting for you when you start doing things YOU love.

STOP OVER ANALYZING. LIFE IS SIMPLE.

OPEN YOUR MIND, ARMS and HEART to NEW things and people. We are united in our differences.

Some OPPORTUNITIES only come ONCE, seize them.

TRAVEL OFTEN: getting lost will help you to FIND YOURSELF.

All EMOTIONS are BEAUTIFUL.

When you EAT, APPRECIATE every last bite.

Ask the next PERSON you see what their PASSION is. SHARE your ispiring DREAM with them.

LIFE IS ABOUT THE PEOPLE YOU MEET and the THINGS YOU CREATE WITH THEM, so go out and start creating.

Life is short, LIVE YOUR DREAM and SHARE YOUR PASSIONS.

"The Holstee Manifesto"

So thank you to all the people that crossed my way during these four years and turned my PhD into an awesome experience, chemically and personally speaking.

Special thanks go...to ***Pau***, because apart from our daily fights and disagreements about everything, he has been the main person that invested time, knowledge and patience in trying to understand with me the magic of my chemistry. *Nos echaremos mucho de menos jefe, estoy segura*!

To my ***PB4***, 'cause there is not a better place to work, laugh, sing and share chemistry and emotions at the same time...forever labmates, forever friends (at

least with most of them!). Between all, I would like to thank **Monica,** brilliant teacher of Spanish history and political affairs. *Gracias por las largas conversaciones poco nerdy y muy interesantes, por el cariño que me has guardado siempre, hasta cuando me fui a USA y por las noches de fiesta, claro! Por cierto, no me olvidaré del juez Garzón en toda mi vida!* To the shining **Gemma,** my sun in the darkness of Microsoft Office. *Gracias por tu ayuda, por las sonrisas y los abrazos que han acompañado estos meses de escritura…Vente conmigo*!!! To **Albano** & our Friday mojito nights. I could not survive to the over-stress without *yogurin* (*ahora si que estoy convencida que el PB4 esta "on fire*", *Del todo*!). To **Marcos**...for having always the nicest words in the worst chemical moments, but mainly for sharing with me the experience of a pipette in the finger...*Marcos, yo y el dedo del amor…en la Clinica Matt! Muchisimas gracias, que haré yo sin el latin lover del lab…mah!* To **Virginia**, *mi gemela de melena*, for introducing me into the Spanish music culture, *con Mecano y Joan Manuel Serrat. Pues te guardo con el recuerdo de la noche de vuestra llegada, en la Vaqueria*! To **Laura**, because there are few people that really understand that "*no estoy loca, solo fuera de contexto*"! *Muchisima suerte con todo…la Galicia parece ganar en mis recuerdos mas bonitos (excluida la noche que tu y Ana me llevaste al hospital, claro*!). To **Eddy, "**the party animal**",** for the funny moments spent inside and outside the lab (save energies also for my party!) and to **Louis** & his contagious great American laugh! To **Nelson** (*cuida mi vitrina*!), **Bea** (*no habrá que hacer mas pedidos con código raro, ole'*) and all the previous labmates. Starting from **Inma** & all her identities and going back to **Bego**, **Ana**, **Almudena**, **Guzman** and mami-**M.Angeles** (*el primordial PB4 que me enseñò que en el mundo hay que hablar español, el ingles no hace falta*!). And of course to **Carmela** (stai gia' pensando a cosa cucinare a cena?!?!). Thanks also to the guys that visited the lab during the summer; it was definetely lot of fun together, Big **Tony,** Mazote **Ruben** de Parla, **David**, **Zack** and **Calden,** great desk neighbours. And to the people met in the Master: **Nuria** (porque las fallas se hacen en Valencia y no en Sevilla)**, Miriam** (estimadora de reinas de torso)**, Cristina, Merce, Oriol, Isidoro** and mainly to **Carlo**, because this experience started with his help and will nicely finish together. Ammetti che nonostante le mail strane, ne e' valsa la pena farmi sbarcare a Tarraco! Dai, dai, dai che ce la facciamo!!!

Acknowledgements

A huge thank you flies also to USA. Thanks to ***Amar*** for giving me the unique opportunity of working in a great lab made of great people; to **Eddie**, 'cause I could not expect a better friend to live in full the American life style, enjoy coffee + bagel every morning and having party; to **Kevin**, forever and ever, for the neverending patience. And for initiating me to the triazolophane world-hell as well as to the American football + barbeque + CornHole game tradition. To my officemates **Craig** and **Chris** for the nice talks and the drinking games at the Upstairs Pub. And of course to **Simon, Yuran** and sweety **Lucy**. A huge thank you goes also to **Felicia**, **Alice** and their nice smiles. As well to **Pucheng Ke** and **Bruce** (I miss our lunches at the Union!). Finally, standing ovation to my flatmate **Laura** to understand what living in USA means for an European...but mainly to teach me how to cook a 40 Kg Thanksgiving Day Turkey!

Many Many Many thanks to the people met also outside the lab. To the ones mentioned here. To the ones that surely I forgot. And to the ones that asked explicitly for personal acknowledgements after the support offered during these last months (gracias **Jon**!).

Thanks to **Caterina** and **Ana,** because I had a memorable beginning with the first and a fantastic ending with the second. ***Grazie Cat!*** per tutto e forse anche più di tutto...i ricordi più emozionanti son sicuramente i nostri e un semplice grazie non sará mai sufficiente! ***Gracias a Ana***...pues quien podía saber que un simple viaje a Lisboa podía ser el inicio de más y más viajes super chulos, de cenas italo-gallegas con vino buenísimo y una amistad tan preciosa con sabor a locura (no habría sobrevivido a Tarragona sin ti, ya lo sabes)! ***Grazie a Margherita*****,** for her nice smile, the long reassuring talks and the moments at Arrabassada...una amicizia breve ma efficace! To **Alba**, because it was friendship at first sight...Carnaval será siempre mi recuerdo más bonito! To **John**, **Kian** and **Danny**...we definetely had the worst Spanish teacher, but it was the best course company I could meet, ever! To **James**, because the nights at the Cau had always a different taste with him...at all! To **Sara,** personal bon ton teacher...credo che dopo il viaggio a NY e soprattutto la visita alla Statua della Libertà, siam pronte ad affrontare qualsiasi avventura insieme! Un agradecimiento especial también para **Amparo** y **Alexandra**: conoceros ha sido más que un placer, gracias por vuestras sonrisas y alegría!

Acknowledgements

I would also like to thank the whole Italian community because...we always make the difference...it was nice to share moments like the annual Christmas dinner and the Internation football matches. Un grazie speciale va ovviamente a **Daniele**, per i copyright della copertina (scherzo...dai che mi mancheranno i nostri momenti chat-gossip:"Ansè? Ciocià?") e **Antonello** (sempre con la parola giusta detta al momento giusto nella maniera più giusta). A **Salassa,** prova vivente che anche al Nord si può essere simpatici e parlare il dialetto romano...o almeno ce provi! **Antò-Bazzo**...te sei incluso!

Per concludere, ringrazio ***mamma e papà***, per la libertà di scelta in ogni singolo momento di vita. Per accettare ogni mia decisione e condividere le numerose esperienze che, seppur poco comuni negli standard del paesello, mi han permesso di essere la persona che sono...semplicemente fantastica! Un grazie speciale anche a ***nonno Domenico***, il sostenitore più accanito, ***Sonia***, per l'affetto tangibile anche a Km di distanza, ***Ileano***, fratellozzo ineguagliabile dai preziosi consigli di vita e design, e ***Rosalia*** per gli sms sempre piacevolmente inaspettati.

The work contained in this thesis has been possible thanks to ICIQ Research Support Unit and to the financial support of *Ministerio de Educación y Ciencia* FPU (Formación de Profesorado Universitario) Fellowship (AP2008-02355), to Ministerio de Ciencia e Innovacion, Generalitat de Catalunya and the ICIQ Fundation.

UNIVERSITAT ROVIRA I VIRGILI

Institut
Català
d'Investigació
Química

To the ones that love me, unconditionally

Graphical Abstract

The work presented in this thesis focuses on the design and synthesis of Supramolecular Hosts.

Three different classes of receptors are shown for *ion pair binding*. In particular, a new family of aryl-extended calix[4]pyrroles with two and four phosphonate groups have been synthesized for the complexation of ion-pairs. Likewise, the design and synthesis of functionalized triazolophanes for inclusion of linear polyatomic anions is presented.

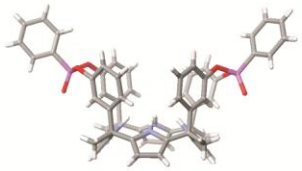

***bis*-phosphonate calix[4]pyrrole**

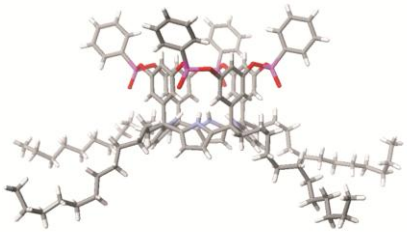

***tetra*-phosphonate calix[4]pyrrole**

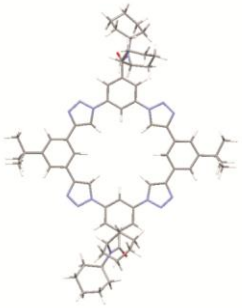

Triazolophane

Derivatives of calix[4]pyrroles have been also prepared for the *selective inclusion* of the high energy conformer of *N*-methylmorpholine *N*-oxide. The value of the inclusion is tested by studying the modification of the reactivity of the *N*-oxide in reactions in which it is usually used as sacrificial oxidant.

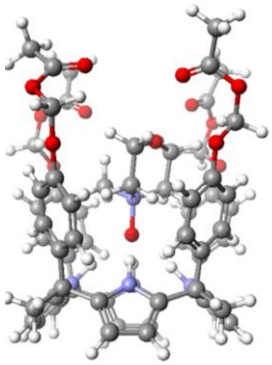

Finally, the design and synthesis of resorcin[4]arene-derivatives capable to include neutral and ionic species and able to work as ligands for *supramolecular catalysis* are presented.

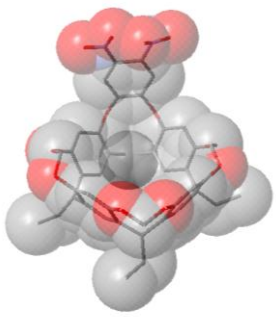

Table of Contents

Table of Contents

CHAPTER I

General Introduction

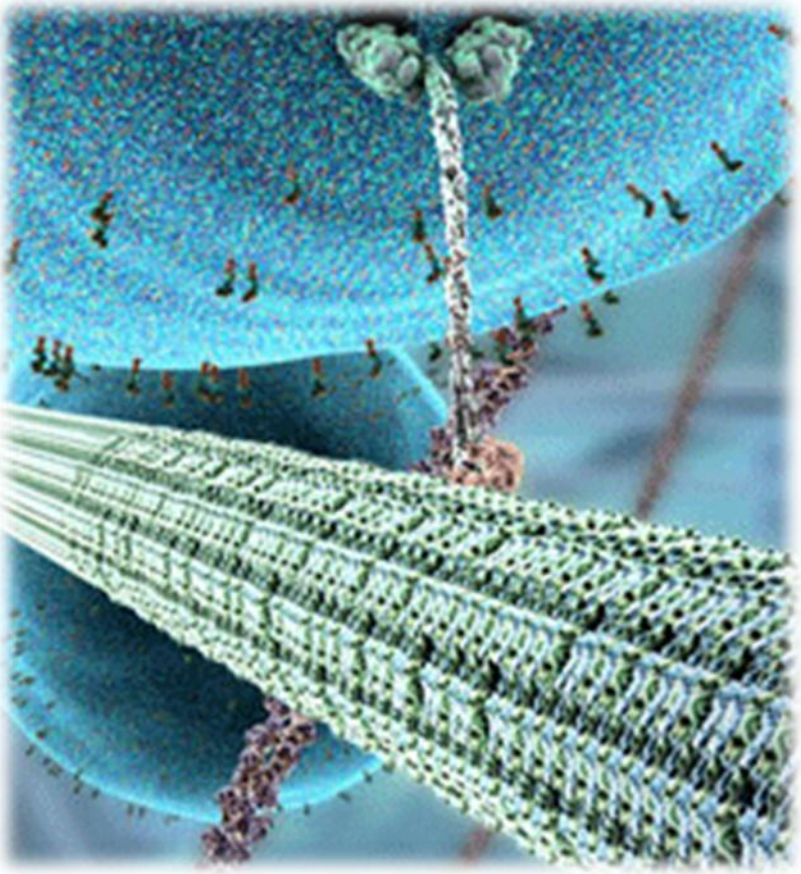

"The Inner Life of the Cell" *Copyright 2007 The Presidents and Fellows of Harvard College*

1. 1 Introduction

Supramolecular Chemistry has evolved extraordinarily since Lehn established its importance in the late 80s.[1] Nowadays, the host-guest chemistry has grown away from its limited *lock-and-key* image to cover a huge variety of interesting fields with fascinating potential and real applications.[2] Its original labeling as "Chemistry of Life", since the use of weak and reversible forces evokes the supramolecular interactions occurring between proteins, has assumed a more complex personality with more versatile topics, which have promoted a quick development and a parallel increasing interest in the scientific community. Among the wide range of applications of supramolecular chemistry, the development of new pharmaceutical therapies by understanding the interactions at a drug binding site has been one of the most important in the biological field.[3] More recently, this singular branch of chemistry has also gained interest in the development of new materials for nanotechnology applications.[4] In this line, molecular machines represent the most interesting evidence of synergy between supramolecular chemistry and nanotechnology.[5,6,7] Key applications of "non-covalent" interactions established between molecules include also the design and constructions of catalysts, polymers and sensors[8,9,10] as well as the creation of encapsulation systems like molecular capsules, micelles and dendrimers able to create microenvironments suitable for catalytic reactions.[11]

This thesis deals mainly with *Supramolecular Host Design.* Accordingly, this work has been organized to show its application in three different areas of interest in supramolecular chemistry studies: *Ion Pair Binding*, *Molecular Inclusion* and *Supramolecular Catalysis*.

Ion-Pair Receptors

The design and synthesis of ion-pair receptors represent an area of significant future growth in supramolecular chemistry due to their potential applications as membrane transporters, salt solubilisation agents and sensors. In solution, broadly speaking, we can distinguish three different states of ion-pairs.[12] In polar solvents, particularly in aqueous media, solvation energy overcomes the

electrostatic mutual attraction of ion pairs and hence the predominant species are solvent-separated ion pairs. This ion solvation is particularly advantageous in organic synthesis for example, where dipolar, aprotic solvents such as acetonitrile are used to effectively solvate cations, leaving reactive anions relatively free to undergo reactions such as nucleophilic substitution with a substrate (also known as *naked anion effect*). In less polar media, ions are often poorly solvated and form either contact ion pairs, in which an individual pair of oppositely charged ions are directly bonded *via* electrostatic interactions or aggregated contact ion pairs in which a number of ions form a small cluster which is itself solvated by the surrounding medium. The binding anions or cations in non-polar media involve a considerable enthalpic cost associated with breaking the interaction of the contact ion pair. This is confirmed by the different order of magnitude determined for the values of ion-pair dissociation constants (K_{ipd}) in solvents of different polarity (Figure 1.1). For example, in non-polar chlorinated solvents, tetra-alkyl ammonium salts $R_4N^+X^-$ [(R) Me, *n*-Pr, *n*-Bu; (X) PF_6, $B(C_6H_5)_4$, ClO_4, Cl, SCN] exhibite an ion-pair dissociation constant values in the range of 10^{-4} to 5 x 10^{-5} M^{-1}. On the contrary, in more polar solvents like acetonitrile the K_{ipd} values estimated for the same salts are of the order of 2-4 x 10^{-2} M^{-1}, that is two to three orders of magnitude larger. Finally, zwitterions can also be considered as intramolecular ion-paired species, since they are neutral molecules with both positive and negative parts. The classic examples of zwitterions are the amino acids in which the carboxylic acid group generally protonates the amine moiety.

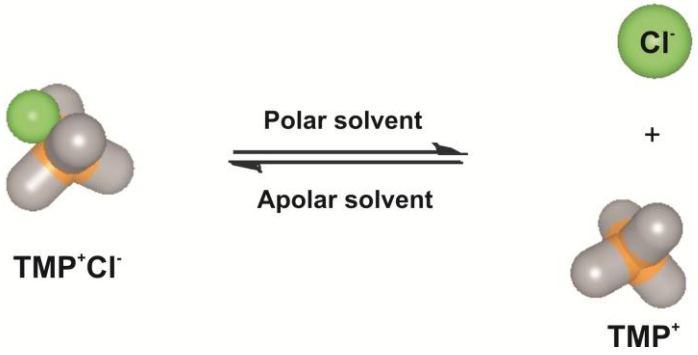

Figure 1.1. Ionic species involved in apolar (mainly ion-pair) and polar (mainly dissociated ions) solvents.

Over the past thirty years, a large number of macrocyclic receptors have been synthesized and evaluated for their abilities to bind cations.[13,14,15,16,17,18] More recently, increased attention has been directed towards the development of receptors for anions and ion-pairs.[19,20,21,22,23,24] Compared to simple ion receptors (monotopic receptors), which are able to bind either a cation or an anion, ion-pair receptors (heteroditopic receptors) might offer considerably advantages in term of affinity and selectivity. In many cases, ion-pair receptors display enhanced affinity with respect to simple ion receptors, as a consequence of the existence of direct or indirect cooperative interactions between the co-bound ions. Ion-pair receptors can be formed by a binary mixture of a monotopic cation receptor with a monotopic anion receptor (dual receptor strategy) or by a single molecule ditopic receptor with defined cation and anion binding sites (ditopic receptor strategy). For clarity, we described below one example for each kind of strategy.

On the one hand, Parisi *et al.*[25] demonstrated that the effective binding of targeted ion-paired organic salts (like N-acetyl-lysine methyl ester hydrochloride) can be achieved by a suitable combination of cationic (calix[6]arene derivative **1**) and anionic (calix[6]pyrrole derivative **2**) receptors (Figure 1.2). The observed synergic factors can be ascribed to the assisted dissociation of the ion pair by a combined action of the two receptors. The authors stated that as a result of the negligible electrostatic interaction between the charged components of the salt when confined in the cavity of their complementary host the conditional association constants measurable by this approach may be regarded as close to those expected in an ideal case where the counterion is absent.

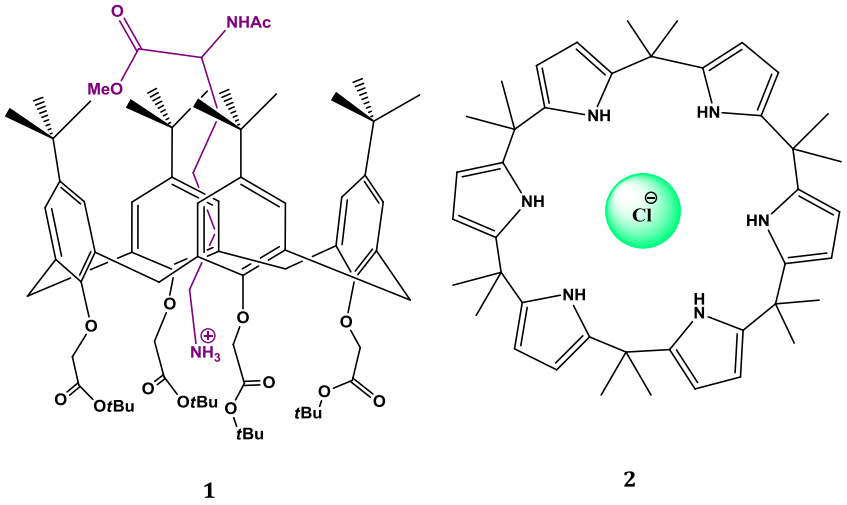

1 2

Figure 1.2. Binary 1:1 host system formed by the cationic N-Ac-Lys-OMe · H^+ @ calix[6]arene receptor **1** and the anionic Cl^- @ calix[6]pyrrole receptor **2**.

On the other hand, an interesting unimolecular heteroditopic receptor based on a calix[4]arene bis(benzo-15-crown-5) molecule **3** (Figure 1.3) was reported by Beer *et al.*[26] In polar organic solvents, the potassium cation complexed by the calix[4]arene receptor **3** enhances the strength of the binding of chloride, benzoate and dihydrogen phosphate anions *via* favourable preorganization and electrostatic effects. The multitopic properties of this receptor will be described later.

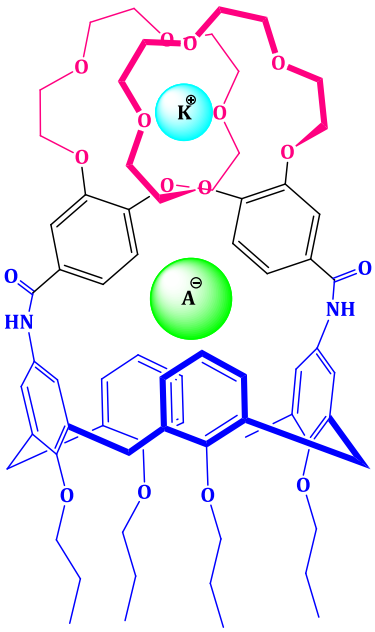

3

Figure 1.3. Calix[4]arene-based heteroditopic receptor **3** reported by Beer and co-workers.

Ion pair receptors achieve anion recognition mainly through hydrogen bonding donors[27] (urea, amide, hydroxyl groups, imidazolium or pyrroles units), Lewis acidic sites[28] (boron, aluminium and uranyl) and positively charged polyammonium groups[29]. In contrast, the majority of ion pair receptors afford cation recognition through lone pair electron donors like crown ethers and π-electron donors such as functionalized calixarenes[30]. Our attention focused on ion pair receptors based on pyrrole units since they constitute the starting building block for some of the receptors described in this thesis. First described in 1886 by Baeyer,[31] the tetrapyrrolic macrocycle **4** (Figure 1.4), called calix[4]pyrrole, was found in 1996 by Sessler et al. to be able to bind certain anions in organic solvents.[32] In 2005, Moyer, Sessler, Gale and coworkers confirmed that calix[4]pyrrole **4** can act as an ion pair receptor for various cesium salts and certain organic halide salts in the solid state.[33] X-ray crystal structures of several cesium and organic cation-containing anion complexes of calix[4]pyrroles **4** revealed that the anions are bound to the pyrrolic NH protons via hydrogen bonds. These interactions induce the calix[4]pyrrole core to adopt the cone conformation in solution and provide an electron rich bowl-shaped cavity opposite to the bound

anion into which, e.g., the cesium cation is bound via a combination of π–cation and cation-dipole interactions.

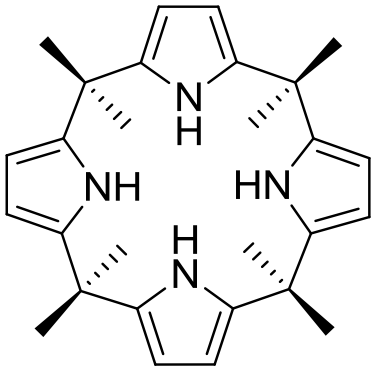

4

Figure 1.4. *meso*-Octamethylcalix[4]pyrrole **4**

Further evidence that calix[4]pyrrole **4** is effective for ion pair recognition came from liquid–liquid extraction studies carried out by Wintergerst *et al.*[34] This study demonstrated that compound **4** can extract CsCl and CsBr, but not $CsNO_3$, from an aqueous phase into nitrobenzene, a relatively polar organic phase. The solvent extraction process was modeled in terms of three thermochemical steps (Figure 1.5).

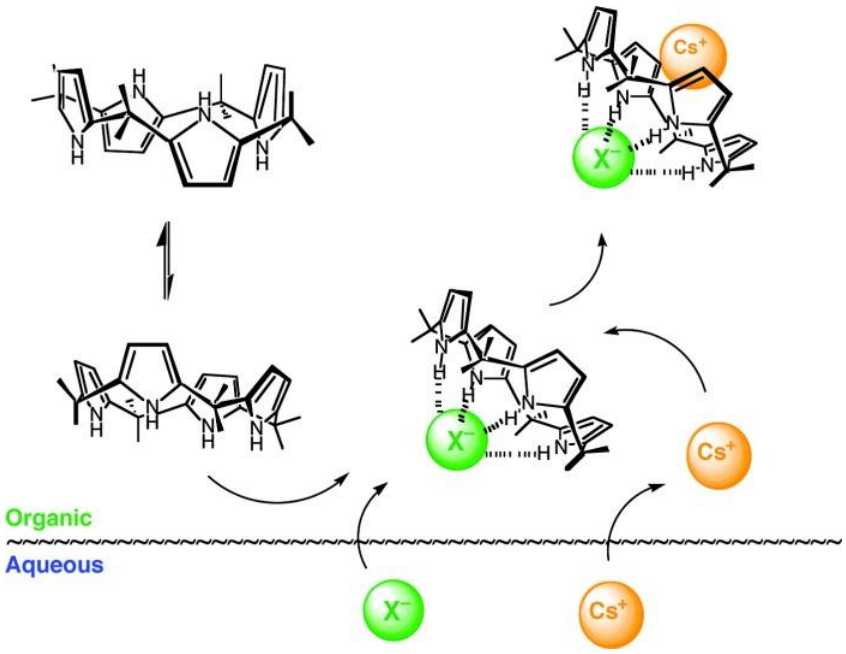

Figure 1.5. Proposed thermodynamic steps used to model cesium salt extraction by calix[4]pyrrole **4**. *Copyright 2008 of American Chemistry Society.*

The first one involves a partitioning of the cesium cations and the halide anions into the nitrobenzene phase from the water phase. The second step involves a conformational change of the calix[4]pyrrole in order to adopt the cone conformation, a geometry it maintains as the result of halide anion binding. The final step involves the cesium cation binding within the bowl-shaped calix cavity created as the result of the conformational change taking place in step 2. These steps can take place concurrently, so calix[4]pyrrole **4** binds both the cesium cation and a halide anion (Cl^- or Br^-).

Very recently, transmembrane anion transport experiments were carried out with calix[4]pyrrole **4.**[35] It was found that this simple-to-obtain receptor transports CsCl across phospholipid bilayers with significant selectivity and with an enhanced efficiency relative to other alkaline chloride salts. Such findings supported once again that calix[4]pyrrole **4** acted as an ion pair receptor under appropriate conditions.

The advantage of creating heteroditopic receptors over monotopic ones relies on the consequent stronger binding, following the heuristic principle that "*binding both is binding better*".[36] Higher binding constants are measured for the complexes derived form heteroditopic receptors, especially in low dielectric constant media. However, due to the general use of a simplified binding model, which does not take

into account the dissociation of the ion-pair nor the formation of an ion-paired complex, the experimentally determined magnitudes for the binding constants of the complexes with monotopic and heteroditopic receptors vary significantly upon receptor concentration, the specific ionic guest (type of salt used as anion precursor), the cation concentration, and the nature of other ions present in the medium. Ion-pair binding can occur in a sequential or concurrent way affording an analogous ion-paired complex.[37] In the case of sequential binding, the receptor can bind one ion of the ion pair on its own. Once bound, this first ion enhances the affinity for the other ion of the ion pair through an allosteric effect or by providing an additional binding driving force, commonly a direct or solvent-mediated electrostatic interaction with its counter ion. In this first design, we can include *cascade complexes* (Figure 1.6-a). By contrast, in the case of concurrent ion pair binding, the receptor literally forms a simultaneous complex with the anion and cation of the ion pair. Typically, this results in a complex where the two ions of the ion pair are in direct contact or spatially separated via one or more molecules of solvent or by the receptor skeleton. Ditopic receptors for separated ions (Figure 1.6-b) can experience a conformational change after the binding of the first ion that improves the affinity for the counter-ion. However, the Coulombic penalty that must be paid to enforce charge separation affects the affinity of the ion-pair binding with regard to the receptors for associated ion-pairs (Figure 1.6-c). Subsequently, ion-pair recognition can be dramatically enhanced by binding a contact ion pair.

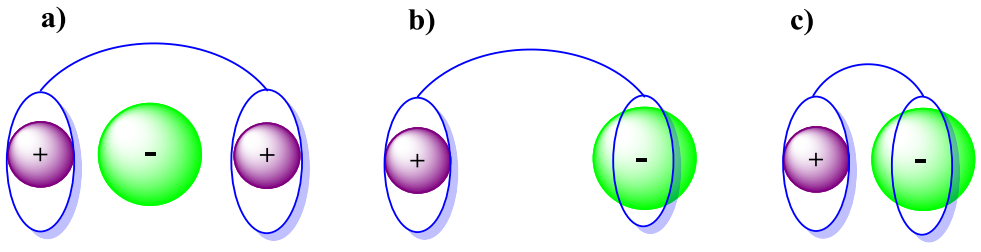

Figure 1.6. Common designs of ditopic receptors: a) Cascade complex. Heteroditopic receptor for separated ion pairs (b) and contact ion pairs (c).[37]

An alternative but analogous way of classifying ion pair receptors is based on the binding geometry adopted by the bound ion pair.[38] In this context three different

binding modes can be defined. These limiting modes are depicted in Figure 1.7 and differ in how the ion pair is held within a host molecule. The first involves a contact ion pair, wherein the anion and the cation are in direct contact (Figure 1.7 a); the second, called solvent-bridged ion pair, is where one or more solvent molecules bridge the gap between the anion and the co-bound cation (Figure 1.7 b), while the third one consists of a host-separated ion pair, wherein the anion and the cation are bound relatively far one from another, usually by the receptor framework (Figure 1.7 c).

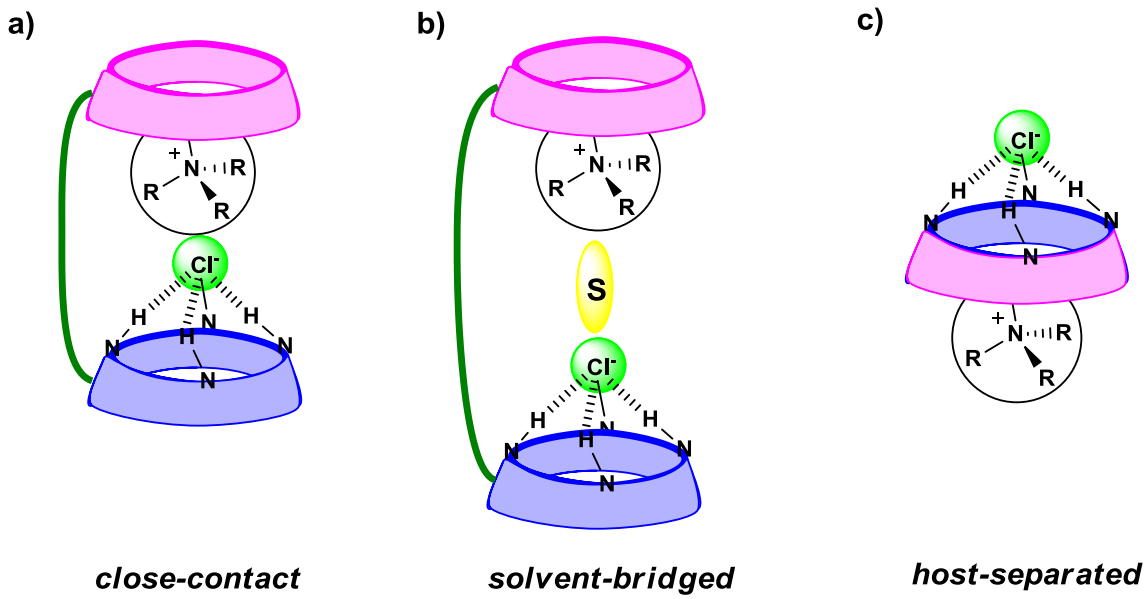

Figure 1.7. Limiting ion-pair interactions relevant to receptor-mediated ion-pair recognition: (a) contact, (b) solvent-bridged, and (c) host separated.

Calix[4]pyrrole–calix[4]arene linked receptor **5** (Figure 1.8) constitute a rare example of ion pairs host that is able to adopt the three different recognition modes referred above.[39] The preferred recognition mode is determined by the size of the ion pair, in particular by the size of the anion, while the same cation is used (i.e. cesium). When the anion is fluoride, CsF binds to receptor **5** as a solvent-separated ion-pair with a water molecule bridging the cation and the anion. The recognition of Cs^+ or F^- only takes place when both ions are present in solution (Figure 1.8-a). In contrast, when the anion is chloride an unusual 2:2 complex ($\mathbf{5}_2 \cdot (CsCl)_2$) is observed, featuring two different binding modes in the solid state. One

of these consists of a contact ion pair with the cesium cation and chloride anion both included within the central binding pocket and in direct contact with one another. The other mode involves a chloride anion bound to the pyrrole NH protons of a calix[4]pyrrole subunit and a cesium cation sandwiched between two cone shaped calix[4]pyrroles originating from separate receptor units. Thus one of the complexes observed in the solid state is a solvent-loosened contact ion pair. The other binding mode observed for CsCl is the receptor separated ion-pair shown in Figure 1.8-b. Finally, in presence of the largest ion pair $CsNO_3$, **5** acts as contact ion pair receptor (Figure 1.8-c).

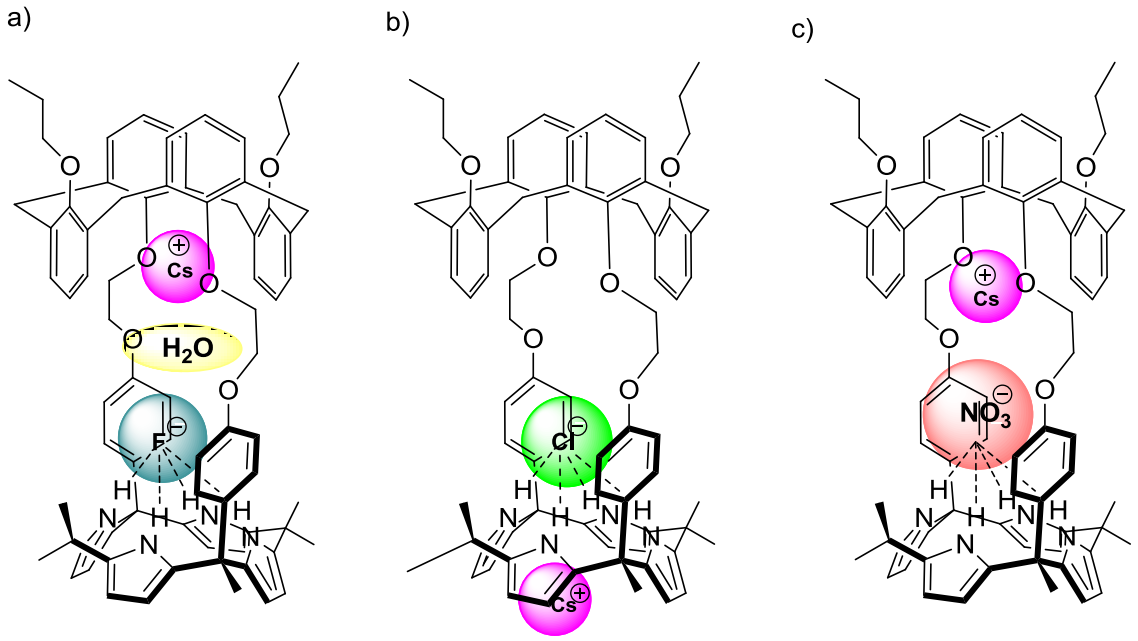

Figure 1.8. Three different ion-pair binding modes for receptor **5**. a) Solvent-separated CsF ion pair $CsF{\cdot}H_2O{\subset}$**5**; b) hots separated CsCl ion pair CsCl@**5**; c) contact $CsNO_3$ ion pair $CsNO_3{\subset}$**5**.

As briefly discussed above, ion-pair recognition is more complex than simple anion or cation recognition processes, since a higher number of equilibria are involved (Figure 1.9). The receptor can bind the anion (K_1) or the cation (K_2) separately as well as the ion pair (K_3). However, while the apparent constants K_1 and/or K_2 are independent of the counterion, concentration-dependent fluctuations are observed in the K_3 values (also named experimental constant $K_{a,exp}$) attributable to ion pairing. Competing ion pairing may also occur outside the receptor (K_{ip}), leading to precipitation of the ion pair itself. This last competing ion pairing and precipitation is quite common in non polar solvents, where ion-pairing effects are stronger.

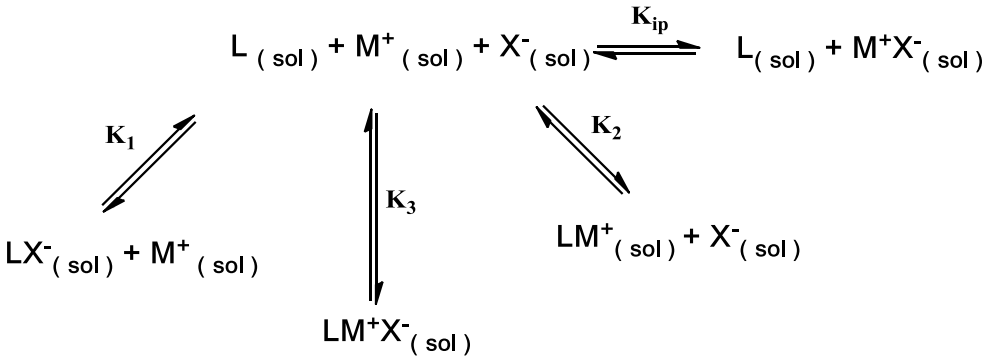

Figure 1.9. Simplified diagram illustrating the various equilibria that can exist in an ion-pair binding system. (X^- : anion; M^+ : cation; L : host).

Moreover, *cooperativity* can also play an important role in an ion-pair binding system since there is more than one binding site. The simplest situation is represented by non-cooperative binding where each ion binds independently of the other. In this case K_3 depends on K_1 and K_2. This occurs when the cation and the anion binding sites are rigid and separated either spatially or by solvent to prevent direct interactions between the cation and anion. Anticooperative binding occurs when the binding of one ion inhibits the binding of the other, whereas cooperative binding is observed when the binding of one ion enhances the binding of the other. Consequently, K_3 is smaller than the sum of K_1 and K_2 for anticooperative binding, and larger for cooperative binding. We are used to associate ion-pair binding to receptors that successfully exploit cooperativity[40], either if they are heteroditopic receptor for separated ion-pairs or for contact ion-pairs. However, there are also cases, though less common, in which the receptor displays both cooperative and anticooperative binding depending on the nature of the ion pair. It is the case of the calix[4]arene-based heteroditopic receptor **3** reported by Beer and co-workers and depicted in Figure 1.3. In this receptor the binding of chloride anion to the amide groups is enhanced 10-fold in the presence of potassium cation (Figure 1.10-a). This cooperative binding is attributed to the potassium-induced conformational change, which preorganizes the amide groups forming the 1:1 potassium/bis-(benzo[15]crown-5 ether) complex, favouring the existence of attractive electrostatic interactions between the anion and the cation. Conversely, anticooperative binding is observed in presence of two sodium cations bound to the individual crown ether moieties, because electrostatic repulsive

interactions established between the two complexed sodium cations prevents the conformational change (Figure 1.10-b).

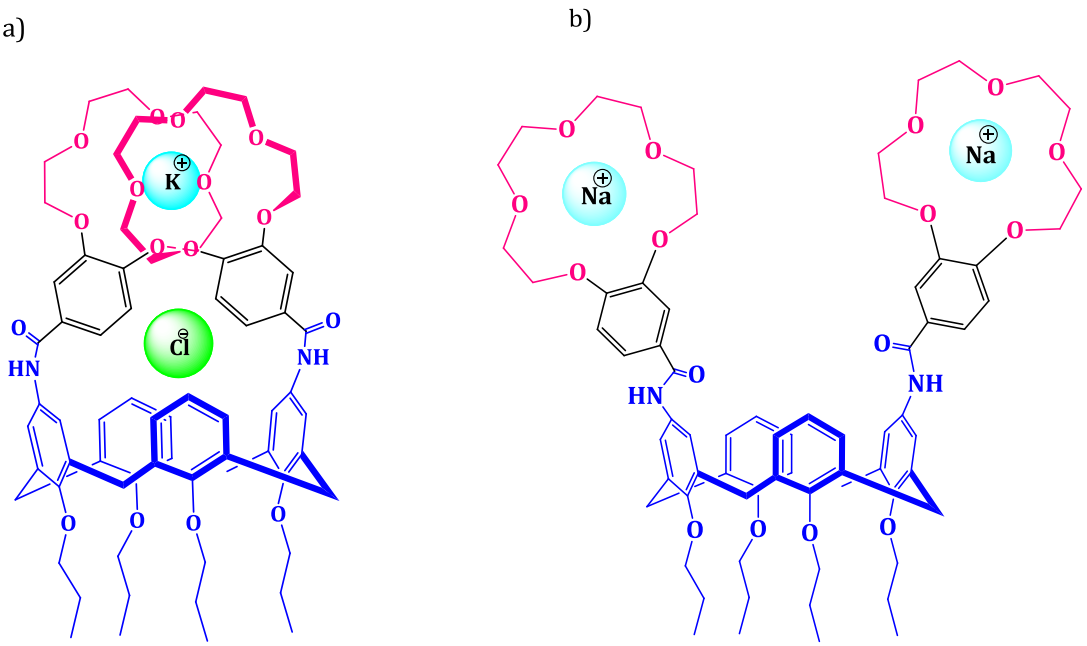

Figure 1.10. Calix[4]arene-based heteroditopic receptor **3:** a) Cooperative binding of KCl and b) anticooperative binding in the presence of two sodium Na^+.

The solvent in which the ion-pair recognition event takes place can also affect to cooperativity (Figure 1.1). Thus, receptor **6** binds fluoride in its calix[4]pyrrole anion binding cavity in $CDCl_3$. No evidence of fluoride binding is observed in a more polar system like 9:1 $CDCl_3/CD_3OD$, due to the stronger solvation of fluoride anion. However, in presence of a cesium cation bound within the crown ether binding unit fluoride complexation is observed again, even in 9:1 $CDCl_3/CD_3OD$ solvent mixture. The binding of the two ions was also found to be non-cooperative in CH_3CN because of the high polarity of the solvent.[41]

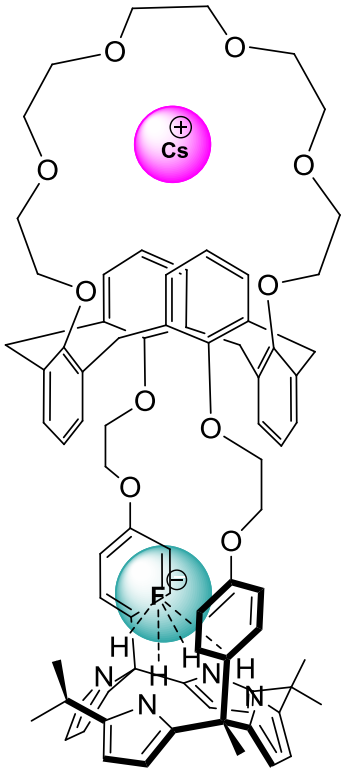

6

Figure 1.11. Receptor for CsF ion pairs reported by Sessler and coworkers.

All these examples suggest that although ion-pairing makes the understanding of the binding processes more complex, it cannot be excluded when studying these systems in apolar environments. The current literature on binding of ion pairs with ditopic receptors is essentially based on 1) crystallographic evidence, which demonstrates the existence of ion-pair complexes but not of cooperative effects, 2) transport through membranes or extraction from aqueous solutions, which is not necessarily dependent on cooperativity, and 3) binding studies in solution, that do not always allow a complete assessment of cooperativity. Usually the magnitude of the association constant related to the ion-pair complexation by a ditopic receptor is assessed by ^{1}H NMR titrations in organic solvents. The chemical shift changes experienced by a single proton signal of one of the binding partners, normally the host, are analyzed using a theoretical 1:1 binding model to derive the binding constant value. The determined value is simply compared to the magnitude of the association constant similarly determined for the same ditopic receptor with the anion or cation of interest in the presence of an innocent counterion, neglecting

other equilibria (ion pairing, higher stoichiometry association, etc.) that may occur in solution. Such a simplified approach is limited for several reasons: 1) systems containing multiple species and/or higher stoichiometry complexes cannot be fitted to a 1:1 binding isotherm; 2) the comparison of a ternary ion pair/receptor complex with a binary ion/receptor complex is wrong, since they have different dimensionality; 3) a three-component species like an ion-paired complex should not be analyzed using a two-species 1:1 binding model; 4) the counterion is not inert and should not be neglected. To overcome these limitations, new methods have been developed for a more detailed and quantitative analysis of the binding processes occurring during the ion-pair complexation with ditopic receptors.[42,43,36]

Molecular inclusion and encapsulation

The inclusion of molecules within molecules[44] is a common technique used in pharmaceutical sciences to protect sensitive compounds and increase their stability and storage over time.[45,46,47,48,49,50,51,52] A well-known example is represented by the encapsulation of drugs inside host molecules like cyclodextrins[53]. In the same vein, hemicarcerands have been studied as cages to stabilize highly reactive species[54] like cyclobutadiene.[55] In this way, species that would rapidly decompose or polymerize even at low temperature can be stored at room temperature inside its host. Likewise, the encapsulation of water sensitive species allows their isolation even in aqueous solution through hydrophobic catalysts.[56] Many examples of guest encapsulation/inclusion have been reported in recent literature.[57,58,59,60,61,62,63,64,65] Between them, the confinement of disfavourable conformations[66,67] and the modulation of the reactivity of a guest with alteration of the modes of reaction in solution represent for us the most interesting ones[68,69,70,71,72] and inspired the work presented in Chapter 5. Although the two recognition processes result similar, it is important to remark the subtle difference existing between inclusion complexation and encapsulation interaction, that lies in whether a guest is included in the cavity of a host or not. In particular, we refer to inclusion complexation when the interaction between the host and the guest occurs by complete or partially accommodation of the guest molecules inside the macrocycle. On the contrary, an encapsulation interaction occurs when the guest resides in the packing structure formed by host molecules.

The process of guest exchange in supramolecular systems consists in the substitution of a non-covalently bound molecule occupying the interior of a larger host molecule by a new guest molecule originally found in the bulk solution. The exchange process can occurs through an associative mechanism, where the bound guest is exchanged with a free guest or solvent molecule by means of a concerted process (SN_2-like), or a dissociative mechanism, where the bound guest departs from the cavity yielding an 'empty' assembly which is trapped by an incoming guest or a solvent molecule (SN_1-like). Depending on the structure of the host molecule, a variety of mechanisms can be envisioned for the exchange process to take place following any of the two mechanisms. If the host molecule is held together by weak forces, rupture of the host can permit guest release or exchange. Conversely, if the host is held in a rigid structure, then guest exchange must occur by the guest squeezing through apertures in the host assembly. Three main mechanistic pathways have been identified to describe the movement of molecules to and from macromolecules: 1) trapping, 2) gating and 3) slippage.[73] We describe below two well-known examples of guest exchange through a gating process in a covalently assembled host and in a hydrogen-bonded host complex.

We already mentioned that the internal cavities of suitable hosts have been used to stabilize highly reactive species. A classic example is the photochemical generation of cyclobutadiene, $(CH)_4$, inside of a hemicarcerand, leading to the first room temperature characterization of this highly reactive molecule. In order to understand the guest exchange pathway, Cram introduced the idea of *constrictive binding* to describe the steric interactions that must be overcome for guest ejection when the apertures of the host are smaller than the guest molecule itself.[74] The fact that guests larger than the portals of the hemicarcerands (Figure 1.12) are able to exchange suggests that the apertures of the assembly are able to expand and contract to facilitate ingress or egress. In such an exchange pathway, smaller guests are able to exchange more rapidly as they require a smaller deformation of the host, whereas exchange of larger guests is retarded due to the required host deformation.

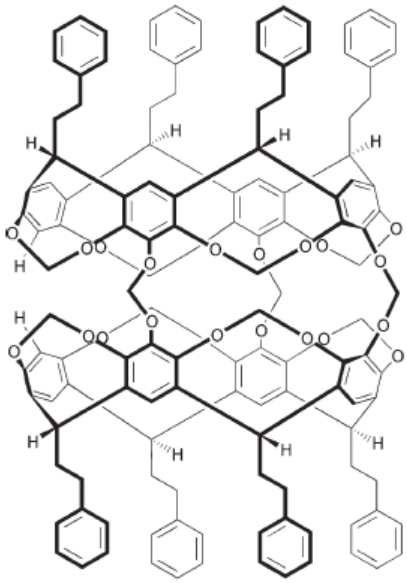

Figure 1.12 Hemicarcerand structure.

Thermodynamically speaking, the *constrictive binding* energy is the free energy which must be provided to the system to reach the transition-state for guest dissociation from the encapsulated state minus the free energy associated with binding ($\Delta G^{\ddagger}_{constrictive} = \Delta G^{\ddagger}_{diss} - (-\Delta G^{\circ})$, Figure 1.13).

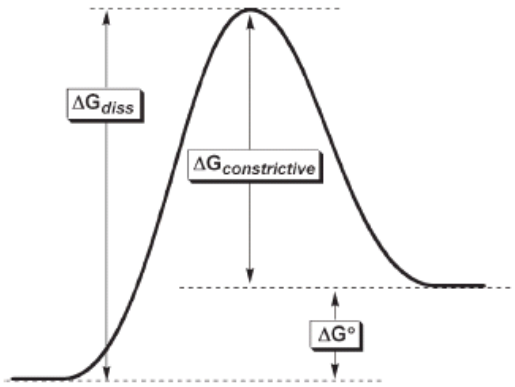

Figure 1.13 Energy diagram for guest release.

A two-steps guest dissociation mechanism has been proposed for these systems, in which the guest dissociates from the host capsule to leave an 'empty' host. This vacant cavity is either trapped by solvent or by the original guest molecule (SN_1 mechanism). Under low concentration of guest the large excess of solvent makes the guest–solvent metathesis essentially irreversible. The first order guest dissociation step is dependent on the identity of the solvent due to the ability of

the solvent to solvate the transition state for guest ejection. Van't Hoff analysis of the hemicarcerand host–guest system revealed that guest encapsulation is both enthalpically and entropically driven. At first glance, the inclusion of a guest molecule inside of a host would appear to be entropically disfavored; however, this schematic is an oversimplification. If the encapsulation process requires complete guest desolvation, the solvent molecules that were restricted in motion due to guest salvation are released into the bulk solution. This phenomenon has been observed in both hydrogen bonding solvents and non-hydrogen bonding solvents. The topic of constrictive binding is not restricted to the specific hemicarcerands outlined above. Many other carcerands and hemicarcerands display this mode of guest exchange. The cohesion of the covalently linked host and the inability of the host itself to dissociate require that portals in the host expand to allow for sterically encumbering guests to exchange through the dilated portals.

A nice example of gating in hydrogen-bonded hosts was reported by the Rebek group, creator of a variety of 'sportsballs' consisting of small identical subunits held together by rigid hydrogen bonds.[75] Hydrogen-bonding dimerization processes have extensively been used by Rebek at *al*. in the creation of hosts possessing an interior cavity capable of encapsulating a variety of guest molecules. The resulting encpasulation complexes are stable in aprotic solvents since protic media generally disrupts the hydrogen-bonding networks that stabilize the host's assembly. We describe here the famous example of Rebek and coworkers "*tennis ball*", named in this way for its small size (internal volume 50–55 Å). When placed in apolar solvents ($CDCl_3$) the two complementary bis-glycouril units dimerize by establishing eight N–H···O hydrogen bonds. Interestingly, the tennis ball is able to entrap small hydrocarbons, like ethane. In this complex, the conformational change of the seven membered ring creates a portal for guests to enter and exit the cavity (for this reason the exchange mechanism is called *gating*). Computational results are in favor of the dissociation–recombination mechanism of the host directing the guest exchange (Figure 1.14).

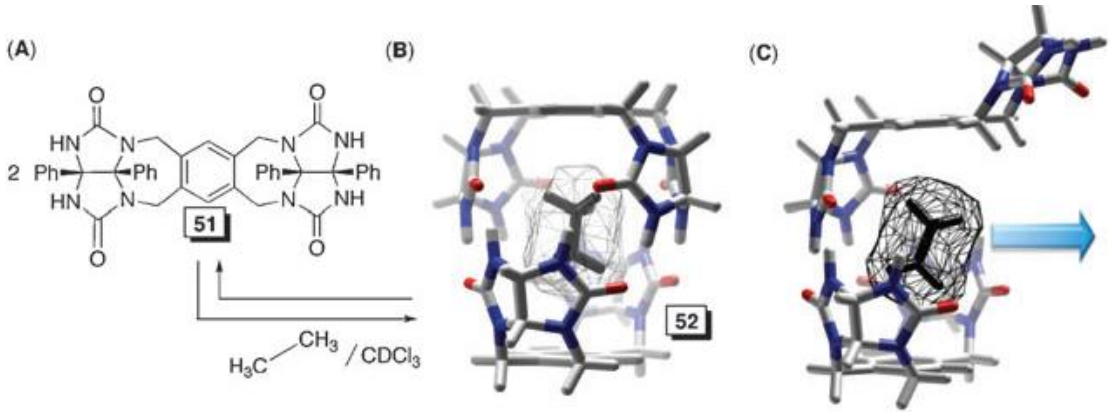

Figure 1.14. Rebek "tennis ball" and guest exchange mechanism. *Copyright 2011 The Royal Society of Chemistry.*

We are interested in focusing the attention of the reader on the analytical methods commonly used in monitoring and characterizing guest encapsulation/exchange processes, since they will be used in the development of this thesis work.[76] A short description of NMR, UV-Vis, mass spectrometry, electrochemistry and calorimetry techniques in guest encapsulation/exchange processes follows.

Nuclear magnetic resonance (NMR)[77] is the most prevalent, and often most useful, spectroscopic method for monitoring host–guest systems. Although supramolecular systems are often especially complex, they are also often highly symmetric, which can lead to greatly simplified NMR spectra. This simplicity can aid in the detection of the proton signal of the guest molecules, but it can also hide small time-averaged structural changes in the host. A number of experiments unique to NMR have been used to monitor host–guest systems. Diffusion-ordered spectroscopy (DOSY), for example, allows for measurement of diffusion coefficients in solution.[78] Host and guest molecules diffusing at an identical rate through solution are characteristic of a stable host–guest complex. In addition, weaker ion-pairing interactions can also be observed using DOSY. One of the most common NMR methods for characterization of supramolecular assemblies is Nuclear Overhauser Effect Spectroscopy (NOESY), which allows for through-space rather than through-bond observation. NOESY is often used to show guest inclusion and can yield valuable information on the relative proximities of guest molecules with different parts of the host. Although mainly used for qualitative observation, quantitative NOE studies have also been used to accurately determine

the solution structure of encapsulated guests. Sharing an identical pulse sequence with NOESY, EXSY (Exchange Spectroscopy) allows for measurement of chemical exchange rates. The practical difference between NOESY and EXSY is that NOESY measures rates of spin cross-relaxation, whereas EXSY measures rate of chemical exchange of spin.[79] Therefore, using EXSY and spin saturation transfer experiments, the rate of guest exchange can be measured. Such methods are amenable as they can cover a wide range of exchange rates ranging from 10^{-2} s^{-1} to 10^{2} s^{-1}.

Mass spectrometry allows for a convenient assessment of the exact stoichiometry of the complex in the gas phase through the analysis of the mass and isotopic composition of the observed ions in the MS spectra.[80,81] One unique benefit of mass spectrometry is that the transition from solution to the gas phase during ionization greatly affects the strengths of weak interactions often involved in supramolecular architectures. For example, in solution, assemblies held together by hydrogen-bonding are easily disrupted by the presence of hydrogen bond donors or acceptors from either protic solvent or other host molecules. In the gas phase, however, hydrogen bonding is greatly strengthened as competitive hydrogen bond donors and acceptors are removed. Similarly, electrostatic interactions such as ion-pairing are greatly enhanced in the gas phase as the competitive solvation of the ion-paired molecules is suppressed. However, other forces, such as Van der Waals interactions and hydrophobic interactions, are substantially weakened as the entropic driving force for dissociation in the gas phase is often too great. Unlike in solution where guest exchange is a dynamic process, in the gas phase guest ejection is essentially irreversible. Therefore, while solution studies show the thermodynamic stability of host–guest complexes, kinetic stability plays a more important role in the gas phase. Similarly, in the high-vacuum environment of mass spectrometry experiments, the entropic contributions of guest encapsulation are greatly affected. While guest ejection is often entropically disfavorable in solution due to the loss of degrees of freedom of the solvent molecules solvating the ejected guest molecule, dissociation of the host–guest complex is entropically favorable in the gas phase. Despite these differences, selective binding can be studied in the gas phase. However, both the method and matrix used in sample preparation can

dramatically influence the relative intensities of species, thereby making quantitative studies difficult. Mass spectrometry measurements of binding processes should be compared with solution-state data to provide valuable information on the role of solvation.

UV-visible spectroscopy[82] constitutes a useful tool for monitoring chemical reactions and chemical equilibria. This spectroscopic method requires that either the supramolecular host molecule or the guest species possess absorption bands in the UV-Vis region. The overall guest exchange process monitored by UV spectroscopy can provide information on the rate of the exchange of one guest for another or on the composition of the equilibria. One of the main advantages of this methodology is the ease of the experimental setup and the ability to monitor very dilute solutions in a wide variety of solvents. Circular dichroism (CD) spectroscopy, which measures the differential absorption of right- and left-handed circularly polarized light, can be used to monitor similar processes involving the optically active complexes.

Electrochemistry experiments[83] are a valuable tool for characterizing supramolecular systems providing useful information on guest exchange dynamics, which are slow in the timescale of the technique. Electrochemical methods require either the host or guest being electroactive. One of the most important electrochemical concepts in the field of supramolecular chemistry is redox-switching. The underlying principle is that the oxidation state of the guest (or host) influences the thermodynamic stability of the host–guest complex. When strong host–guest binding can be induced electrochemically, separate redox waves for the bound and unbound states can be observed in some cases, providing information on the concentration of each species.

Calorimetry[84] is the most exact and unbiased technique for precision thermodynamic measurements. When a guest molecule binds to a host, heat is either released or absorbed. Direct measurement of this heat in isothermal titration calorimetry (ITC) experiments allows for the determination of $\Delta G°$, $\Delta H°$, $\Delta S°$ from a single experiment in which the host complex is titrated with uniform increments of the guest. In comparison to other methods of determining

thermodynamic values, calorimetry is the only method for direct enthalpy measurement. Calorimetry is preferable to van't Hoff thermodynamic studies as ΔH° and ΔG° are determined from a single temperature point, not over a range of temperatures. Van't Hoff analysis makes the assumption that the heat capacity of the system is invariant over the temperature range of the experiment; an assumption which is not needed for calorimetry. Also, anomalous enthalpy–entropy compensation can be avoided by calorimetric methods as measurements of entropy and enthalpy are statistically independent. The analysis of calorimetric data requires an accurate working model for guest binding, and the influence of complicated external factors can greatly complicate interpretation. Guest binding can be complicated by factors such as ion-pairing and solvent reorganization, making the formulation of a suitable theoretical model for the binding processes problematic.

Supramolecular catalysis

The design of highly efficient and selective catalysts is one of the major goals of research in chemistry.[85,86,87,88,89,90,91,92] The remarkable features displayed in this respect by the natural catalysts, the enzymes, have provided major stimulus and inspiration for the development of novel catalysts by either manipulating their natural version or by trying to create artificial catalysts that, unlucky, so far have not display the high efficiency and selectivity displayed by the natural counterparts. Enzymatic reactions involve the binding of a specific substrate and its conversion into a different structure. Consequently, they constitute the essence of a supramolecular process. Molecular receptors bearing appropriate reactive groups in addition to binding sites may complex a substrate (with given stability, selectivity and kinetic features), react with it (with given rates, selectivity and turnover), and release the products, thus regenerating the catalyst for a new cycle. Supramolecular reactivity and catalysis involve two main steps: *binding*, which selects the substrate, and *transformation* of the bound species into products within the formed supramolecule. Both steps take part in the molecular *recognition* of the *productive* substrate and require the correct molecular information in the reactive receptor. Compared to simple uni-molecular reactivity, supramolecular reactions involve a binding step that precedes the reaction itself. Catalysis featuring turn-

over comprises a third step, the release of the substrate. The selection of the substrate is not the only function of the binding step. In order to promote a given reaction, the binding should strain the substrate so as to bring it toward the transition state of the reaction; thus, efficient catalysts should bind the transition state more strongly than the ground state of the substrate in order to lower the free energy of activation. A major role is played by the existence of strong interactions between the substrate and the catalytic receptor in order to facilitate the reaction in several ways. The effects induced by the fixation of the substrate play a critical role in the reaction catalyzed by either synthetic species or enzymes and may result in a sort of *mutual activation* of the two partners. It is then distinguished a thermodynamic effect, in the strong binding that forces the substrate into contact with the reactive groups; a steric effect, that control the fixation of the substrate and is able to distort its ground state structure towards a transition state-like geometry; an electrostatic (electronic, protonic, ionic) effect, consisting of a possible activation of the functional groups of the catalyst (and possibly of the substrate) by modification of their physico-chemical properties (pK_a, polarity, etc.) as a consequence of substrate fixation. This latter process may perturb the charge distributions in both the substrate and the catalyst with respect to their free, unbound states.

The design and study of efficient and selective supramolecular reagents and catalysts may give mechanistic insight into the elementary steps of catalysts, provide new types of chemical reagents, and reveal factors contributing to enzymatic catalysis. Supramolecular metallocatalysts consist on the combination of a recognition subunit (such as a cyclodextrin, a cyclophane, etc.) that selects the substrate with a catalytic metal center, bound to another subunit that represents the reactive site. The complexed metal centers presenting free coordination positions may provide a variety of substrate activation and functionalization properties. Heterotopic co-receptors bind simultaneously a substrate and a metal ion bringing them closer, thus potentially favoring a reaction between them. Approaches towards the development of synthetic metalloenzymes have been reported, based on macrocycles, that involve various metal ions, such as Zn(II), Cu(II), Co(III), in order to promote hydrolysis, epoxidation, hydrogen transfer, etc.

Many model systems[93] have been designed taking advantage of the binding energy to achieve reaction catalysis. In particular, two types of systems can be differentiated: (a) molecular receptors in which the catalytic site is placed close to the binding site designed to bind selectively the reactant and (b) molecular receptors that promote the reaction of two simultaneously complexed reactants.

In this thesis work, we focused our attention on the design and synthesis of catalytic systems of type (a), provided of a *Salphen* or *Terpyridi*ne unit as catalytic centre (Chapter 6). Early examples of supramolecular catalysis emerged from the work of Bender *et al.*, who studied the hydrolysis of *m*-*tert*-butylphenyl acetate in the presence of 2-benzimidazoleacetic acid with α-cyclodextrin.[94] More recently, Kim *et al*. have used a series of functionalized β-cyclodextrin with different polyazamacrocycles.[95] The Zn-complexes of these molecules are carboxypeptidase mimics, with the hydrophobic cavity of the cyclodextrin acting as a binding site for the aromatic residue of *p*-nitrophenyl acetate and the Zn(II) metal centre complexed by the azamacrocycle being the catalytic site. Other recent examples of this kind of methodology can be found in the literature and represent the main source of inspiration for the design and synthesis of the supramolecular ligands presented in this thesis. For example, Rebek *et al.* [96] reported the use of a cavitand armed with a *Zn salen*-type complex as catalyst (Figure 1.15).

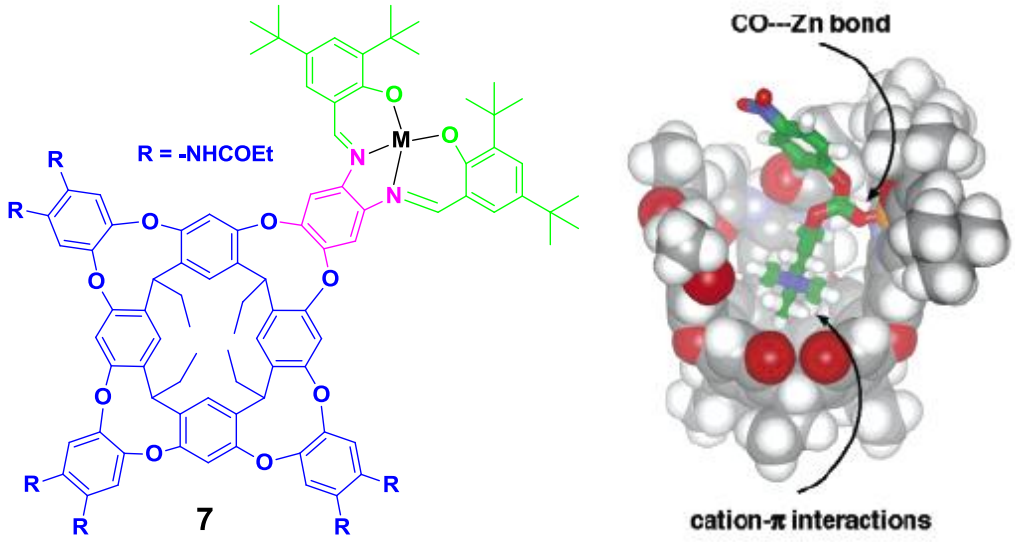

Figure 1.15. Molecular structure of Rebek's Zn-cavitand **7** and CAChe minimized structure of the p-nitrophenylcholine carbonate (PNPCC) included in **7**. *Copyright 2004 of American Chemistry Society.*

Cavitand **7** adopts a vase-like conformation that is stabilized by a seam of hydrogen bonds provided by the six secondary amides. The structure of the catalyst provokes that the dynamic exchange between free and bound guest (reactant) is slow on the ^{1}H NMR time-scale. The exchange is controlled by the folding and unfolding of the cavitand. The Zn-salen-modified cavitand **7** catalyzes the formation of acetylcholine from choline and acetic anhydride. When the guest used is *p*-nitrophenylcholine carbonate (PNPCC) **8,** the Lewis acid zinc(II) activates the well-positioned carbonyl group in the PNPCC@Zn-cavitand towards reaction with external nucleophiles. The energy minimized structure of the PNPCC@Zn-cavitand complex shows that cation-π interactions and C=O···Zn coordination bond occurs simultaneously. In general, the hydrolysis of the carbonate in the absence of the cavitand **7** is slow and only 30% of PNPCC is decomposed after 5h. On the contrary, the acceleration of the reaction rate is more than 50-fold when 1 equiv of cavitand **7** is present in solution. The binding of *p*-nitrophenylcholine carbonate **8** by cavitand **7** results highly selective and no affinity is detected for analogues of PNPCC like **9**. In this case, only the outer face of the salen ligand seems to be accessible to the substrate **9**. When the model of the salen wall but without cavitand is used as catalyst, **10**, the zinc(II) cation acts as Lewis acid and the reaction rate is also increased, although it turned out to be 5 times slower than the reaction catalyzed with the cavitand receptor **7**.

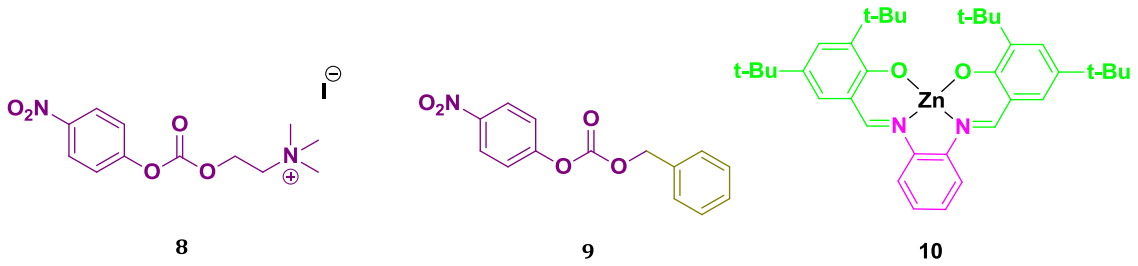

Figure 1.16. p-nitrophenylcholine carbonate **8**, p-nitrophenylcholine carbonate analogue **9** and Salen ligand **10.**

We chose Salphen ligands for the development of new resorcin[4]arene-derivatives for supramolecular catalysis since they are the most well-known and versatile structures in homogeneous catalysis (Chapter 6).[97,98,99,100]

In general, *the Salphen* structure is comprised of two salicylidene imine groups (Schiff base precursors) bridged by a phenyl spacer unit. In most of the catalytic applications, the salen ligand is highly symmetrical and is accessed via a double condensation reaction between a diamine and two equivalents of a salicylaldehyde.[101] Their respective metal salts are generally easily obtained by treatment with acetate-based metal precursors or via activation of the two phenolic positions with a strong base (e.g., BuLi or $ZnEt_2$).[102] The synthesis of nonsymmetrical salphens[103] is generally subject to a number of complications[104] but also increased attention, since the presence of two distinct salicylidene moieties in a complexed form provides a way to tune the catalytic efficiency of the metal center. Also, by preparing unsymmetrical salphen derivatives, it is possible to introduce a diverse variety of functional groups, allowing the application of these ligands for numerous purposes.[105,106,107,108] For all these reasons, various symmetrical[109], non-symmetrical[110] and chiral structures can be derived from this class of molecules. The tetradentate coordination ability of the salphen ligand commonly gives access to highly stabilized metal ions upon complexation and is furthermore well-suited for stabilization of higher oxidation states of catalytic intermediates.[111] Thermal and kinetic stability are desired prerequisites for molecular building blocks, and for this reason metallosalphens have recently been identified as interesting molecules in supramolecular chemistry and material science.[112] In this sense, the Zn(salphen) derivatives have been considered stable

molecular building blocks[113,114,115], although in some cases particular care should be taken with the use of certain coordinative patterns.[116] As most of the enzymes provided with the tetrahedrally coordinated Zn^{2+} ion, Zn(II)salphen complexes [or *N*,*N*′-phenylenebis(salicylideneimine)] also possess a remarkable high Lewis acid character. In these salphen derivatives, the Zn metal center possesses a remarkable Lewis acidity[117] as a result of the unfavorable planar geometry dictated by the tetradentate N_2O_2 ligation of the ligand. Therefore, the coordination geometry in these complexes needs additional ligands to stabilize the Zn ion. This feature has been exploited in various applications to bind ligands at the axial position to afford stable pentacoordinated species; as well it has proven to be extremely valuable in the construction of various supramolecular systems, in chemical sensing[118] and for discrimination of nitroaromatics.[119]

In the same way, terpyridine ligands can act as supramolecular synthetic catalyst and are capable of orienting the substrate towards the reaction center, as described by Crabtree and coworkers (Figure 1. 17)[120].

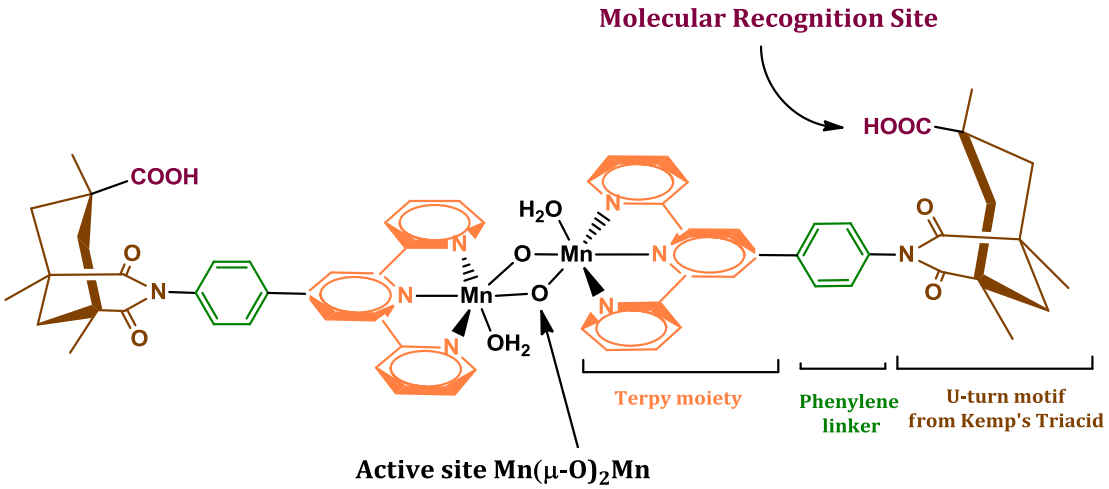

11

Figure 1. 17. Molecular structure of Crabtree's ligand **11**.

The authors combined molecular recognition through hydrogen bonds and C-H activation to obtain high turnover catalytic regioselective functionalization of sp^3 C-H bonds remote from the –COOH recognition group. The catalyst contains a di-μ-

oxo dimanganese catalytic core and two ligands that are based on the covalent connection of a Kemp's triacid unit[121] and provides a well-known U-turn motif having a –COOH group properly oriented for the molecular recognition of another –COOH moiety.[122,123,124,125,126,127,128,129,130] Molecular modelling studies (Figure 1.18) suggested a geometry for the H-bonded complex with ibuprofen (2-(4-isobutylphenyl)propionic acid), which reveals that the methylene C-H of the substrate is closest to the metal center and consequently should be oxidized more easily. If the oxidation operates via the catalyst-substrate complex predicted by the model complex, then this regioselective oxidation product should be the major component of the reaction mixture. When ibuprofen was treated with the catalyst, the selectivity for the regioselective product (97.5 : 2.5) was raised more than 10-fold when compared to the value obtained with a catalyst lacking the –COOH group (77 : 23). Oxidation of an alkyl carboxylic acid using the same catalysts led not only to regioselective oxygenation but also to diastereoselection of a single isomer. With a 0.1% catalyst-to-substrate ratio, a total turnover number of 580 was attained without loss of regioselectivity.

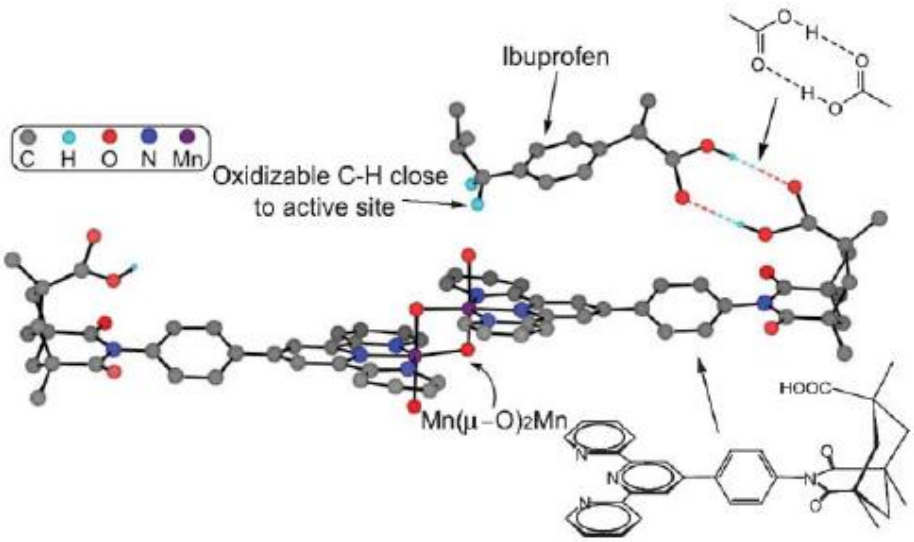

Figure 1.18 Molecular model of the supramolecular catalyst (CAChe minimized) docked with ibuprofen. *Copyright 2006 American Association for the Advancement of Science.*

For these reasons, we also selected the terpyridine ligand for the preparation of supramolecular catalysts based on the resorcin[4]arene scaffold (Chapter 6).

1. 2 Aims of this thesis

Due to the importance that ion-pair receptors and supramolecular catalysts are gaining in recent times and also to the wide variety of their potential applications, we decided to investigate further in these two areas of supramolecular chemisty during the development of the work presented in this thesis.

This PhD thesis deals with three different topics: (a) the design of unprecedented supramolecular receptors and the study of their binding processes with ion pairs (b) the study and application of the inclusion complexes between *N*-oxides and aryl-extended calix[4]pyrroles to modulate chemical reactivity and (c) the design and synthesis of new ligands with potential applications in supramolecular organometallic catalysis.

The project related to the binding studies with ion-pairs involves molecular receptors based on a calix[4]pyrrole and triazolophane scaffolds. More in detail, the goals we wanted to achieve in this line of research can be summarized as follows:

1. Design and synthesis of phosphonate aryl-extended calix[4]pyrroles. An unprecedented class of calix[4]pyrroles functionalized on the upper rim with two and four phosphonate groups, respectively, are targeted as potential receptors for alkylammonium/ammonium chloride salts. Binding studies will be undertaken to prove that these hosts can act as ion-pair receptors in apolar solvents (dichloromethane) and as anionic receptors in polar solvents (acetonitrile). The magnitudes of the association constants values of the complexes will be assessed by ^{1}H and ^{31}P-NMR titration experiments. The obtained thermodynamic data will be corroborated with the results derived form ITC measurements, ESI-MS experiments, and conductometric titrations. The binding geometry of the complexes will be investigated in solution by 2D NMR experiments and in the solid state using X-ray diffraction analysis.
2. Design and synthesis of functionalized Triazolophanes for inclusion of linear polyatomic anions. Our aim consists on the synthesis of new

triazolophane receptors and on studying the binding of monoanionic pseudohalide (F-H-F) anion using ^{1}H and ^{19}F-NMR spectroscopy. The system will represent an example of combining the strongest hydrogen-bond ($FH\cdots F^{-}$) with one of the weakest hydrogen bond interactions that are provided by the CH-of a triazol unit.

3. Synthesis of aryl-extended calix[4]pyrroles for the inclusion of conformationally flexible *N*-oxides typically used as sacrificial agents in oxidation reaction. Our aims in this section include the modulation of the chemical reactivity of *N*-oxides and the modification of the conformational equilibria in which they are involved by molecular inclusion. We envisaged the selective inclusion of the high energy conformer of *N*-methylmorpholine *N*-oxide (NMMO) within a calix[4]pyrrole having four aromatic ring substituents in the *meso* position. The value of the inclusion complex in modifying the normal chemical reactivity of the *N*-oxide will be tested by studying the outcome of reactions in which the NMMO is commonly used as sacrificial oxidant (e.g. oxidation of primary and secondary alcohol to carbonyl derivatives with tetrapropylammonium perruthenate). The progress of the oxidation reaction will be monitored by ^{1}H NMR spectroscopy and gas chromatography analysis of the reaction mixtures, both in the presence of free *N*-methylmorpholine *N*-oxide or of its inclusion complex with an aryl-extended calix[4]pyrrole (*N*-oxide@calix[4]pyrrole).

In the project dealing with the design of ligands for supramolecular catalysis, our proposal consisted in the design of molecules featuring an aromatic cavity or cleft capable to include neutral and ionic species decorated with covalently attached binding units for metal centers. To achieve our objectives, the research plan consisted on:

1. Preparation of trimethylene-bridged resorcinarene scaffold. The idea is to obtain a very simple construction unit featuring an aromatic cavity deep enough for the inclusion of positively charged unsaturated substrate or biologically active molecule (e.g. choline) by cation-π interactions.

2. Synthesis of derivatives of the trimethylene-bridged cavitand that can be used as ligands for supramolecular organometallic catalysis. The working plan consists in the placement of an extended aromatic wall (a dinitrophenyl unit) at the upper rim of the trimethylene-bridged resorcinarene. The aromatic bridging unit will be further elaborated to contain terpyridine and salen ligands. Future experiments (not included in this work) are planned to study the catalytic epoxidation of olefinic substrates with the terpyridine derivatives as Ru-complexes. On the other hand, the salen catalysts is planned to be tested in the acylation reaction of choline using acetyl imidazole as reactant. Both substrates can be simultaneously bound to the salen trimethylene bridged cavitand through cation-π interactions and Zn-N coordination bond, respectively.

1. 3 Summary

The present PhD Thesis is divided in 7 different chapters including the present introduction (chapter 1), the results and discussion part (chapters 2-6) and finally the general conclusions (chapter 7).

After this short introduction in the supramolecular chemistry field, we describe *in Chapter 2* the dynamics, thermodynamics and complex geometries of three diasteromeric *bis*-phosphonate cavitands based on an aryl extended calix[4]pyrrole tetraol scaffold that differ in the relative spatial orientation of the P=O groups installed in their upper rims (PO *in-in*, PO *out-out*, PO *in-out*). We demonstrate that these compounds act as heteroditopic receptors for ion pairs forming ion-paired 1:1 complexes with alkylammonium (quaternary and primary) chloride salts in dichloromethane (DCM) solution and in the solid-state. In the case of tetraalkyl-phosphonium/ammonium chloride guests, the host featuring the two P=O groups directed outwardly with respect to the aromatic cavity produces the more thermodynamically stable complexes. Conversely, for the primary alkyl ammonium chloride the most effective receptor is the diastereoisomer with the two P=O groups converging on top of the aromatic cavity. In the non-polar DCM solvent, the size of the quaternary cation has a strong impact in the thermodynamic stability of the complexes and their binding geometry. We also report that the 1:1 complexes of the *bis*-phosphonate *out-out* host with the chloride salts have a *separated* arrangement of the bound ion-pair. In contrast, those of the the *bis*-phosphonate *in-in* host display a *close-contact* arrangement. We also investigate the same complexation processes in acetonitrile (CH_3CN) solution. The receptors show an analogous trend in their binding affinities for quaternary phosphonium/ammonium chloride salts to the one seen in DCM solution. However, in CH_3CN solution the magnitude of the binding affinities is significantly reduced and the size of the cation does not have an important effect on them. The preparation of more complex *tetra*-phosphonate calix[4]pyrroles reveals dynamics, thermodynamics and complex geometries similar to the *bis*-phosphonate cavitands. However, the binding studies confirm that *four* phosphonate walls ensure stronger binding of tetraalkyl-

phosphonium/ammonium chloride guests respect to only two walls (*Chapter3*). In *Chapter 4* we present the design and synthesis of new derivatives of macrocyclic triazolophane receptors. Although they bear only triazole- and phenyl-derived CH hydrogen bond donors, these receptors show good binding strengths towards ion-pairs. We then report the preliminary NMR spectroscopy binding studies toward the linear bifluoride anion (HF_2^-) in polar solvents. In *Chapter 5* we show that aryl-extended calix[4]pyrroles are also able to form highly stable complexes with *N*-oxides of *N*-methylmorpholine (NMMO). The inclusion of the high energy conformer of the NMMO (not observed in the NMR timescale at room temperature) represents an interesting tool to examine and manipulate the properties of small molecules in confined space. *Chapter 6* presents the design and synthesis of a novel class of resorcinarene supramolecular catalysts. In particular, we show the complete synthesis of Terpyridine and Salphen derivatives for possible future applications in the catalytic epoxidation of unsaturated substrates and acylation reaction of acetylcholine, respectively.

Finally, the summary and concluding remarks of the work presented in the thesis are provided at *Chapter 7*.

1. 4 Refences and Notes

[1] Lehn, J. M. *Science* **1993**, *260*, 1762.
[2] J. W. Steed, J. A. Atwood, *Supramolecular Chemistry*, 2nd Edition, Wiley, 2009
[3] Bertrand, N.; Gauthier, M. A.; Bouvet, C.; Moreau, P.; Petitjean, A.; Leroux, J. C.; Leblond, J. *J. Controlled Release* **2011**, *155*, 200.
[4] P.A. Gale and J.W. Steed, *Supramolecular Chemistry: From Molecules to Nanomaterials*, Wiley , 2012
[5] Balzani, V.; Gomez-Lopez, M.; Stoddart, J. F. *Acc. Chem. Res.* **1998**, *31*, 405.
[6] Ikeda, T.; Stoddart, J. F. *Science and Technology of Advanced Materials* **2008**, *9*.
[7] Berna, J.; Leigh, D. A.; Lubomska, M.; Mendoza, S. M.; Perez, E. M.; Rudolf, P.; Teobaldi, G.; Zerbetto, F. *Nat. Mater.* **2005**, *4*, 704.
[8] Kurth, D. G. *Science and Technology of Advanced Materials* **2008**, *9*.
[9] Bureekaew, S.; Shimomura, S.; Kitagawa, S. *Science and Technology of Advanced Materials* **2008**, *9*.
[10] Lehn, J. M. *Angew. Chem., Int. Ed. Engl.* **1990**, *29*, 1304.
[11] Ariga, K.; Hill, J. P.; Lee, M. V.; Vinu, A.; Charvet, R.; Acharya, S. *Science and Technology of Advanced Materials* **2008**, *9*.
[12] Marcus, Y.; Hefter, G. *Chem. Rev.* **2006**, *106*, 4585.
[13] Yamato, T.; Rahman, S.; Kitajima, F.; Xi, Z.; Gil, J. T. *J. Chem. Res.* **2006**, 496.
[14] Cametti, M.; Nissinen, M.; Cort, A. D.; Mandolini, L.; Rissanen, K. *Chem. Commun. (Cambridge, U. K.)* **2003**, 2420.
[15] Kim, Y. H.; Hong, J. I. *Chem. Commun. (Cambridge, U. K.)* **2002**, 512.
[16] Mahoney, J. M.; Beatty, A. M.; Smith, B. D. *J. Am. Chem. Soc.* **2001**, *123*, 5847.
[17] Scheerder, J.; vanDuynhoven, J. P. M.; Engbersen, J. F. J.; Reinhoudt, D. N. *Angew. Chem., Int. Ed. Engl.* **1996**, *35*, 1090.
[18] Rudkevich, D. M.; Mercerchalmers, J. D.; Verboom, W.; Ungaro, R.; Dejong, F.; Reinhoudt, D. N. *J. Am. Chem. Soc.* **1995**, *117*, 6124.
[19] Kirkovits, G. J.; Shriver, J. A.; Gale, P. A.; Sessler, J. L. *J. Inclusion Phenom. Macrocyclic Chem.* **2001**, *41*, 69.
[20] Nabeshima, T.; Saiki, T.; Iwabuchi, J.; Akine, S. *J. Am. Chem. Soc.* **2005**, *127*, 5507.
[21] Gong, J. C.; Gibb, B. C. *Chem. Commun. (Cambridge, U. K.)* **2005**, 1393.
[22] Lankshear, M. D.; Cowley, A. R.; Beer, P. D. *Chem. Commun. (Cambridge, U. K.)* **2006**, 612.
[23] Cametti, M.; Nissinen, M.; Cort, A. D.; Mandolini, L.; Rissanen, K. *J. Am. Chem. Soc.* **2007**, *129*, 3641.
[24] Lankshear, M. D.; Dudley, I. M.; Chan, K. M.; Beer, P. D. *New J. Chem.* **2007**, *31*, 684.
[25] Cafeo, G.; Gattuso, G.; Kohnke, F. H.; Notti, A.; Occhipinti, S.; Pappalardo, S.; Parisi, M. F. *Angew. Chem., Int. Ed.* **2002**, *41*, 2122.
[26] Evans, A. J.; Beer, P. D. *Dalton Trans.* **2003**, 4451.
[27] Shi, X. D.; Fettinger, J. C.; Davis, J. T. *Angew. Chem., Int. Ed.* **2001**, *40*, 2827.
[28] Zhao, H. Y.; Gabbai, F. P. *Nature Chem.* **2010**, *2*, 984.
[29] Llinares, J. M.; Powell, D.; Bowman-James, K. *Coord. Chem. Rev.* **2003**, *240*, 57.
[30] Chen, Y.; Wang, D. X.; Huang, Z. T.; Wang, M. X. *Chem. Commun. (Cambridge, U. K.)* **2011**, *47*, 8112.
[31] A. Baeyer, *Ber. Dtsch. Chem. Ges.*, **1886**, *19*, 2184.
[32] Gale, P. A.; Sessler, J. L.; Kral, V.; Lynch, V. *J. Am. Chem. Soc.* **1996**, *118*, 5140.
[33] Custelcean, R.; Delmau, L. H.; Moyer, B. A.; Sessler, J. L.; Cho, W. S.; Gross, D.; Bates, G. W.; Brooks, S. J.; Light, M. E.; Gale, P. A. *Angew. Chem., Int. Ed.* **2005**, *44*, 2537.
[34] Wintergerst, M. P.; Levitskaia, T. G.; Moyer, B. A.; Sessler, J. L.; Delmau, L. H. *J. Am. Chem. Soc.* **2008**, *130*, 4129.
[35] Tong, C. C.; Quesada, R.; Sessler, J. L.; Gale, P. A. *Chem. Commun. (Cambridge, U. K.)* **2008**, 6321.
[36] Roelens, S.; Vacca, A.; Francesconi, O.; Venturi, C. *Chem.--Eur. J.* **2009**, *15*, 8296.
[37] McConnell, A. J.; Beer, P. D. *Angew. Chem., Int. Ed.* **2012**, *51*, 5052.
[38] Kim, S. K.; Sessler, J. L. *Chem. Soc. Rev.* **2010**, *39*, 3784.
[39] Kim, S. K.; Sessler, J. L.; Gross, D. E.; Lee, C. H.; Kim, J. S.; Lynch, V. M.; Delmau, L. H.; Hay, B. P. *J. Am. Chem. Soc.* **2010**, *132*, 5827.
[40] Hunter, C. A.; Anderson, H. L. *Angew. Chem., Int. Ed.* **2009**, *48*, 7488.
[41] Sessler, J. L.; Kim, S. K.; Gross, D. E.; Lee, C. H.; Kim, J. S.; Lynch, V. M. *J. Am. Chem. Soc.* **2008**, *130*, 13162.

[42] Jones, J. W.; Gibson, H. W. *J. Am. Chem. Soc.* **2003**, *125*, 7001.
[43] Llinares, J. M.; Powell, D.; Bowman-James, K. *Coord. Chem. Rev.* **2003**, *240*, 57.
[44] Hof, F.; Rebek, J. *Proc. Natl. Acad. Sci. U. S. A.* **2002**, *99*, 4775.
[45] Raymond, K. N. *Nature* **2009**, *460*, 585.
[46] Mal, P.; Breiner, B.; Rissanen, K.; Nitschke, J. R. *Science* **2009**, *324*, 1697.
[47] Campbell, V. E.; de Hatten, X.; Delsuc, N.; Kauffmann, B.; Huc, I.; Nitschke, J. R. *Chem.--Eur. J.* **2009**, *15*, 6138.
[48] Mal, P.; Schultz, D.; Beyeh, K.; Rissanen, K.; Nitschke, J. R. *Angew. Chem., Int. Ed.* **2008**, *47*, 8297.
[49] Iwasawa, T.; Hooley, R. J.; Rebek, J. *Science* **2007**, *317*, 493.
[50] Warmuth, R.; Marvel, M. A. *Angew. Chem., Int. Ed.* **2000**, *39*, 1117.
[51] Cram, D. J. *Nature* **1992**, *356*, 29.
[52] Cram, D. J. *Science* **1983**, *219*, 1177.
[53] Liu, L.; Guo, Q. X. *J. Inclusion Phenom. Macrocyclic Chem.* **2002**, *42*, 1.
[54] Warmuth, R. *Angew. Chem., Int. Ed. Engl.* **1997**, *36*, 1347.
[55] Cram, D. J.; Tanner, M. E.; Thomas, R. *Angew. Chem., Int. Ed. Engl.* **1991**, *30*, 1024.
[56] *Molecular Encapsulation*: Organic Reactions in Constrained Systems, U. H. Brinker, J. L. Mieusset, Wiley, 2010
[57] Qiu, Y. H.; Yi, S.; Kaifer, A. E. *J. Org. Chem.* **2012**, *77*, 4622.
[58] Little, M. A.; Donkin, J.; Fisher, J.; Halcrow, M. A.; Loder, J.; Hardie, M. J. *Angew. Chem., Int. Ed.* **2012**, *51*, 764.
[59] Yoshizawa, M.; Kusukawa, T.; Fujita, M.; Yamaguchi, K. *J. Am. Chem. Soc.* **2000**, *122*, 6311.
[60] Hof, F.; Craig, S. L.; Nuckolls, C.; Rebek, J. *Angew. Chem., Int. Ed.* **2002**, *41*, 1488.
[61] Sarmentero, M. A.; Fernandez-Perez, H.; Zuidema, E.; Bo, C.; Vidal-Ferran, A.; Ballester, P. *Angew. Chem., Int. Ed.* **2010**, *49*, 7489.
[62] Podkoscielny, D.; Hooley, R. J.; Rebek, J.; Kaifer, A. E. *Org. Lett.* **2008**, *10*, 2865.
[63] Leontiev, A. V.; Saleh, A. W.; Rudkevich, D. M. *Org. Lett.* **2007**, *9*, 1753.
[64] Chen, Y.; Liu, Y. *Chem. Soc. Rev.* **2010**, *39*, 495.
[65] Song, L. X.; Bai, L.; Xu, X. M.; He, J.; Pan, S. Z. *Coord. Chem. Rev.* **2009**, *253*, 1276.
[66] Ajami, D.; Rebek, J. *Nature Chem.* **2009**, *1*, 87.
[67] Ams, M. R.; Ajami, D.; Craig, S. L.; Yang, J. S.; Rebek, J. *J. Am. Chem. Soc.* **2009**, *131*, 13190.
[68] Djernes, K. E.; Moshe, O.; Mettry, M.; Richards, D. D.; Hooley, R. J. *Org. Lett.* **2012**, *14*, 788.
[69] Breiner, B.; Clegg, J. K.; Nitschke, J. R. *Chemical Science* **2011**, *2*, 51.
[70] Minten, I. J.; Claessen, V. I.; Blank, K.; Rowan, A. E.; Nolte, R. J. M.; Cornelissen, J. J. L. M. *Chemical Science* **2011**, *2*, 358.
[71] Restorp, P.; Rebek, J. *J. Am. Chem. Soc.* **2008**, *130*, 11850.
[72] Kawano, M.; Kobayashi, Y.; Ozeki, T.; Fujita, M. *J. Am. Chem. Soc.* **2006**, *128*, 6558.
[73] Rieth, S.; Hermann, K.; Wang, B. Y.; Badjic, J. D. *Chem. Soc. Rev.* **2011**, *40*, 1609.
[74] Cram, D. J.; Tanner, M. E.; Knobler, C. B. *J. Am. Chem. Soc.* **1991**, *113*, 7717.
[75] Wyler, R.; Demendoza, J.; Rebek, J. *Angew. Chem., Int. Ed. Engl.* **1993**, *32*, 1699.
[76] Pluth, M. D.; Raymond, K. N. *Chem. Soc. Rev.* **2007**, *36*, 161.
[77] Rudkevich, D. M.; Hilmersson, G.; Rebek, J. *J. Am. Chem. Soc.* **1998**, *120*, 12216.
[78] Cohen, Y.; Avram, L.; Frish, L. *Angew. Chem., Int. Ed.* **2005**, *44*, 520.
[79] Perrin, C. L.; Dwyer, T. J. *Chem. Rev.* **1990**, *90*, 935.
[80] Andersen, U. N.; Seeber, G.; Fiedler, D.; Raymond, K. N.; Lin, D.; Harris, D. *J. Am. Soc. Mass Spectrom.* **2006**, *17*, 292.
[81] Schalley, C. A.; Baytekin, B.; Baytekin, H. T.; Engeser, M.; Felder, T.; Rang, A. *J. Phys. Org. Chem.* **2006**, *19*, 479.
[82] Crupi, V.; Ficarra, R.; Guardo, M.; Majolino, D.; Stancanelli, R.; Venuti, V. *J. Pharm. Biomed. Anal.* **2007**, *44*, 110.
[83] Ko, Y. H.; Kim, E.; Hwang, I.; Kim, K. *Chem. Commun. (Cambridge, U. K.)* **2007**, 1305.
[84] Schmidtchen, F. P. *Chem.--Eur. J.* **2002**, *8*, 3522.
[85] Berryman, O. B.; Sather, A. C.; Lledo, A.; Rebek, J. *Angew. Chem., Int. Ed.* **2011**, *50*, 9400.
[86] Pluth, M. D.; Bergman, R. G.; Raymond, K. N. *Acc. Chem. Res.* **2009**, *42*, 1650.
[87] Yoshizawa, M.; Tamura, M.; Fujita, M. *Science* **2006**, *312*, 251.
[88] Kleij, A. W.; Reek, J. N. H. *Chem.--Eur. J.* **2006**, *12*, 4219.

[89] Slagt, V. F.; Kamer, P. C. J.; van Leeuwen, P. W. N. M.; Reek, J. N. H. *J. Am. Chem. Soc.* **2004**, *126*, 1526.
[90] Gissot, A.; Rebek, J. *J. Am. Chem. Soc.* **2004**, *126*, 7424.
[91] Purse, B. W.; Ballester, P.; Rebek, J. *J. Am. Chem. Soc.* **2003**, *125*, 14682.
[92] Piet W. N. M. van Leeuwen, Comprehensive Supramolecular Chemistry, Vol. 10 (Ed.: D. N. Reinhoudt), Wiley-VCH, Weinheim, 1996.
[93] Piet W. N. M. van Leeuwen, *Supramolecular catalysis,* WYLEY-VCH Verlag GmbH & Co. KGaA, , 2008
[94] Komiyama, M.; Breaux, E. J.; Bender, M. L. *Bioorg. Chem.* **1977**, *6*, 127.
[95] Kim, D. H.; Lee, S. S. *Bioorg. Med. Chem.* **2000**, *8*, 647.
[96] Richeter, S.; Rebek, J. *J. Am. Chem. Soc.* **2004**, *126*, 16280.
[97] McGarrigle, E. M.; Gilheany, D. G. *Chem. Rev.* **2005**, *105*, 1563.
[98] Jacobsen, E. N. *Acc. Chem. Res.* **2000**, *33*, 421.
[99] Atwood, D. A.; Harvey, M. J. *Chem. Rev.* **2001**, *101*, 37.
[100] Canali, L.; Sherrington, D. C. *Chem. Soc. Rev.* **1999**, *28*, 85.
[101] Morris, G. A.; Zhou, H. Y.; Stern, C. L.; Nguyen, S. T. *Inorg. Chem.* **2001**, *40*, 3222.
[102] Larrow, J. F.; Jacobsen, E. N.; Gao, Y.; Hong, Y. P.; Nie, X. Y.; Zepp, C. M. *J. Org. Chem.* **1994**, *59*, 1939.
[103] Kleij, A. W. *Eur. J. Inorg. Chem.* **2009**, 193.
[104] Renehan, M. F.; Schanz, H. J.; McGarrigle, E. M.; Dalton, C. T.; Daly, A. M.; Gilheany, D. G. *J. Mol. Catal. A: Chem.* **2005**, *231*, 205.
[105] Wezenberg, S. J.; Kleij, A. W. *Angew. Chem., Int. Ed.* **2008**, *47*, 2354.
[106] Zheng, X. L.; Jones, C. W.; Weck, M. *Chem.--Eur. J.* **2006**, *12*, 576.
[107] Kleij, A. W.; Tooke, D. M.; Spek, A. L.; Reek, J. N. H. *Eur. J. Inorg. Chem.* **2005**, 4626.
[108] Munoz-Hernandez, M. A.; Keizer, T. S.; Parkin, S.; Patrick, B.; Atwood, D. A. *Organometallics* **2000**, *19*, 4416.
[109] Jing, H. W.; Edulji, S. K.; Gibbs, J. M.; Stern, C. L.; Zhou, H. Y.; Nguyen, S. T. *Inorg. Chem.* **2004**, *43*, 4315.
[110] Holbach, M.; Zheng, X. L.; Burd, C.; Jones, C. W.; Weck, M. *J. Org. Chem.* **2006**, *71*, 2903.
[111] Sammis, G. M.; Danjo, H.; Jacobsen, E. N. *J. Am. Chem. Soc.* **2004**, *126*, 9928.
[112] Gianneschi, N. C.; Cho, S. H.; Nguyen, S. T.; Mirkin, C. A. *Angew. Chem., Int. Ed.* **2004**, *43*, 5503.
[113] Kleij, A. W. *Dalton Trans.* **2009**, 4635.
[114] Kuil, M.; Goudriaan, P. E.; Kleij, A. W.; Tooke, D. M.; Spek, A. L.; van Leeuwen, P. W. N. M.; Reek, J. N. H. *Dalton Trans.* **2007**, 2311.
[115] Kleij, A. W.; Kuil, M.; Tooke, D. M.; Spek, A. L.; Reek, J. N. H. *Inorg. Chem.* **2007**, *46*, 5829.
[116] Escudero-Adan, E. C.; Benet-Buchholz, J.; Kleij, A. W. *Dalton Trans.* **2008**, 734.
[117] Kleij, A. W.; Kuil, M.; Tooke, D. M.; Lutz, M.; Spek, A. L.; Reek, J. N. H. *Chem.--Eur. J.* **2005**, *11*, 4743.
[118] Wezenberg, S. J.; Escudero-Adan, E. C.; Benet-Buchholz, J.; Kleij, A. W. *Org. Lett.* **2008**, *10*, 3311.
[119] Germain, M. E.; Knapp, M. J. *J. Am. Chem. Soc.* **2008**, *130*, 5422.
[120] Das, S.; Incarvito, C. D.; Crabtree, R. H.; Brudvig, G. W. *Science* **2006**, *312*, 1941.
[121] Kemp, D. S.; Petrakis, K. S. *J. Org. Chem.* **1981**, *46*, 5140.
[122] Shenoy, S. R.; Crisostomo, F. R. P.; Iwasawa, T.; Rebek, J. *J. Am. Chem. Soc.* **2008**, *130*, 5658.
[123] Stoll, I.; Mix, A.; Rozhenko, A. B.; Neumann, B.; Stammler, H. G.; Mattay, J. *Tetrahedron* **2008**, *64*, 3813.
[124] Park, H. K.; Chang, S. K. *Bull. Korean Chem. Soc.* **2000**, *21*, 1052.
[125] Kim, N. Y.; Park, S. W.; Chang, S. K. *Bull. Korean Chem. Soc.* **1997**, *18*, 519.
[126] Matthews, C. J.; Heath, S. L.; Clegg, W.; Lockhart, J. C. *J. Chem. Soc., Perkin Trans. 2* **1997**, 665.
[127] Rebek, J. *Pure Appl. Chem.* **1989**, *61*, 1517.
[128] Marshall, L.; Parris, K.; Rebek, J.; Luis, S. V.; Burguete, M. I. *J. Am. Chem. Soc.* **1988**, *110*, 5192.
[129] Rebek, J.; Askew, B.; Killoran, M.; Nemeth, D.; Lin, F. T. *J. Am. Chem. Soc.* **1987**, *109*, 2426.
[130] Rebek, J.; Marshall, L.; Wolak, R.; Parris, K.; Killoran, M.; Askew, B.; Nemeth, D.; Islam, N. *J. Am. Chem. Soc.* **1985**, *107*, 7476.

CHAPTER II

Synthesis and Binding studies of Bis-Phosphonate Calix[4]pyrroles[I]

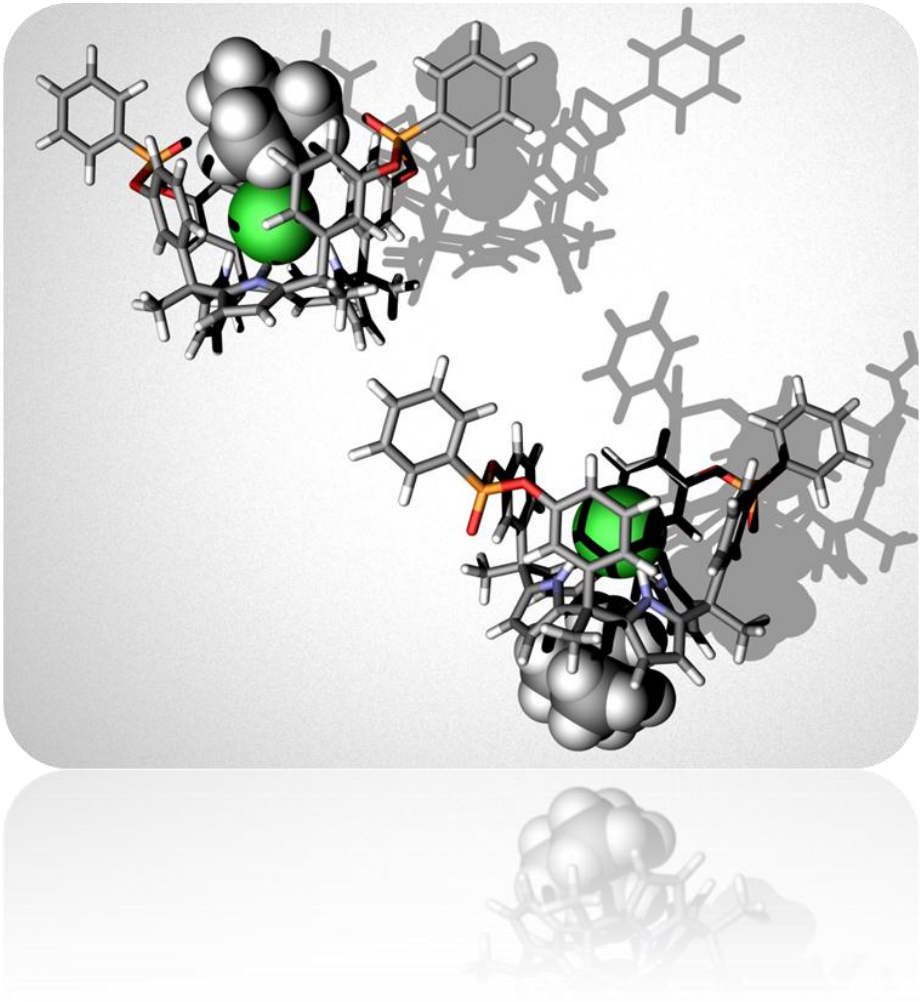

[I] The work presented in this chapter has been published in *J. Am. Chem. Soc.*, **2012**, *134*, 13121.

2. 1 Introduction

Calix[4]pyrroles are a well known class of neutral receptors for selective anion-binding.[1] In the free state, calix[4]pyrrole receptors exhibit different types of conformations i.e. 1,3-alternate and cone.[2,3] Anion binding fixes the calix[4]pyrrole scaffold into the cone conformation.[4] In this conformation, the calix[4]pyrrole unit displays a bowl-shaped cavity delimited by the four pyrrole rings opposite to the bound anion. This shallow and electron-rich aromatic cavity begs for the inclusion of electropositive guests. Aryl-extended calix[4]pyrroles **1** are obtained by substituting each of the four *meso* carbon atoms of the parent octamethyl compound **2** with one aryl group. This substitution results in four possible configurational isomers displaying either a supplementary cavity or a cleft, defined by the fixed aromatic walls.[5] When the *α,α,α,α*-isomers of aryl extended calix[4]pyrroles adopt the cone conformation, the additional deep aromatic cavity is open only at one end. The closed end of the deep aromatic cavity is delimited by four convergent pyrrole NHs (Figure 2.1).

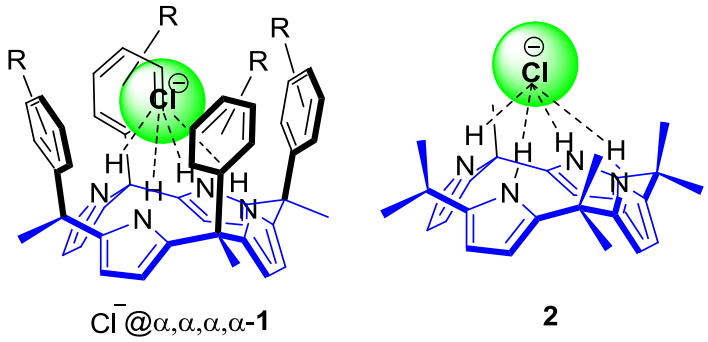

Figure 2.1. Structures of the α,α,α,α-**1**-isomer of aryl-extended calix[4]pyrrole and of the octamethylcalix[4]pyrrole **2** involved in the formation of anonic complexes with chloride.

The size and volume of this *endo* functionalized cavity is large enough to include halides. Similarly to the process described for the parent calix[4]pyrroles, the inclusion/binding of the halide by the *α,α,α,α*-isomer fixes the receptor in the cone conformation inducing the formation of a shallow and electron-rich aromatic cavity opposite to the anion in the negatively charged complex.

Bis-phosphonate bridged cavitands and their tetraphosphonate analogs, derived from resorcin[4]arene are known to be excellent molecular receptors for cationic species such as ammonium[6,7] or methylpyridinium[8,9] or even neutral guests like alcohols.[10,11,12,13] The number of bridging P=O groups, placed at the upper rim of resorcin[4]arene scaffold, in combination with their relative orientation with respect to the aromatic cavity are crucial in defining the binding properties of the receptors. In particular, high stability constants were measured for supramolecular complexes involving intracavity ammonium and methylpyridium guests if complexation occurs through the cooperative effect of several converging and inwardly directed P=O groups. Hydrogen-bonding and/or cation-dipole interactions established by the P=O groups and the included organic cation are assisted by additional cation-π interactions with the aromatic rings of the resorcinarene cavity.

We present here the design of unprecedented ditopic receptors for ion-pair recognition. We combined the known anion binding properties of aryl-extended calix[4]pyrrole receptors **1** with the recognition characteristics displayed by resorcin[4]arene phosphonate cavitands like **3ii** towards alkylammonium cations (Figure 2.2). Our synthetic plan involved the installation of several phosponate groups in the upper rim of an aryl-extended calix[4]pyrrole scaffold. The phosphonate groups would be introduced as bridges between two adjacent *meso*-phenyl substituents similarly to the approach used in the resorcin[4]arene based receptors.[14] The introduction of the phosphonate bridges should preorganize the aromatic cavity of the aryl extended calix[4]pyrrole receptors by reducing the number of potential conformations and providing a cavitand-like structure. We expected that the phosphorylated upper rim installed in the **4ii** diastereoisomer of a calix[4]pyrrole based cavitand and its deep aromatic cavity, functionalized with four convergent pyrrole NHs, could act cooperatively for the selective inclusion of ion-pairs. The resulting ion-paired 1:1 complex was expected to display a preferential *contact* binding arrangement of the ions.

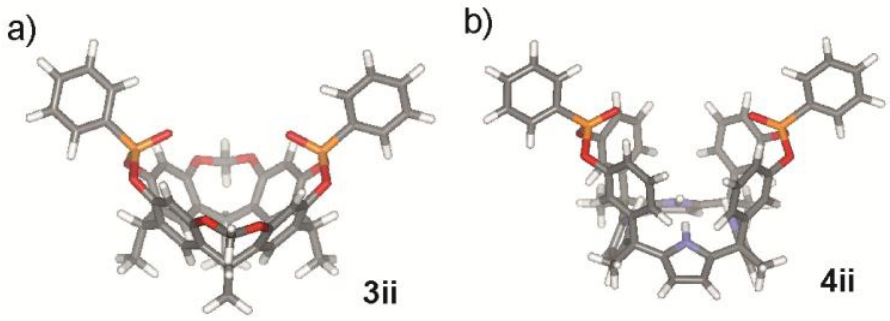

Figure 2.2. Energy minimized structures of two bis-phosphonate cavitands: a) **3ii** designed for the recognition of methylalkylammonium using a calix[4]arene scaffold and b) **4ii**, designed for ion-pair recognition of alkylammonium chloride salts, based on an aryl extended calix[4]pyrrole scaffold.

2. 2 Results and Discussion

We describe here the synthesis of the new family of aryl-extended calix[4]pyrroles **4** with two phoshonate groups as bridging groups in their upper rim. Three stereoisomeric receptors displaying different configurations of the two P=O groups (ii, io, oo where i = in; o = out) have been prepared. We also disclose the binding properties of the three stereoisomers of **4**, both in solution and in the solid state, with several alkylammonium ion-pairs.

2.2. 1 Synthesis

We encountered serious synthetic difficulties in the installation of four phosphonate groups to the upper rim of the known tetramethyl calix[4]pyrrole-resorcinarene hybrid.[15] For this reason, we selected tetrol **1a** as an alternative parent aryl extended calix[4]pyrrole for the installation of only two phosphonate bridging groups.

The original synthetic pathway for the preparation of phosphonate cavitands **4** consisted in a two step procedure already applied in the preparation of phosphonate resorcinarenes (Scheme 2.1).[16,17] First, *α,α,α,α*-**1a** was reacted for 3 hrs at 70 ºC with dichloro(phenyl)phosphine using freshly distilled pyridine as solvent. This reaction is expected to yield di-bridged phenyl-phosphinito cavitands (P-bridge receptors) as a mixture of stereoisomers. The obtained mixture was oxidized "in situ" by addition of a 1:1 solution of hydrogen peroxide and

chloroform to give the corresponding mixture of stereoisomers of *bis*-phosphonate cavitands **4**. Disappointingly, the two step synthetic strategy leaded to the formation of more complex reaction mixtures than the single step protocol. The isolation of pure steroisomers of **4** from that mixture was tedious and very time consuming. In addition, we detected in the two steps reaction crude the presence of thermodynamically highly stable inclusion complexes of pyridine-*N*-oxide with the stereoisomers of **4**. These inclusion complexes even survived column chromatography. Single crystals of the pyridine-*N*-oxide inclusion complex with **4io** suitable for X-ray diffraction grew from acetonitrile solution. The pyridine-*N*-oxide must be produced during the "in situ" oxidation of the phenyl-phosphinito cavitands because we used pyridine as solvent in the first synthetic step. Additional efforts to optimize the two step reaction conditions (less harsh oxidative conditions, use of a bulkier base like 2,6-dimethyl pyridine, addition of a co-solvent) resulted useless.

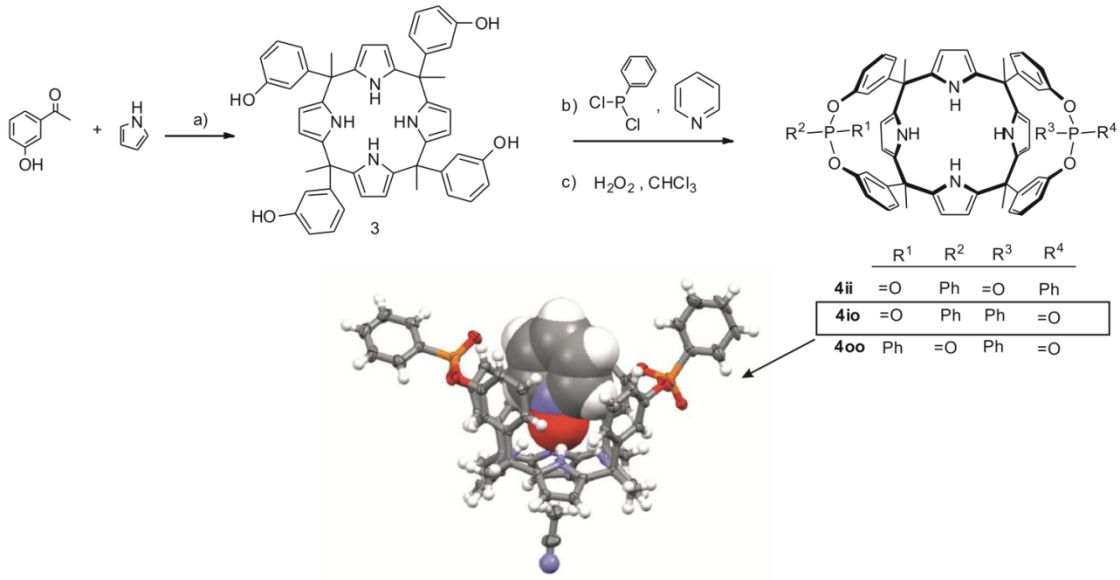

Scheme 2.1. Synthetic scheme for the proposed preparation of bis-phosphonate calix[4]pyrrole receptors and solid state structure of the inclusion complex of pyridine-*N*-oxide (shown in CPK) with the phosphonate stereoisomer **4io**. The inclusion of the *N*-oxide in the deep aromatic cavity induces the receptor to adopt the cone conformation. Note that one molecule of acetonitrile is bound opposite to the included *N*-oxide in the shallow cavity defined by the pyrrole units of the calix[4]pyrrole cone conformation.

Subsequently, the synthesis of the three diastereoisomeric phosphonate cavitand receptors **4** was achieved as depicted in Scheme 2.2.

Bis-Phosphonate Calix[4]pyrroles

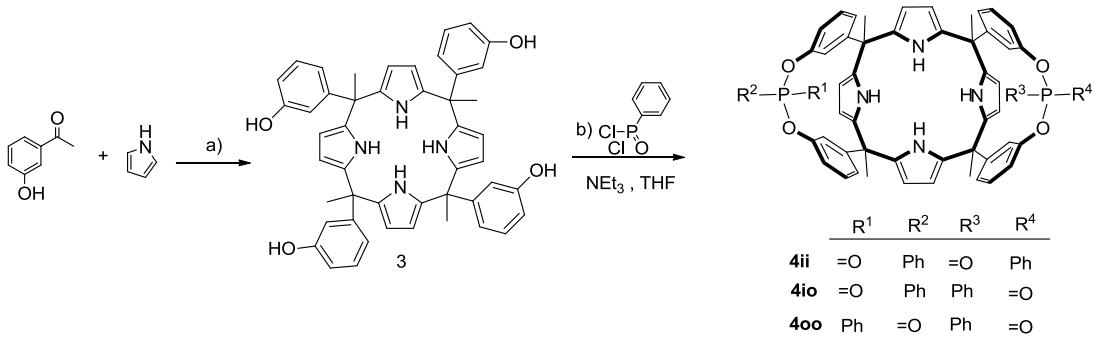

Scheme 2.2. Synthetic scheme for the preparation of bis-phosphonate calix[4]pyrrole receptors 4.

meta-Hydroxyphenylmethylcalix[4]pyrrole **1a** was obtained as a mixture of configurational isomers by condensation of freshly distilled pyrrole with 3-hydroxyacetophenone under acidic conditions following literature procedures.[18] The configurationally pure *α,α,α,α*-**1a** isomer was isolated by crystallization of the mixture of isomers from acetonitrile solution. Room temperature reaction of the *α,α,α,α*-**1a** tetrol and dichloro(phenyl)phosphane oxide[19] in the presence of triethylamine in tetrahydrofuran solution during two hours produced a mixture of the three *bis*-phosphonate stereoisomers **4ii**, **4io** and **4oo**. Each pure steroisomer was isolated by semipreparative HPLC (Spherisorb silica 250 × 20 mm, 5 μm) using DCM:MeOH 99:1 as eluant and crystallized from acetonitrile solution in yields ranging from 10 to 25% (Figure 2. 3).

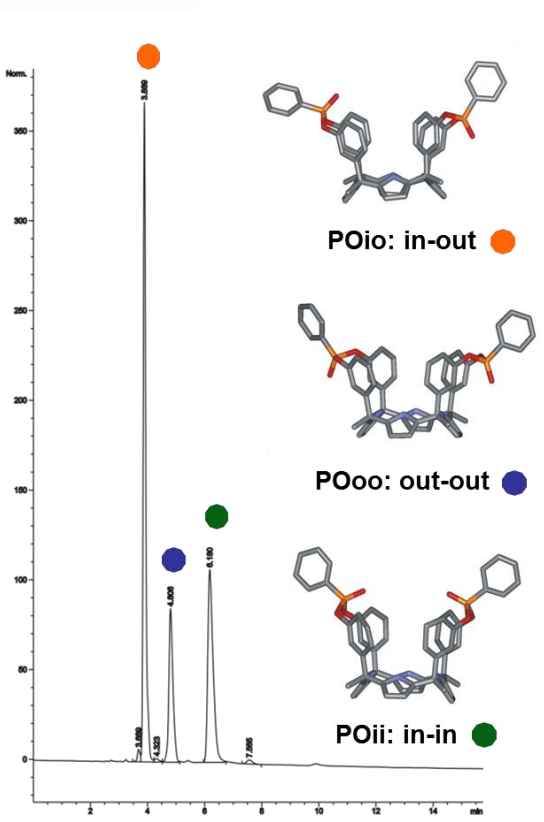

Figure 2. 3 Normal phase - HPLC chromatogram of the three bis-phosphonate stereoisomers separated using DCM : MeOH 99 : 1 as eluent mixture at 19 mL/min.

2.2. 2 Configurational assignment

We performed the configurational assignment of the three diastereoisomers of **4** by a combination of ^{1}H NMR spectroscopy and single crystal X-ray crystallographic analysis. In all cases, the calix[4]pyrrole core adopts the cone conformation with one molecule of acetonitrile included in the deep aromatic cavity and hydrogen bonded to the four pyrrole NHs. In the solid state, the fourteen membered rings delineated by the bridged phosphonate-group, two *meso*-phenyl groups, their corresponding *meso*-carbons and one pyrrole ring showed a preferred conformation in which the phenyl substituent of the phosphorous atoms is directed away from the pyrrole unit. This conformation is observed for all the macrocycles. Receptors **4ii** and **4oo** possess C_{2v} symmetry and showed a reduced number of proton signals in their ^{1}H NMR spectra compared to **4io**. We performed the complete assignment of the signals observed in the ^{1}H NMR spectra of the three stereoisomers by means of 2D experiments. Figure 2.4 shows the downfield region of the ^{1}H NMR spectra of the **4io** stereoisomer having C_s symmetry. Three

broad singlets resonating at δ = 8.29, 8.09, and 7.88 ppm with relative intensities 1:2:1 were assigned to the NH protons. The two pyrrole rings not involved in the 14-member macrocyles display β-pyrrole protons that are chemically non-equivalent (H_f, H_g) and were assigned to the signals resonating at δ= 5.96 and 5.91 ppm. On the contrary, the other two pyrrole rings that are included in the macrocycles although experiencing different magnetic environments have chemically equivalent β-pyrrole protons. We assigned the signals resonating at δ = 6.24 and 6.2 ppm to the β-pyrrole protons H_d and H_e of the pyrrole rings in the macrocycles containing the phosphonate-in and phosphonate-out bridges, respectively. The ^{31}P NMR of **4io** displays two different signals resonating at δ = 15.5 and 13.2 ppm corresponding to the two chemically non-equivalent phosphorus nuclei. The signals of the *ortho*-protons in the two chemically non-equivalent phenyl phosphonate groups show the signs of $^3J_{P\text{-}H}$ (~ 14 Hz) coupling.

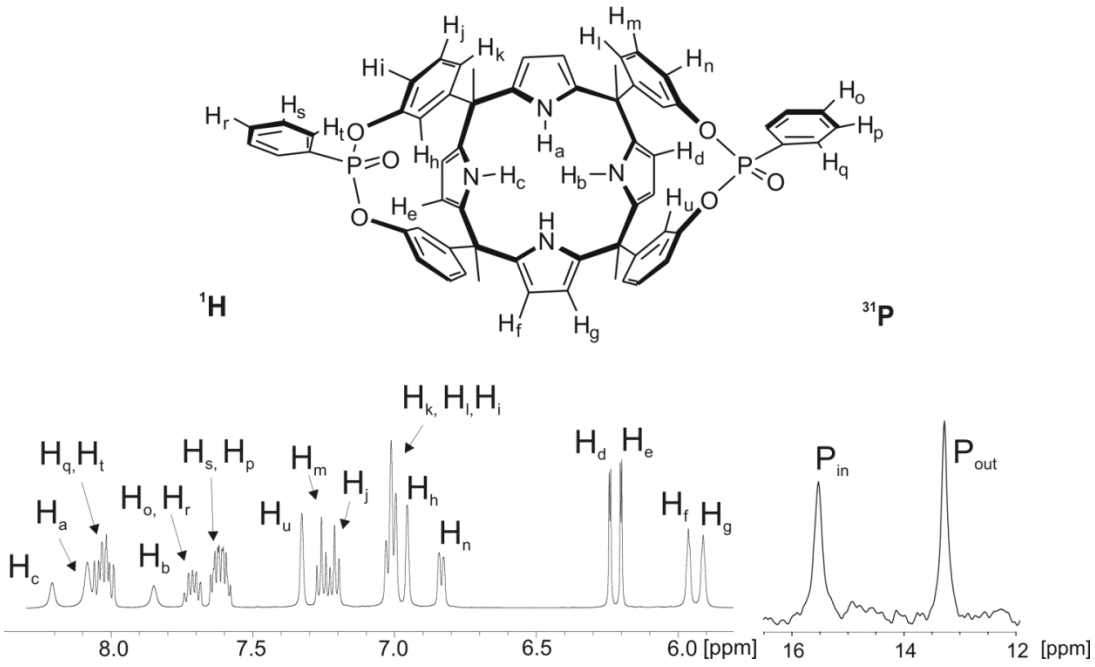

Figure 2.4. Selected downfield region of the ^1H-NMR and ^{31}P-NMR spectra (400 MHz) of the **4io** stereoisomer at 298 K in DCM solution. The proton assignment is shown in the molecular structure of the **4io** receptor represented on top.

In Figure 2.5 is reported the downfield region of the ^1H NMR and the ^{31}P NMR spectra of the **4oo** stereoisomer. Two broad singlets resonating at δ = 8.04 and 7.49 ppm with relative intensities 1:1 were assigned to the NH protons. The two

pyrrole rings not involved in the 14-member macrocyles display chemically equivalent β-pyrrole protons (H_c) and were assigned to the signals resonating at δ = 6.32 ppm. On the contrary, the protons H_d of the other two pyrrole rings resonate at δ = 5.50 ppm. The ^{31}P NMR of **4oo** displays only one signal resonating at δ = 12.5 ppm corresponding to the two chemically equivalent phosphorus nuclei.

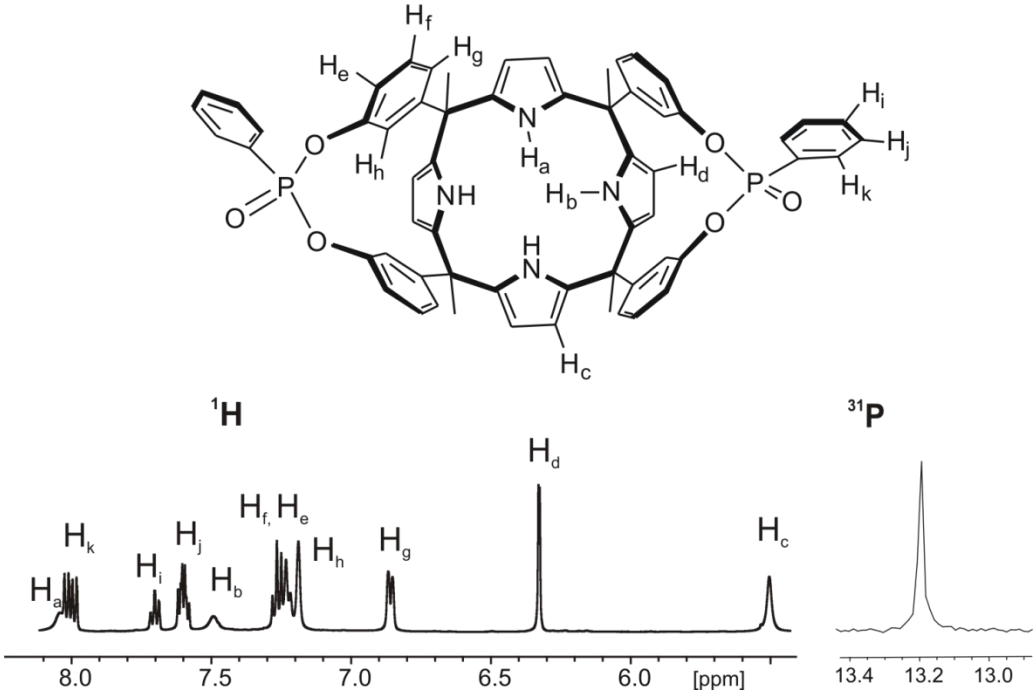

Figure 2.5. Selected downfield region of the ^{1}H-NMR and ^{31}P-NMR spectra (400 MHz) of the **4oo** stereoisomer at 298 K in DCM solution. The proton assignment is shown in the molecular structure of the **4oo** receptor represented on top.

Finally, we report the ^{1}H NMR and the ^{31}P NMR spectra of the **4ii** stereoisomer. Only one singlet resonating at δ = 8.18 ppm is observed for the NH protons. The β-pyrrole protons of the two pyrrole rings not involved in the 14-member macrocyles resonate at δ = 6.17 ppm. On the contrary, the protons H_d resonate at δ = 6.05 ppm. The *meso*-phenyl protons H_h and H_e are shifted upfield at 6.94 and 6.96 ppm respect to the 4oo stereoisomer (H_h = 7.18 ppm and H_e = 7.22 ppm). We attribute this change of chemical shift to the different environment that these protons explore when the oxygens of the phosphonate groups point inside the cavity of the **4ii** isomer. The ^{31}P NMR of **4ii** shows only one signal resonating at δ = 14.64 ppm corresponding to the two chemically equivalent phosphorus nuclei.

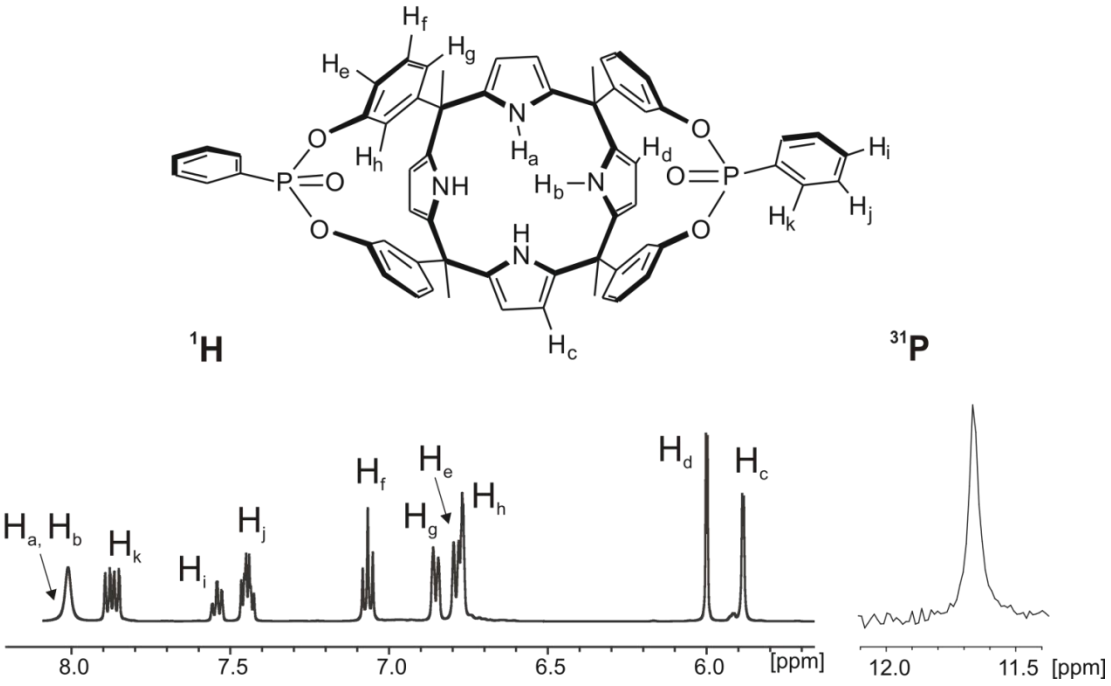

Figure 2.6. Selected downfield region of the ^{1}H-NMR and ^{31}P-NMR spectra (400 MHz) of the **4ii** stereoisomer at 298 K in DCM solution. The proton assignment is shown in the molecular structure of the **4ii** receptor represented on top.

The receptors showed a moderate tendency for aggregation in dichloromethane solution. We performed dilution experiments in the range of 1 mM to 14 mM using ^{1}H NMR spectroscopy. The fit of the chemical shift changes observed for selected signals of the protons to a simple dimerization model allowed us to estimate dimerization constant values of the order 10-50 M^{-1}. We considered the tendency to aggregation (< 10%) observed for these receptors to be negligible at the concentrations (~ 1mM) typically used for the binding experiments. In particular, the fit of the β-pyrrolic protons chemical shift of the **4io** stereoisomer by HyperNMR software allowed us to estimate a constant for the formation of the dimer specie ~ 15 M^{-1}. When the concentration of **4io** is ~ 5mM, that represents the highest concentration at which we performed the experiments, only 13% of dimer is formed in solution. The trimer specie starts to appear at a concentration of **4io** higher than 7 mM with a constant K ~ 100 M^{-1}.

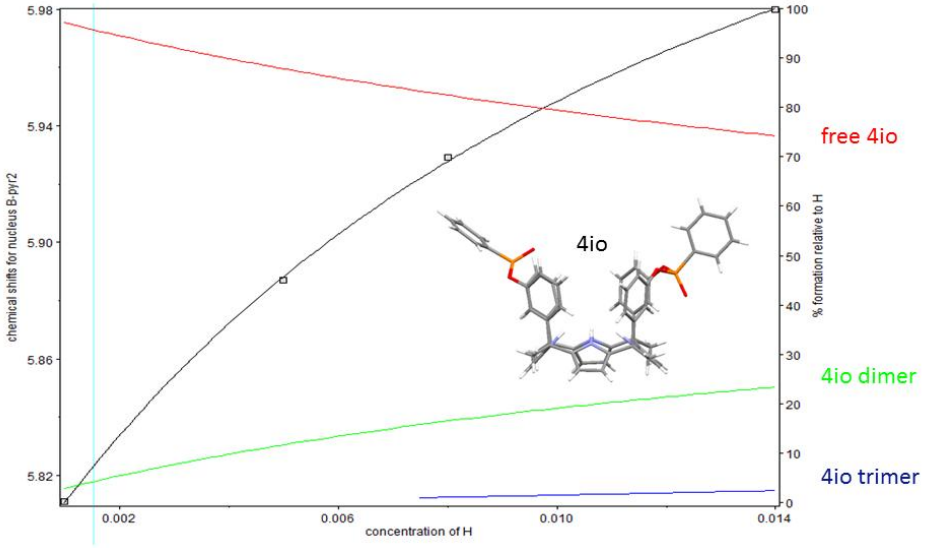

Figure 2.7. Speciation curve of **4io** obtained by fitting the data of ^{1}H NMR dilution experiments.

In the same way, the fit of the β-pyrrolic protons chemical shift of the **4oo** and **4ii** stereoisomers by HyperNMR software revealed that the dimerization process occurs with a constant of ~ 16 M^{-1} and 32 M^{-1}, respectively. At a concentration of receptor of ~ 5mM, only 14% and 20% of dimer is formed in solution. The trimer specie start to appear at a concentration of **4oo** higher than 8 mM with a constant K ~ 100 M^{-1}.

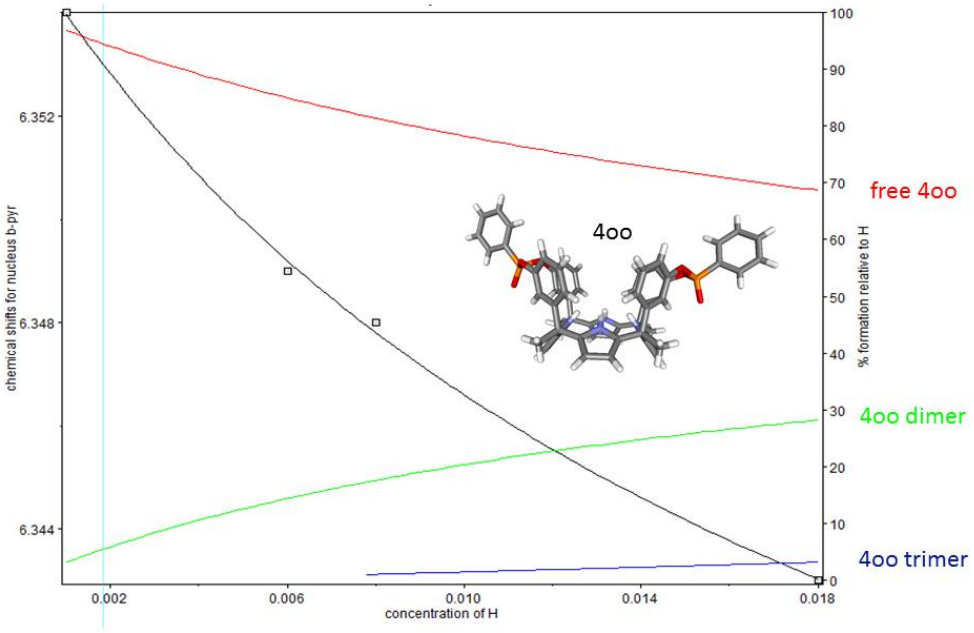

a)

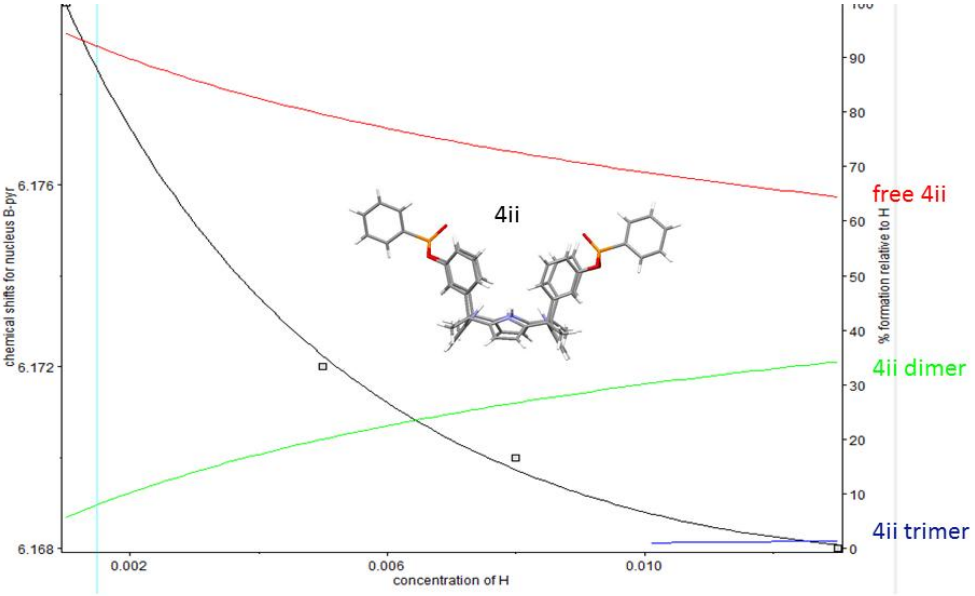

b)

Figure 2.8. On the top: a) Speciation curve of **4oo** obtained by fitting the data of ^{1}H NMR dilution experiments. On the bottom: b) Speciation curve of **4ii** obtained by fitting the data of ^{1}H NMR dilution experiments. At 5 mM of **4ii**, that represent the highest concentration at which we performed the experiments, about 20% of the dimer specie is formed (K ~ 32 M^{-1}). The trimer is formed at a concentration of **4ii** higher than 10 mM (K ~ 1000 M^{-1}).

2.2. 3 Binding studies

Aryl-extended calix[4]pyrrole ***6***

Before undertaking the studies of the binding properties of the series of diastereoisomeric receptors **4** with alkylammonium salts in dichloromethane (DCM) solution, we decided to investigate the complexation of these guests with aryl-extended calix[4]pyrrole **6** (Figure 2.1). The goal of this study was twofold. On the one hand, we wanted to determine or estimate the binding constant values of the complexes formed between more conformationally flexible aryl extended calixpyrrole **6** and the salts in non-polar solvent to be able to use them as references in the forthcoming study of receptors **4**. On the other hand, we were keen to determine the influence that the cation's size exerts on the binding constant values of **6**. Our previous studies with aryl-extended calix[4]pyrrole receptors and chloride quaternary ammonium salts were performed in acetonitrile (ACN) solution and we did not evaluate the cation's size effect with these hosts.[20] It is worth noting that Sessler, Gale, Schmidtchen et al.[21,1] recently described the existence of substantial cation's size modulation effects in the binding affinities of

meso-octamethylcalix[4]pyrrole **2** with alkylphosphonium and alkylammonium chlorides salts in non-polar solvents i.e. DCM.

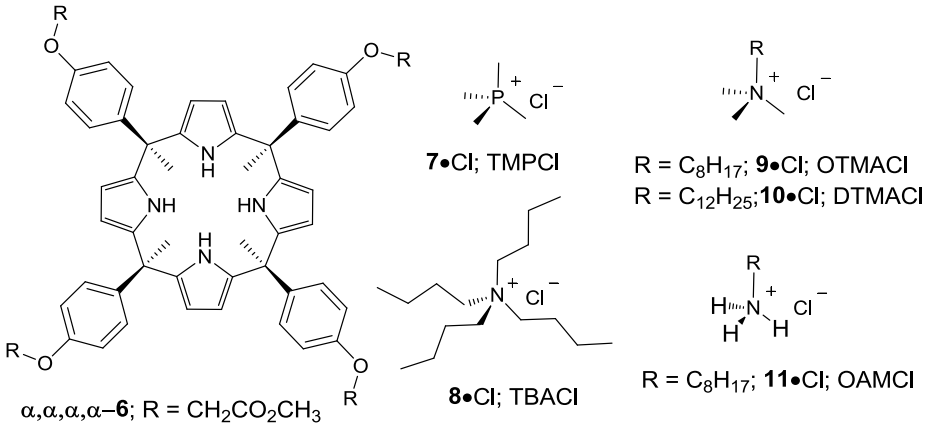

Figure 2.9. Line drawing structures of aryl-extended calix[4]pyrrole **6**, tetramethyl phosphopnium chloride (TMPCl) **7**•Cl, tetrabutylammonium chloride (TBACl) **8**•Cl, octyltrimethylammonium chloride (OTMACl) **9**•Cl, dodecyltrimethylammoniun chloride (DTMACl) **10**•Cl and octylammonium chloride (OAMCl) **11**•Cl.

The addition of less than one equivalent of TMPCl, **7**•Cl, to a 1mM DCM solution of **6** produced separated proton signals for the free and bound receptor. This observation indicated that the chemical exchange between free and bound host is slow on the ^{1}H NMR timescale. Similar exchange dynamics were observed in the complexation of chloride with closely related aryl-extended calix[4]pyrrole receptors in ACN solution.[20] We determined the stoichiometry of the formed complex as 1:1 and estimated an association constant value ($K_{a,exp}$) larger than 10^4 M^{-1} because in the presence of one equivalent of TMPCl only the signals for the bound receptor were detected in the ^{1}H-NMR spectrum of the mixture. The inclusion of the chloride in the deep aromatic cavity of **6** was evidenced by the observation of a strong downfield shift in the signal of the NH protons and moderate upfield shifts for the phenyl protons of the bound receptor.

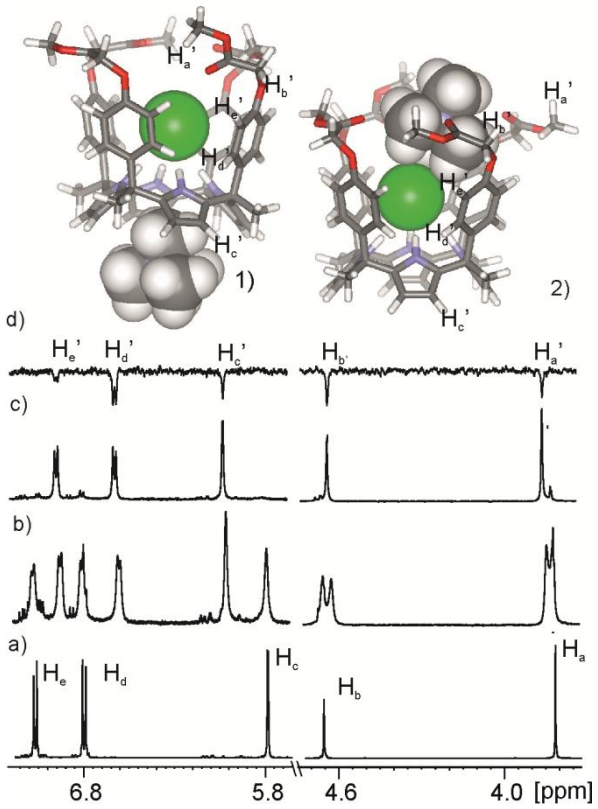

Figure 2.10. Sections of the ^{1}H-NMR spectra acquired during the titration of **6** with TMPCl: a) 0 equivalents; b) 0.5 equivalents; c) 1 equivalent; d) GOESY experiment with selective excitation of the signal of the methyl protons of TMP of c. Top: Proposed binding geometries for the ion-paired TMPCl@**6** complex in DCM solution 1) ion-separated, 2) close contact.

Because we were working in a non-polar solvent (DCM), we considered that the 1:1 complex should have an ion-paired nature. Evidence of the concomitant complexation of the cation could be inferred from the upfield shift experienced by the signal of the methyl groups of TMP. To map out the preferred location of the TMP cation in the solution binding geometry of the 1:1 complex, TMPCl@**6**, we performed GOESY (gradient enhanced nuclear Overhauser effect spectroscopy) experiments (Figure 2.10 d). Selective irradiation of the signal of the methyl groups of bound TMP produced inverted signals for several protons of the bound receptor. This result is indicative of the existence of intermolecular contacts between the protons of TMP and the receptor due to their close spatial proximity in the complex. In particular, the negative NOE observed for the β-pyrrole protons and the *meso*-methyl groups suggested the placement of the TMP cation in the shallow, electron rich aromatic cavity defined by the four pyrrole rings opposite to the included anion. Likewise, irradiation of the signal for the *meso*-methyl protons

of **6** induced a weak but detectable negative intermolecular NOE peak to the TMP protons. Taken together, these results gave support to a putative binding geometry for the 1:1 ion-paired complex in DCM solution exhibiting an ion-pair separated arrangement (Figure 2.10 - 1). However, the same GOESY experiment also revealed the existence of intermolecular NOEs between the TMP protons and the signals of the methyl and α-methylene protons of the ester groups of **6**. These intermolecular contacts suggested that, in solution, the TMP cation might also be complexed, to a certain extent, close to the COOMe groups of **6** (ion-dipole interactions and CH···O hydrogen bonds). Based on the latter result, we propose an additional binding geometry in solution for the 1:1 complex. In this alternative geometry the ion-pair displays a *close-contact* or intimate arrangement of the ions, both being included in the deep aromatic cavity of receptor **6** (Figure 2.10 - 2). Unfortunately, the relative proportion of the two proposed binding geometries for the 1:1 complex, which probably co-exist in solution, cannot be exactly determined from the results obtained in the GOESY experiment.

In striking contrast with the observations presented above, the addition of one equivalent of TBACl, **8**•Cl, to a 1 mM solution of **6** in DCM did not produce noticeable changes in the chemical shift values of the proton signals of the aryl-extended calix[4]pyrrole receptor. In particular, the ^{1}H NMR titration of a 14.6 mM solution of **6** with incremental amount of TBACl showed fast exchange dynamics for most of the protons of the host. The titration data were fitted by HyperNMR software to a 1:1 binding model affording a $K_{a,exp} = 1 \pm 0.2 \times 10^{1}$ M^{-1}. We report in Figure 2.11 the speciation curves corresponding to the titration. After addition of 10 equivalents of TBACl, only 35% of host is present as complex (blue curve), while the missing 75% is still free (green curve).

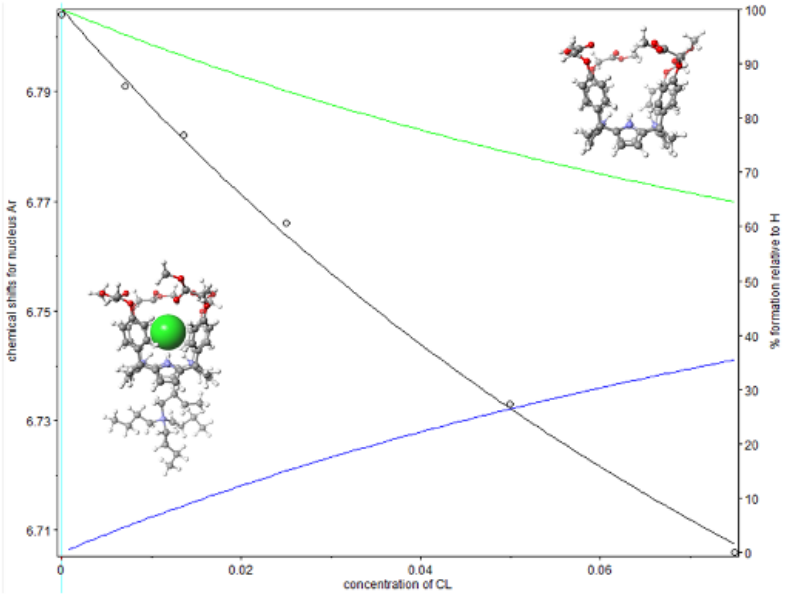

Figure 2.11. Plot of the chemical shift changes experienced by the signal of the aromatic proton Hc at δ = 6.8 ppm in the meso-phenyl substituent of [**6**] = 14.6 mM (black circles) upon titration with incremental amounts of TBACl.

This finding indicated that in DCM solution the binding affinity of receptor **6** for TBACl is strongly reduced compared to TMPCl. As mentioned above, Sessler, Gale, Schmidtchen et al. already noticed strong counter cation-effects in the complexation of **2** with ammonium salts. They reported association constants values of the order of 10^5 M^{-1} and 10^2 M^{-1} for the complexes of **2** with OTMACl and TBACl, respectively. A likely explanation for this significant counter-cation effect was put forward by the same authors suggesting a stepwise binding mechanism, whereby the calix[4]pyrrole receptor **2** binds the chloride anion initially to form a cone-conformation 1:1 complex with an electron-rich bowl-shaped cavity opposed to the bound chloride. The formed 1:1 anionic complex subsequently interacts with the cation to yield an ion-paired complex (Scheme 2.3).

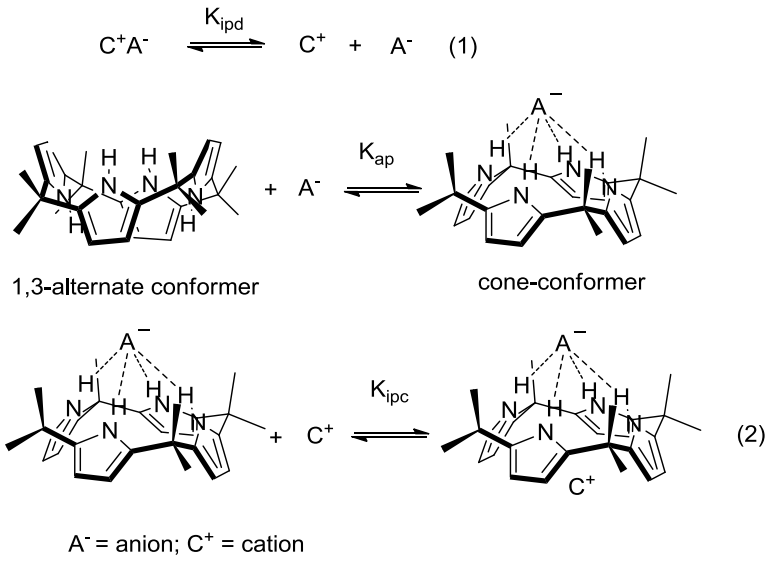

Scheme 2.3. Proposed equilibria involved in the solution binding of ion-pair salts in low dielectric constant solvents with ditopic receptor meso-octamethylcalix[4]pyrrole **2**.

The magnitude of the latter cation complexation is strongly dependent on the match between the cavity and the cation's size. In DCM solution strong ion pairing is expected for both the organic salt and the 1:1 complex. The assumption that relatively large cations are more prone to dissociation in non-polar DCM solution, thus increasing the available concentration of free anion proved to be inconsistent with the reported data and also with the results described here.

A mathematical treatment of the equilibria involved in the complexation of ionic species in low dielectric constant media by neutral guest, which explicitly considers both ion pairing processes (1) and (2) has been reported and validated experimentally.[22] The study demonstrated that the existence of ion-pairing processes in solution provokes that the experimentally determined values in the form of $K_{a,exp}$ (3) are concentration dependent. For this reason, the application of the complete equilibrium treatment requires the determination of $K_{a,exp}$ values in different range of concentrations. In this and the following sections of the chapter, we do not explicitly consider in the calculation of the reported association constant values the ion-pair dissociation equilibrium of the salt (1) or the ion-pairing equilibrium yielding the neutral 1:1 complex (2).[23] We were restricted by the solubility of the receptors and the sensitivity of ^{1}H NMR spectroscopy to use a reduced range of concentrations for our investigations. For this reason and as

frequently encountered in literature, the values reported here for the association constant in DCM solutions correspond to experimental binding constant, $K_{a,exp}$, of the form:

$$H\ (host) + C^+A^- = H \bullet C^+A^- ;\ K_{a,exp} = [H \bullet C^+A^-]/\ [H]\ [C^+A^-]\ \text{in}\ M^{-1}\ \text{units}\ (3)$$

This treatment implicitly assumes that the salt ion-pair is the active component and that the complex is fully ion-paired (an equivalent expression applies when both the guest salt and the complex are 100% dissociated (see solvent effect), however, is quite improbable in low dielectric constant solvent).

*Bis-phosphonate calix[4]pyrroles **4***

The interaction of the three stereoisomers of **4** with TMPCl, **7**•Cl, was probed in DCM solution using ^{1}H NMR and ^{31}P NMR titrations. We initially focused in the evaluation of the binding properties featured by the stereoisomer **4ii**, specifically designed to function as a ditopic receptor for TMPCl. Nevertheless, we also considered the binding properties of the other two stereisomers **4oo** and **4io** with TMPCl. These two latter hosts were very useful in teaching us basic lessons on the fundamental nature of the interactions driving ion-pair recognition with bis-phosphonate calix[4]pyrrole receptors **4**. The three stereomeric caviatnds **4** are readily soluble in DCM. Titration experiments were performed by sequentially adding 0.5 and 1 equivalent of TMPCl to NMR tubes containing individual DCM solutions of each stereoisomer. The initial addition of 0.5 equivalents of TMPCl to **4ii** induced the appearance of a new set of proton signals in the ^{1}H NMR spectrum of the mixture and two new phosphorous signals in its ^{31}P NMR spectrum. The new signals in the ^{31}P NMR spectrum were assigned to the phosphorous atoms of bound **4ii** (broad, δ = 12.9 ppm) and the phosphorous atom of TMP (δ = 24.3 ppm) involved in the TMP**C**l@**4ii** complex. The phosphorous atoms of free **4ii** and free TMP**C**l resonated at δ = 14.6 ppm and δ = 26.9 ppm, respectively. In turn, the new set of proton signals was assigned to the protons of the bound receptor in the TMPCl@**4ii** complex. The integral ratio of proton signals for the free and bound **4ii** was 1:1. The signals of the bound pyrrole NHs experienced significant downfield shifts ($\Delta\delta$ > 3.5 ppm) as a result of their involvement in the formation of hydrogen

bonds with the included chloride. One of the signals of the β-pyrrole protons and all the signals of the aromatic protons of the *meso*-phenyl substituents of **4ii** also experienced noticeable upfield shifts in the bound receptor. On the contrary, the signals of the phenyl-phosphonate protons were almost unaffected (Figure 2.12).

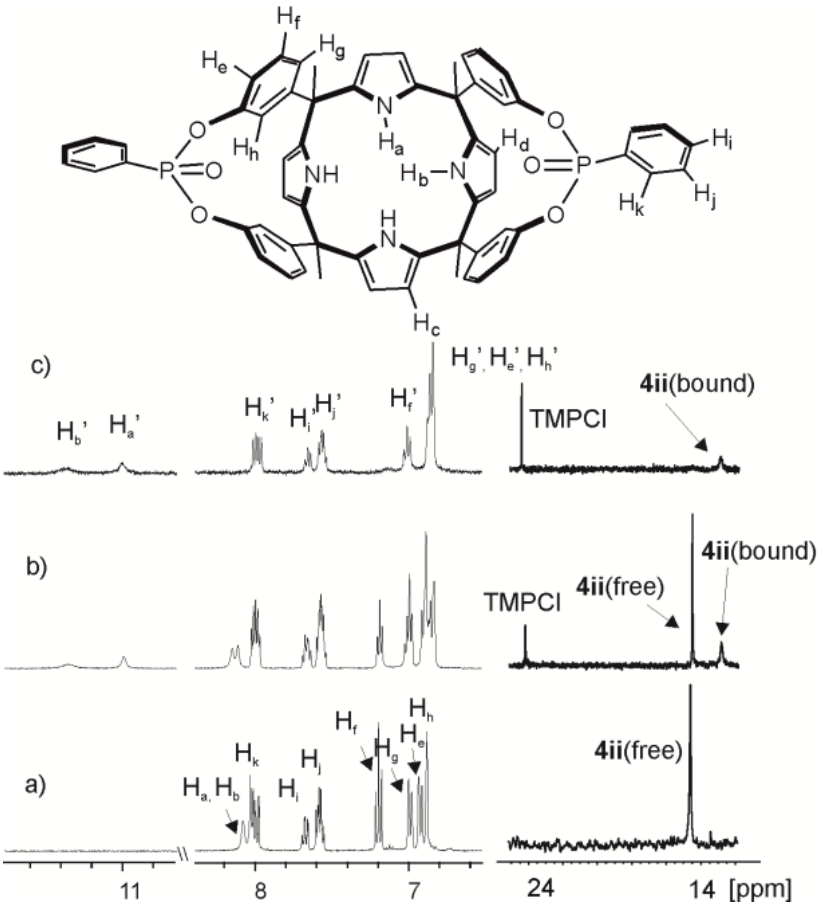

Figure 2.12. Selected regions of the ^{1}H and ^{31}P NMR spectra acquired during the titration of **4ii** with ClTMP: a) 0 equivalents; b) 0.5 equivalents; and c) 1 equivalent added.

Taken together, these observations suggested the existence of a conformational change of the calix[4]pyrrole core in the free **4ii**, probably from 1,3-alternate to cone, induced by complexation with TMPCl. The observation of separate proton signals for the free and bound receptor **4ii** indicated that the chemical exchange between them is slow on the ^{1}H NMR timescale. We had observed a similar exchange dynamics with aryl extended calix[4]pyrrole **6**. In addition, the signal of the methyl protons of the TMP cation experienced a significant upfield shift (δ = 1.16 ppm; $\Delta\delta$ = - 1.01 ppm). The addition of one equivalent of TMPCl induced the

exclusive observation of the signals assigned to the proton and phosphorous atoms in the TMPCl@**4ii** complex. This results indicated that the value of the experimental association constant, $K_{a,exp}$, for the TMPCl@**4ii** complex is higher than 10^4 M^{-1} and cannot be measured accurately by ^1H NMR titrations. When more than 1 equivalent of TMPCl was added the chemical shifts of the proton signals of the bound **4ii** receptor were not affected, however, the proton signal of the methyl groups of TMP cation and its phosphorous atom shifted downfield. This observation was indicative of the existence of a fast exchange on the ^1H NMR timescale between free and bound TMP cations. The observation of different exchange dynamics between free and bound receptor and between free and bound cation pointed to the existence of two different exchange processes. Due to the inclusion of the anion in the deep aromatic cavity of **4ii**, the chemical exchange between free and bound host requires a conformational change of the calix[4]pyrrole core.[24] Conversely, the chemical exchange between free and bound TMP cation can occur without this requirement. The TMP cation is located at the periphery of the anionic inclusion complex, either close to the phosphonato groups of the upper rim or partially included in the shallow aromatic cavity distal to the bound anion that is defined by the pyrrole rings of the calix[4]pyrrole core in cone conformation. A 2D ROESY experiment carried out in the sample containing 1 equivalent of TMPCl revealed the existence of negative cross peaks between the doublet of the methyl protons of TMP and the aromatic *para* protons (H_e) of the *meso*-phenyl substituent pointing towards the upper rim of the receptor. The existence of such intermolecular close-contact testified for the preferred location of the TMP cation close to the upper rim and the inwardly directed phosphonato groups of **4ii**, experiencing both cation-dipole with the phosphonate groups and charge-charge interactions with the included chloride. We concluded that the preferred binding geometry of the TMPCl@**4ii** complex in solution is that of a *close-contact* ion-pair arrangement.

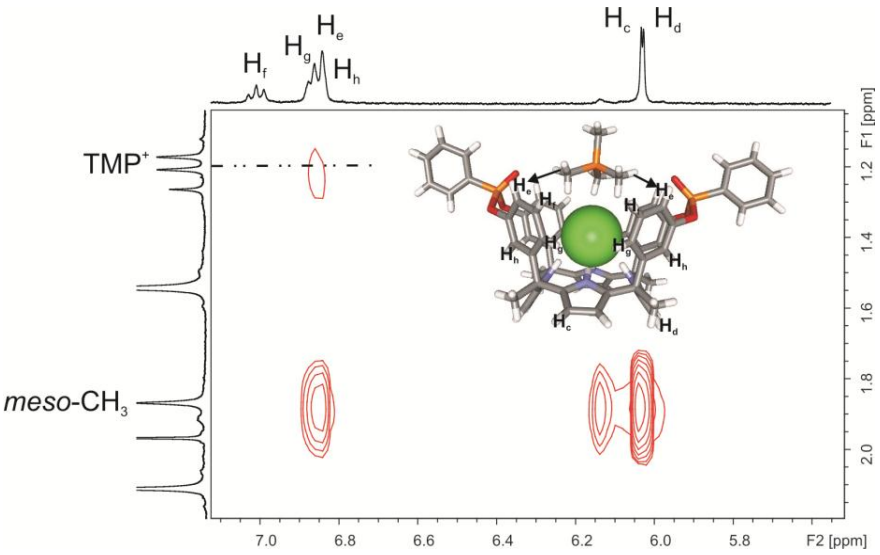

Figure 2.13. Selected region of a 2D-ROESY experiment performed on a 4.6 mM dichloromethane solution of **4ii** containing 0.9 equivalents of TMPCl.

Single crystals of the TMPCl@**4ii** complex suitable for X-ray diffraction were grown from dichloromethane solution. The binding geometry proposed in solution is supported by the formation of the *endo*-cavity anionic complex TMPCl@**4ii** in the solid state. Unfortunately, the packing of the crystal showed the formation of a columnar motif of TMPCl@**4ii** complexes and did not provide an unambiguous response to the preferred placement of the TMP cation with respect of the anion in the solid-state (Figure 2.14).

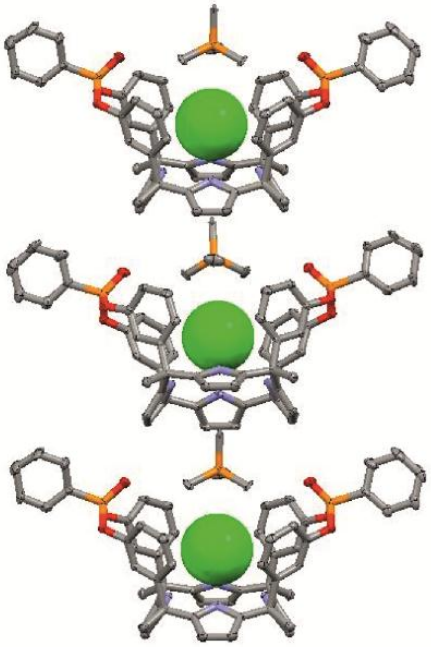

Figure 2.14. Section of the crystal packing of the TMPCl@**4ii** complex. The columnar arrangement of the TMPCl@**4ii** complex does not allow distinguishing the preferred charge neutralization with the TMP cation located in the upper rim or in the shallow aromatic opposite to the included anion. For clarity, hydrogen atoms and solvent molecules are removed.

The general dynamics and thermodynamics trends observed in the NMR titrations of stereoisomer **4io** and **4oo** with TMPCl paralleled those described above for **4ii**. It is worth noting, however, that when 0.5 or 1 equivalents of TMPCl are added to 1 mM dichloromethane solutions of **4io** and **4oo** the chemical shift value of the signal corresponding to the methyl groups the TMP cation is noticeably upfield shifted ($\delta \approx 0.67$ ppm; $\Delta\delta = -1.5$ ppm) compared to the one registered in the case of **4ii** ($\delta = 1.16$ ppm; $\Delta\delta = -1.01$ ppm) as shown in Figure 2.15.

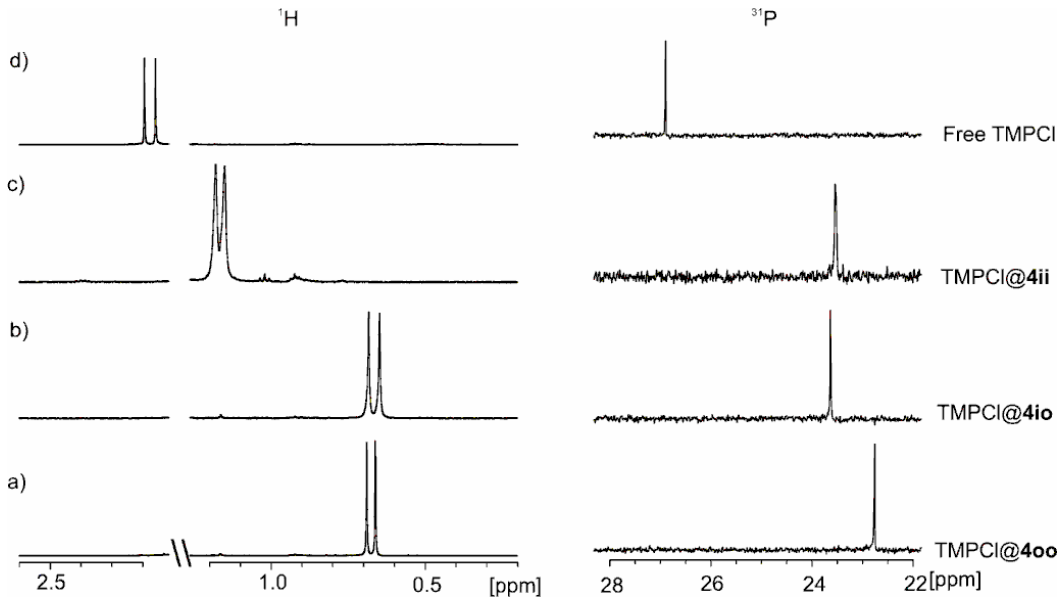

Figure 2.15. Selected regions of the ^{1}H-NMR and ^{31}P-NMR spectra of a 4.6 mM dichloromethane solution of a) **4oo**, b) **4io** and c) **4ii** with 0.5 equivalents of TMPCl added, d) free TMPCl.

2D ROESY experiments performed on equimolar dichloromethane solutions of the receptors **4io** or **4oo** with TMPCl displayed intense cross-peaks between the signal of the methyl protons of TMP and the signals of the β-pyrrole protons of the receptors (Figure 2.16). The observed intermolecular NOE cross-peak between the protons of TMP^{+} and the β-pyrrolic protons (Hd', Hc') of bound **4oo** indicate that the cation is preferentially located in the calix[4]pyrrole cup opposite to the bound chloride. For the **4io** receptor a much weaker cross peak was also spotted between the signals of TMP and the *para* aromatic proton in two of the *meso*-phenyl substituents, indicating that placement of the cation within the ion-paired complex can take place in two possible binding sites.

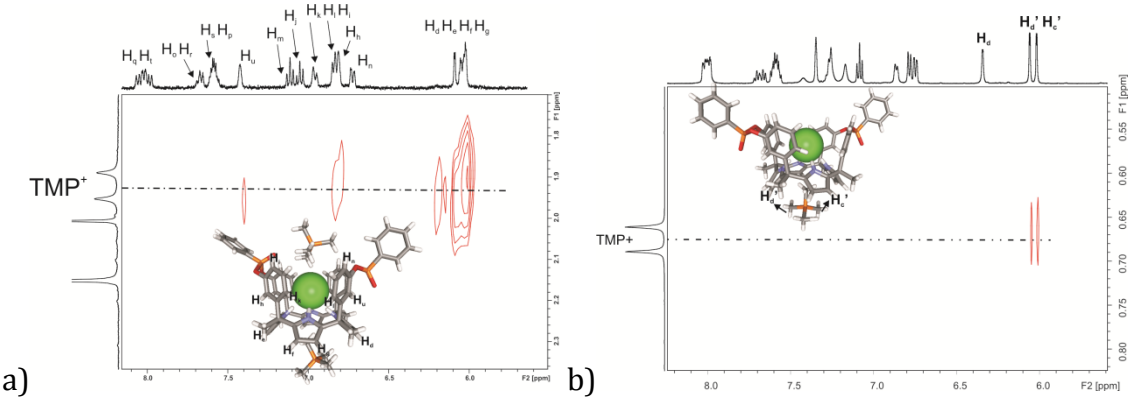

a) b)

Figure 2.16. Selected region of a 2D-ROESY experiment performed on a 4.6 mM dichloromethane solution of: a) **4io** with 1.0 equivalents of TMPCl. b) Selected region of the 2D-ROESY experiment performed on a 4.6 mM dichloromethane solution of **4oo** with 0.5 equivalents of TMPCl.

Taken together, these results suggested that, in solution, for the 1:1 complexes TMPCl@**4oo** and TMPCl@**4io** the TMP cation is preferentially located in the shallow aromatic cavity defined by the pyrrole rings stabilized by cation-π interactions. In the specific case of the TMPCl@**4io** complex, the binding geometry locating the TMP in the upper rim close to the inwardly directed phosphonato group was also detected. In short, the energetically favoured binding geometries for the complexes TMPCl@**4io** and TMPCl@**4oo** in solution displayed an ion-pair *separated* arrangement. The formation of chloride *endo* cavity complexes with **4oo** and **4io** receptors in solution was supported by the structures of the complexes obtained in the solid-state. Disappointingly, the columnar motif displayed by the packing of the crystals of the complexes TMPCl@**4oo** and TMPCl@**4io** was not conclusive in resolving the issue of the preferred placement of the TMP cation also in the solid state (Figure 2.17).

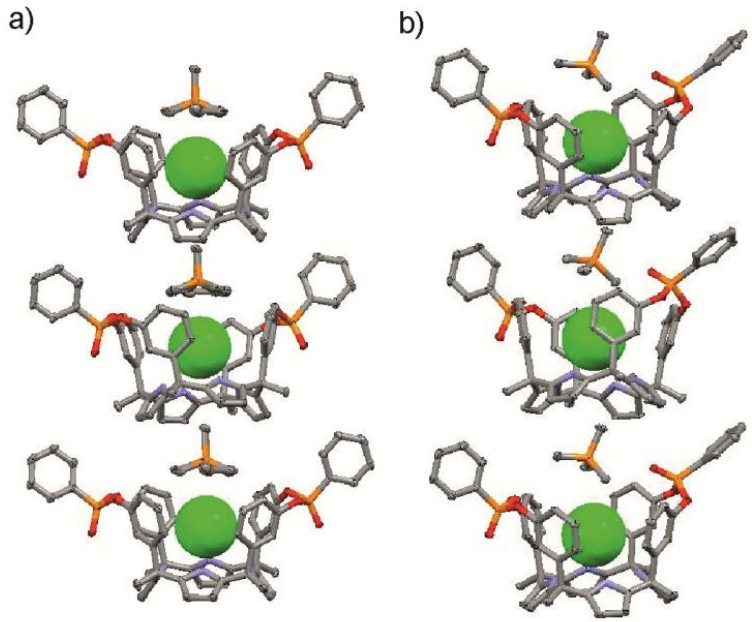

Figure 2.17. Sections of the crystal packing of the: a) TMPCl@**4oo** complex and b) TMPCl@**4io**. For clarity, hydrogen atoms and solvent molecules are removed. Chloride is shown as CPK model.

The results of ^{1}H and ^{31}P titration experiments performed between the series of receptors **4** and methyl pyridinium chloride as guest parallel the observations made for TMPCl.

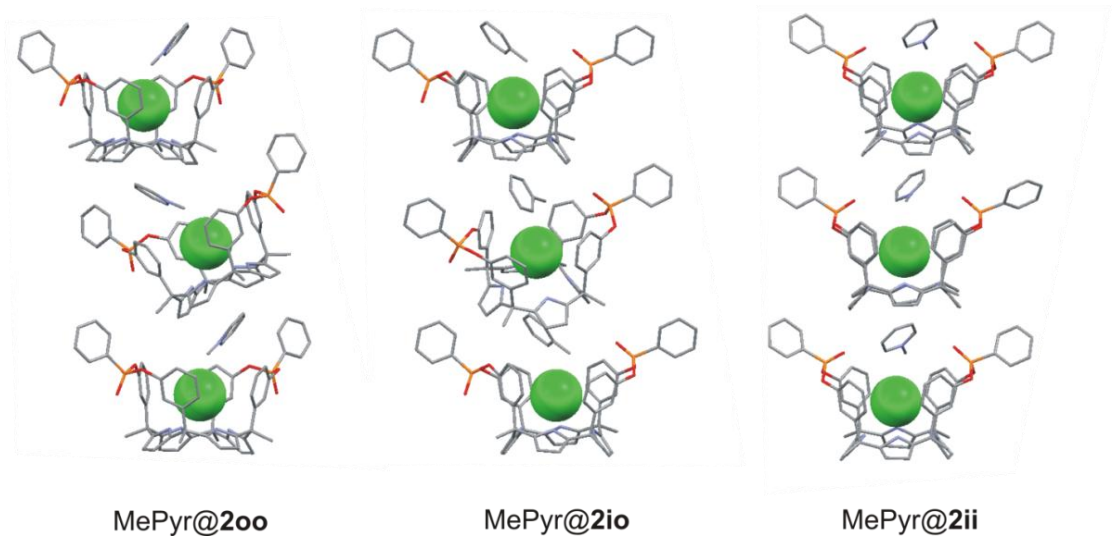

Figure 2.18. Sections of the crystal packing of the MethylPyridiniumChloride@**4oo,** MethylPyridiniumChloride@**4io** and MethylPyridiniumChloride@**4ii**. For clarity, hydrogen atoms and solvent molecules are removed. Chloride is shown as CPK model.

The inclusion complexes formed in solution were supported by the obtained solid-state structures. The columnar motifs displayed by the complexes in the packing of

the crystals did not help in clarifying an unambiguous placement of the cation in the complexes (Figure 2.18).

The ditopic character of **4oo** was also evidenced in ESI-MS experiments of a solution containing TMPCl. We used negative and positive detection modes with capillary voltages form 0-500 V. We observed ion-peaks at m/z 1019 corresponding to the anionic complex Cl^-@**4oo** in negative ESI.

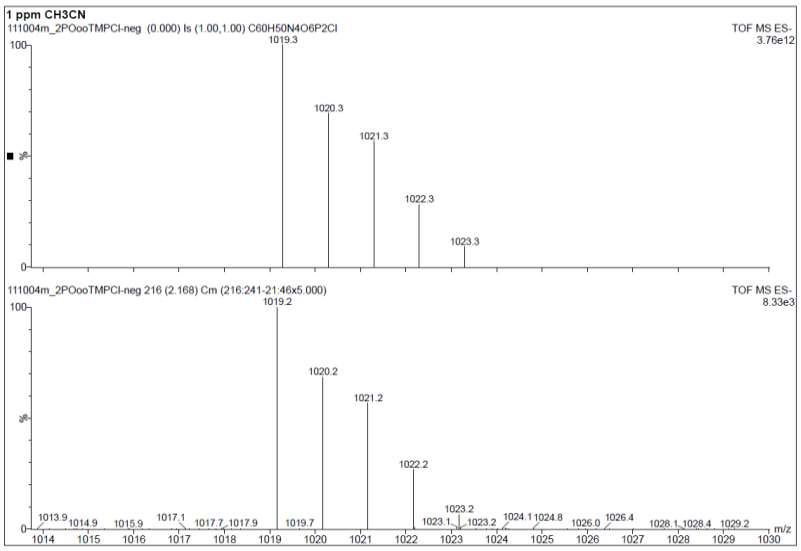

Figure 2.19. Negative ESI-MS Expansion at 5000V (at the bottom) and calculated isotopic distribution (on the top) for the ion peak with m/z 1019.2 corresponding to the anionic complex **4oo**@Cl^- obtained by spraying a solution containing the **4oo** stereoisomer and TMPCl.

While in positive ESI we detected the peak at m/z 1075 corresponding to the cationic complex TMP^+@**4oo.**

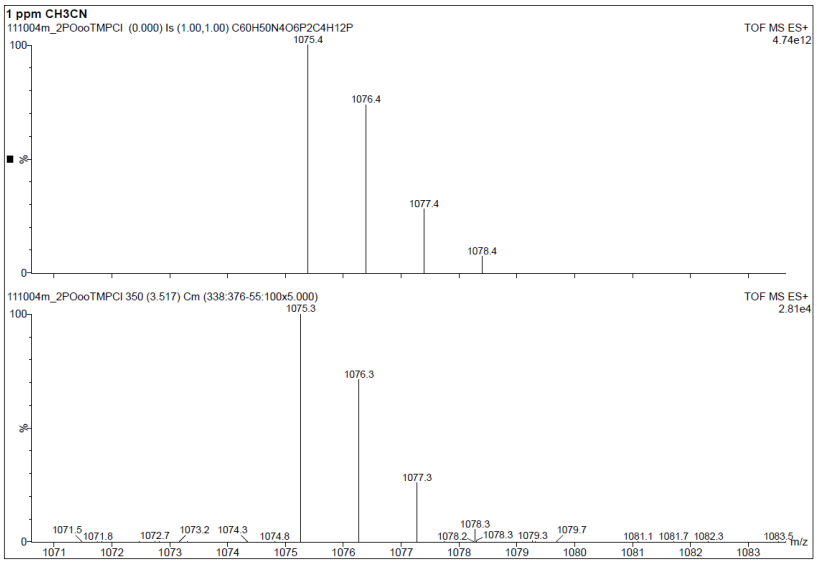

Figure 2.20. Positive ESI-MS Expansion at 5000V (at the bottom) and calculated isotopic distribution (on the top) for the ion peak with m/z 1075.3 corresponding to the cationic complex **4oo**@TMP$^+$ obtained by spraying a solution containing the **4oo** stereoisomer and TMPCl.

In order to rank the magnitudes of the binding affinities of receptor series **4** with TMPCl, we performed pairwise competitive binding experiments. We prepared ~1 mM solutions containing a close to equimolar mixture of two bis-phosphonate receptors and TMPCl in deuterated dichloromethane. The extent of chloride complexation attained by each receptor in the solution was assessed using ^{1}H and ^{31}P NMR spectroscopy. As commented above, the interaction of receptors **4** with chloride induced a considerable downfield shift of the NH proton signals. The NH protons in chloride-bound receptors **4** resonated in the region of 10-12 ppm completely separated from the rest. In any combination of two receptors, we observed two different sets of signals corresponding to the NH protons hydrogen bonded to chloride in each one of the TMPCl@**4** complex (Figure 2.21). In the aromatic region of the ^{1}H NMR spectra of the mixtures, we also could identify separate signals for some protons in the free and bound state of both receptors. In addition, the ^{31}P NMR spectra of all solution mixtures displayed different signals for the phosphorus atoms of the two receptors, both in the free and bound state. The integral areas of selected proton signals for each receptor, in both free and bound state, were used to calculate the ratio of association constant values for the two TMPCl@**4** complexes present in the pairwise competitive experiments by means of the following equation (4):

$$K_{a,exp}(\text{TMPCl@}\mathbf{4xx})/K_{a,exp}(\text{TMPCl@}\mathbf{4yy}) =$$
$$(\text{FB}(\mathbf{4xx})/\text{FB}(\mathbf{4yy})) \times (\text{FF}(\mathbf{4yy})/\text{FF}(\mathbf{4xx})) \quad (4)$$

FF= fraction free; FB= fraction bound

Because of uneven NOE enhancements of the signals by decoupling and long longitudinal relaxation times, the ^{31}P NMR spectra of the mixtures were only used to qualitatively corroborate the relative extent in which the two TMPCl complexes were formed in solution that we derived from the ^{1}H NMR analysis of the mixture. We measured that Ka,exp(TMPCl@**4oo**) is approximately four-fold larger than Ka,exp(TMPCl@**4ii**) and that Ka,exp(TMPCl@**4io**) is two-fold larger than to Ka,exp(TMPCl@**4ii**). Consequently, Ka,exp(TMPCl@**4oo**) must be close to 2-fold larger than Ka,exp(TMPCl@**4io**). The presumed ratio of constants was also confirmed experimentally by a direct pairwise competition experiment between **4oo** and **4io**. In short, the experimentally measured order of binding affinities for the receptor series **4** towards ClTMP is as follows: Ka,exp(TMPCl@**4oo**) ≈ 2 × Ka,exp(TMPCl@4**io**) ≈ 4 × Ka,exp(TMPCl@**4ii**).

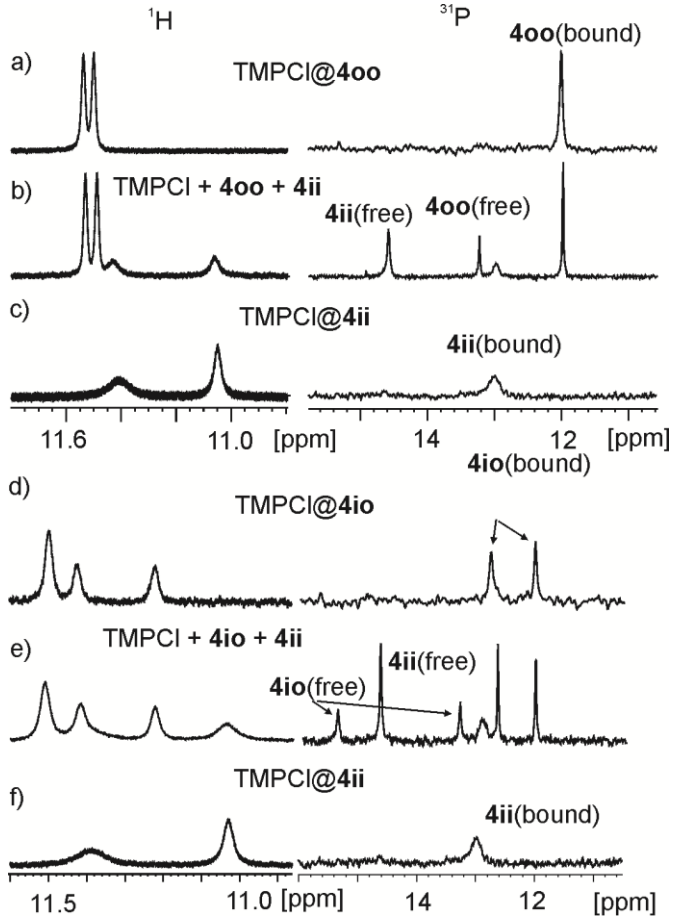

Figure 2.21. Selected regions of the ^{1}H and ^{31}P NMR spectra of: a) TMPCl@**4oo**, b) TMPCl + **4oo** + **4ii**, c) TMPCl@**4ii**, d) TMPCl@**4io**, e) TMPCl + **4io** + **4ii**, and f) TMPCl@**4ii**.

This result was completely unexpected for us. In fact our expectations were completely opposite. We thought that the **4ii** stereoisomer capable of binding the ion-pair of the salt in a *close contact* arrangement and providing stabilizing cation-dipole and CH···O interactions to the bound TMP moiety when located close to the upper rim should afford the more energetically favourable 1:1 complex, probably followed by the steroisomer **4io**. We rationalized the experimentally measured order of binding affinities of the receptor series **4** towards TMPCl by invoking an stepwise binding mechanism, as previously proposed for octamethyl calix[4]pyrrole receptor **2**. In the case at hand, however, we surmise that the magnitude of the initial binding of the chloride anion to form the 1:1 anionic complex is strongly dependent on the spatial orientation of the phosphonate bridging groups. The subsequent complexation of the TMP cation and its placement within the ion-paired 1:1 complex, which is indeed mandated by the

spatial arrangement of the phosphonate groups of the steroisomeric receptor *vide supra*, provided an almost constant energetic contribution to the overall binding. In the **4ii** stereoisomer the two oxygen atoms of the phosphonate groups are pointing inwardly with respect to the deep cavity in which the chloride is included. Most likely, the existence of repulsive electrostatic interactions between the partial negative charges of the inwardly directed oxygen atoms of the phosphonate groups and their dipoles with the included chloride is responsible for the energetic disadvantage of TMPCl@**4ii** complex with respect to TMPCl@**4oo** and TMPCl@**4io**. The orientation of the dipole moment of the phosphonate groups changes substantially on the basis of the molecular structure of stereoisomers **4**. In this sense, for the **4io a**and **4ii** stereoisomers one or the two negative ends of the dipoles assigned to the phosphonate groups, respectively, point towards the included chloride. However, for the **4oo** stereoisomer is the positive end of both dipole moments of the phosphonate groups that are directed towards the included chloride. Isothermal titration calorimetry (ITC) experiments allowed to quantify the magnitudes of the binding constants for the receptor series **4** with TMPCl in DCM solution. From the results of these experiments we were also able to determine the thermochemical data for the complexation. In general, the binding processes showed a reduced heat release (heat *vs* time). We obtained a good fit for the integrated heat to a theoretical binding isotherm corresponding to the formation of a 1:1 complex. The inflection point of the sigmoideal binding isotherms coincides with a molar ratio value close to 1. The obtained trend and ratio of the determined binding affinity values are in complete agreement with the results obtained in the pairwise competitive experiments that were analyzed by ^{1}H NMR spectroscopy ($K_{a,exp}$(TMPCl@**4oo**)= 8 ± 1 × 10^5 M^{-1}; ΔG = – 8.0 kcal/mol; ΔH = – 3.3 kcal/mol; TΔH = – 4.7 kcal/mol; $K_{a,exp}$(TMPCl@**4io**) = 5 ± 1 × 10^5 M^{-1}; ΔG = – 7.7 kcal/mol; ΔH = – 3.1 kcal/mol; TΔH = – 4.6 kcal/mol; $K_{a,exp}$(TMPCl@**4ii**) = 2 ± 0.5 × 10^5 M^{-1}; ΔG = – 7.2 kcal/mol; ΔH = – 1.9 kcal/mol; TΔH = – 5.3 kcal/mol). All processes were both enthalpically and entropically driven. The strong and favourable entropic component measured for all complexation processes suggests that solvation/desolvation effects must play a crucial role.

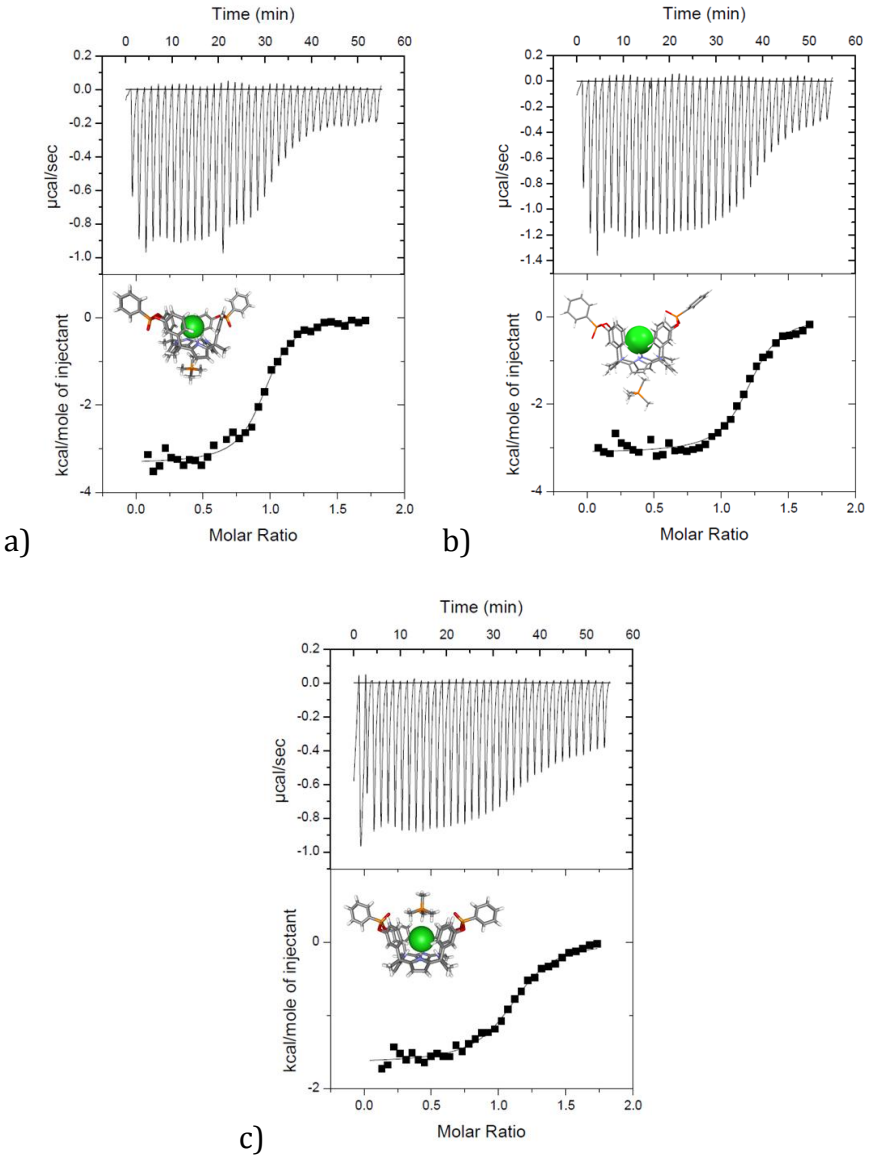

Figure 2.22. Raw data and binding isotherm for the ITC titration of a) TMPCl into **4oo**, b) TMPCl into **4io** and c) TMPCl into **4ii**. The titrations were performed in dichloromethane at 25°C. The enthalpy of binding for each injection is plotted against the ratio of concentrations of TMPCl/**4**.

Counter-ion effect

As commented above, we also wanted to evaluate the effect that the size of the cation present in the ion-pair of the chloride salt used as guest produced on the absolute and relative binding affinities with the receptor series. For this reason, we investigated the complexation properties of the receptor series **4** with two additional chloride salts: 1-dodecyltrimethylammonium chloride, **10**•Cl, DTMACl and tetrabutylammonium chloride **8**•Cl, TBACl. The results of the binding experiments with receptor series **4** and DTMACl (dynamics, thermodynamics and

complex geometries) were analogous to the ones we described above for TMPCl. By means of pairwise competitive binding experiments we determined the following relationship of binding constants for DTMACl as guest: $K_{a,exp}$(DTMACl@**4oo**) ≈ 2 × $K_{a,exp}$(DTMACl@**4io**) ≈ 4 × $K_{a,exp}$(DTMACl@**4ii**). The analogy of the results obtained with DTMACl and TMPCl as guests indicated that although the two cations of these salts have different sizes both can be similarly accommodated in the cationic binding pockets of the receptors. That is, if the DTMA cation directs the long alkyl chain away from the binding pockets of the receptor it becomes almost equal in size and shape to the TMP cation.[25] Due to statistical effects, however, we surmise that the complexes of receptors **4** with TMPCl should be slightly more stable thermodynamically than with DTMACl.

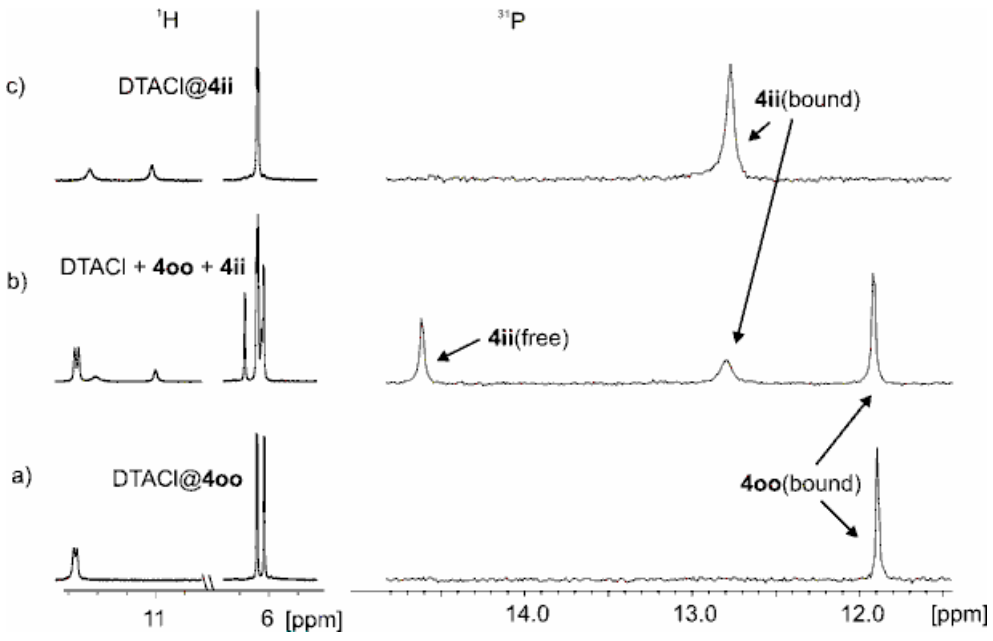

1)

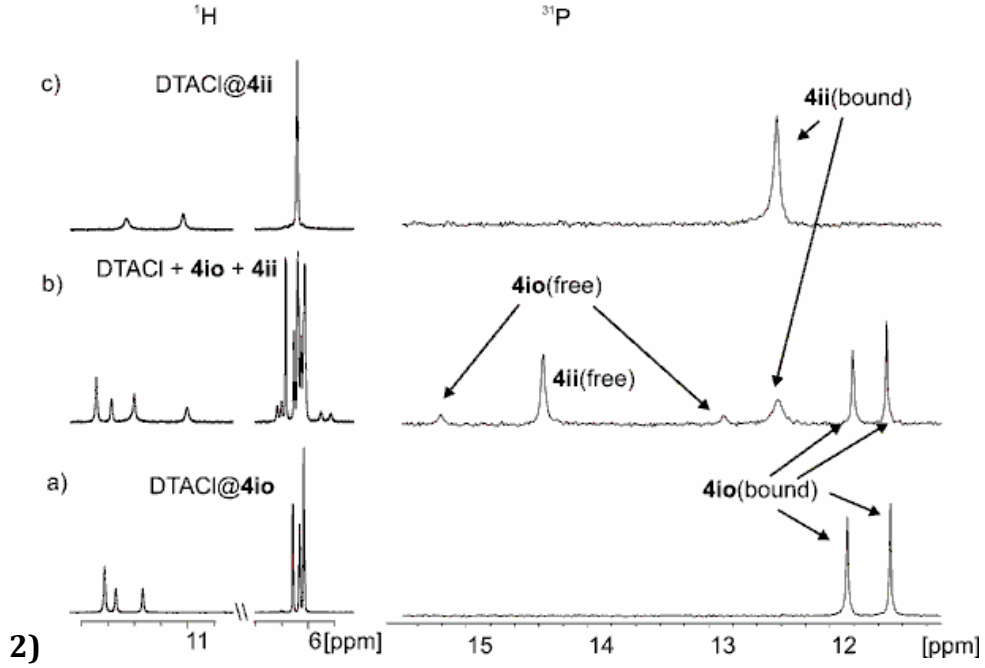

Figure 2.23. Selected regions of the ^{1}H-NMR and ^{31}P-NMR spectra in DCM-d_2 solutions of: 1 a) DTACl@**4oo**, b) an equimolar mixture of DTACl + **4oo** + **4ii**, c) DTACl@**4ii**; 2) a) DTACl@**4io**, b) an equimolar mixture of DTACl + **4io** + **4ii**, c) DTACl@**4ii**.

The results obtained in the complexation experiments of the receptor series **4** with TBACl are worth to be commented in more detail. Addition of 0.5 equivalent of TBACl to separated 1 mM deuterated dichloromethane solutions of the three stereoisomers produced the appearance of diagnostic signals of complex formation, in the corresponding ^{1}H NMR spectra of the mixtures. For the three cases, the exchange dynamics of the complexation processes were slow/intermediate on the ^{1}H NMR timescale. We observed separated signals for some protons in the free and bound receptors and broadening of other proton signals. Integration of selected proton signals for free and bound receptor after addition of 1 equivalent of TBACl, allowed us to estimate that the binding constants $K_{a,exp}$ for TBACl@**4oo** is in the order of 10^4 M^{-1}. 2D ROESY experiment shows NOEs between the α and β protons of TBA^+ with the *β*-pyrrolic protons (H_d) of bound **4oo** indicate that the cation is located in the cup of the calix[4]pyrrole opposite to the bound anion.

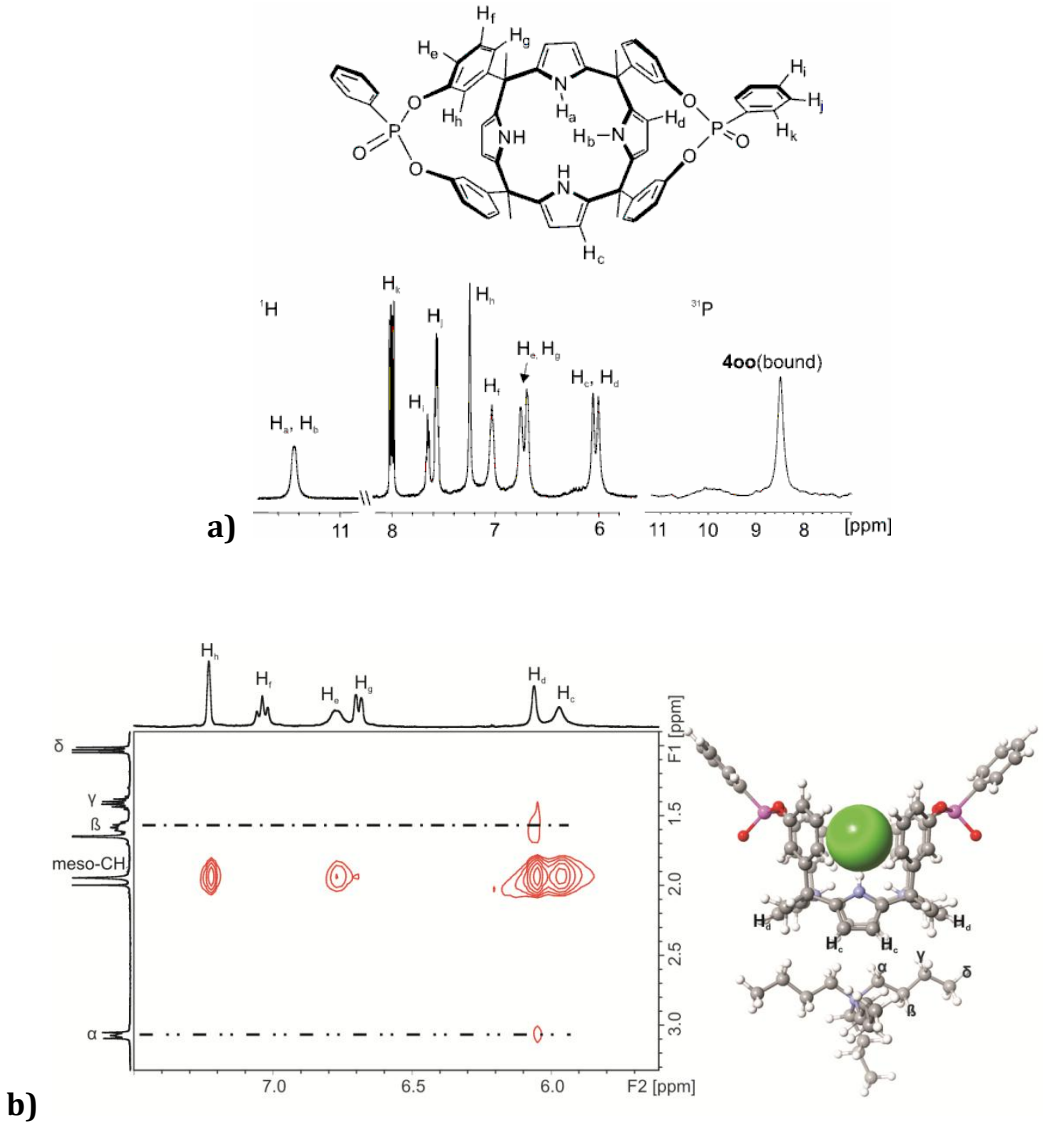

Figure 2.24. a) Selected regions of the ^{1}H-NMR and ^{31}P-NMR spectra of a 3.45 mM solution of **4oo** in DCM- d_2 after addition of 0.95 equivalents of TBACl and b) 2D-ROESY experiment. The CAChe energy minimized structure of TBACl@**4oo** is shown at the right.

Conversely, the addition of 1 equivalent of TBACl to the solution of **4ii** induced the formation of the 1:1 complex TBACl@**4ii** to a much reduced extent, $K_{a,exp}$(TBACl@**4ii**) ≈ 5±1 × 10^2 M^{-1}. 2D ROESY experiments reveal no NOE cross peaks between the protons of TBA^+ and the signals of **4ii**.

Bis-Phosphonate Calix[4]pyrroles

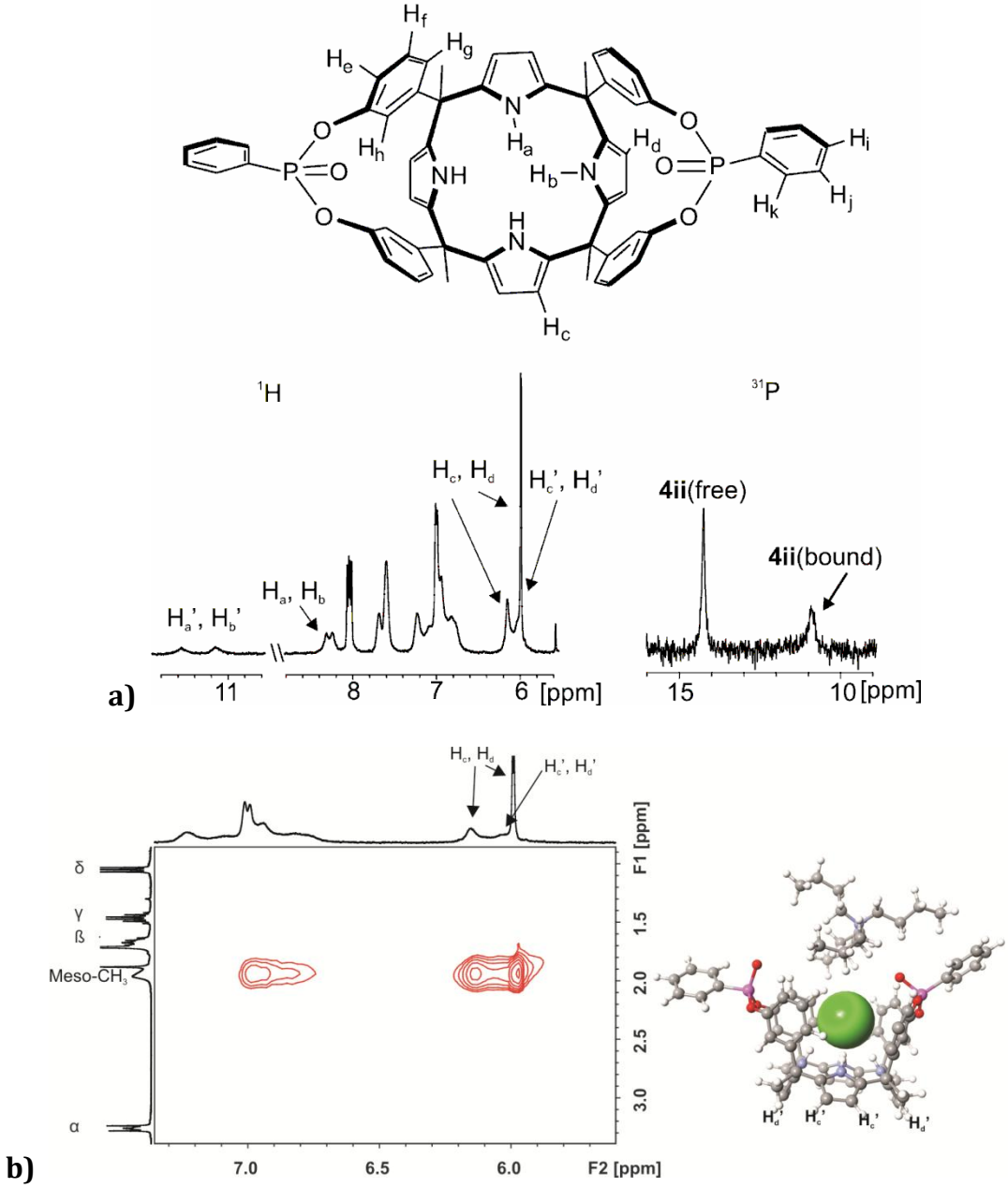

Figure 2. 25 a) Selected regions of the ^{1}H-NMR ^{31}P-NMR spectra of a 3.0 mM DCM-d_2 solution of **4ii** after addition of 1.0 equivalents of TBACl in dichloromethane. b) 2D-ROESY experiment performed on a 3.6 mM dichloromethane-d_2 solution of **4ii** with 1.2 equivalents of TBACl.

While the $K_{a,exp}$ for TBACl@**4io** had a value of 2 ± 0.5 × 10^3 M^{-1}. In this case, the 2D-ROESY experiment shows NOEs between the α and β protons of TBA^+ with the *β*-pyrrolic protons (H_d) of bound **4io** indicating that the cation is located in the cup of the calix[4]pyrrole opposite to the bound anion.

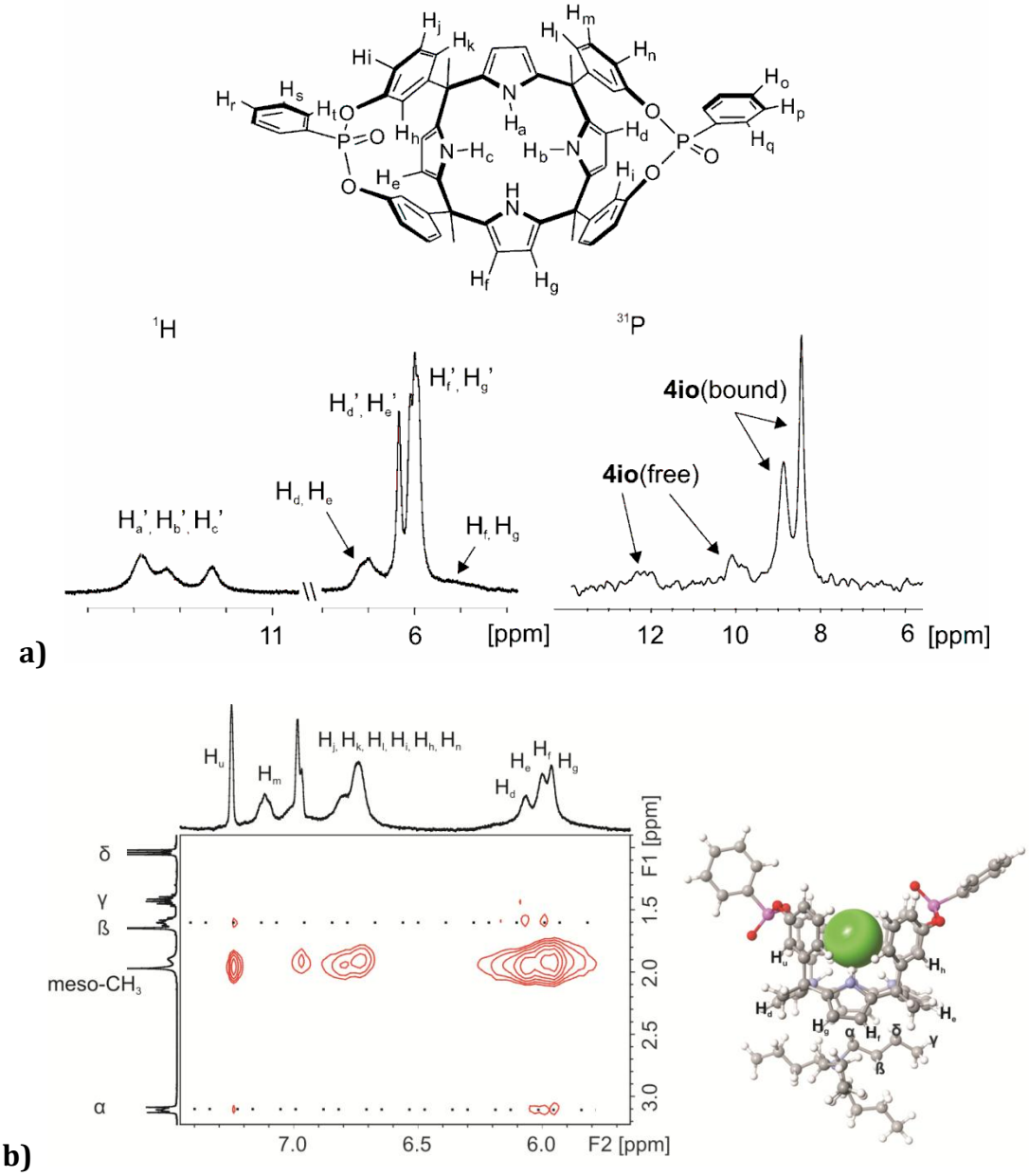

Figure 2.26 . (a) Selected regions of the ^{1}H-NMR and ^{31}P-NMR spectra of a 3.45 mM solution of **4io** in DCM-d_2 solution after addition of 1.0 equivalent of TBACl and (b) 2D-ROESY experiment. The CAChe energy minimized structure of TBACl@**4io** is shown at the right.

We performed a pairwise competitive experiment between receptors **4oo** and **4io** with TBACl (Figure 2.27) demonstrating the superior binding affinity of **4oo** for this salt ($K_{a,exp}$(TBACl@**4oo**)/$K_{a,exp}$(TBACl@**4io**) ≈ 5) in order to understand the reason of the different binding strength in the two hosts. These results demonstrated that the general trend in binding affinities determined above for the receptor series **4** with TMPCl and DTMACl was also maintained for the TBACl. However, the magnitude of the binding affinities of **4ii** and **4io** towards TBACl

were significantly reduced compared to those estimated for TMPCl and DTMACl. Most likely, the mismatch that exists between the size of the TBA cation and that of the receptor's binding sites significantly reduced the energetics of complexation.

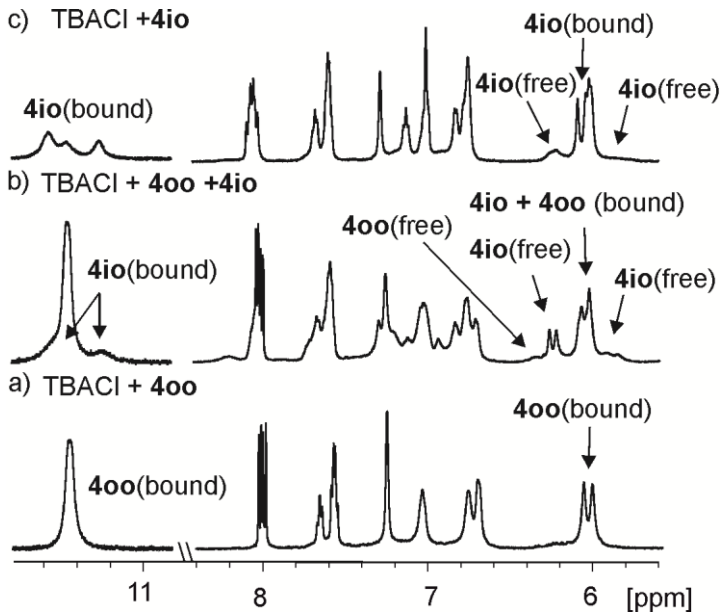

Figure 2.27. Selected regions of the ^{1}H spectra of: a) TBACl + **4oo**, b) TBACl + **4oo** + **4io** and c) TBACl + **4io**.

Remarkably, the magnitude of the binding affinity featured by the phosphonate receptor **4oo** towards TBACl was three and two orders of magnitude larger than those determined for the more conformationally flexible aryl-extended calix[4]pyrrole **6** and the *meso*-octamethylcalix[4]pyrrole **2**, respectively.

2.2.4 Conformational and Electrostatic factors influencing the complexation process of receptor 4oo with ion-pair salts.

In an attempt to dissect the electrostatic and conformational rigidity contributions provided by the phosphonate groups of the **4oo** receptor to the overall binding energy of the TMPCl salt, we also determined the binding properties of the synthesized cavitand calix[4]pyrrole **5** towards this salt. The comparison of the binding properties exhibited by **5** with those of **4oo** should reveal the effect provided mainly by the electrostatic factors of the phosphonate groups to the ion-pair binding.

Bis-methylene bridged cavitand **5** was synthesized from the reaction of *α,α,α,α*-**1a** tetrol with dibromomethane using dry potassium carbonate as base in dry DMSO solution heated to 80˚C for 3 hours. The pure compound **5** was isolated in 10% yield using semipreparative reverse-phase HPLC. The presence of two methylene bridges in the upper rim of **5** endorsed this cavitand with a conformational rigidity similar to that of the phosphonate receptor series **4**.

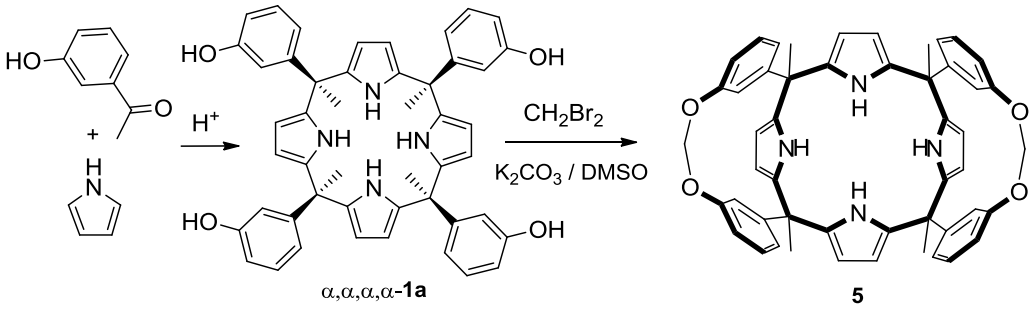

Figure 2.28. Synthetic schemes for the preparations of **5** from precursor **1a**.

Bis-methylene bridged host **5** formed a 1:1 complex with TMPCl in deuterated DCM for which we could estimate, using 1H NMR titrations, a binding affinity constant value Ka,exp(ClTMP@**5**) > 1 × 10^4 M^{-1}. We observed slow exchange dynamics for the binding process. The signal of methyl protons of bound TMP cation resonate at δ = 0.67 ppm suggesting its inclusion in the shallow aromatic cavity provided by the pyrrole rings in cone conformation that is distal to the bound chloride. In the downfield region of the ^{1}H NMR spectrum of the ClTMP@**5** complex, we detected two signals for the pyrrole NH protons hydrogen bonded to the chloride resonating at δ = 11.62 and 11.20 ppm. We performed competitive pairwise binding experiments involving receptors **6**, **4oo** and **5** with TMPCl in DCM solution. The ratio of the integrals for selected signals of the protons in the free and bound receptors and the application of equation (1) allowed us to derive the following relationship for the stability constants values of the complexes Ka,exp(TMPCl@**4oo**) ≈ 10 × Ka,exp(TMPCl@**5**) ≈ 40 × Ka,exp(TMPCl@**6**).

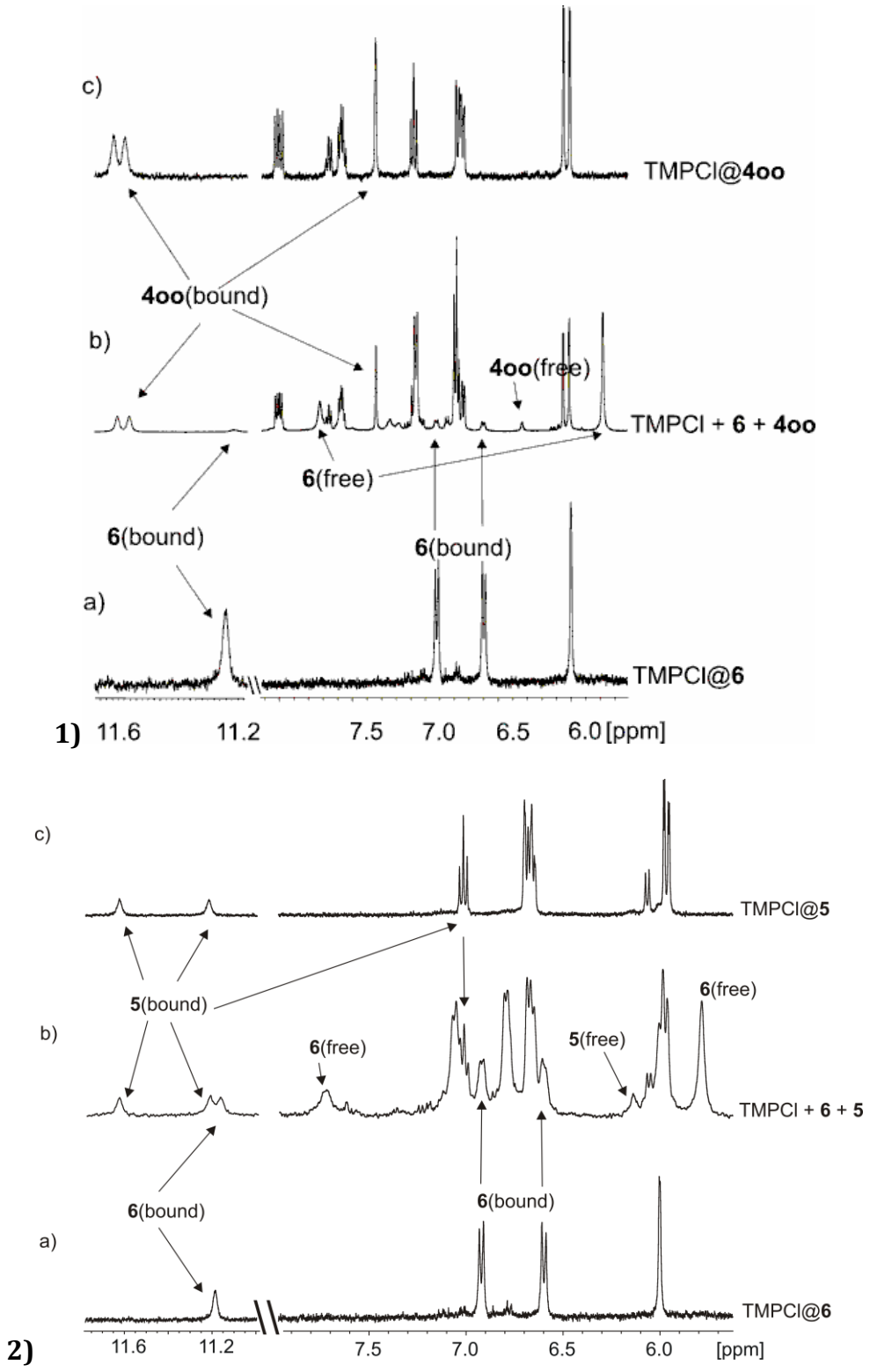

Figure 2.29. Selected regions of the ^{1}H-NMR spectra in DCM-d_2 solution of: 1): a) TMPCl@**6**, b) an equimolar mixture of TMPCl + **6** + **4oo** and c) TMPCl@**4oo**. 2): a) TMPCl@**6**, b) an equimolar mixture of TMPCl + **6** + **5** and c) TMPCl@**5**.

Thus, we concluded that the bridging phosphonato groups installed in the upper rim of the **4oo** receptor offered electrostatic and conformational advantages

compared to **6**, which can be quantified in - 2.2 kcal/mol. The overall gain in binding energy of **4oo** with respect to **6** can be dissected in the two components by the use of receptor **5** as reference. We had considered that receptor **4oo** and **5** are similarly restricted conformationally (preorganized) for the binding of TMPCl. Complexation of TMPCl with **5**, however, lacks of the electrostatic interactions provided by the phosphonate groups installed in **4oo**. We assigned the measured difference in the binding energies of TMPCl with **4oo** and **5**, -1.4 kcal/mol, mainly to the existence of electrostatic interactions in the TMPCl@**4oo**. Consequently, the preorganization effect build into the scaffolds of bridged receptors **4oo** can be quantified approximately as - 2.2 – (-1.4) = - 0.8 kcal/mol using aryl-extended calix[4]pyrrole **6** as reference. These back of the envelop calculations indicate that both effects, preorganization and electrostatic interactions, are important for the effective binding of organic ion-pairs by receptor **4oo**. For the TMPCl@**4oo** complex the TMP cation is not directly interacting with the phosphonato groups but exhibiting a separated arrangement of the in-pair in solution.

2.2.5 Recognition of primary alkylammonium salt by receptor series 4.

P=O bridged cavitands derived from resorcin[4]arene are well known hydrogen-bonding receptors for alkylammonium ions.[26] By means of gas-phase binding studies, it was shown that the number and spatial orientation of the P=O binding groups in these receptors have a dramatic influence on their ability to form hydrogen bonded complex with primary, secondary and tertiary methylammonium ions.[27,28] Thus, we became interested in evaluating the effect that the geometrical differences provided by the calix[4]pyrrole phosphonate cavitand series **4** produced in the complexation of octylammonium chloride OAMCl ion-pair, **11**•Cl, also in DCM solution. We also wanted to determined, if possible, the relative thermodynamic stabilities of the complexes formed by the receptor series **4** with primary and tertiary alkylammonium salts. Molecular modelling studies indicated that OAMCl can be engaged in an interaction of its alkylammonium group (hydrogen bonds, CH··O and cation—dipole interactions) simultaneously with the two P=O groups of diastereoisomer **4ii** (Figure 2.30 a). Geometrical constrains eliminate this bidentate binding possibility for the other two diastereoisomeric receptors.

We performed ^{1}H NMR titration experiments by adding 0.5 and 1 equivalent of OAMCl to separated 1 mM solutions of stereoisomers **4oo** and **4ii** in deuterared DCM. We observed that both complexation processes featured slow exchange dynamics on the ^{1}H NMR timescale. In particular, for stereoisomer **4ii** the addition of 1 equivalent of the salt induced the exclusive observation of proton signals corresponding to the bound host. This result indicated that the binding constant value for the 1:1 complex of OAMCl@**4ii** can be estimated as higher than 10^4 M^{-1}. The complexation induced shifts observed for some signals of the protons in the octylammonium cation **11** were significant. The signal of the ammonium group moved upfield $\Delta\delta$ = - 2.0 ppm, as well as that of the methylene in α position, $\Delta\delta\alpha$ - 0.73 ppm, and the one for β methylene, $\Delta\delta\beta$ = - 0.26 ppm. The placement of the cation in the upper rim and the close-contact ion-paired geometry assigned to the OAMCl@**4ii** complex (Figure 2.30b) were supported by the existence of intermolecular close contacts between the *meso*-phenyl protons (*para* and *meta*) and the methylene protons (mainly *α* and *γ*) of the alkyl chain of **11**, which produced the corresponding cross-peaks in the ROESY spectrum of the complex.

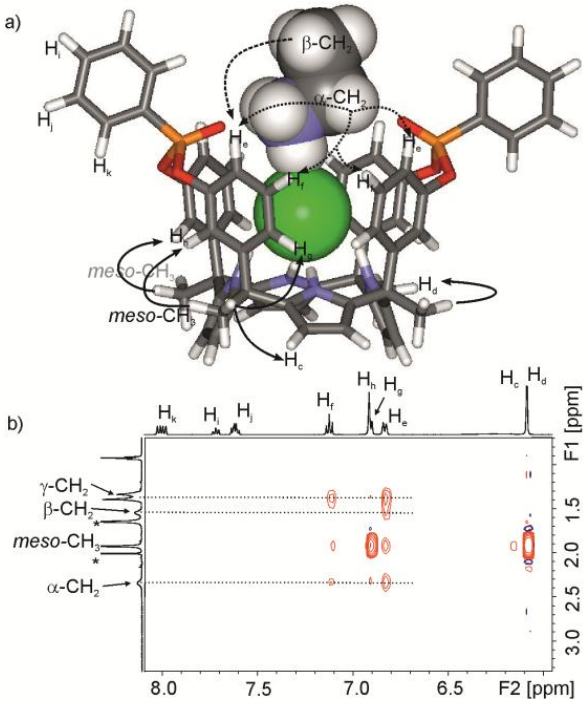

Figure 2.30. a) CAChe energy minimized structure (PM6) of the OAMCl@**4ii** complex highlighting the bidentate binding mode of the alkylammonium cation located in the upper rim. For clarity, the alkyl group shown for OAM cation is ethyl and the salt ion-pair is displayed as CPK model; b) Selected region of a 2D-ROESY experiment performed on a dichloromethane solution containing an

equimolar mixture of **4ii** and OMACl. Intermolecular (dotted lines) and intramolecular (solid lines) NOEs are indicated by arrows in a.

In striking contrast, the addition of 1 equivalent of OAMCl to the dichloromethane solution of receptor **4oo** revealed the co-existence of proton signals both for the free and bound host. Integration of proton signals for free and bound host allowed us to determined the stability constant value for the 1:1 complex as $K_{a,exp}$(OAMCl@**4oo**) = 2±1 × 10^3 M^{-1}. A careful analysis of the ^{1}H NMR spectrum of **4oo** containing 0.5 equivalent of OMACl revealed that the signals of the methylene protons of the cation in α and β position with respect to the ammonium group were massively upfield shifted, $\Delta\delta_\alpha$ = - 2.2 and $\Delta\delta_\beta$ = - 0.91 ppm, suggesting a deep inclusion in the shallow and electron rich aromatic cavity opposed to the bound chloride (Figure 2.31 a). The signal for the protons of the ammonium group of OAMCl also experienced a dramatic upfield shift ($\Delta\delta$ = - 5.6). Probably, the complexation induced shift of the ammonium protons signals is partially caused by the shielding effect of the aromatic cavity in which the cation is located. Nevertheless, we propose that the change in geometry experienced by the ion-pair of the salt from a *close-contact* arrangement in the free-state to *ion-separated* arrangement in the ion-paired complex OAMCl@**4oo** must play an important role in the observed chemical shift change. In complete agreement with the proposed *ion-separated* binding geometry assigned to the OAMCl@**4oo**, the ROESY experiment carried out on a solution containing an equimolar mixture of the two binding partners (~ 75% complex formation) displayed the exclusive existence of intermolecular cross peak between the signals of the β-pyrrole protons of the host and the α methylene protons in the octylammonium cation (Figure 2.31).

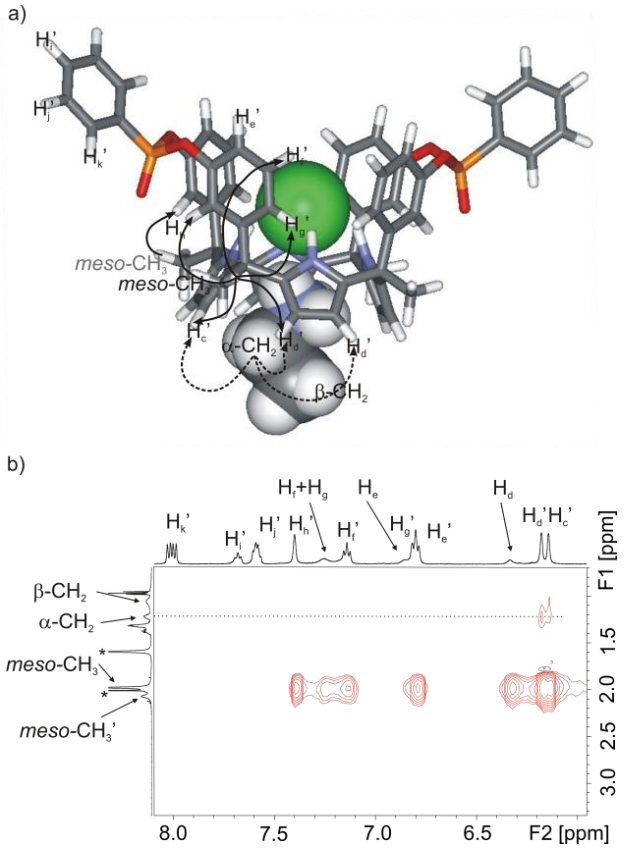

Figure 2.31. a) CAChe energy minimized structure (PM6) of the OAMCl@**4oo** complex with the alkylammonium cation located in the electron-rich aromatic cup distal to the bound chloride. For clarity, the alkyl group shown for **11** is ethyl and the salt ion-pair is displayed as CPK model; b) Selected region of a 2D-ROESY experiment performed on a dichloromethane solution containing an equimolar mixture of **4oo** and OAMCl. Separate signals for the free and bound protons of the receptors are still distinguishable. Primed letters indicate proton signals of the free receptor. Intermolecular (dotted lines) and intramolecular (solid lines) NOEs are indicated by arrows in a.

From all the results of the above experiments, we concluded that the spatial location of the cation in the binding geometries of the 1:1 complexes formed by the receptor series **4** and quaternary ammonium salts is analogous to that of the complexes derived from a primary alkylammonium salt. Most likely, ion-dipole with or without the assistance of hydrogen bonding interactions with the phophonato groups are responsible to the selective spatial location of both types of cations. Interestingly, the trend of the relative thermodynamic stabilities of the complexes is complete reversed on changing from quaternary to primary ammonium salts. Thus, quaternary ammonium salts formed the more thermodynamically stable complexes with the **4oo** receptor. On the contrary, a primary ammonium salt binds more tightly with the **4ii** receptor. Favourable hydrogen bonding interactions established between the primary alkylammonium

residue and the phosphonate groups[29] in the **4ii** receptors compensate for the reduced binding energy provided in the initial interaction of the chloride with this receptor compared to **4oo**. Unfortunately, pairwise competitive binding experiments in solution were not conclusive for rating the binding affinities of **4ii** with respect to TMPCl and OAMCl, that is quaternary *versus* a primary ammonium salt.

2.2.6 Effect of the solvent in the binding of tetralkylammonium/ammonium chloride salts

The nature of the solvents has a strong impact on the behavior of 1:1 electrolytes. In low permittivity media, such as DCM, ion pair formation is likely to occur. The extent of ion-pair formation is concentration dependent and, based on existing information, it is reasonable to consider that at 1 mM concentration alkylammonium salts are mainly ion-paired in DCM.[30,31,32] On the contrary, in high permittivity solvents, such as acetonitrile (ACN) alkylammonium salts at 1mM concentration are predominantly ionic species. Conductance measurements are practical in establishing these points. The absence of ions in solution correlates with the observation of no conductance.

When the guest salt and the complex are both 100% dissociated equation (5) applies referring to the 1:1 complexation process of a mono charged anion:

$$H + A^- = H \bullet A^- \; ; \; K_{a,exp} = [H \bullet A^-] / [H]\,[A^-] \text{ in units of } M^{-1} \quad (5)$$

The application of equation (5) explicitly assumes that the ligand is present as a monomer and the cation is not participating in the binding process. The selection of ACN as solvent allows the direct assessment of the selectivity of the receptor series **4** towards chloride without having to worry about the effect of the different cations. At 298 K only receptor **4oo** is significantly soluble in ACN. The solubility of receptor **4io** was 0.5 mg/mL (~ 0.5 mM) and receptor **4ii** is not soluble enough to be detected by ^{1}H NMR spectroscopy. The ^{1}H NMR titrations of receptors **4oo** and **4io** in ACN solution with TMPCl showed slow exchange dynamics for the binding process. From the integral values of selected signals for protons in the free and bound receptors we calculated the following binding constants values $K_{a,exp}$(TMPCl@**4oo**) = 7.0±2 × 10^3 M^{-1} and $K_{a,exp}$(TMPCl@**4io**) = 2.0±1 × 10^3 M^{-1}. The

magnitudes of the binding constants are significantly reduced compared to the values we estimated/determined in DCM solution, however, the ratio of binding constant values $K_{a,exp}$(TMPCl@**4oo**)/$K_{a,exp}$(TMPCl@**4io**) is similar to the one we calculated in DCM solution.

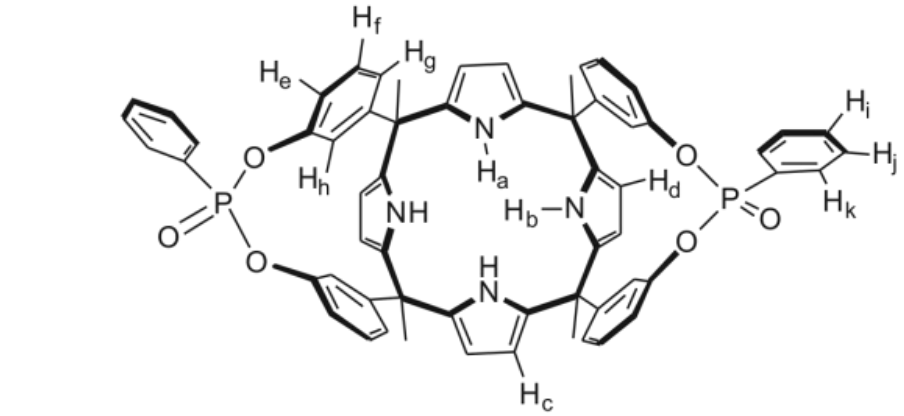

1)

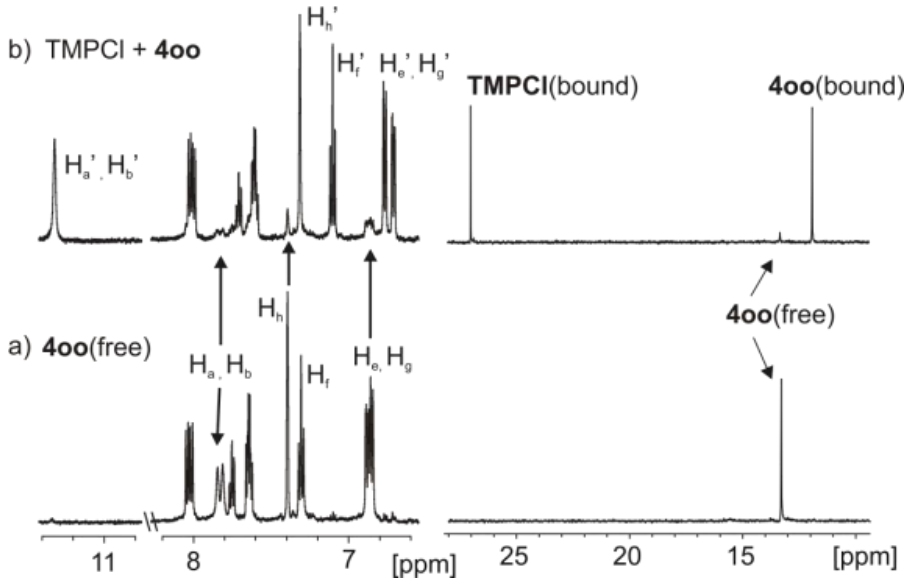

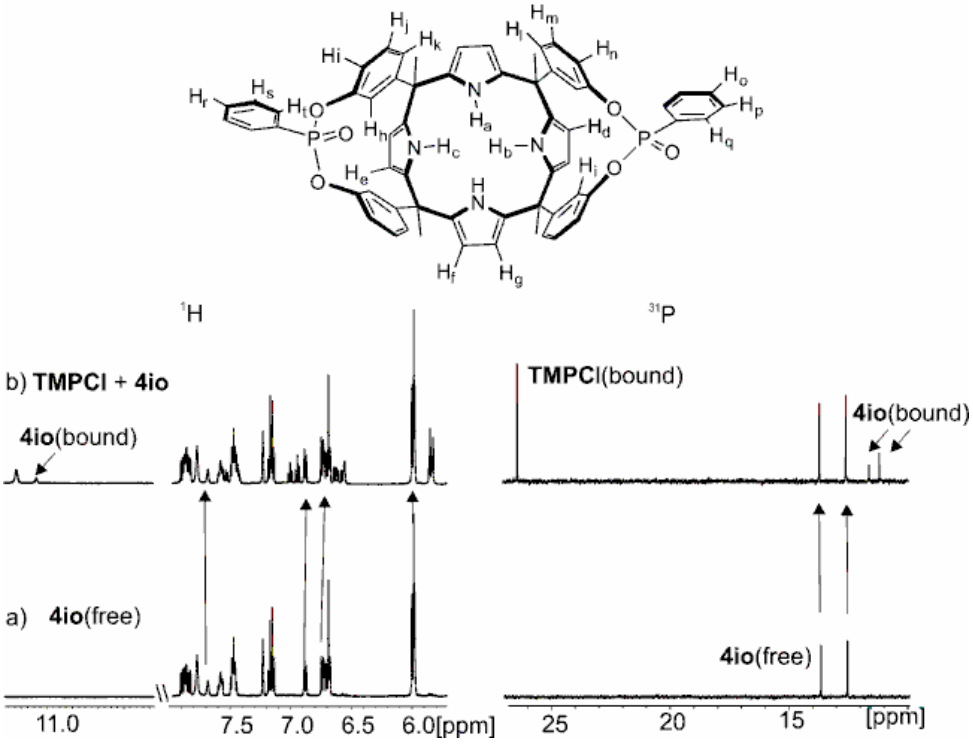

Figure 2.32. Selected regions of ^{1}H-NMR and ^{31}P-NMR spectra of: 1): 3.03 mM solution of **4oo** in ACN-d_3 after addition of a) 0 equivalents and b) 1.0 equivalent of TMPCl. 2): 0.3 mM solution of **4io** in ACN-d_3 after addition of a) 0 equivalents and b) 1.0 equivalent of TMPCl.

This result is in support of our hypothesis stating that the binding of the quaternary ammonium cation, in DCM solution, to the initially formed anionic complex Cl^{-}@**4** although not being site-identical was energetically very similar in the three diastereoisomeric complexes. We postulated that the observed selectivity for the three receptors in DCM derived directly from their affinity to the chloride and was not influenced by the cation binding.

The two receptors, **4oo** and **4io**, were also titrated against the battery of all alkylammonium salts. In all cases, the interaction of the anion with the receptor induced a large downfield shift of the NH protons and produced the observation of two different set of proton signals assigned to the free and bound host. The values of the measured binding constants were in the order of 10^3 M^{-1}, reinforcing the idea that the cation is not significantly involved in the formation of ion-paired complexes in ACN solution. For any salt, the value for the binding constant with the **4oo** receptor was between four to the five-fold larger than with **4io**. In the specific case of TBACl, this ratio was also evaluated through a direct pairwise competitive experiment affording $K_{a,exp}$(TBACl@**4oo**)/$K_{a,exp}$(TBACl@**4io**) ≈ 5 (Figure 2.33).

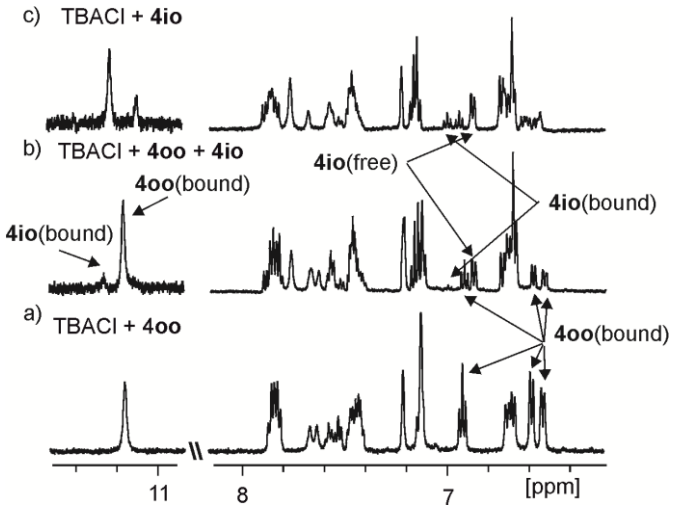

Figure 2.33. Selected regions of the ^{1}H spectra in ACN solution at 298 K of mixtures containing equimolar amounts of : a) TBACl + **4oo**, b) TBACl + **4oo** + **4io**, c) TBACl + **4io**.

Finally, we performed a conductometric titration for the pair **4oo** and TBACl in ACN. The plot of molar conductance Λ_m(S cm^2 mol^{-1}), against the receptor/ion concentration ratio [**4oo**]/[Cl$^-$] is shown in Figure 2.34. The observation of a significant conductance value (158 S cm^2 mol^{-1}) at [**4oo**]/[Cl$^-$] = 0, which is very close to the Λ_m^o value for TBACl in this solvent was a clear indication that the salt was mainly in the form of ionic species.[33] The incremental addition of **4oo** to the ACN solution of [TBACl]= 9.8 × 10^{-5} M^{-1} induced a decrease in the molar conductance. This is due to the complexation of the chloride by the receptor. The volume of the Cl$^-$@**4oo** complex is larger than that of the free chloride. Therefore, the diffusion rate of the complex in solution is reduced compared to that of the free chloride. The conductometric titration curve can be adjusted to two different linear segments that intersect close to the expected value of [**4oo**]/[Cl$^-$] ratio for the formation of a 1:1 complex. This result strongly supports the use of equation (5) in determining binding affinity constant of receptors **4oo** and **4io** with chloride in ACN solution.

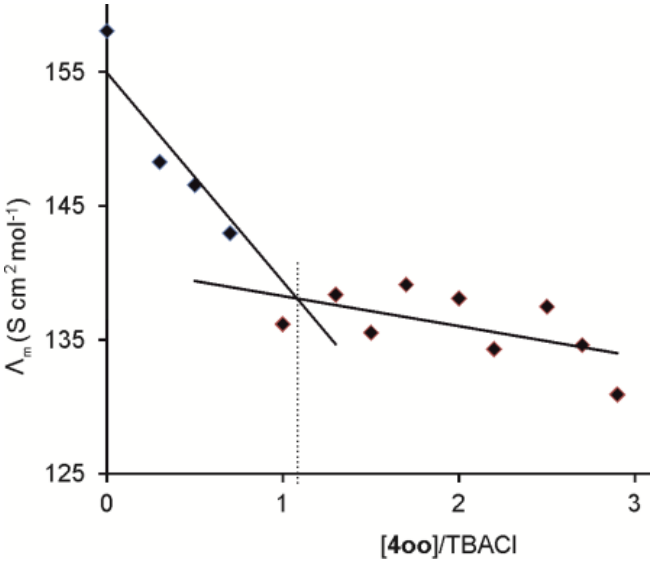

Figure 2.34. Conductometric titration curve of chloride anion (TBACl) with **4oo** in ACN solution at 298 K.

2. 3 Conclusions

We have designed and synthesized unprecedented *bis*-phosphonate calix[4]pyrrole cavitands **4**. The synthetic methodology allowed the isolation of three diastereomeric bis-phosphonato cavitands that were fully characterized by a combination of NMR spectroscopy and X-ray diffraction techniques. The three diastereisomeric receptors differ by the relative spatial orientation of the two phosphonate groups installed in the upper rim of the common aryl-extended calix[4]pyrrole scaffold. We have evaluated the binding properties of the three bis-phosphonate receptors with a series of tetraalkylammonium chloride salts and one primary alkylammonium chloride in DCM and ACN solutions. In DCM solution, the three diastereomeric hosts formed thermodynamically (Ka > 10^4 M^{-1}) and kinetically highly stable 1:1 ion-paired complexes with quaternary trimethylphosphonium/ammonium chloride salts like TMPCl and DTMACl. In solution, the relative orientation of the P=O groups with respect to the aromatic cavity has a strong impact on the binding properties of the receptor and in the geometry of its ion-paired complex. Thus, the **4ii** stereoisomer with the two P=O groups inwardly oriented provided the smallest magnitudes in binding constant for the 1:1 complex with the chloride quats and displayed a *contact* arrangement of

the ion-pair. The **4oo** host featuring outwardly oriented P=O groups produced the more thermodynamically stable 1:1 complexes with the same chloride salts and displayed a *separated* arrangement of the ion-pair. We rationalize the observed trend in binding affinities as a consequence of stepwise binding mechanism. The magnitude of the initial binding of the chloride to form the 1:1 anionic complex must be strongly dependent on the spatial orientation of the phosphonate bridging groups. The subsequent complexation of the quat cation and its placement within the ion-paired 1:1 complex, which is indeed mandated by the spatial arrangement of the phosphonate groups, should afford an almost constant energetic contribution to the overall binding. The use of TBACl as guest provokes a reduction in the thermodynamic stabilities of the corresponding 1:1 ion-paired complexes. For a primary alkylammonium chloride the arrangement of the ion-pair in the complexes is similarly controlled by the relative orientation of the P=O groups in the hosts. Surprisingly, however, the trend in binding affinities for their 1:1 complexes is reversed compared to that measured for the quaternary ammonium salts. Favorable hydrogen bonding interactions established between the primary alkylammonium residue and the phosphate groups in the **4ii** receptors pay-back for the reduced binding energy provided by the initial interaction of the chloride with this receptor compared to **4oo**. In ACN solution the alkylammonium chloride salts and their complexes with the receptor series are mainly ionic species. Consequently, the cation is not significantly involved in the binding process. In this solvent, the binding affinities we determined for the bis-phosphonate cavitands with chloride salts having alkylammonium cations of different sizes or substitution levels, quaternary or primary, are always of the order of 10^3 M^{-1}. We measured that $K_{a,exp}$(TMPCl@**4oo**)/$K_{a,exp}$(TMPCl@**4io**) ≈ 4, both in DCM and ACN solutions. This result supports the hypothesis that binding of the quaternary ammonium cation in DCM solution even occurring at different sites of the host is energetically very similar for the two diastereoisomeric hosts.

2. 4 Experimental Section

General information and instrumentation

All syntheses were carried out using chemicals as purchased from commercial sources unless otherwise noted. All commercial solvents and chemicals were of reagent grade quality and were used without further purification except as noted. When required, dried and deoxygenated solvents supplied by Sigma-Aldrich Solvent Purification System (SPS-200-6) were used. Thin-layer chromatography (TLC) and flash column chromatography were performed with DC-Alufolien Kieselgel 60 F254 (Merck) and silica gel 60A for chromatography (SDS) respectively. ^{1}H and ^{31}P NMR spectra were recorded on a Bruker Avance 400 (400.1 MHz for ^{1}H NMR) and Bruker Avance 500 (500.1 MHz for ^{1}H NMR) ultrashield spectrometer; Mass Spectrometry experiments on a LCT Premier, Waters-Micromass ESI or Autoflex, Bruker Daltonics MALDI. FT-IR measurements were carried out on a Bruker Optics FTIR Alpha spectrometer equipped with a DTGS detector, KBr beam splitter at 4 cm^{-1} resolution. Isothermal titration calorimetry experiments (ITC) were performed using a Microcal VP-ITC Microcalorimeter. The conductometric titrations were performed by Mettler-Toledo conductimeter, using a 84µS/cm sensor previously calibrated with a 0.00056 M KCl solution.

Binding studies

<u>^{1}H NMR dilution experiments of *bis*-phosphonate calix[4]pyrroles in DCM solution.</u>

The ^{1}H NMR dilution experiments of **4** were carried out on a Bruker 400MHz spectrometer, at 298 K. Solutions were prepared by weighting separately the three diastereoisomers in three different volumetric flasks of 1 mL in order to make a moderately concentrated stock solution (**4ii**: 13.2 mM; **4oo**: 17.6 mM; **4io**: 14.2 mM). A ^{1}H NMR spectrum of 0.5 mL of **4ii**, **4oo** and **4io** stock solution was recorded for each stereoisomer. Then each NMR tube solution was sequentially diluted by transferring specific volumes of solvent by a volumetric pipette, for a total of three sequential dilutions per host solution (8 mM; 5 mM; 1 mM). The

oligomerization process shows a fast exchange in the NMR timescale in all cases, and the constants were determined by monitoring the chemical shift changes of the β- pyrrolic protons as incremental volume of solvent was added. The value of the association constant was calculated using the software HyperNMR

^{1}H NMR binding experiment of **6** with TBACl in DCM solution. The complexation behaviour of **6** toward TBACl was studied by ^{1}H NMR on a Bruker 400MHz spectrometer, at 298 K. The association constant was determined by adding aliquots of a 1.5 x 10^{-1} M solution of TBACl in CD_2Cl_2 into the NMR tube containing a 1.46 x 10^{-2} M solution of **6** in the same solvent. The concentration of the receptor was variable throughout the titration. The complexation of TBACl shows a fast exchange in the NMR timescale. The association constant between **6** and the chloride anion was determined as $K_{a,exp}$ = 1±0.2 × 10^1 M^{-1} by monitoring the chemical changes of the protons resonating at 6.80 ppm (*meso*-phenyl protons) and 4.65 ppm (methylene protons of the lateral chain) in the ^{1}H NMR spectrum as incremental amounts of the guest were added (0.5; 1; 2; 5; 10 equivalents of TBACl). The value of the association constant was calculated using the software HyperNMR. The data were fitted to a simple 1:1 binding model.

The conductometric titrations were performed in 25 mL vials equipped with a magnetic stirring bar and placed on top of a stirring plate. The conductivity of a pure acetonitrile solution afforded a value of 0.22μS/cm. A solution of [TBACl] = 0.98 x 10^{-4} M in acetonitrile gave a conductivity value of 15.49 μS/cm. We placed 20 mL of the above solution in the 25 mL vial and added incremental amounts of a **[4oo] =** 1.7 x 10^{-3} M solution in the same solvent. After each addition the mixture was stirred for 2 minutes to ensure a good mixing of all the components. The measurement of the conductance of the solution was performed after switching off stirring. The process of stirring and measurement was repeated until a constant value for the conductance was obtained.

The ESI-MS experiments were carried out using an Electrospray Ionization source combined with a Time-of-Flight mass spectrometer (ESI-TOF), operating in negative and positive mode. The samples were continuously sprayed using nitrogen as drying gas (desolvation at 510 L/hr). The injection rate was

maintained constant at 20 µL/min. The voltage applied at the ESI needle was increased from 0V to 500V, while a voltage of 0V was applied to the cone. The source and desolvation temperatures were set to 120 °C and 200 °C, respectively.

Synthesis

meso-Tetramethyltetrakis(hydroxyphenyl) calix[4]pyrrole 1a:

3-hydroxy acetophenone (6.0 g, 44 mmol) was dissolved in HPLC grade MeOH (200 mL) and methanesulfonic acid was added dropwise (1.4 mL, 22.03 mmol). The solution turned from pale yellow to red after addition of freshly distilled pyrrole (3 mL, 44 mmol). The reaction was protected from light and refluxed for 3 hrs. Then quenched by addition of triethylamine (4 mL) and distilled water (200 mL). MeOH was evaporated and the aqueous solution extracted with AcOEt (3 × 200 mL). The collected organic fractions were dried over sodium sulphate and the solvent removed under reduced pressure. The desired isomer was filtered off by crystallization of the reaction crude from CH_3CN (20 mL) as white solid with a yield of 2%. ^{1}H-NMR (400 MHz, CD_3CN) δ_H ppm 7.96 (bs, 4H), 7.10 (t, 4H), 6.58 (dd, 4H), 6.51 (dd, 4H), 6.42 (bt, 4H), 6.04 (d, 8H), 2.15 (bs, 4H), 1.88 (s, 12H).

Bis-phosphonate cavitands 4:

To a solution of calix[4]pyrrole **1a** (200 mg, 0.270 mmol) in dry THF (10 mL) and freshly distilled triethylamine (0.753 mL, 5.40 mmol), phenylphosphonic dichloride (0.095 mL, 0.675 mmol) was added dropwise under argon atmosphere. The reaction mixture was stirred for 2 hrs at room temperature. The solvent was removed *in vacuo* and water (50 mL) was added to solubilise the triethylammonium chloride salt. The suspension was extracted with CH_2Cl_2 (2 × 50 mL). The organic extracts were combined, dried, filtered and the solvent removed *in vacuo*. The ^{1}H-NMR spectrum of the residue indicated the presence of a mixture of three diastereoisomers **4io, 4oo**, **4ii**. The reaction crude was first purified by Combiflash (SiO_2; CH_2Cl_2 : MeOH 99:1) in order to remove the oligomers/polymers formed during the reaction with 60% overall yield. The fraction containing the three diastereomers was purified by semipreparative HPLC (Spherisorb silica 250 × 20 mm, 5 µm; SiO_2; CH_2Cl_2 : MeOH 99:1) to yield each separated isomer **4io, 4oo**

and **4ii** as a white solid (Retention times: 4.8 minutes, 6.19 minutes and 9.8 minutes, respectively). The isomers can be further purified by crystallization from acetonitrile.

Experimental data **4io** (white solid, 30%). M.p.: T > 200ºC (slow decomposition); ^{1}H-NMR (500 MHz, CD_2Cl_2, 25°C): δ (ppm) = 8.20 (bs, 1H), 8.08 (bs, 2H), 8.02 (m, $^{3}J_{H-P}$ ~ 14 Hz, $^{3}J_{H-H}$ ~ 7.3 Hz, $^{4}J_{H-H}$ ~ 1.2 Hz, 4H), 7.84 (bs, 1H), 7.71 (m, $^{3}J_{H-H}$ ~ 7.3 Hz, $^{4}J_{H-H} \approx {}^{5}J_{H-P}$ ~ 1.2 Hz, 2H), 7.61 (m, $^{3}J_{H-H}$ ~ 7.3 Hz, $^{4}J_{H-P}$ ~ 4.8 Hz, 4H), 7.32 (s, 2H), 7.25 (t, $^{3}J_{H-H}$ ~ 7.98 Hz, 2H), 7.21 (t, $^{3}J_{H-H}$ ~ 7.98 Hz, 2H), 7.02 (d, $^{3}J_{H-H}$ ~ 7.98 Hz, 2H), 7.01 (d, $^{3}J_{H-H}$ ~ 7.98 Hz, 2H), 7.00 (d, $^{3}J_{H-H}$ ~ 7.98 Hz, 2H), 6.95 (s, 2H), 6.83 (d, $^{3}J_{H-H}$ ~ 7.98 Hz, 2H), 6.23 (d, $^{4}J_{H-H}$ ~ 2.17 Hz, 2H), 6.2 (d, $^{4}J_{H-H}$ ~ 2.17 Hz, 2H), 5.96 (t, $^{4}J_{H-H} \approx {}^{3}J_{H-H}$ ~ 2.17 Hz, 2H), 5.91 (t, $^{4}J_{H-H} \approx {}^{3}J_{H-H}$ ~ 2.17 Hz, 2H), 2.02 (s, 6H), 2.0 (s, 6H). ^{31}P-NMR (500 MHz, CD_2Cl_2, 25°C): δ = (ppm) 15.53 (P(O)in), 13.27 (P(O)out). HR-MALDI-MS: *m/z* calculated for $C_{60}H_{50}N_4O_6P_2$ 984.32, found 984.31; FT-IR ν (cm^{-1}) 3000 (P-CH_{Ar} streaching, 1580 (P-Ar aromatic ring in-plane stretching), 1480-1427 (P-Ar aromatic ring in-plane stretching), 1265,1228,1202 PO stretching; 942 (interaction between aromatic ring vibration and P-C stretching); elemental analysis calculated for $C_{60}H_{50}N_4O_6P_2$ + (3 × CH_3OH) (%): C, 69.99; H, 5.78; N, 5.18; found: C, 69.82; H, 5.34; N, 5.81.

Experimental data **4oo** (white solid, 10%). M.p.: T > 180 ºC (slow decomposition); ^{1}H-NMR (500 MHz, CD_2Cl_2, 25°C): δ (ppm) = 8.04 (bs, 2H), 8.00 (m, $^{3}J_{H-P}$ ~ 14 Hz, $^{3}J_{H-H}$ ~ 7.3 Hz, $^{4}J_{H-H}$ ~ 1.2 Hz, 4H), 7.70 (m, $^{3}J_{H-H}$ ~ 7.3 Hz, $^{4}J_{H-H} \approx {}^{5}J_{H-P}$ ~ 1.2 Hz, 2H), 7.60 (m, $^{3}J_{H-H}$ ~ 7.3 Hz, $^{4}J_{H-P}$ ~ 4.8 Hz, 4H), 7.49 (bs, 2H), 7.26 (t, $^{3}J_{H-H}$ ~ 7.7 Hz, 4H), 7.22 (d, $^{3}J_{H-H}$ ~ 7.7 Hz, 4H), 7.18 (s, 4H), 6.86 (d, $^{3}J_{H-H}$ ~ 7.7 Hz, 4H), 6.32 (d, $^{4}J_{H-H}$ ~ 2.65 Hz, 4H), 5.50 (bs, 4H), 2.07 (s, 12H); ^{31}P-NMR (500 MHz, CD_2Cl_2, 25°C): δ (ppm) = 12.5; HR-MALDI-MS: m/z calculated for $C_{60}H_{50}N_4O_6P_2$ 984.32, found 984.3; FT-IR ν (cm^{-1}) 3000 (P-CH_{Ar} stretching), 1580 and 1480-1427 (P-Ar aromatic ring in-plane stretching), 1272,1232,1201 (PO stretching), 847 (interaction between aromatic ring vibration and P-C stretching); elemental analysis calculated for $C_{60}H_{50}N_4O_6P_2$ + (2 × CH_3OH) (%): C, 70.98; H, 5.57; N, 5.34; found: C, 70.03; H, 5.60; N, 5.38.

Experimental data **4ii** (white solid, 22%). M.p.: T > 230ºC (slow decomposition); ^{1}H-NMR (500 MHz, CD_2Cl_2, 25°C): δ (ppm) = 8.18 (bs, 4H), 8.04 (m, $^{3}J_{H-P}$ ~ 14 Hz, $^{3}J_{H-H}$ ~ 7.3 Hz, $^{4}J_{H-H}$ ~ 1.2 Hz, 4H), 7.71 (m, $^{3}J_{H-H}$ ~ 7.3 Hz, $^{4}J_{H-H} \approx {}^{5}J_{H-P}$ ~ 1.2 Hz, 2H), 7.61 (m, $^{3}J_{H-H}$ ~ 7.3 Hz, $^{4}J_{H-P}$ ~ 4.8 Hz, 4H), 7.24 (t, $^{3}J_{H-H}$ ~ 7.9 Hz, 4H), 7.02 (d, $^{3}J_{H-H}$ ~ 7.9 Hz, 4H), 6.96 (d, $^{3}J_{H-H}$ ~ 7.9 Hz, 4H), 6.94 (s, 4H), 6.17 (d, $^{4}J_{H-H}$ ~ 2.55 Hz, 4H), 6.05 (d, $^{4}J_{H-H}$ ~ 2.55 Hz, 4H), 1.80 ppm (s, 12H); ^{31}P-NMR (500 MHz, CD_2Cl_2, 25°C) δ (ppm): 14.64 (s, P(O)); HR-MALDI-MS: *m/z* calculated for $C_{60}H_{50}N_4O_6P_2$ 984.32, found: 984.32; FT-IR ν (cm^{-1}) 3000 (P-CH_{Ar} streaching), 1580 (P-Ar aromatic ring in-plane stretching), 1480-1427 (P-Ar aromatic ring in-plane stretching), 1265,1228,1202 (PO stretching), 942 (interaction between aromatic ring vibration and P-C stretching); elemental analysis calculated for $C_{60}H_{50}N_4O_6P_2$ + (2 × CH_3CN) (%): C, 72.04; H, 5.29; N, 7.88; found: C, 71.44; H, 5.27; N, 7.93.

Bis-methylene cavitand 5.

Calix[4]pyrrole **1a** (0.300 g, 0.405 mmol) and oven-dried K_2CO_3 (0.213 g, 1.539 mmol) were dissolved in dry DMSO (10 mL). CH_2Br_2 (57 µL, 0.806 mmol) was added, under nitrogen, and the mixture was stirred at 80°C for 3 hrs. The solvent was removed in vacuo and the crude was washed with water (5 mL) and extracted with CH_2Cl_2 (3 × 5 mL). The residue was purified by semipreparative HPLC (Sunfire prepC 100 x 4.6 mm, 5 micron), using a 60:40 THF : H_2O mixture as eluant (Retention time = 7.9 minutes). From the collected fraction containing the desired compound, THF was evaporated under reduced pressure and the water fraction was lyophilised yielding 5 as a yellowish solid in 10% yield. M.p.: decomposition at T > 160°C. 1H-NMR (400 MHz, CD2Cl2) δ (ppm) 7.67 (bs, 2H), 7.52 (bs, 2H), 7.18 (t, 3J~7.55 Hz, 4H), 6.89 (d, 3J~7.55 Hz, 4H), 6.81 (d, 3J~7.55 Hz, 4H), 6.60 (bs, 4H), 6.14 (d, 4J~2.60 Hz, 4H), 5.88 (bs, 4H+2H), 5.55 (d, Jgem~7.18 Hz, 2H), 1.96 (s, 12H). 13C-NMR (500 MHz, CD2Cl2) δ (ppm) 28.32, 44.6, 92, 105.75, 117.07, 118.27, 121.21, 128.71, 137.2, 138.1, 150.7, 156.1; ESI-TOF ES^+: m/z calculated for $C_{50}H_{44}N_4O_4$ ($[M+H]^+$) 765.34, found 765.3 $[M+H]^+$.

2. 5 References and Notes

[1] Sessler, J. L.; Gross, D. E.; Cho, W. S.; Lynch, V. M.; Schmidtchen, F. P.; Bates, G. W.; Light, M. E.; Gale, P. A. *J. Am. Chem. Soc.* **2006**, *128*, 12281.
[2] Blas, J. R.; Marquez, M.; Sessler, J. L.; Luque, F. J.; Orozco, M. *J. Am. Chem. Soc.* **2002**, *124*, 12796.
[3] Blas, J. R.; Lopez-Bes, J. M.; Marquez, M.; Sessler, J. L.; Luque, F. J.; Orozco, M. *Chem. Eur. J.* **2007**, *13*, 1108.
[4] Gale, P. A.; Sessler, J. L.; Kral, V.; Lynch, V. *J. Am. Chem. Soc.* **1996**, *118*, 5140.
[5] Anzenbacher, P.; Jursikova, K.; Lynch, V. M.; Gale, P. A.; Sessler, J. L. *J. Am. Chem. Soc.* **1999**, *121*, 11020.
[6] Kalenius, E.; Neitola, R.; Suman, M.; Dalcanale, E.; Vainiotalo, P. *J. Am. Soc. Mass Spectrom.* **2010**, *21*, 440.
[7] Irico, A.; Vincenti, M.; Dalcanale, E. *Chem. Eur. J.* **2001**, *7*, 2034.
[8] Menozzi, D.; Biavardi, E.; Massera, C.; Schmidtchen, F. P.; Cornia, A.; Dalcanale, E. *Supramol. Chem.* **2010**, *22*, 768.
[9] Prodi, L.; Biavardi, E.; Battistini, G.; Montalti, M.; Yebeutchou, R. M.; Dalcanale, E. *Chem. Commun.* **2008**, 1638.
[10] Pinalli, R.; Nachtigall, F. F.; Ugozzoli, F.; Dalcanale, E. *Angew. Chem., Int. Ed.* **1999**, *38*, 2377.
[11] Suman, M.; Freddi, M.; Massera, C.; Ugozzoli, F.; Dalcanale, E. *J. Am. Chem. Soc.* **2003**, *125*, 12068.
[12] Melegari, M.; Suman, M.; Pirondini, L.; Moiani, D.; Massera, C.; Ugozzoli, F.; Kalenius, E.; Vainiotalo, P.; Mulatier, J. C.; Dutasta, J. P.; Dalcanale, E. *Chem.--Eur. J.* **2008**, *14*, 5772.
[13] Ventola, E.; Vainiotalo, P.; Suman, M.; Dalcanale, E. *J. Am. Soc. Mass Spectrom.* **2006**, *17*, 213.
[14] Delangle, P.; Mulatier, J. C.; Tinant, B.; Declercq, J. P.; Dutasta, J. P. *Eur. J. Org. Chem.* **2001**, 3695.
[15] Gil-Ramirez, G.; Benet-Buchholz, J.; Escudero-Adan, E. C.; Ballester, P. *J. Am. Chem. Soc.* **2007**, *129*, 3820.
[16] Yebeutchou, R. M.; Tancini, F.; Demitri, N.; Geremia, S.; Mendichi, R.; Dalcanale, E. *Angew. Chem., Int. Ed.* **2008**, *47*, 4504.
[17] Tancini, F.; Yebeutchou, R. M.; Pirondini, L.; De Zorzi, R.; Geremia, S.; Scherman, O. A.; Dalcanale, E. *Chem.--Eur. J.* **2010**, *16*, 14313.
[18] Bonomo, L.; Solari, E.; Toraman, G.; Scopelliti, R.; Latronico, M.; Floriani, C. *Chem. Commun.* **1999**, 2413.
[19] Roncucci, P.; Pirondini, L.; Paderni, G.; Massera, C.; Dalcanale, E.; Azov, V. A.; Diederich, F. *Chem.--Eur. J.* **2006**, *12*, 4775.
[20] Gil-Ramirez, G.; Escudero-Adan, E. C.; Benet-Buchholz, J.; Ballester, P. *Angew. Chem., Int. Ed.* **2008**, *47*, 4114.
[21] Gross, D. E.; Schmidtchen, F. P.; Antonius, W.; Gale, P. A.; Lynch, V. M.; Sessler, J. L. *Chem. Eur. J.* **2008**, *14*, 7822.
[22] Jones, J. W.; Gibson, H. W. *J. Am. Chem. Soc.* **2003**, *125*, 7001.
[23] Values for the dissociation equilibrium of alkylammonium ion-pair salts in low dielectric constant solvents can be found in literature, however, the difficulties associated with the accurate determination of the concentrations of the anionic and the ion-paired complexes refrain us to use the complete binding model in the analysis of the titration data.
[24] Verdejo, B.; Gil-Ramirez, G.; Ballester, P. *J. Am. Chem. Soc.* **2009**, *131*, 3178.
[25] The X-ray structure of the DTMACl@**4ii** complex supports this hypothesis.
[26] Lippmann, T.; Wilde, H.; Dalcanale, E.; Mavilla, L.; Mann, G.; Heyer, U.; Spera, S. *J. Org. Chem.* **1995**, *60*, 235.
[27] Irico, A.; Vincenti, M.; Dalcanale, E. *Chem. Eur. J.* **2001**, *7*, 2034.
[28] Kalenius, E.; Moiani, D.; Dalcanale, E.; Vainiotalo, P. *Chem. Commun.* **2007**, 3865.
[29] Tancini, F.; Gottschalk, T.; Schweizer, W. B.; Diederich, F.; Dalcanale, E. *Chem. Eur. J.* **2010**, *16*, 7813.
[30] Hunter, C. A.; Low, C. M. R.; Rotger, C.; Vinter, J. G.; Zonta, C. *Proc. Natl. Acad. Sci. U. S. A.* **2002**, *99*, 4873.
[31] Hunter, C. A.; Low, C. M. R.; Rotger, C.; Vinter, J. G.; Zonta, C. *Chem. Commun.* **2003**, 834.
[32] Bartoli, S.; Roelens, S. *J. Am. Chem. Soc.* **1999**, *121*, 11908.

[33] A DCM solution of [TBACl] = 1 $\times 10^{-4}$ M^{-1} gave a reading of molar conductance of Λ_m = 49 S cm^{-2} $mol^{-1.}$

CHAPTER III

Synthesis and Binding Studies of Tetra-phosphonate calix[4]pyrroles

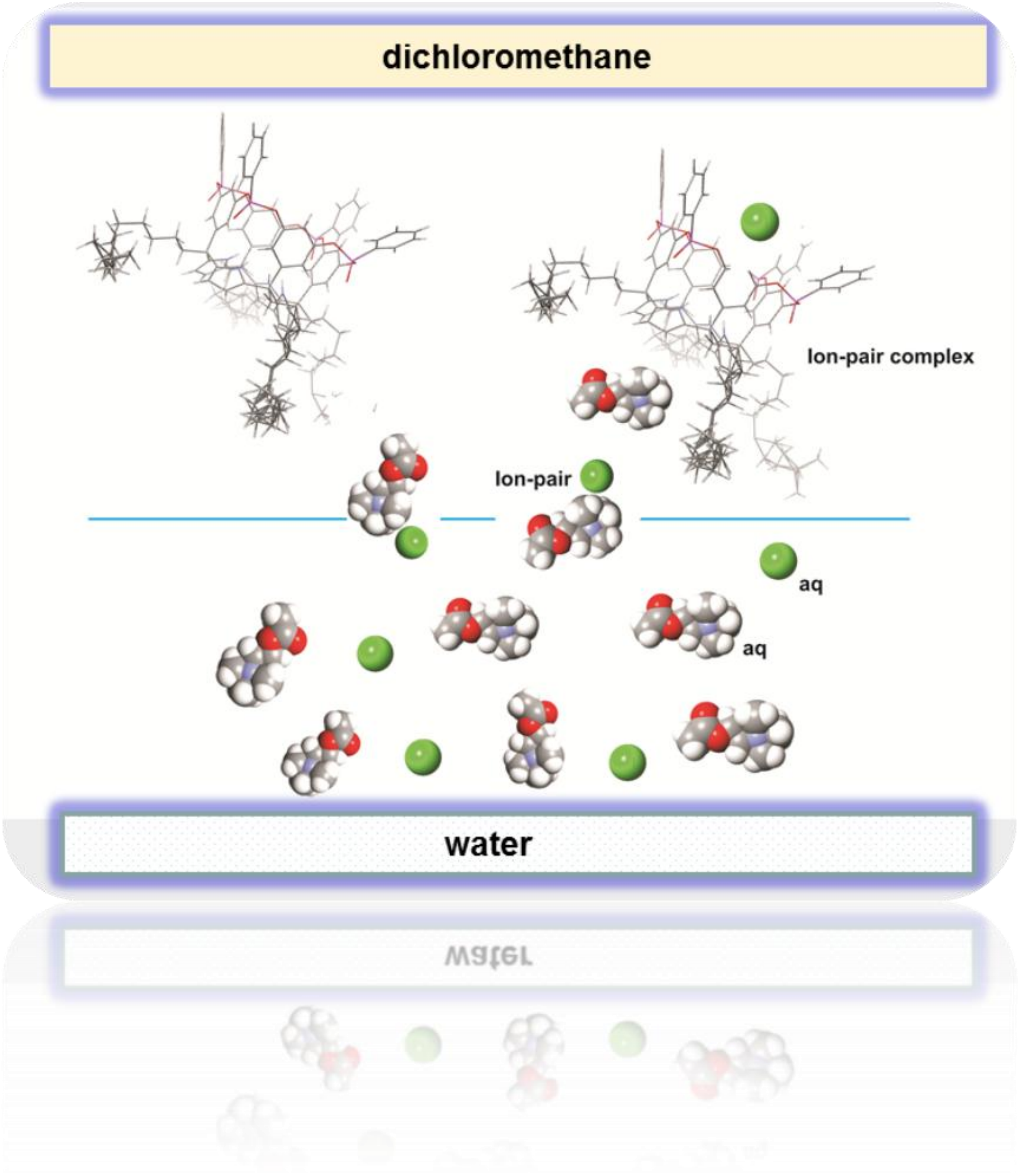

3. 1 Introduction

The binding properties displayed by tetraphosphonate cavitands derived from resorcin[4]arenes in the recognition of cations and hydrogen-bond donor molecules[1,2,3,4], as well as alcohols[5] and ammonium substrates[6,7], prompted us to further investigate the synthesis of tetraphosphonate calix[4]pyrroles derivatives. We disclose here the synthesis and binding properties of a series of two heteroditopic calix[4]pyrroles receptors **2**, conformationally more rigid than the *bis*-phosphonate counterparts described in *Chapter 2*, due to the installation of four phosphonate bridging groups at the upper rim. In addition, receptors **2** are equipped with four long alkyl chains substituted in the *meso*-carbons instead of simple methyl groups (Figure 3.1). The presence of *meso*-alkyl substituents in the lower rim renders receptors **2** to be significantly more soluble in DCM solution than *bis*-phosphonates **1**. The aim of the study of the binding properties of receptors series **2** with alkylammonium salts is twofold. On the one hand, we wanted to quantify the effect on the the binding strengh of ion-paired complexes with alkylammonium/ammonium chloride salts exerted by the four phosphonate groups compared to two. On the other hand, we were interested in increasing the solubility of the phosphonate calix[4]pyrroles in organic solvents in order to evaluate their potential applications as membrane transporters.

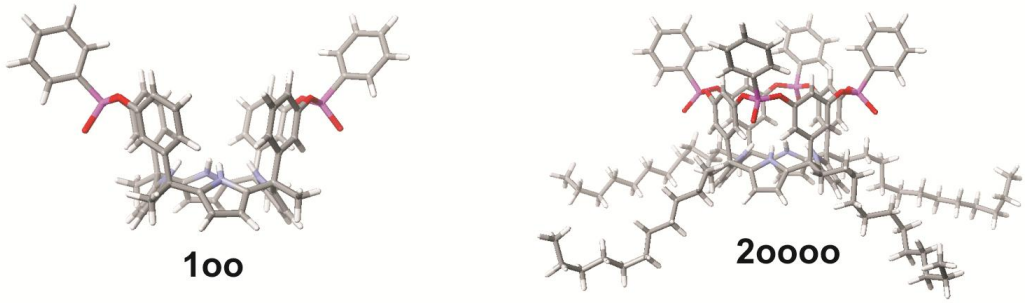

Figure 3.1 Energy minimized structure of: a) bis-phosphonate calix[4]pyrrole **1oo** and b) tetra-phosphonate calix[4]pyrrole **2oooo**.

3. 2 Results and discussion

3.2. 1 Synthesis

The installation of the four phosphonate walls in the upper rim of the lipophilic octol precursor **3**[8,9] was achieved following a synthetic procedure analogous to the one described for the preparation of *bis*-phosphonate cavitands **1** (Scheme 3.1). In particular, octol *α,α,α,α*-**3** was reacted with dichloro(phenyl)phosphane oxide, in presence of triethylamine, in tetrahydrofuran solution. The pure stereoisomers, **2oooo** and **2oooi**, were isolated by semipreparative HPLC (Spherisorb silica 250 x 20 mm, 5 μm) using DCM : Hexane 60 : 40 as eluent and crystallized from acetonitrile solution in 3% and 9% yields, respectively.

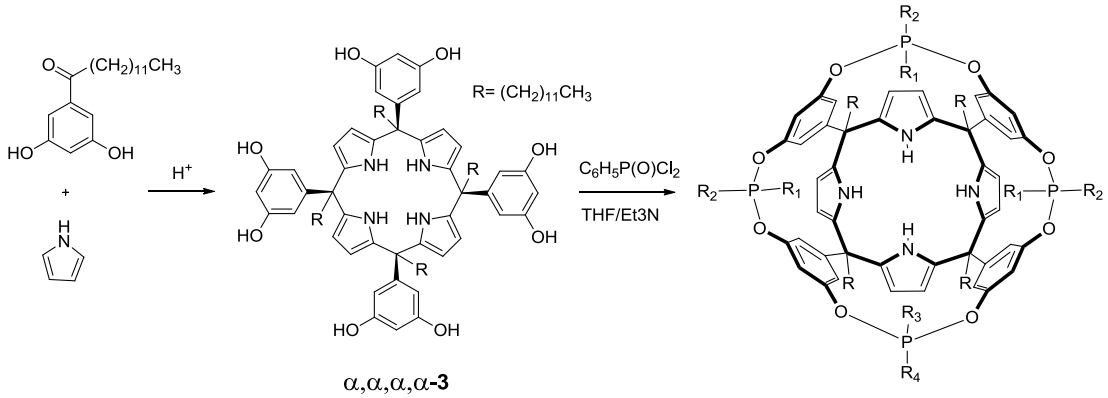

	R1	R2	R3	R4
2oooo	Ph	=O	Ph	=O
2oooi	Ph	=O	=O	Ph

Scheme 3.1. Synthetic scheme for the preparation of tetra-phosphonate calix[4]pyrrole diastereomers receptors **2**.

Only two of the six possible diastereoisomers were isolated from the reaction crude of the acid catalyzed condensation of pyrrol and the lipohilic alkyl-aryl ketone.[10,11] We observed that the reaction produced mainly two diastereomers displaying a clear preference to direct the oxygen atoms of the phosphonate groups outwardly with respect to the calix[4]pyrrole cavity. We were able to isolate from the crude reaction mixture the stereoisomer **2oooo**(o=out) with the four oxygens directed outside the cavity of the receptor and the stereoisomer

2oooi(o=out; i=in) in which one of the three oxygens points towards the inner cavity of the calix[4]pyrrole. This result was not completely unexpected. It is reported in literature that the incorporation of four phosphate groups in the resorcin[4]arene scaffold led to a slight preference for the outward orientation of at least three of the P=O moieties in spite of the steric hindrance experienced by the inwardly directed phenyl groups. In the phosphonato cavitands derived from resorcin[4]arene the iiii isomer is absent. This result has been explained by the existence of a strong preference of the molecules to fill the cavity with at least one phenyl group. The selective preparation of the stereoisomer iiii has been reported only in presence of a specific template, usually a solvent and/or a reactant present in the reaction mixture (i.e. pyridine, triethylamine, etc.).[12,13,14]

3.2. 2 Configurational assignment

We performed the complete assignment of the proton signals observed in the ^{1}H NMR spectra of the two diastereoisomers by means of 2D experiments. Single crystals of **2oooo** were grown by slow evaporation from acetonitrile solution and corroborate the structural assignment (Figure 3.2). Crystals of **2oooi** were also isolated from acetonitrile and dichloromethane solutions but they were not suitable for X-ray crystallographic analysis. In the solid state, the **2oooo** calix[4]pyrrole receptor adopts the cone conformation with one molecule of acetonitrile included in its aromatic cavity and hydrogen bonded to the four pyrrole NHs. A second molecule of acetonitrile is located in the cup provided by the four pyrrole rings. The phenyl substituents in the phosphorous atoms are directed away from the cavity. Moreover, the phophonate bridges introduced at the upper rim significantly reduce the conformational flexibility of the cavitand receptor **2oooo.**

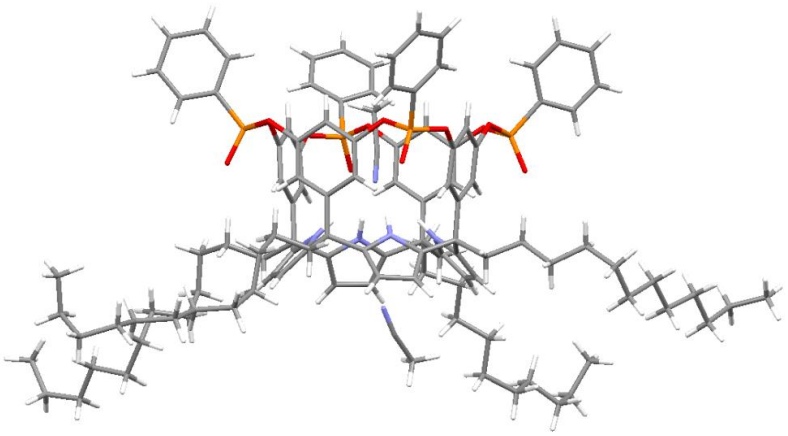

Figure 3.2 Solid state structure of the diastereoisomer **2oooo**.

Receptor **2oooo** presents a ^{1}H NMR spectra compatible with a C_{4v} symmetry and a reduced number of proton signals compared to **2oooi**. Due to the symmetry of the molecule, the NH protons appear as single signal resonating at δ = 7.5 ppm. The β-pyrrolic protons H_b appear as a doublet at δ = 6.17 ppm. Using 2D ROESY experiments it was also possible to assign the *meso*-aromatic protons H_c and H_d to the signals resonating at δ = 7.37 ppm and 6.36 ppm, respectively. The *ortho*-protons H_k show a $J_{H\text{-}P}$ coupling ~ 14 Hz and resonate at δ = 8 ppm. The ^{31}P NMR spectrum of **2oooo** displays one signal at δ = 13.63 ppm corresponding to the four chemically equivalent phosphorus atoms.

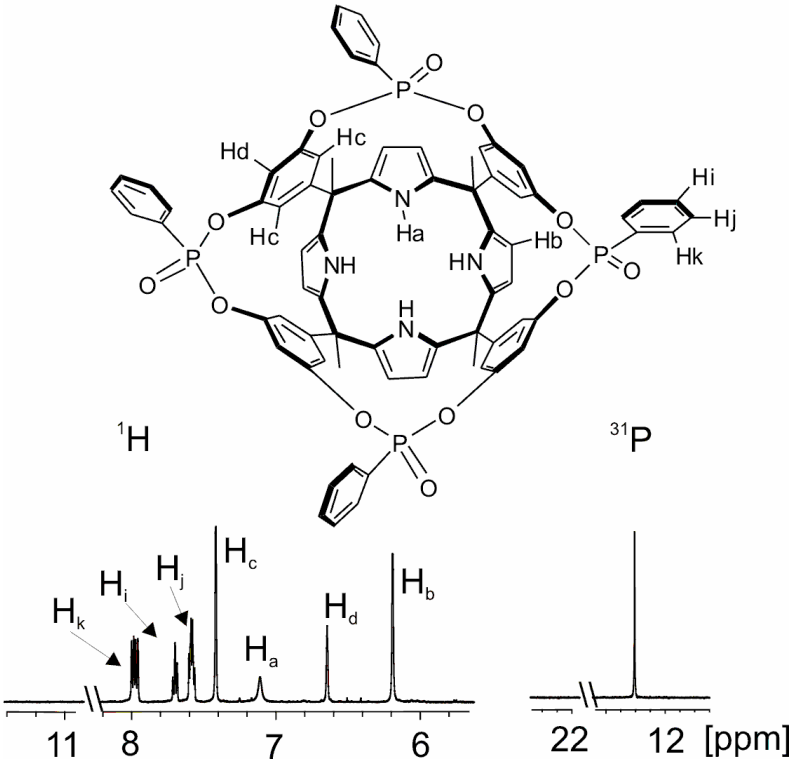

Figure 3.3. Selected downfield region of the ^{1}H and ^{31}P NMR spectra (400MHz) of the **2oooo** stereoisomer at 298 K in $CDCl_3$ solution. The proton assignment is shown in the structure of the **2oooo** receptor represented at the top.

The downfield region of the ^{1}H NMR spectra of the **2oooi** stereoisomer having C_s symmetry is shown in Figure 3.4. Three broad triplets resonating at δ = 7.79, 7.76, and 7.72 ppm with relative intensities 1:2:1 were assigned to the NH protons (H_a, H_b, H_c) of the calix[4]pyrrole core. The signal of the β-pyrrolic protons H_g involved in the fourteen-membered macrocyclic unit with the inwardly orientated P=O group with respect to the cavity is shifted upfield compared to the β-pyrrolic protons having outwardly orientated P=O groups and resonate at δ = 6.045 ppm. The *ortho*-protons H_k, H_v and H_r are chemically non-equivalent and show a J_{H-P} coupling ~ 14 Hz and resonate at 8 ppm. The ^{31}P NMR spectrum of **2oooi** displays only two different but broad signals resonating at δ = 14.37 and 12.96 ppm corresponding to the three chemically non-equivalent phosphorus nuclei. Based on integration values, the phosphorus atoms with oxygens outwardly directed with respect to the calix[4]pyrrole cavity resonated at higher field with respect to the one with the oxygen inwardly directed.

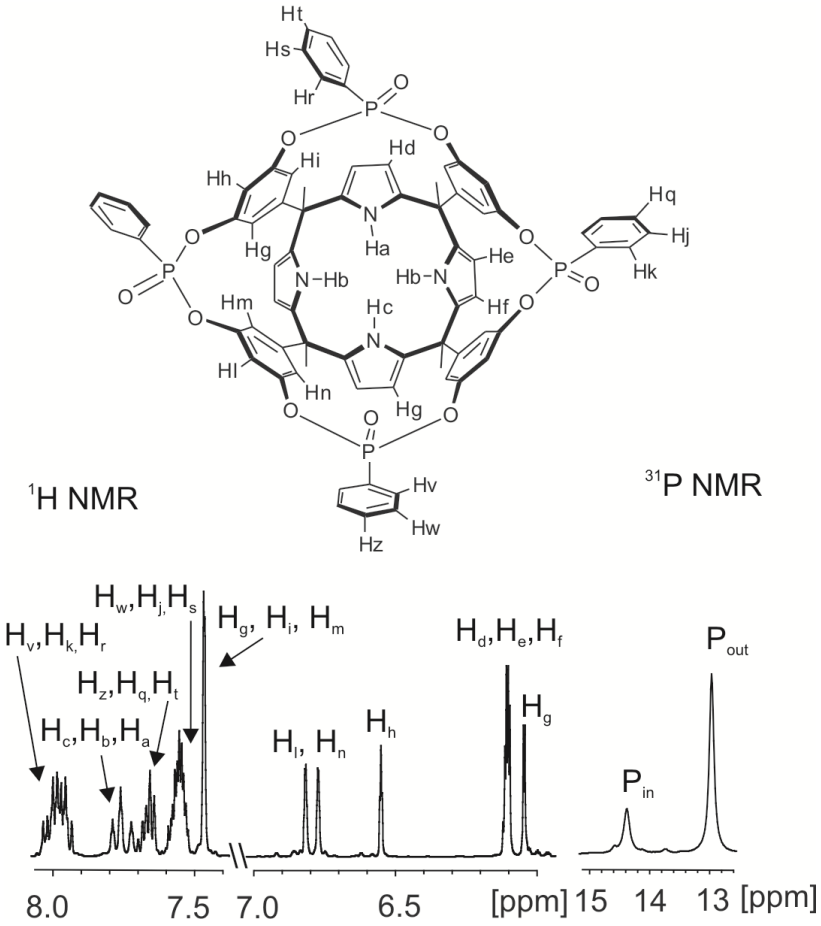

Figure 3.4. Selected downfield region of the ^{1}H and ^{31}P NMR spectra (400MHz) of the **2oooi** stereoisomer at 298 K in CDCl3 solution. The proton assignment is shown in the molecule of the **2oooi** receptor represented in the top.

3.2.3 Binding studies in dichloromethane

The interaction of the two stereoisomers **2oooo** and **2oooi** with TMPCl was probed in DCM solution through direct and pairwise competitive experiments, using ^{1}H and ^{31}P NMR spectroscopic techniques. The results derived from the ^{31}P NMR spectra were used only for a qualitatively analysis and to corroborate the data obtained in ^{1}H NMR spectra. Direct titration experiments were performed by adding two doses of 0.5 equivalent of TMPCl to NMR tubes containing individual DCM solutions of each stereoisomer. The initial addition of 0.5 equivalents of TMPCl to **2oooo** induced the appearance of new proton signals in the ^{1}H NMR spectrum and two new phosphorous signals in the ^{31}P NMR spectrum. The observation of separate proton signals for the free and bound receptor **2oooo** is indicative of the existence of slow chemical exchange between them on the NMR timescale. The new signals observed in the ^{31}P NMR spectrum were assigned to the phosphorous atoms

of bound **2oooo** (broad, δ = 11.5 ppm) and the phosphorous atom of bound TMP (δ = 22.9 ppm) involved in the TMPCl@**2oooo** complex. The phosphorous atoms of free **2oooo** and free TMPCl resonated at δ = 13.0 ppm and δ = 26.9 ppm, respectively. The integral ratio of proton signals for the free and bound **2oooo** resulted 1:1. The signals of the bound pyrrole NHs experienced significant downfield shifts (Δδ ~ 4.15 ppm) as a result of the formation of hydrogen bonds with the included chloride. The signals of the β-pyrrole protons and all the signals of the aromatic protons of the *meso*-phenyl substituents of **2oooo** experienced upfield shifts in the bound receptor. While the signals of the phenyl-phosphonate protons resulted slightly shifted upfied, they were almost unaffected by the complexation (Figure 3. 5). The signal of the methyl protons of the TMP cation experienced a significant upfield shift (δ = 0.659 ppm; Δδ = - 1.471 ppm). The addition of one equivalent of TMPCl induced the exclusive observation of the signals assigned to the proton and phosphorous atoms of the TMPCl@**2oooo** complex. These observations indicated that the value of the experimental association constant, $K_{a,exp}$, for the TMPCl@**2oooo** complex can be estimated as higher than 10^4 M^{-1} and cannot be measured accurately by ^{1}H NMR titrations. When more than 1 equivalent of TMPCl was added, the chemical shifts of the proton signals of the bound **2oooo** receptor were not affected. However, the proton signal of the methyl groups of TMP cation and the signal of its phosphorous atom shifted downfield. This observation was indicative of the existence of a fast exchange on the ^{1}H NMR timescale between free and bound TMP cations. The observation of different exchange dynamics between free and bound receptor and between free and bound cation confirmed the existence of two different exchange processes as we already discussed for the *bis*-phosphonate calix[4]pyrroles **1**. Also in this case, the self-exchange of the included anion or the exchange of a solvent molecule by an anion requires a conformational change of **2oooo**. On the contrary, the chemical exchange between free and bound TMP cation can take places directly.

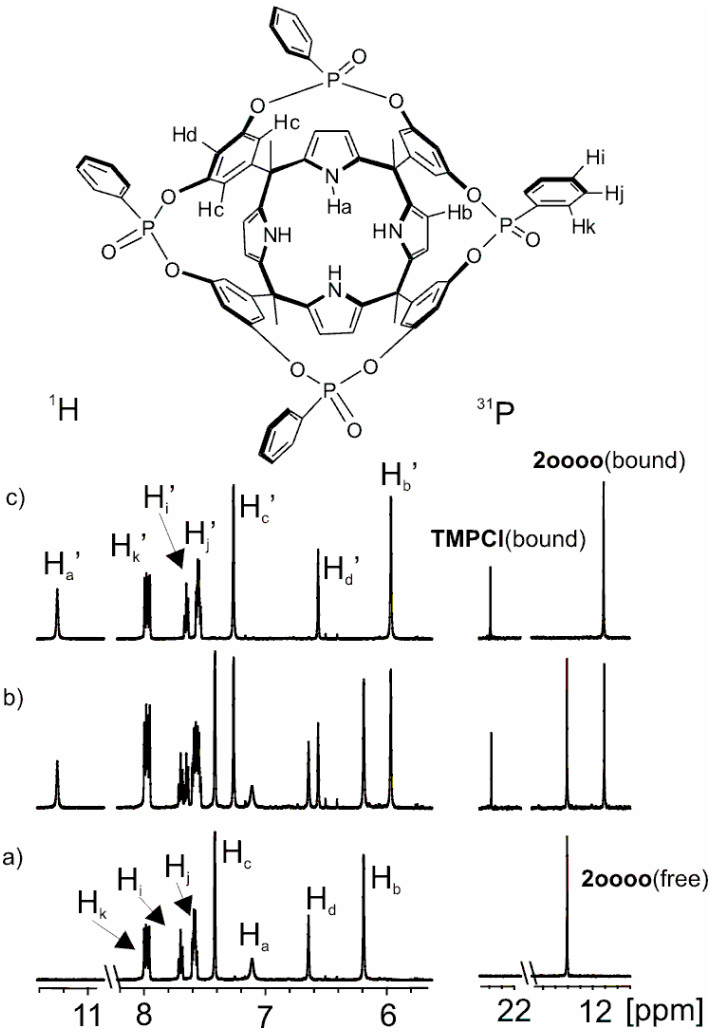

Figure 3. 5. Selected regions of the ^{1}H and ^{31}P NMR spectra of the titration of **2oooo** with TMPCl: a) 0 equivalents; b) 0.5 equivalents; and c) 1 equivalent added.

A 2D ROESY experiment carried out in DCM solution containing equimolar amounts of **2oooo** and TMPCl revealed the existence of negative cross peaks between the doublet of the methyl protons of TMP and the β-pyrrolic protons (H_b) of the receptor. Consequently, we postulate that the preferred binding geometry for the TMPCl@**2oooo** complex in solution is that of a receptor *separated* ion-pair arrangement (Figure 3.6).

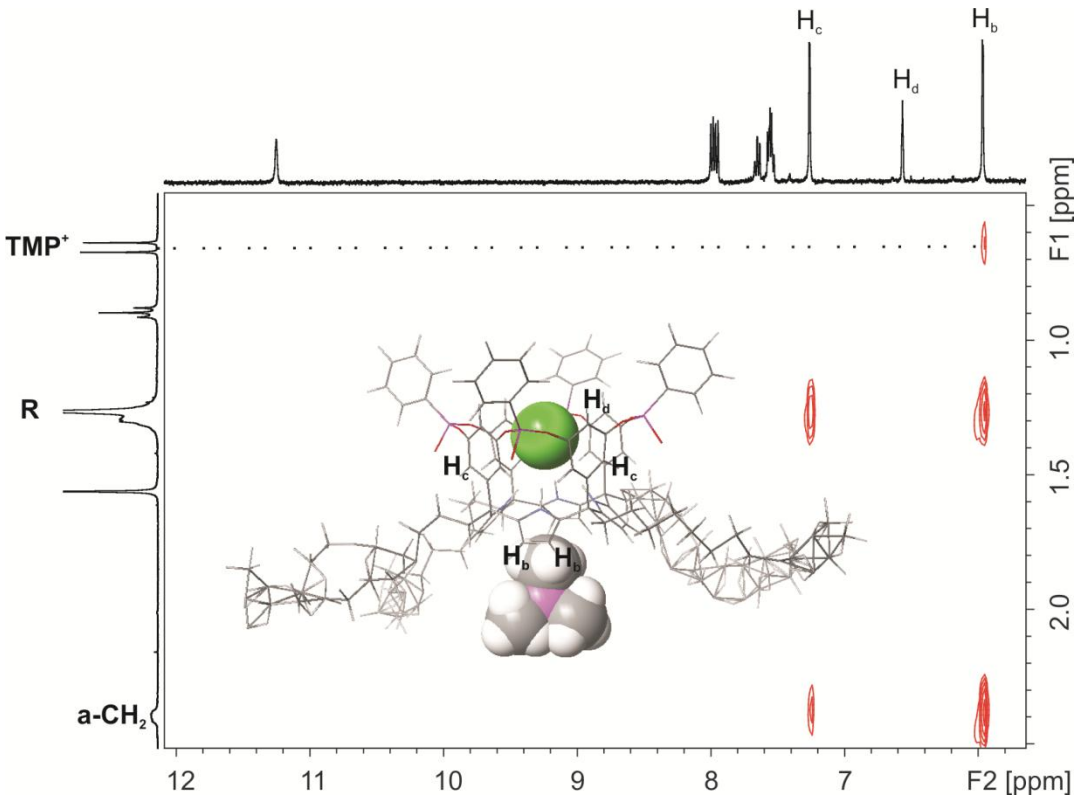

Figure 3.6. Selected region of the 2D-ROESY experiment performed on a dichloromethane solution of **2oooo** with 1.0 equivalents of TMPCl. The observed intermolecular NOE cross-peak between the protons of TMP^+ and the β-pyrrolic protons (Hb) of bound **2oooo** indicate that the cation is located in the calix[4]pyrrole cup opposite to the bound chloride.

^1H and ^{31}P NMR titration experiments performed between **2oooi** and TMPCl indicated that the binding process occurs following the same dynamic and thermodynamic trends observed for the formation of TMPCl@**2oooo**. Interestingly, when 1 equivalent of TMPCl is added to a dichloromethane solution of **2oooi,** the chemical shift value of the signal corresponding to the methyl groups of the TMP cation is still noticeably upfield shifted ($\delta \approx 0.663$ ppm; $\Delta\delta = -1.43$ ppm).

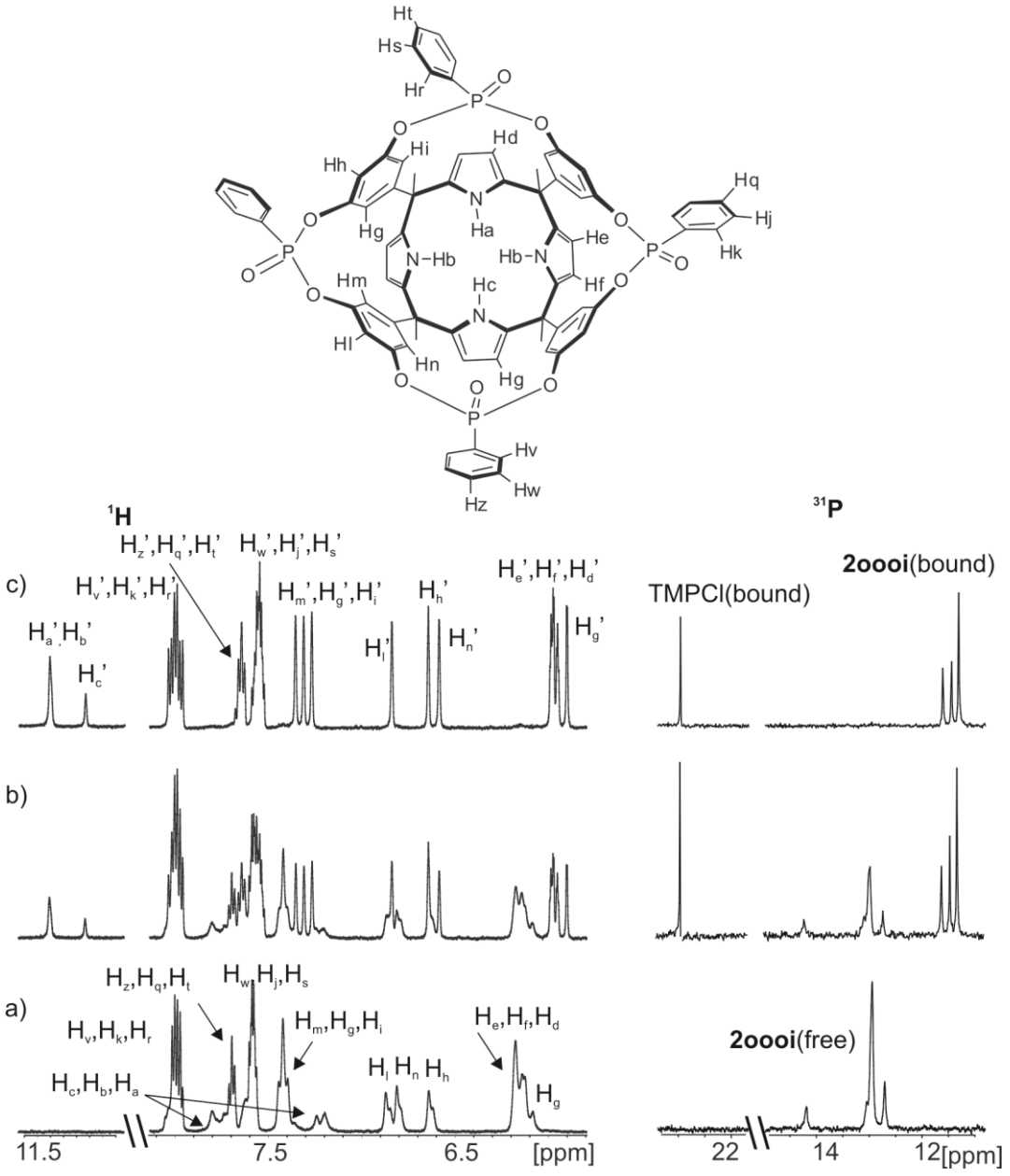

Figure 3.7. Selected regions of the ^{1}H-NMR and ^{31}P-NMR spectra of a dichloromethane solution of **2oooi** after the addition of a) 0, b) 0.5 and c) 1.0 equivalent of TMPCl.

A 2D ROESY experiment performed with a dichloromethane solution containing equimolar amounts of the receptors **2oooi** and TMPCl salt displayed intense cross-peaks between the signal of the methyl protons of TMP and the signals of the β-pyrrole protons of the receptors. Taken together, these results suggest that the TMPCl@**2oooi** complex also adopts a *separated* ion-pair arrangement in solution. The presence of a single phosphonate group with an oxygen atom inwardly

oriented is not enough to induce the switching in the binding mode of the complex (Figure 3.8).

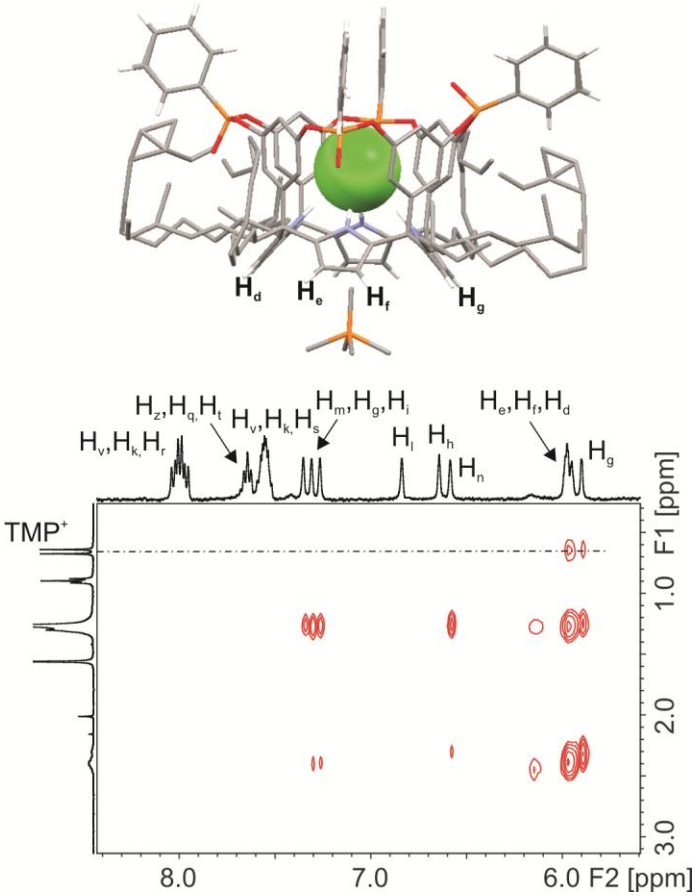

Figure 3.8. Solid state structure of the ion-pair complex TMPCl@**2oooi** and selected region of the 2D-ROESY experiment of a dichloromethane solution containing an equimolar mixture of **2oooi** and TMPCl.

The formation of the ion-pair complex TMPCl@**2oooi** in solution was also supported by solid state data (Figure 3.8). Single crystals suitable for X-ray diffraction analysis grew from a dichloromethane solution containing equimolar amounts of **2oooi** and TMPCl. The solution of the diffraction data revealed the existence of the inclusion complex TMPCl@**2oooi** also in the solid state. Unfortunately, the columnar packing of the TMPCl@**2oooi** complex in the crystal did not provide an unambiguous answer for the preferred placement of the TMP cation with respect the deep included anion in the solid state.

Pairwise competitive binding experiments were carried out in order to measure the relative binding affinities of the two stereoisomers **2** with TMPCl. We prepared ~1

mM solutions containing a close to equimolar mixture of the two *tetra*-phosphonate receptors **2** and TMPCl in deuterated dichloromethane. The binding process was monitored using ^{1}H and ^{31}P NMR spectroscopy, similarly to the case of the direct titration experiments commented above. The interaction of receptors **2** with chloride induced a considerable downfield shift of the NH pyrrole signals. We observed different sets of signals corresponding to the NH protons hydrogen bonded to chloride for each TMPCl@**2** complexes (Figure 3.9). In the aromatic region of the ^{1}H NMR spectra of the mixture, we also could identify separate signals for some protons of the free and bound state of both receptors. In addition, the ^{31}P NMR spectrum displayed different signals for the phosphorus atoms of the two receptors, both in the free and bound state.

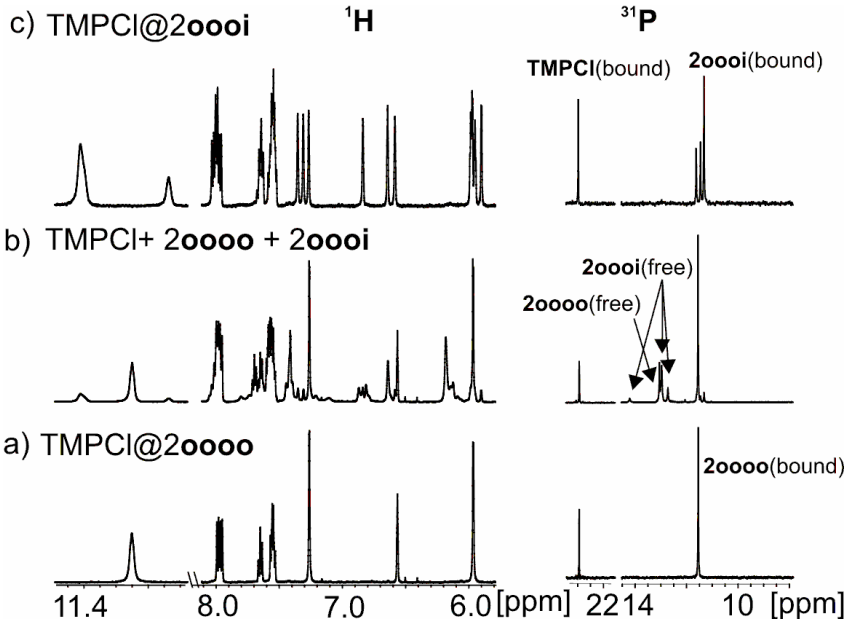

Figure 3.9. Selected regions of the ^{1}H and ^{31}P NMR spectra of: a) TMPCl@**2oooo**; b) TMPCl + **2oooo** + **2oooi**; and c) TMPCl@**2oooi**.

The integral values of selected proton signals for each receptor, in both free and bound state, were used to calculate the ratio of association constant values. We measured that $K_{a,exp}$(TMPCl@**2oooo**) is approximately four-fold larger than $K_{a,exp}$(TMPCl@**2oooi**). This result did not surprise us. As we already learned through the study of simpler *bis*-phosphonate calix[4]pyrroles **1**, the magnitude of the binding constant for the ion-paired complex TMPCl@**1** are correlated well with the strengh of the initial interaction of the chloride anion to form the 1:1 anionic

complex. In turn, this latter interaction strenght is strongly dependent on the spatial orientation of the phosphonate bridging groups, while the complexation of the TMP cation provides an almost constant energetic contribution to the overall binding. We have assigned to the existence of repulsive electrostatic interactions between the partial negative charges of the inwardly directed oxygen atoms of the phosphonate group and their dipoles with the included chloride a destabilizing effect. Consequently, the TMPCl@**2oooi** complex was expected to be energetically less favorable than the TMPCl@**2oooo** complex. The value obtained for the ratio of stability of the tetraphosphonato receptor series encouraged us to perform additional competitive experiments between the *tetra*-phosphonate calix[4]pyrrole **2oooo** and the simpler *bis*-phosphonate stereoisomer **1oo** counterparts. We selected TMPCl as a guest and performed a pairwise competitive experiment. The ^{1}H NMR and ^{31}P NMR spectra of a DCM solution containing an equimolar mixture of the two receptors and TMPCl showed protons signals corresponding to the exclusive formation of the TMPCl@**2oooo** complex and the expected signals for the protons of **1oo** free cavitand. Consequently, we estimated that $K_{a,exp}$(TMPCl@**2oooo**) must be 100-fold larger than $K_{a,exp}$(TMPCl@**1oo**). It is worth noting that in the ^{31}P NMR spectrum of the above mixture the signal of the phosphorus atom for **1oo** showed a reduced upfiled-shift ($\Delta\delta$ = - 0.74 ppm) compared to the chemical shift measured in a solution containing **1oo** alone. Most likely, this shift is produced by the existence of aggregation processes between the *bis* and *tetra*-phosphonate receptors.

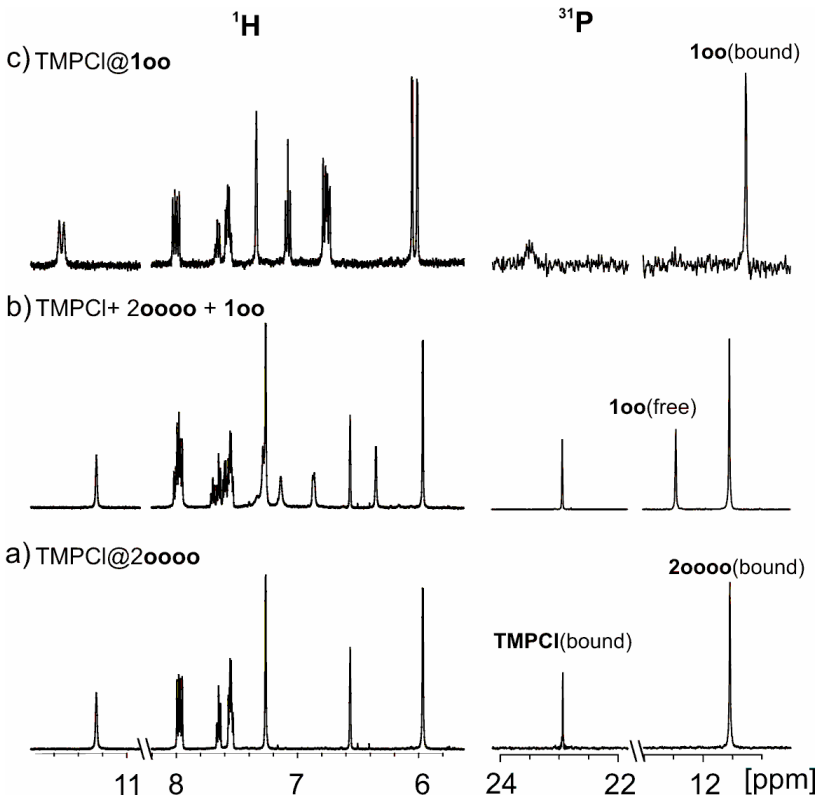

Figure 3.10. Selected regions of the ^{1}H and ^{31}P NMR spectra at 298 K of DCM solutions of: a) TMPCl@**2oooo**; b) TMPCl + **2oooo** + **1oo**; and c) TMPCl@**1oo**.

An analogous competitive experiment performed between **2oooi** and **1oo** using TMPCl as guest was used to calculate $K_{a,exp}$(TMPCl@**2ooo**), that is approximately 80-fold larger than $K_{a,exp}$(TMPCl@**1oo**).

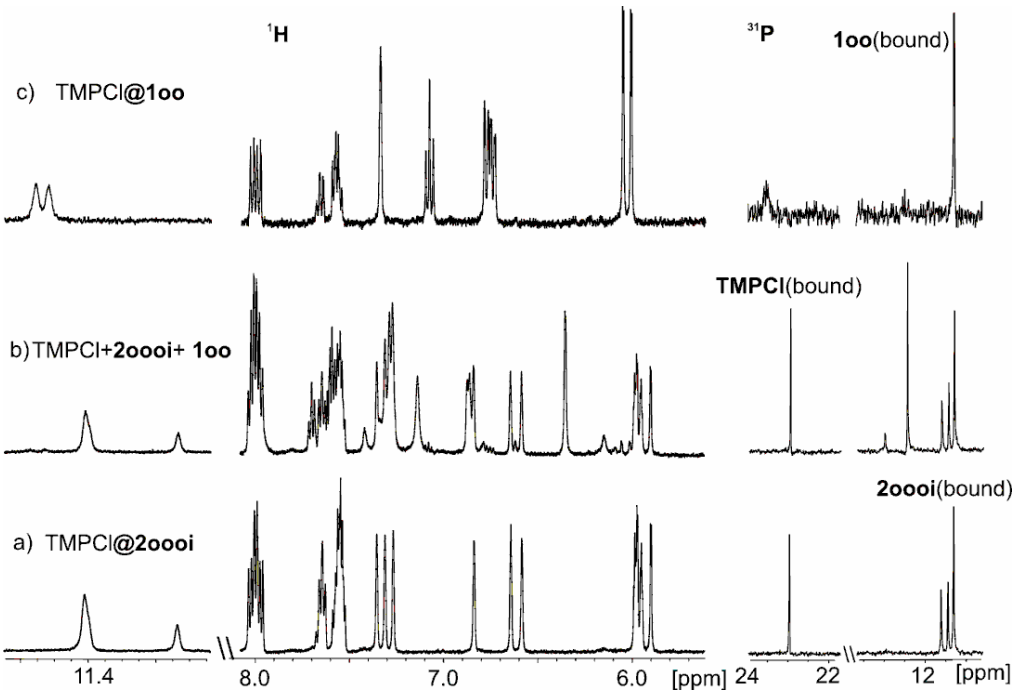

Figure 3.11. Selected regions of the ^{1}H-NMR and ^{31}P-NMR spectra of DCM-d_2 solutions of a) TMPCl@**2oooi**; b) an equimolar mixture of **2oooi**, **1oo** and TMPCl; c) TMPCl@**1oo.**

The results obtained in the experiments described above testify the superior binding properties of the *tetra*-phosphonate calix[4]pyrroles **2** receptors for the ion-paired complexation of TMPCl with respect to the *bis*-phosphonates **1**. We attribute the higher binding strength displayed by **2** in the complexation of TMPCl to the existence of an increased number of electrostatic interactions and the higher conformational rigidity imparted by the four phosphonate groups (instead of two) in the complexation of the TMPCl salt. These effects are maximized in the case of the **2oooo** stereoisomer. ESI-MS experiments performed using negative and positive detection modes and capillary voltages in the range of 0-500 V confirmed the NMR data. We also performed isothermal titration calorimetry (ITC) experiments at 298 K to quantify the binding constants of the receptor series **2** with TMPCl in DCM solution. We obtained a good fit for the integrated heat data to the theoretical binding isotherm for the formation of a 1:1 complex. We calculated that $K_{a,exp}$(TMPCl@**2oooo**) is 5 ± 3.5 × 10^{7} M^{-1} while $K_{a,exp}$(TMPCl@**2oooi**) is 1.5 ± 0.2 × 10^{7} M^{-1}. The ratio of the experimentally determined binding constant values is in complete agreement with the results obtained from the NMR pairwise competitive experiments. These experiments were also useful for the calculation of values of the thermodynamic constants of the complexation processes. In general, the

binding processes showed a small heat release (heat *vs* time). The complexation of TMPCl by the receptors series **2** was both enthalpically and entropically driven. The strong and favourable entropic component measured for the two complexation processes suggests that solvation/desolvation effects must play a crucial role.

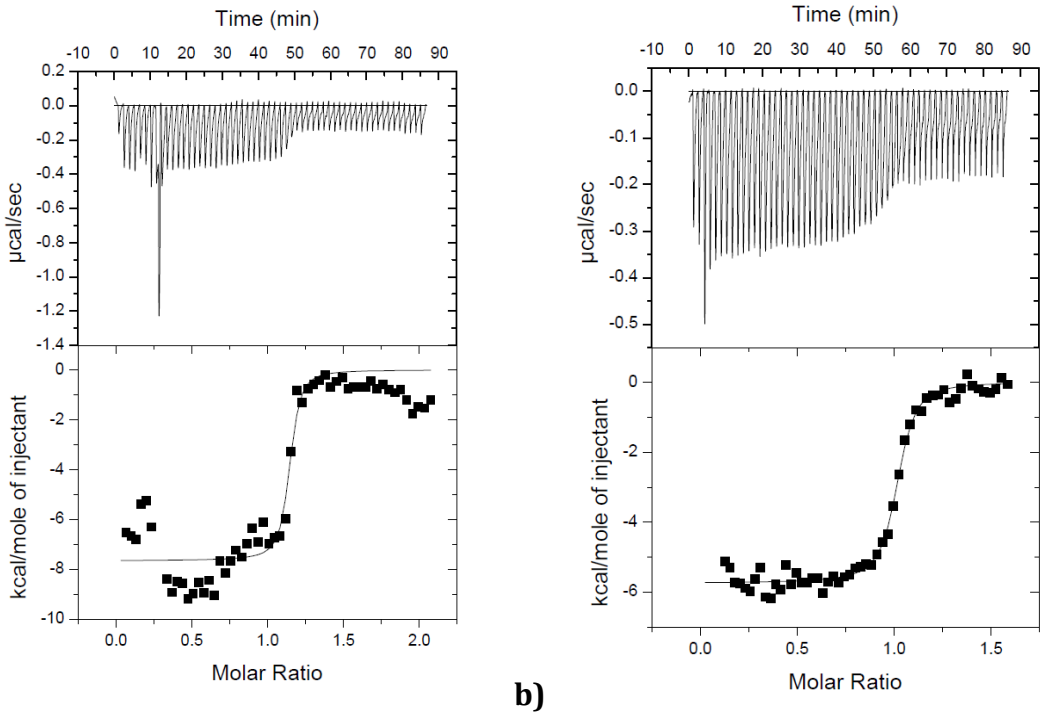

Figure 3.12. Top: Raw data heat vs time. Bottom: Fit of the integrated heat (squares) to the theoretical binding isotherm for a 1:1 complex formation of a)TMPCl titrated into a DCM solution of **2oooo** and b)TMPCl titrated into a DCM solution of **2oooi**. The titrations were performed at 25 °C. The integrated heat for each injection is plotted against the concentrations' ratio TMPCl/**2**.

We were also interested in evaluating the effect that the addition of two phosphonate groups at the upper rim of the calix[4]pyrrole could have on the complexation of a primary ammonium salt i.e. octylammonium chloride (OAMCl). We knew that OAMCl established hydrogen bonds, CH··O and cation-dipole interactions with the two P=O groups of the bisphosphonate **1ii** diastereoisomers. In this sense the OAMCl@**1ii** complex is the more thermodynamically stable complex formed by the *bis*-phosphonate receptor series **1**. These favorable interactions are responsible for the exclusive *close-contact* arrangement of the ion-pair in the OAMCl@**1ii** complex. We performed ^{1}H and ^{31}P NMR titration experiments by sequential addition of two doses of 0.5 equivalent of OAMCl to

individual 1 mM DCM-d_2 solutions of stereoisomers **2oooo** and **2oooi**. In both cases, the complexation process showed slow exchange on the ^{1}H NMR timescale and the addition of 1 equivalent of the salt induced the exclusive observation of proton signals corresponding to the bound host. This latter observation indicated that the binding constant values for the 1:1 complexes OAMCl@**2** are higher than 10^4 M^{-1}. A pairwise competitive experiments of the two stereoisomers with OAMCl evidenced that the **2oooi** stereoisomer was a slightly better receptor for the primary ammonium chloride salts than the **2oooo** stereoisomer (Figure 3.13). Integration of selected proton signals allowed us to calculated the following relationship: $K_{a,exp}$ (OAMCl@**2oooi**) > 2 $K_{a,exp}$ (OAMCl@**2oooo**).

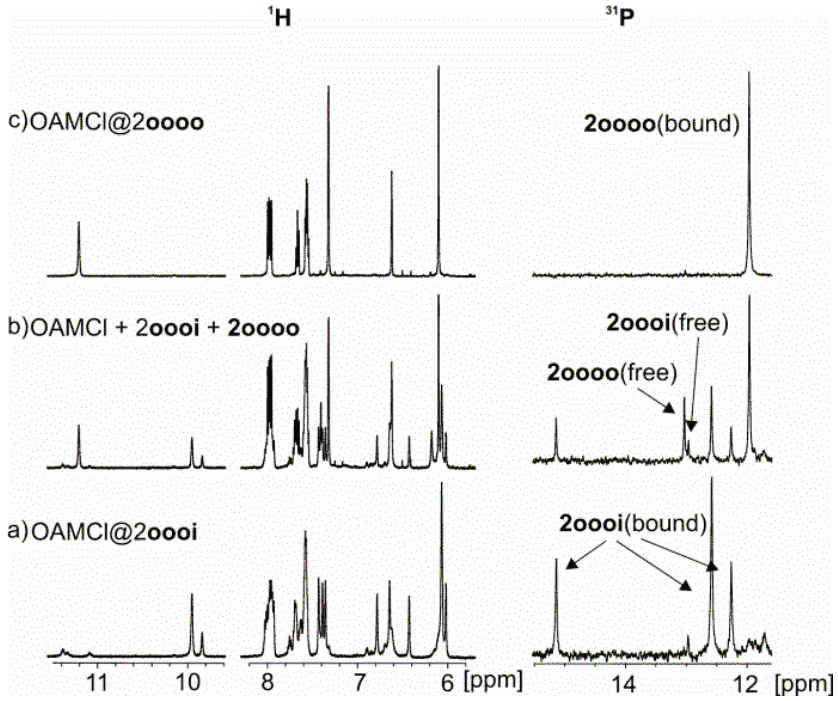

Figure 3.13. Selected regions of the ^{1}H and ^{31}P NMR spectra of DCM-d_2 solutions of: a) OAMCl@**2oooi**; b) equimolar mixture of OAMCl + **2oooi** + **2oooo**; and c) OAMCl @**2oooo**.

The ^{1}H NMR spectrum of the OAMCl@**2oooi** complex indicated that the signal of the methylene protons in α position with respect to the nitrogen atom of the OAMCl shifted upfield to δ = 2.55 ppm (Δδ = - 0.45 ppm). In the case of the **2oooo** receptor the same methylene signal resonates at δ = 0.79 pppm (Δδ = - 2.2 ppm). Taken in concert, these observations strongly support the existence in solution of a significant increase in the binding geometry having a *close-contact* ion-pair

arrangement for the complex formed by *tetra*-phosphonate calix[4]pyrroles **2oooi** with OAMCl compared to the OAMCl@**2oooo** complex. Moreover, the difference in the magnitudes of the association constants we determined for the OAMCl@**2oooi** and OAMCl@**2oooo** is comparable with the *bis*-phosphonate calix[4]pyrroles. The association constant value for the OAMCl@**1io** complex was two-fold higher than OAMCl@**1oo**. A pairwise competitive experiment performed using a ~ 1 mM solution of the **2oooi** and **1io** receptors containing 1 equivalent of OAMCl demonstrated the superior binding properties of the **2oooi** receptor, $K_{a,exp}$(OAMCl@**2oooi**) > 10 $K_{a,exp}$ (OAMCl@**1io**). This is not a surprising result if one simply considers the conformational advantages installed in the *tetra*-phosphonate receptors compared to the *bis*-phosphonate cavitands. Finally, we performed a pairwise competitive experiment in an equimolar mixture of the *tetra* phosphonate calix[4]pyrrole **2oooi**, the *bis* phosphonate calix[4]pyrrole **1ii** and OAMCl. We calculated the following relationship for the stability constants $K_{a,exp}$ (OAMCl@**1ii**) > 2 $K_{a,exp}$ (OAMCl@**2oooi**). This result indicates that the conformational rigidity (preorganization) of the receptor is not the only factor that is important for the increase in the binding affinity of the OAMCl with phosphonate calix[4]pyrroles. Clearly, the existence of ditopic electrostatic interactions between the primary alkylammmonium cation and two phosphonate inwardly directed groups outperforms the conformational advantage (Figure 3.14).

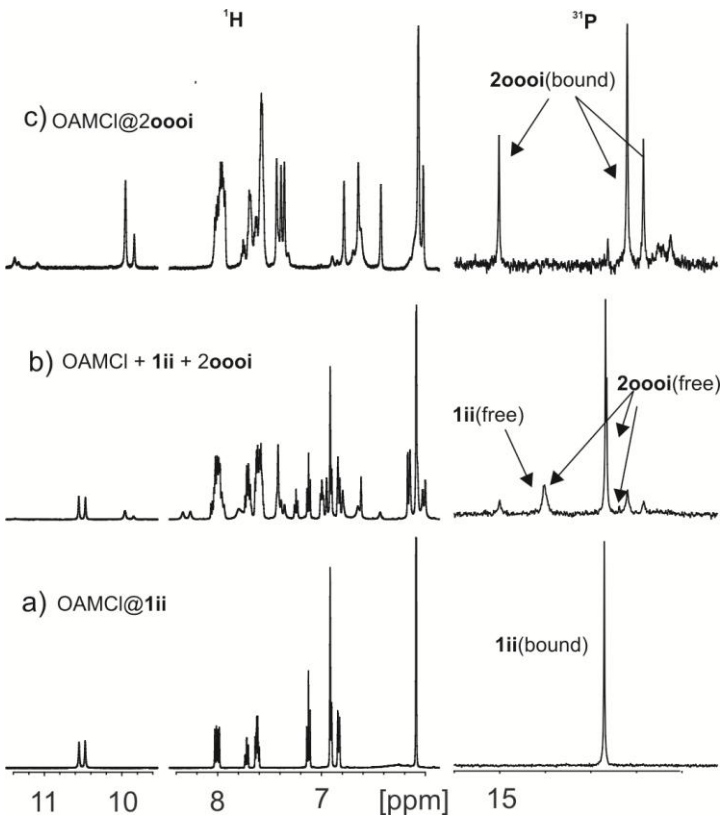

Figure 3.14. Selected regions of the ^{1}H and ^{31}P NMR spectra of DCM solutions of: a) OAMCl@**1ii**; b) equimolar mixture of OAMCl + **1ii** + **2oooi**; and c) OAMCl @**2oooi**.

3.2.4 Studies of *tetra*-phosphonate calix[4]pyrroles as salt solubilizers and membrane transporters

The ion-pair recognition process occurring between *tetra* phosphonate calix[4]pyrroles **2** and quaternary ammonium salts was further investigated with acetylcholine chloride (AcChCl), a biological active molecule involved in processes of transport of neuronal information[15,16] and memory[17]. Several examples of macrocycles are already reported in literature for the recognition in solution of this guest[18] like cyclophane hosts[19,20], calixarenes[21] and resorcarenes[22,23,24,25]. Direct binding experiments between the **2** serie with AcChCl showed dynamics, thermodynamics and geometries for AcChCl@**2** similar to TMPCl@**2** complexes. ^{1}H and ^{31}P NMR experiments show association constants > 10^{4} M^{-1}. The AcCh cation, although has different size respect to TMP cation, is easily accommodated in the calix[4]pyrroles cavity. We were interested in evaluating the ability of *tetra* phosphonate calix[4]pyrroles **2** in the extraction of acetylcholine chloride from aqueous solution and in the transport through membranes. We chose the

stereoisomer **2oooi** since it was the one available in higher amount at the moment of the experiments.

We already discussed in the *General Introduction* of Chapter 1 that ion pairing is strongly dependent on the polarity of the solvent. Thus, the general equation for the transfer of ion pairs between immiscible solvents involves the equilibrium:

$$C^+_{aq} + A^-_{aq} \rightleftharpoons C^+ A^-_{org} \qquad (1)$$

where C^+_{aq} and A^-_{aq} represent the individual cation and anion in the aqueous phase and $C^+A^-_{org}$ the cation and anion involved in the formation of the ion pair complex, in the organic phase. Subsequently, the extraction of acetylcholine chloride ($AcCh^+Cl^-$) into an organic phase mediated by a salt receptor (**2oooi** in our case) occurs through a two-step process. The first equilibrium, K_{exIP}, involves partitioning of the salt into the organic phase and the second equilibrium, K_a, concerns association of the partitioned salt with the receptor. These steps occur simultaneously and involve the Cl anion binding through the pyrrolic NHs of the receptor and the AcCh cation accommodation in the electron rich cup of the calix[4]pyrrole[26].

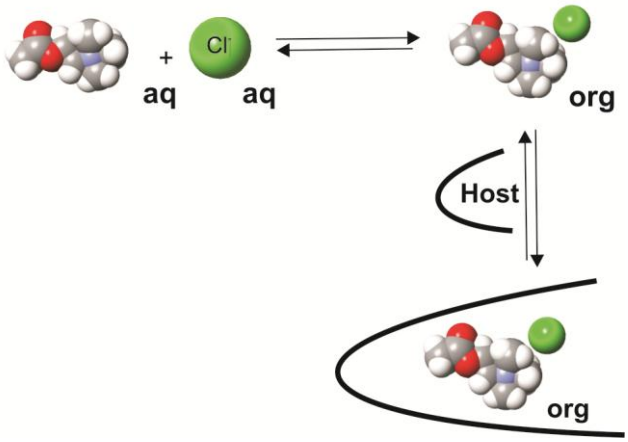

Figure 3.15. Two-process step for the extraction of AcChCl using a salt receptor.

The ability displayed by ion-pairs receptors **2** to increase the apparent solubility of salts in organic solvents (as shown for the cases of TMPCl and AcChCl) is based on these equilbria and bodes well for their application in the development of salt solubilization agents.[27] We also wanted to evaluate the ability of **2oooi** as ion-pair

carrier (AcChCl) in transport experiments between two aqueous solutions separated by a dichloromethane layer acting as a simple model of a lipohilic liquid membrane.[28,29] The U-tube-type Pressman cell with a "dichloromethane" membrane was used to study the transport of AcChl chloride and is represented in Figure 3.16. It consists of a U-tube with an "*α*" or "*source phase*" consisting of 10 mL of a 5.78 mM water solution of AcChCl. And a "*β*" or "*receiving phase*", containing 10 mL of MilliQ water. The organic transport layer consisted on a dichloromethane solution, placed between the two aqueous phases, 10-fold more diluted (0.5 mM) than the source phase and exclusively containing receptor **2oooi**. The U-tube-type cell was equipped with a magnetic stirrer to ensure constant stirring of the membrane phase. We followed the transport of AcChl chloride between the two arms (limbs) of the cell using conductimetry measurements. The choice of this technique was dictated by the advantages provided by conductivity measurements in the quantification of the concentration of ion-pairs in solution compared to other techniques like UV-vis or HPLC. Conductimeters are quite inexpensive and commercial available. The new generation of advanced instruments ensures high accuracy in the conductivity measurements. Moreover, conductimetry can be applied for the determination of concentrations of all electrolytes in almost any solvent and over wide ranges of temperature and pressure. The sensibility of the new conductimeters allows measurements to be performed at relatively low concentrations of the electrolytes (around 10^{-4} M).

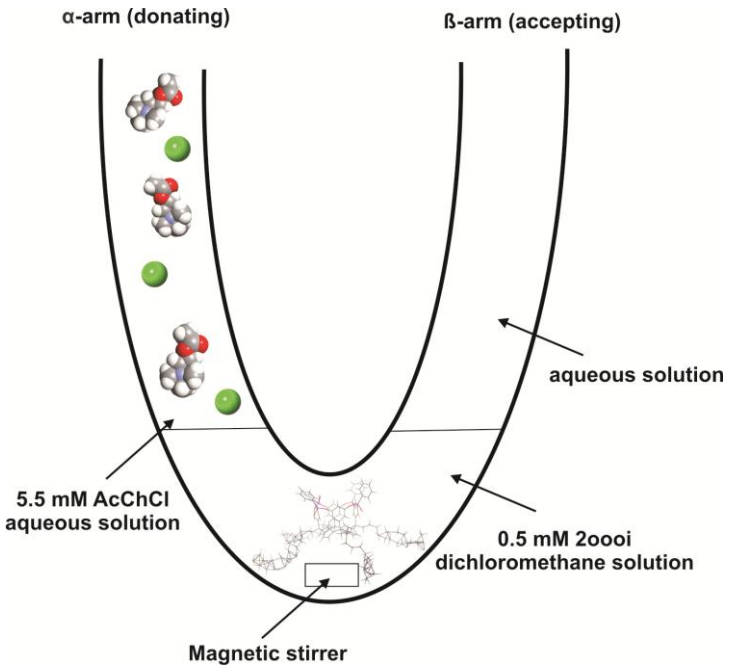

Figure 3.16. U-tube-type cell used for the study of transport experiments of a 5.5 mM aqueous solution of acetylcholine chloride through a 0.5 mM dichloromethane solution of **2oooi**.

The transport experiment consisted in monitoring the change in the conductimetry values at both arms of the U-tube type cell during 24 hours. Preliminary conductometric measurements performed as blank with the α and β arms containing only MilliQ water and no receptor in the organic phase, afforded conductivity values (Λ) < 1 Siemens. The measured conductivity of 5.5 mM aqueous solution of AcChCl resulted of 352 Siemens.

In the initial phases of the transport experiment, the AcChCl molecules diffuse quickly from the donating phase solution to the organic layer resulting in a decrease of conductivity from 352 Siemens to 112 Siemens. We observed an analogous drop of conductance value for the source phase in the control experiment performed in the absence of added receptor in the organic phase. We must conclude that the liquid/liquid partitioning process must play the most important role in the extraction process between the source and membrane layer for both the reference and the receptor mediated systems.

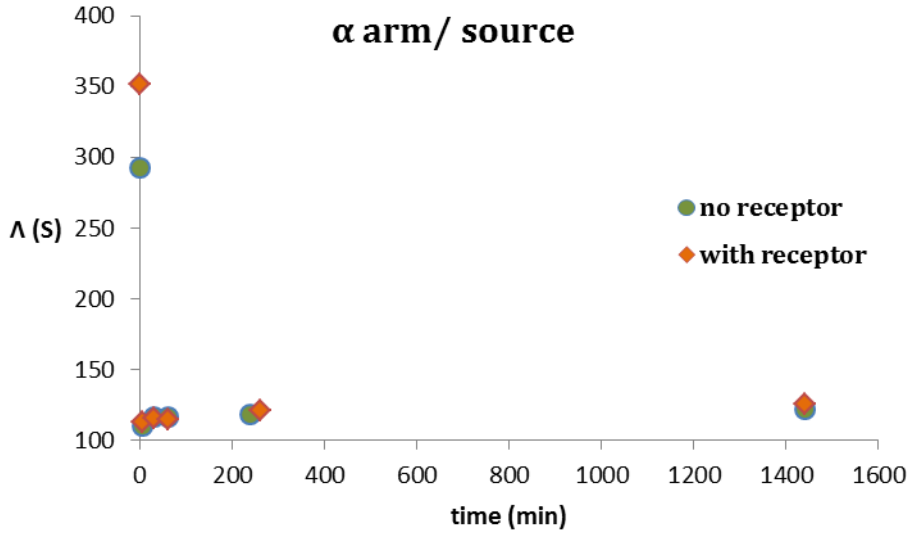

Figure 3.17. Conductance measurements of acetylcholine chloride aqueous solution at the α arm (source aqueous solution) of the U-tube-type cell.

In the receiving phase the transport of guest in absence of host seems to be slighty slower than in the presence of host, although in both cases similar amounts of acetylcholine chloride are extracted at the end of the transport experiment. This result might suggest that the receptor has a moderate effect on the rate of guest transport through the membrane. Linear plots of conductance variation versus time for the receiving *β phase* at the beginning of the experiment both in the absence and in presence of the receptor indicated that the transport processes reaches equilibrium after two hours. Probably, the concentrations we selected for the source and the membrane phases were too low to measure any relevant difference or even significant values for transport and extraction in the experiments we performed.

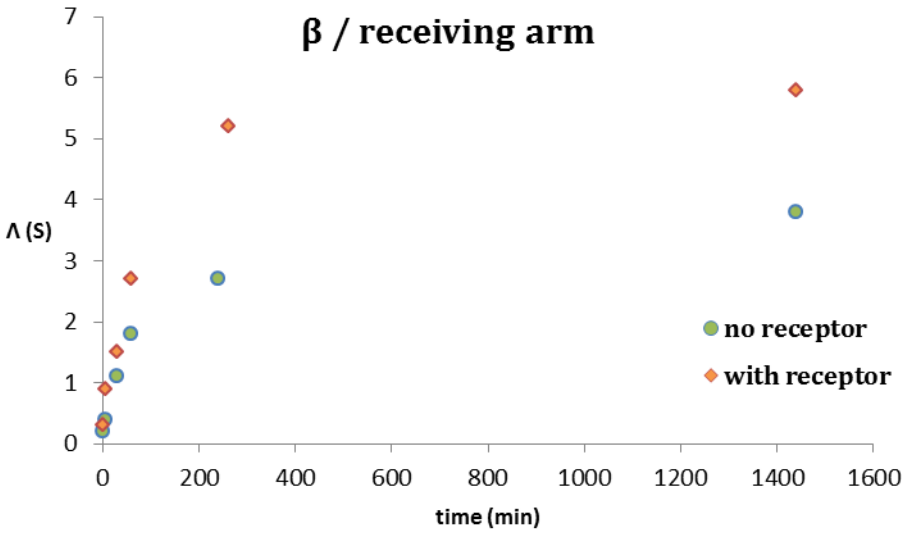

Figure 3.18. Conductance measurements of acetylcholine chloride aqueous solution at the β arm (receiving aqueous solution) of the U-tube.

We must conclude that, at the concentration at which we worked, *tetra*-phosphonate calix[4]pyrroles did not result excellent membrane carriers. Moreover, the strong binding between **2oooi** and the acetylcholine chloride does not favor the release of the guest into the receiving phase.

3.2.5 Solvent effect : binding studies in acetonitrile

The experiments performed in dichloromethane allowed us to study the tetra-phosphonate receptors **2** as ion-pair receptors. In polar solvents, such as acetonitrile (ACN), it is possible to analyze the binding and selectivity of the receptors **2** towards chloride without having to worry about the effect of the cation. Binding studies perfomed in ACN allowed us to compare the binding strength of a *tetra*-phosphonate cavitand **2** versus a bis-phosphonate cavitand **1**. We chose to compite the **2oooo** and **1oo** stereoisomers, because they were the best receptors in dichloromethane solution among their series of stereoisomers. The solubility of receptor **2oooo** in ACN at 298 K is 0.1 mg/mL (~ 0.1 mM). While **2oooi** is not soluble enough to be detected by ^{1}H NMR spectroscopy. The ^{1}H NMR spectrum of receptor **2oooo** in ACN solution suggested that this stereoisomer adopts the cone conformation and includes one solvent yielding the ACN@**2oooo** complex. The inclusion of one molecule of ACN in the aromatic cavity of **2oooo** was also observed

in its solid state structure. The addition of less than 1 equivalent of TMPCl produced a slow chemical exchange on NMR timescale between the free and bound receptor. From the integral values of selected signals for the protons in the free and bound receptors we calculated the binding constant value as $K_{a,exp}$ (Cl@**2oooo**) = 1.4±2 × 10^4 M^{-1}. As expected, the magnitude of the binding constant is significantly reduced compared to the value we estimated/determined in DCM solution. The TMP cation is not significantly involved in the formation of the complex, as can be inferred from the slight upfield shift experienced by the protons of the TMP cation (δ = 1.79 ppm; Δδ = - 0.06 ppm). However, it is important to note that the association constant value for TMPCl@**2oooo** complex (1.4±2 × 10^4 M^{-1}) is two-fold larger than the one calculated the *bis*-phosphonate cavitand **1oo** in the same solvent (7±2 x 10^3 M^{-1}). A pairwise competitive experiment between **2oooo** and **1oo** with TMPCl was performed to corroborate the ratio of the stability constants. The integration values of signals for the protons in free and bound **2oooo** and **1oo** after the addition of ~ 1 equivalent of TMPCl were used to calculated a value of $K_{a,exp}$(TMPCl@**2oooo**)/ $K_{a,exp}$(TMPCl@**1oo**) ~ 6.0, which is in line with the result derived from direct titration experiment of each stereoisomer with TMPCl (Figure 3.19).

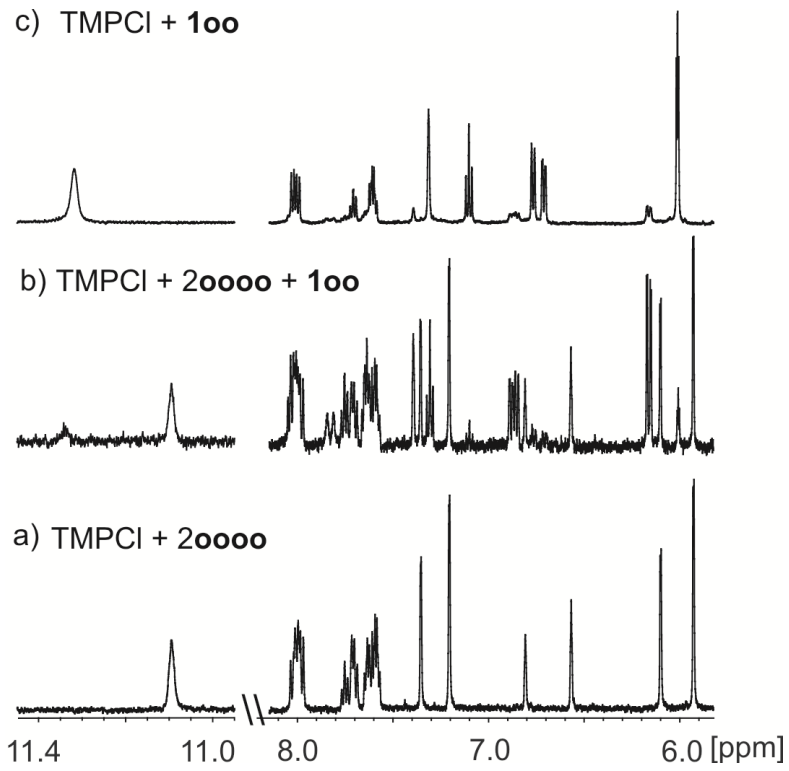

Figure 3.19. Selected regions of the ^{1}H NMR spectrum of: a) TMPCl + 4oooo; b) TMPCl + 2oooo + 1oo; and c) TMPCl + 1oo in acetonitrile-d_3.

3. 3 Conclusions

A series of two *tetra*-phosphonate cavitands based on calix[4]pyrrole scaffold have been synthesized. The two diastereoisomers form 1:1 complexes with alkylammonium/ammonium chloride salts with association constants larger than 10^4 M^{-1}. In the case of TMPCl as guest, the existence of one oxygen pointing inside the calix[4]pyrrole cavity in the stereoisomer **2oooi** reduces the strength of binding, probably due to the existence of electrostatic repulsion between the inwardly oriented oxygen and the included chloride. These data confirm the fully outwardly oriented phosphonate stereoisomer **2oooo** the best receptor for ion pairs between the *tetra*-phosphonate series. Subsequently, the geometry adopted by TMPCl@**2** complexes is a *separated* arrangement in which the TMP cation is located in the electron rich cup of the calix[4]pyrrole. When OAMCl is used as guest, the OAM cation is preferentially locked in the upper rim of **2oooi** in which it establishes hydrogen bonding interactions with the inwardly oriented phosphonate group. In this case, the OAMCl@**2oooi** complex adopts a *close contact*

geometry. In polar solvents like acetonitrile the association constants are strongly reduced as consequence of the ion pair dissociation and removal of the cation effect on the overall binding. Competitive experiments performed between *tetra*-phosphonate and *bis*-phosphonate calix[4]pyrroles toward alkylammonium/ammonium chloride salts reveal the former having association constants 100 fold (alkylammonium chloride salts) and 10 fold higher (ammonium chloride salts) than the latter.

3. 4 Experimental Section

General information and instrumentation

All syntheses were carried out using chemicals as purchased from commercial sources unless otherwise noted. When required, dried and deoxygenated solvents supplied by a Solvent Purification System (SPS-200-6) were used. Thin-layer chromatography (TLC) and flash column chromatography were performed with DC-Alufolien Kieselgel 60 F254 (Merck) and silica gel 60A for chromatography (SDS) respectively. ^{1}H and ^{31}P NMR spectra were recorded on a Bruker Avance 400 (400.1 MHz for ^{1}H NMR) and Bruker Avance 500 (500.1 MHz for ^{1}H NMR) ultrashield spectrometer; Mass Spectrometry experiments on a LCT Premier, Waters-Micromass ESI or Autoflex, Bruker Daltonics MALDI. FT-IR measurements were carried out on a Bruker Optics FTIR Alpha spectrometer equipped with a DTGS detector, KBr beam splitter at 4 cm^{-1} resolution. Isothermal titration calorimetry experiments (ITC) were performed using a Microcal VP-ITC Microcalorimeter.

Synthesis

To a solution of calix[4]pyrrole **3** (500 mg, 0.352mmol) in dry THF (10 mL) and freshly distilled triethylamine (0.980 mL, 7.03 mmol), phenylphosphonic dichloride (0.247 mL, 1.758 mmol) was added dropwise under argon atmosphere. The reaction mixture was stirred for 2 hrs at room temperature. The solvent was

removed *in vacuo* and water (50 mL) was added. The grey precipitate was filtered off and purified by Combiflash (SiO_2; CH_2Cl_2) in order to remove the oligomers/polymers formed during the reaction with 39% overall yield. The fraction containing the two diastereomers was purified by semipreparative HPLC (Spherisorb silica 250 × 20 mm, 5 µm; SiO_2; CH_2Cl_2 : Hexane 60:40; flow rate: 15 mL/min) to yield each separated isomer **2oooo** and **2oooi** as a white solid (Figure 3. 20, retention times: 4.3 minutes and 5.3 minutes, respectively). The isomers can be further purified by crystallization from acetonitrile.

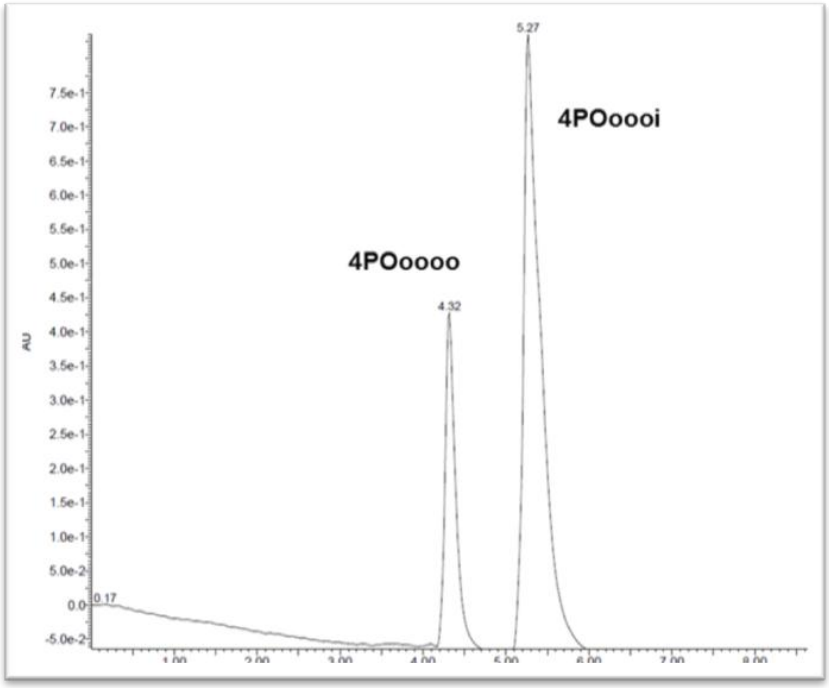

Figure 3. 20 Normal phase - HPLC chromatogram of tetra-phosphonates reaction crude using a mixture of DCM : Hexane 60 : 40 as eluent.

Experimental data **2oooo** (white solid, 3%). ^{1}H-NMR (400 MHz, $CDCl_3$, 25°C): δ (ppm) = 7.94 (m, $^3J_{H-P}$ ~ 14 Hz, $^3J_{H-H}$ ~ 7.3 Hz, $^4J_{H-H}$ ~ 1.2 Hz, 8H), 7.65 (m, $^3J_{H-H}$ ~ 7.3 Hz, $^4J_{H-H} \approx {}^5J_{H-P}$ ~ 1.2 Hz, 4H), 7.53 (m, $^3J_{H-H}$ ~ 7.3 Hz, $^4J_{H-P}$ ~ 4.8 Hz, 8H), 7.53 (bs, 4H), 7.37 (d, $^4J_{H-H}$ ~ 1.75 Hz, 8H), 6.56 (t, $^4J_{H-H}$ ~ 1.75 Hz, 4H), 6.17 (d, $^4J_{H-H}$ ~ 2.27 Hz, 8H), 2.45 (m, 8H), 1.27 (m, 80H), 0.88 (t, $^3J_{H-H}$ ~ 7.0 Hz, 12H). ^{31}P-NMR (400 MHz, $CDCl_3$, 25°C): δ = (ppm) 13.63. HR-MALDI-MS: *m/z* calculated for $C_{116}H_{144}N_4O_{12}P_4$ 1908.9731, found 1908.9699; FT-IR ν (cm^{-1}) 2921-2851 (P-CH_{Ar} streaching, 1592 (P-Ar aromatic ring in-plane stretching), 1426 (P-Ar aromatic ring in-plane stretching), 1293 (PO stretching); elemental analysis calculated for

$C_{116}H_{144}N_4O_{12}P_4$ + $C_7H_{12}Cl_2N_2$ (2 x CH_3CN) + CH_2Cl_2 (%): C, 70.17; H, 7.47; N, 3.99; found: C, 69.68; H, 7.99; N, 4.25.

Experimental data **2oooi** (white solid, 9%). ^{1}H-NMR (400 MHz, $CDCl_3$, 25°C): δ (ppm) = 7.97 (m, $^3J_{H-P}$ ~ 14 Hz, $^3J_{H-H}$ ~ 7.3 Hz, $^4J_{H-H}$ ~ 1.2 Hz, 8H), 7.79 (t, $^4J_{H-H}$ ~ 2.3 Hz, 1H), 7.76 (t, $^4J_{H-H}$ ~ 3.0 Hz, 2H), 7.72 (t, $^4J_{H-H}$ ~ 2.3 Hz, 1H), 7.66 (m, $^3J_{H-H}$ ~ 7.3 Hz, $^4J_{H-H} \approx {}^5J_{H-P}$ ~ 1.2 Hz, 4H), 7.55 (m, $^3J_{H-H}$ ~ 7.3 Hz, $^4J_{H-P}$ ~ 4.8 Hz, 8H), 7.46 (t, $^4J_{H-H}$ ~ 2.0 Hz, 2H), 7.46 (t, $^4J_{H-H}$ ~ 2.0 Hz, 2H), 7.46 (t, $^4J_{H-H}$ ~ 2.0 Hz, 2H), 6.81 (t, $^4J_{H-H}$ ~ 2.0 Hz, 2H), 6.77 (t, $^4J_{H-H}$ ~ 3.3 Hz, 2H), 6.55 (t, $^4J_{H-H}$ ~ 3.3 Hz, 2H), 6.18 (d, $^4J_{H-H}$ ~ 2.3 Hz, 2H), 6.15 (t, $^4J_{H-H}$ ~ 3.0 Hz, 2H), 6.12 (t, $^4J_{H-H}$ ~ 3.0 Hz, 2H), 6.08 (d, $^4J_{H-H}$ ~ 2.3 Hz, 2H), 2.45 (m, 8H), 1.27 (m, 80H), 0.89 (t, $^3J_{H-H}$ ~ 7.0 Hz, 12H); ^{31}P-NMR (400 MHz, $CDCl_3$, 25°C): δ (ppm) = 14.37 (P(O)in), 12.96 (P(O)out); HR-MALDI-MS: m/z calculated for $C_{116}H_{144}N_4O_{12}P_4$ 1908.9731, found 1908.9866; FT-IR ν (cm^{-1}) 2921-2850 (P-CH_{Ar} stretching), 1593(P-Ar aromatic ring in-plane stretching), 1430 (P-Ar aromatic ring in-plane stretching), 1294 (PO stretching); elemental analysis calculated for $C_{116}H_{144}N_4O_{12}P_4$ + $C_4H_6N_2$ (2 x CH_3CN) (%): C, 72.34; H, 7.59; N, 4.22; found: C, 71.65; H, 7.34; N, 3.54.

Binding studies

The ESI-MS experiments were carried out using an Electrospray Ionization source combined with a Time-of-Flight mass analyzer (ESI-TOF), operating in negative or positive mode. The samples were continuously sprayed using nitrogen as drying gas (desolvation at 510 L/hr). The injection rate was maintained constant at 20μL/min. The voltage applied at the ESI needle was increased from 0V to 500V, while a voltage of 0V was applied to the cone. The source and desolvation temperatures were set to 120 °C and 200 °C, respectively.

2. 6 References and Notes

[1] Dutasta, J. P. *New Aspects in Phosphorus Chemistry Iv* **2004**, *232*, 55.
[2] Delangle, P.; Mulatier, J. C.; Tinant, B.; Declercq, J. P.; Dutasta, J. P. *Eur. J. Org. Chem.* **2001**, 3695.
[3] Yebeutchou, R. M.; Tancini, F.; Demitri, N.; Geremia, S.; Mendichi, R.; Dalcanale, E. *Angew. Chem., Int. Ed.* **2008**, *47*, 4504.
[4] Melegari, M.; Suman, M.; Pirondini, L.; Moiani, D.; Massera, C.; Ugozzoli, F.; Kalenius, E.; Vainiotalo, P.; Mulatier, J. C.; Dutasta, J. P.; Dalcanale, E. *Chem.--Eur. J.* **2008**, *14*, 5772.
[5] Ventola, E.; Vainiotalo, P.; Suman, M.; Dalcanale, E. *J. Am. Soc. Mass Spectrom.* **2006**, *17*, 213.
[6] Kalenius, E.; Moiani, D.; Dalcanale, E.; Vainiotalo, P. *Chem. Commun.* **2007**, 3865.
[7] Kalenius, E.; Neitola, R.; Suman, M.; Dalcanale, E.; Vainiotalo, P. *J. Am. Soc. Mass Spectrom.* **2010**, *21*, 440.
[8] Slovak, S.; Evan-Salem, T.; Cohen, Y. *Org. Lett.* **2010**, *12*, 4864.
[9] Master thesis A. Galán, "Lipophilic cavitands based on Calix[4]pyrrole scaffolds. Molecular recognition studies with anions and N-oxides", **2012.**
[10] Lippmann, T.; Wilde, H.; Dalcanale, E.; Mavilla, L.; Mann, G.; Heyer, U.; Spera, S. *J. Org. Chem.* **1995**, *60*, 235.
[11] Jacopozzi, P.; Dalcanale, E.; Spera, S.; Chrisstoffels, L. A. J.; Reinhoudt, D. N.; Lippmann, T.; Mann, G. *J. Chem. Soc., Perkin Trans. 2* **1998**, 671.
[12] Delangle, P.; Dutasta, J. P. *Tetrahedron Lett.* **1995**, *36*, 9325.
[13] Tancini, F.; Yebeutchou, R. M.; Pirondini, L.; De Zorzi, R.; Geremia, S.; Scherman, O. A.; Dalcanale, E. *Chem.--Eur. J.* **2010**, *16*, 14313.
[14] Delangle, P.; Mulatier, J. C.; Tinant, B.; Declercq, J. P.; Dutasta, J. P. *Eur. J. Org. Chem.* **2001**, 3695.
[15] Chas, M.; Gil-Ramirez, G.; Escudero-Adan, E. C.; Benet-Buchholz, J.; Ballester, P. *Org. Lett.* **2010**, *12*, 1740.
[16] Ragozzino, M. E.; Unick, K. E.; Gold, P. E. *Proc. Natl. Acad. Sci. U. S. A.* **1996**, *93*, 4693.
[17] Nirogi, R.; Mudigonda, K.; Kandikere, V.; Ponnamaneni, R. *Biomed. Chromatogr.* **2010**, *24*, 39.
[18] A. Späth, B. König, *Beilstein J. Org. Chem. 6* **(2010)** 32.
[19] Bartoli, S.; Roelens, S. *J. Am. Chem. Soc.* **2002**, *124*, 8307.
[20] Sarri, P.; Venturi, P. S. F.; Cuda, F.; Roelens, S. *J. Org. Chem.* **2004**, *69*, 3654.
[21] Ballester, P.; Sarmentero, M. A. *Org. Lett.* **2006**, *8*, 3477.
[22] Murayama, K.; Aoki, K. *Chem. Commun.* **1997**, 119.
[23] Ballester, P.; Shivanyuk, A.; Far, A. R.; Rebek, J. *J. Am. Chem. Soc.* **2002**, *124*, 14014.
[24] Hof, F.; Trembleau, L.; Ullrich, E. C.; Rebek, J. *Angew. Chem., Int. Ed.* **2003**, *42*, 3150.
[25] Abdoul-Carime, H.; Harb, M. M.; Montano, C. G.; Cecile, T.; Farizon, B.; Farizon, M.; Vachon, J.; Harthong, S.; Dutasta, J. P.; Jeanneau, E.; Mark, T. D. *Chem. Phys. Lett.* **2012**, *533*, 82.
[26] Wintergerst, M. P.; Levitskaia, T. G.; Moyer, B. A.; Sessler, J. L.; Delmau, L. H. *J. Am. Chem. Soc.* **2008**, *130*, 4129.
[27] Pelizzi, N.; Casnati, A.; Friggeri, A.; Ungaro, R. *J. Chem. Soc., Perkin Trans. 2* **1998**, 1307.
[28]Rudkevich, D. M.; Mercerchalmers, J. D.; Verboom, W.; Ungaro, R.; Dejong, F.; Reinhoudt, D. N. *J. Am. Chem. Soc.* **1995**, *117*, 6124.
[29] Mahoney, J. M.; Nawaratna, G. U.; Beatty, A. M.; Duggan, P. J.; Smith, B. D. *Inorg. Chem.* **2004**, *43*, 5902.

CHAPTER IV

Synthesis of Triazolophane-based Receptors for Linear Bifluoride Ions[I]

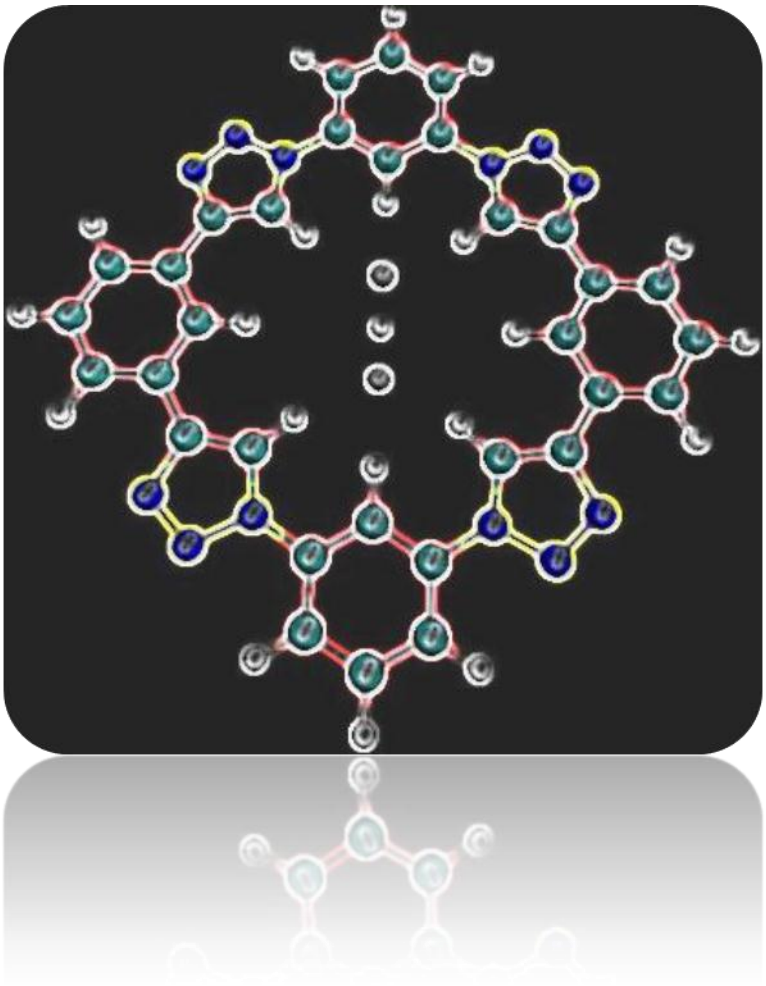

[I] The work presented in this chapter has been carried out in the laboratory of Prof. Amar Flood, in Indiana University (USA), under the supervision of K. P. McDonald.

4. 1 Introduction

In *Chapters 2* and *3* we have presented the design, synthesis and binding studies of *calix[4]pyrrole*-based ion pairs receptors in order to bind chloride anions. The binding process occurs through the formation of H-bonds between the chloride and the four polarized NH pyrrolic donors. We report here the design and synthesis of a new *triazolophane*-based receptor and the preliminary binding studies toward monoanionic pseudohalides such as the bifluoride ion HF_2^-.

Triazolophanes represent a new class of macrocycles in which the binding of anions like chloride occurs by triazole and phenyl-derived CH hydrogen bond donors.[1,2,3,4,5,6,7,8] These receptors show extraordinary binding constants, of the order > 10^6 M^{-1}, and the binding affinities for chloride result two orders of magnitude higher than the parent Sessler's calix[4]pyrrole, even though the process of complexation occurs by using weak CH hydrogen bonds. Recently, A. Flood's group[9] has highlighted that both electrostatic and structural features of the triazolophane-based receptors are responsible for the high binding strength, selectivity and guest regulation. In particular, they showed that triazolophanes bind chloride tightly because the triazole's CH donors are sufficiently polarized for hydrogen bonding and the receptors do not require a pre-reorganization to achieve the chloride binding.[10,11,12] On the contrary, an energetic penalty of ~ one-third of the entire Cl^- stabilization energy is required by calix[4]pyrroles to reorganize the macrocycle from 1,3-alternate to cone conformation and to establish H-bonds with the anion, as described in the previous chapters.

The work presented here consisted in the synthesis of a new triazolophane-derivative (Figure 4. 1) for the binding of the monoanionic pseudohalide (HF_2^-) anion using ^1H and ^{19}F-NMR spectroscopy. In particular, the idea was to combine the strongest hydrogen-bond ($FH\cdots F^-$) with one of the weakest hydrogen bond interactions that are provided by the CHs of a triazole unit. The structure of the macrocycle is defined by three different types of C-H hydrogen-bond donors: four equivalent strong donors from the triazoles (H^T) and two pairs of weaker phenylene C-H donors, coming from the N-linked phenylenes (H^N, north-south)

and from the C-linked phenylenes (H^C, east-west). Moreover, the receptor presents a dicyclohexylamido moiety on the two N-linked phenylenes (north and south direction) which polarize the triazole C-H hydrogen donors and increase the solubility of the macromolecule in organic solvents. *Tert*-butyl groups on the C-linked phenylenes (east and west direction) minimize the π-π stacking between the receptor molecules.

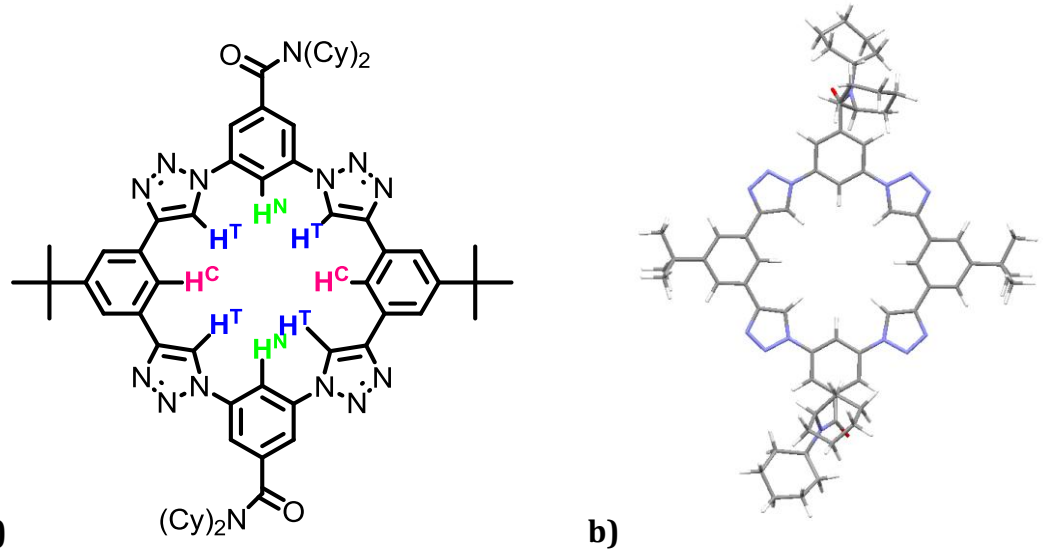

Figure 4. 1 Structure of the desired triazolophane (a, on the left) and the corresponding minimized structure obtained by Spartan software (b, on the right).

The inclusion of the "bifluoride" anion in the triazolophane skeleton has been previously modeled and calculated inside the parent triazolophane, as shown in Figure 4. 2.

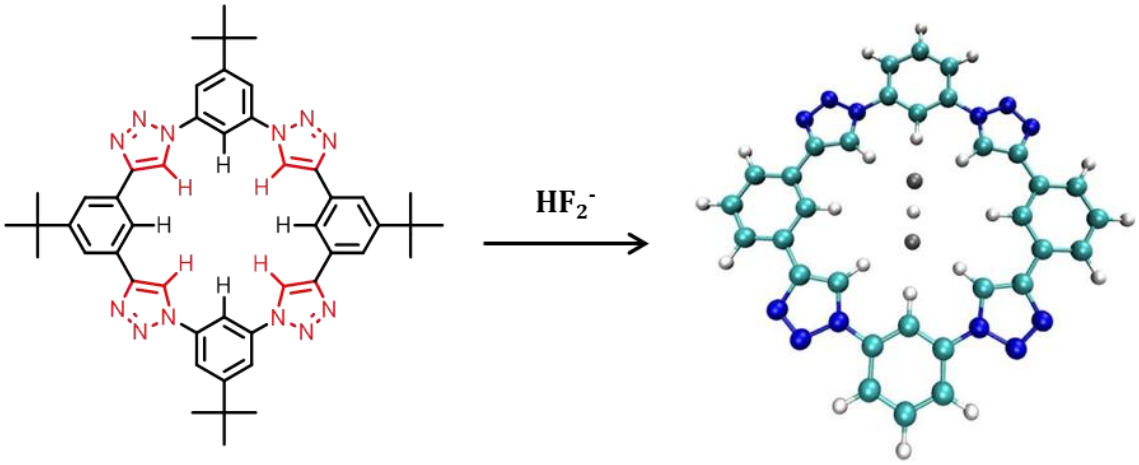

Figure 4. 2 Structure of the parent triazolophane receptor (left) and minimized geometry of the "bifluoride" anion inside the parent triazolophane (right).

Inclusion of pseudohalides, in particular cyanide, within a rigid macrocyclic triazolophane receptor by using strong C-H hydrogen bonds has already been reported in Flood's group and it has been corroborated both by theory and experimental data.[13] In the same way, examples of encapsulation of bifluoride are reported for tricyclic hosts in the literature.[14,15,16,17] The choice of developing synthetic receptors for HF_2^- recognition was dictated not only by our interest in binding linear guests but also by the interesting properties that fluoride compounds currently exhibit.[18] Moreover, it is known that bifluoride HF_2^- anion results more stable than fluoride F^- in organic solvents.[19] In apolar media and in the presence of water the following equilibrium takes place and results to be time dependent:

$$2\ TBAF + H_2O \rightleftharpoons TBAHF_2 + TBAOH \quad (1)$$

The water can be contained in the solvent or in the tetrabutylammonium fluoride (TBAF) itself, being the salt commercially available as trihydrate (it is not easy to produce dry TBAF[20] because of its decomposition by Hoffmann elimination, occurring even at room temperature[21]). It has been observed that the proportion of HF_2^- increases drastically with dilution of fluoride solutions and usually fluoride exists mainly in the bihalide form in 0.5 mM solution.[19] Subsequently, the HF_2^- results highly stable in solution, even over time.

4. 2 Results and Discussion

4.2. 1 Synthesis

The synthesis of the desired triazolophane-derivative **10** has been achieved by preparing the two main building blocks **4** and **8**, as reported in Scheme 4. 1. The N,N-dicyclohexyl-3,5-diazido-1-phenylamide **4** has been prepared from 3,5-diamino-1-phenyl carboxylic acid **1** by the formation of an azonium salt, giving the 3,5-diazide-1-phenyl carboxylic acid **2.** The synthesis of **2** resulted more successful with a $H_2SO_{4(aq)}$:Acetonitrile mixture than using CH_3COOH[11] for the *in situ* preparation of the nitrous acid. The chloride derivative **3** of 3,5-diazide-1-phenyl carboxylic acid **2** was directly reacted with the corresponding dicyclohexylamine in presence of triethylamine to give **4**. The 3,5-diethynyl-1-tert-butyl-benzene **8** building block was prepared from the 4-tert-butyl-aniline **5.** The corresponding 2,6-diiodo-4-tert-butyl-aniline **6** was reacted with $NaNO_2/H_2SO_4$ in boiling EtOH to give the corresponding 3,5-diiodo-1-tert-butyl-benzene **7** in 50% yield. The same reaction was carried out at room temperature and atmospheric pressure, using H_2O_2 as source of nitrous acid and H_2SO_4 as hydrogen donor.[22] The reaction resulted faster and easy in handling. The *tert*-butyl-diethynyl benzene **8** was obtained through Sonogashira reaction followed by TMS deprotection. The two components **4** and **8** were reacted together in a 1:10 ratio by click chemistry generating the precursor **9** as diethynyl derivative in which only five rings of the eight required for the desired macrocycle are present.[23] The final macrocyclization reaction was carried out under pseudo-high dilution conditions reacting the pre-macrocycle **9** with N,N-dicyclohexyl-3,5-diazido-1-phenylamide **4** in 1:1 ratio. The desired macrocycle was isolated with low yield (3%) exploring different chromatographic conditions and characterized by ^{1}H-NMR and ESI-MS.

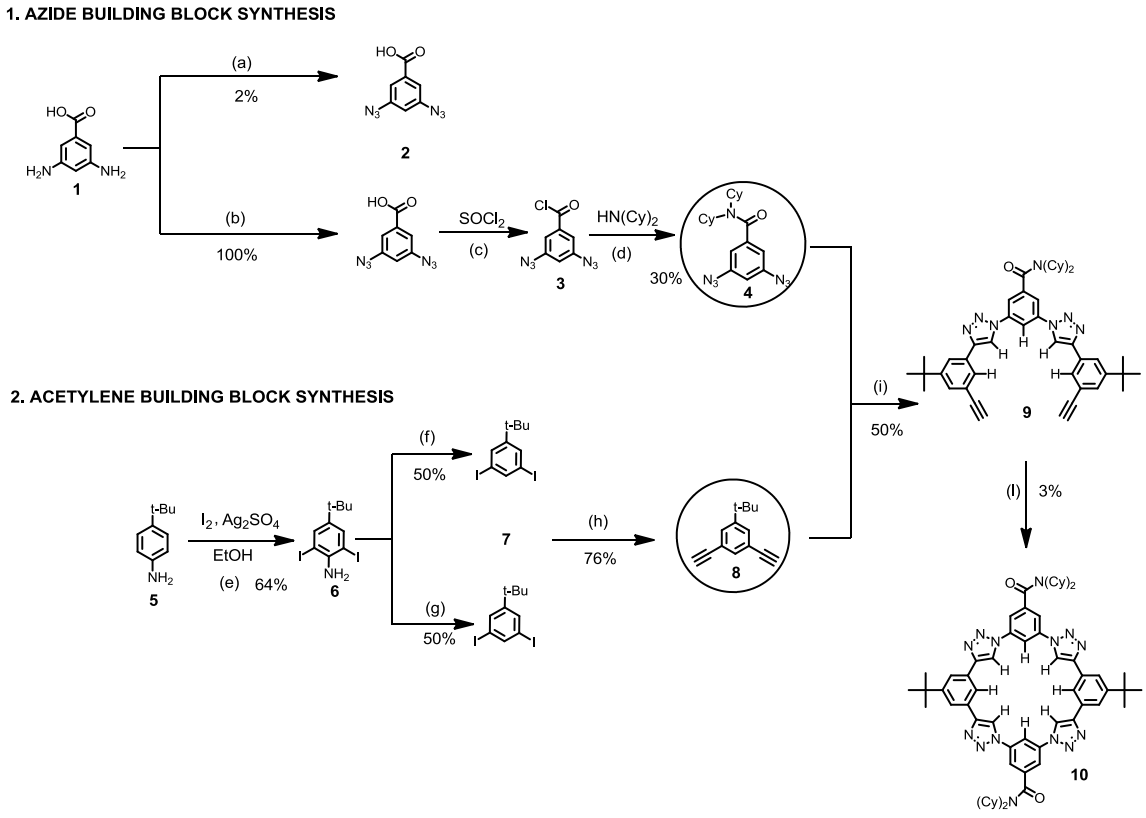

Scheme 4. 1 Triazolophane **10** synthesis. Azide building block synthesis: a) 1M glacial acetic acid, t-butyl nitrite, 0°C, 1 h; sodium azide, 0°C, 5 hrs; b) H_2SO_4 (aq) : ACN, t-butyl nitrite, 0°C, 30'; sodium azide, 0°C, 2 hrs; c) $SOCl_2$, DMF, THF, 50°C, 2hrs; d) dicyclohexylamine, $CHCl_3$, TEA, r.t., 24hrs. Acetylene building block synthesis: e) iodine, silver sulphate, EtOH, r.t., 1h; f) H_2SO_4, sodium nitrite, EtOH, reflux, 24hrs; g) H_2O_2, H_2SO_4, THF, r.t., 2hrs; h) TMS, CuI, $Pd(PPh_3)_2Cl_2$, i-Pr_2NH, 1hr and K_2CO_3/MeOH, THF, 2hrs; i) CuI/DBU, toluene, 1hr, 60°C; l) CuI/DBU, toluene, 1hr, 70°C overnight.

The yield related to the last synthetic step, from which we isolated the desired macrocycle **10**, was low due to the difficulties encountered in the purification of the receptor. The ^{1}H-NMR spectrum of triazolophane **10** showed broad signals when isolated by chromatography. However, addition of an excess of tetrabutylammonium chloride (TBACl) salt to the host solution gave sharp signals for the formation of the TBACl@**10** complex species. The excess of salt was removed by washing the sample with water, even though traces of tetrabutylammonium cation were still present in the ^{1}H-NMR spectrum. The downfield region of the ^{1}H-NMR spectrum of **10** presents four sets of aromatic protons, in which the peak for the triazole CHs (H_T) resonates at δ = 9.5 ppm and the protons of the inner phenylene CHs (H_N and H_C) at δ = 8.1 ppm. Finally, we

attribute the two peaks at δ = 7.9 ppm and δ = 7.8 ppm to the outwardly oriented protons H_a and H_b of the phenyl rings forming the macrocycle.

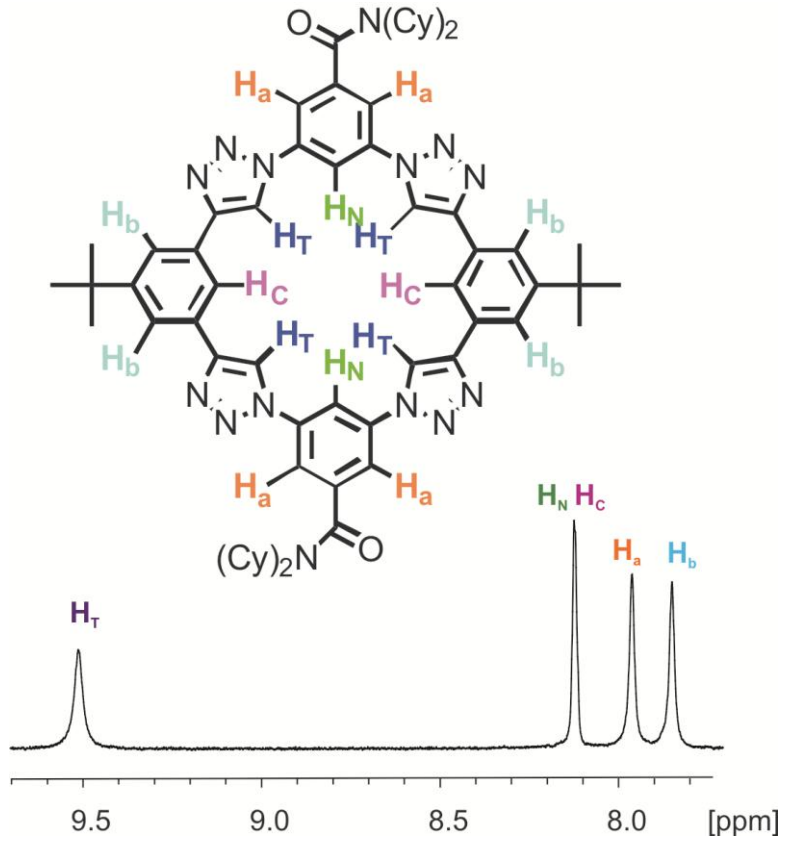

Figure 4. 3 Expansion of the downfield region of the ^{1}H-NMR spectrum of triazolophane **10** in dichloromethane-d_2 solution.

Unluckily, due to the presence of TBA^+ as impurity in the receptor solution, the binding studies monitored by ^{1}H and ^{19}F-NMR between the receptor **10** and tetrabutylammonium bifluoride[24] ($TBAHF_2$) have been used only for a qualitative interpretation of the data collected from the experiments.

4.2. 2 Binding Studies

In order to understand the dynamics of the binding process of triazolophane **10** and tetrabutylammonium bifluoride ($TBAHF_2$), we considered all the possible equilibria occurring in solution. The solution-phase binding model includes the formation of 1:1 and 2:1 complexes, due to the strong π-π stacking interaction between the aromatic rings of the host molecules, and an ion pairing process that involves the HF_2^- anion and the TBA^+ counter-ion.

$$\mathbf{10} + HF_2^- \overset{K_{1:1}}{=} \mathbf{10} \cdot HF_2^- \qquad \text{1:1 complex} \qquad (2)$$

$$\mathbf{10} \cdot HF_2^- + \mathbf{10} \overset{K_{2:1}}{=} \mathbf{10}_2 \cdot HF_2^- \qquad \text{2:1 complex} \qquad (3)$$

$$TBA^+ + HF_2^- \overset{K_{ip}}{=} TBAHF_2 \qquad \text{salt ion pairing} \qquad (4)$$

The ^{1}H-NMR titration of a 0.5 mM solution of triazolophane **10** with $TBAHF_2$ confirmed the established binding model (Figure 4. 4). The receptor shows a slow chemical exchange at NMR timescale. Upon addition of 0.2 equivalents of guest, a new set of triazole CH protons H_T appears downfield at δ = 10.4 ppm in addition to the ones of the free macrocycle at δ = 9.5 ppm (Δδ = 0.9 ppm), corresponding to the formation of the 2:1 complex $TBAHF_2$@$\mathbf{10}_2$. An evident shift is also detected for the inner protons H_N and H_C up to δ = 8.8 ppm (Δδ = 0.7 ppm) as consequence of the bifluoride complexation. The evident shifts shown by the inner protons H_T, H_N and H_C indicate that the bifluoride is hydrogen bonded inside the cavity of the triazolophane **10**. On the contrary, the outwardly oriented aromatic protons H_a and H_b at δ = 7.9 ppm and at δ = 7.8 ppm move slightly downfield to δ = 8.25 and 8.23 ppm, respectively. After addition of 0.8 equivalents of $TBAHF_2$ to the triazolophane solution, new peaks appear as consequence of the 1:1 complex $TBAHF_2$@**10** formation. The triazole CH signal at δ = 10.4 ppm splits in an additional peak at δ = 10.3 ppm due to the co-existence of the 2:1 and 1:1 complexes in solution. The peaks of the protons H_N and H_C corresponding to the 1:1 complex $TBAHF_2$@**10** resonate at δ = 8.9 ppm, H_a at δ = 8.28 ppm and H_b at δ = 8.20 ppm. The ultimate saturation of the 1:1 complex was achieved after addition of 20 equivalents of $TBAHF_2$. These data confirm the importance of including both the 2:1 and 1:1 equilibria (equations 2 and 3) in the analysis of the binding process of triazolophane **10** with $TBAHF_2$.

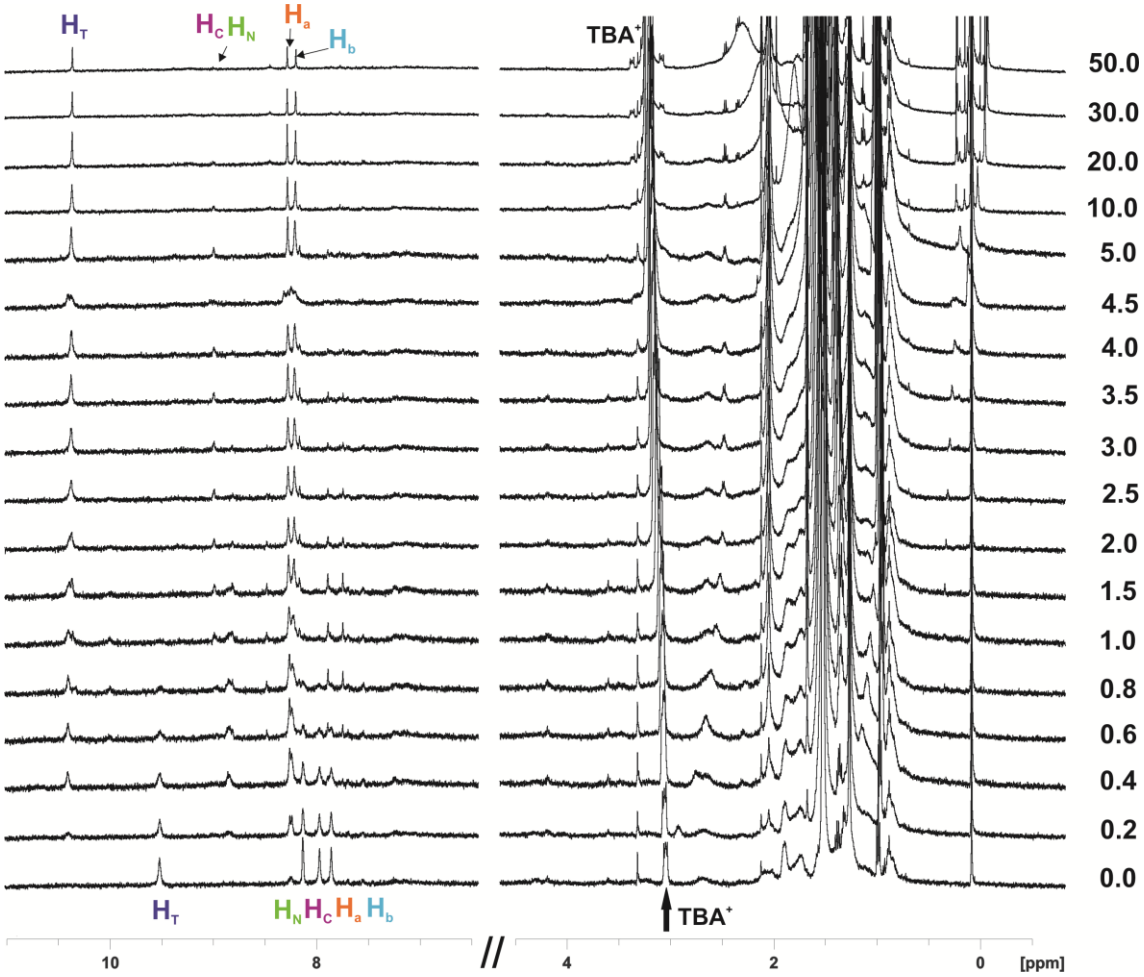

Figure 4. 4 ^{1}H-NMR spectra of the titration experiment of a 0.5 mM solution of the triazolophane **10** upon addition of $TBAHF_2$ in CD_2Cl_2 (from 0.2 to 50 equivalents). The signals of the spectra between 0.2 and 0.8 equivalent refer only to the protons of the 2:1 complex; between 1 and 5 equivalents to the protons of both 2:1 and 1:1 complexes; after 5 equivalents only to the 1:1 complex.

The upfield shift of the α-methylene proton of the TBA^+ cation from δ = 3.2 ppm ($TBAHF_2$ free) to 3 ppm ($TBAHF_2$@**10**) after addition of 0.2 equivalents of $TBAHF_2$ corroborates the presence of the ion-pair equilibrium process (equation 4). Since the cation can compete with the triazolophane for binding the anion, it is important to consider also this equilibrium and isolate its influence from the 1:1 binding process. The plot of the chemical shift δ of the TBA cation versus the equivalents of guest added shows that a saturation point is obtained for the 2:1 complex after the addition of 5 equivalents of guest (Figure 4. 5).

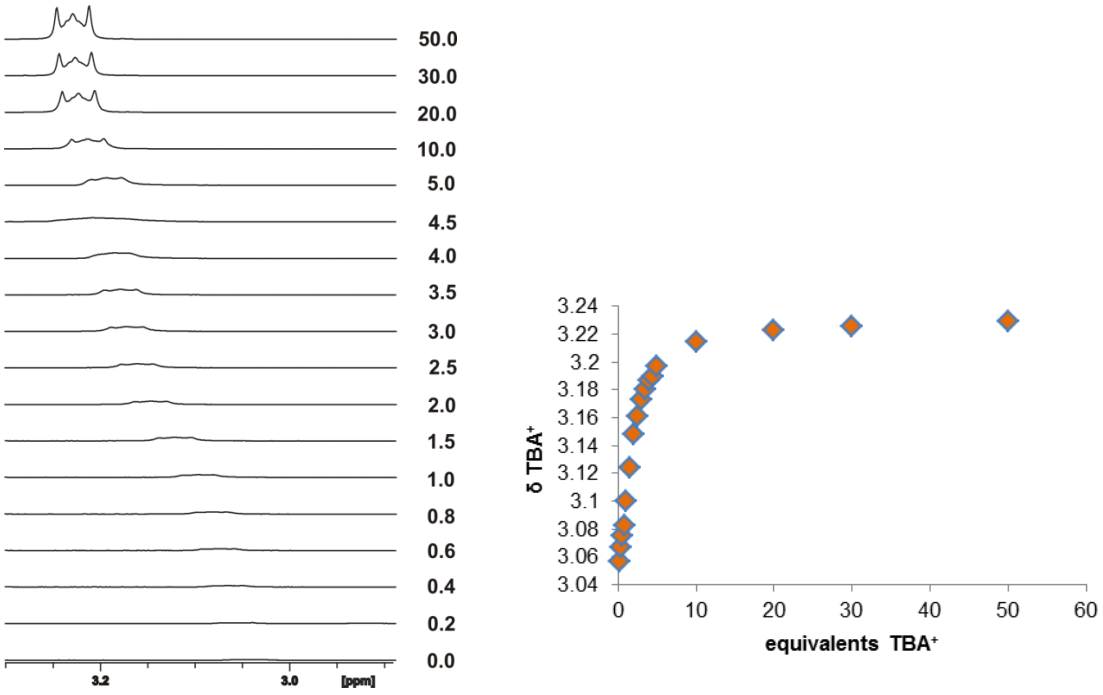

Figure 4. 5 Partial ^{1}H-NMR spectra and chemical shift plotting of the TBA cation upon addition of $TBAHF_2$ to a 0.5 mM solution of the triazolophane **10** in CD_2Cl_2.

Simulated speciation curve generated for the ^{1}H-NMR titration of the 0.5 mM solution of the triazolophane **10** with $TBAHF_2$ in CD_2Cl_2 by using HySS2009 software[25] shows clearly all the species and equilibria present in solution. The association constants used in the simulation were estimated to be of the order of 10^5 M^{-1} for the 1:1 complex ($K_{1:1}$, equation 2), of 10^8 M^{-1} for 2:1 complex ($K_{2:1}$, equation 3) and around 10^4 M^{-1} for the $TBAHF_2$ ion pairing constant (K_{ip}, equation 4). A UV-Vis dilution experiment was performed to determine the $TBAHF_2$ ion pairing constant K_{ip} in dichloromethane according to preliminary HySS simulation (solutions from 1 μM to 1 mM). However, the intensity of the absorbance resulted too low and it was not possible to fit the data to get an acceptable measurement of the association constant K_{ip} for $TBAHF_2$. For this reason, we used the ion pairing constant K_{ip} value already reported for the TBACN[13]. The speciation curves of Figure 4. 6 shows that the free receptor **10** (red line) is consumed after addition of $TBAHF_2$. The concentration of the 2:1 complex $TBAHF_2$@$\mathbf{10}_2$ decreases after addition of 5 equivalents of guest (blue line) and < 10% is still present at the end of the titration. In the same way, the concentration of the 1:1 complex $TBAHF_2$@**10** (green line) increases as long as the guest is added to the host solution until a

saturation point is reached (~ 20 equivalents of $TBAHF_2$ added, end of the titration).

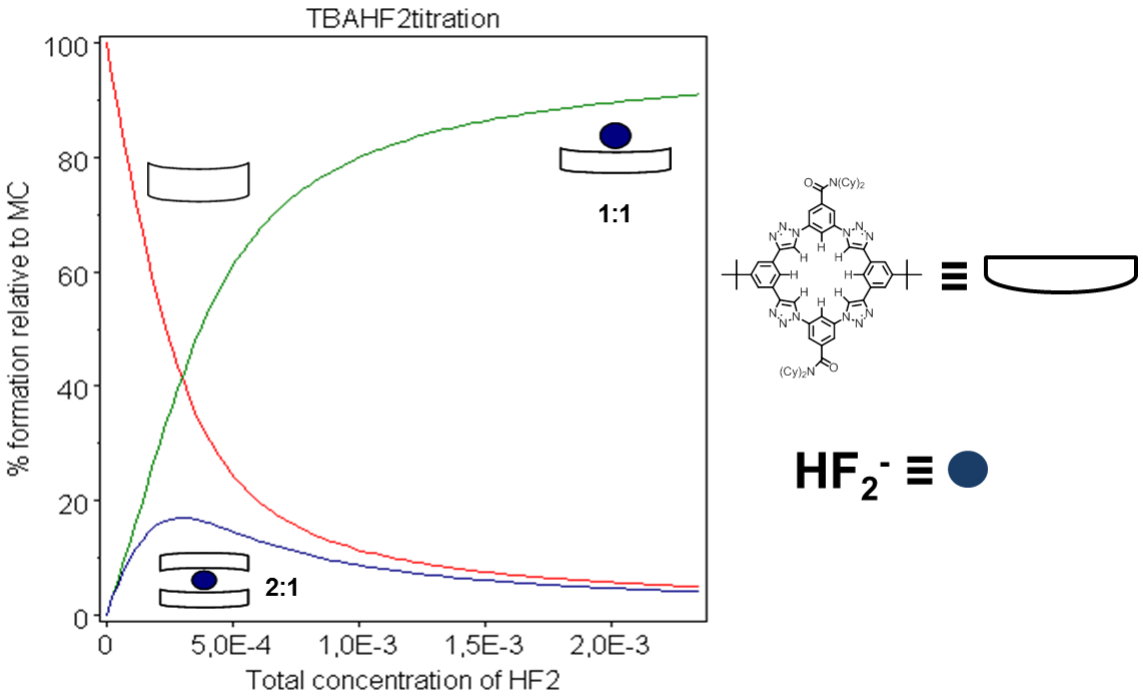

Figure 4. 6 Speciation curve generated using HySS software for the titration of [**10**] = 0.5 mM (red line) with $TBAHF_2$, in which both 2:1 complex (blue line) and 1:1 complex (green line) curves are indicated. (MC = macrocycle). The concentration of HF_2^- is in M unit.

An additional NMR titration was carried out at higher concentration (5 mM) of triazolophane **10** and the binding process with $TBAHF_2$ was followed by ^1H and ^{19}F-NMR. As expected, higher concentration of macrocycle increases the persistence of the 2:1 complex in solution and favors the formation of complexes with higher stoichiometry. The ^{19}F-NMR experiment corroborates the ^1H-NMR data (Figure 4. 7). The addition of 0.2 equivalents of guest generates a signal at δ = -117 ppm corresponding to the 2:1 complex $TBAHF_2$@**10**$_2$. With 0.4 equivalents of $TBAHF_2$ in solution it is also possible to distinguish the peak of the 1:1 complex $TBAHF_2$@**10** at δ = -124 ppm. Upon addition of 1.8 equivalents of guest two new signals appears at δ = -154 ppm and at δ = -128 ppm. We attribute these peaks to the $TBAHF_2$ (δ = -154 ppm) and to the hydrated fluoride ion (δ = -128 ppm) as explained in the introduction of this chapter (equation 1).[26,27,28]

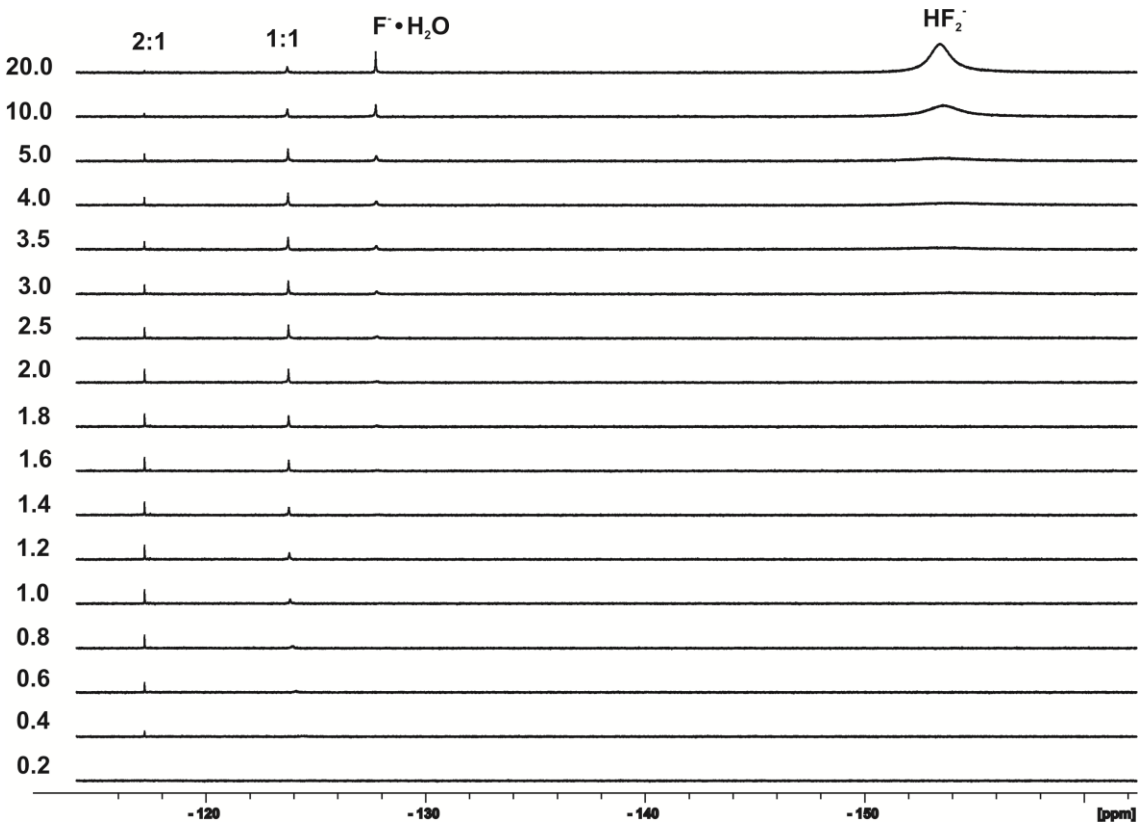

Figure 4. 7 ^{19}F-NMR titration experiment of a 5 mM solution of triazolophane **10** upon addition of $TBAHF_2$ in CD_2Cl_2.

4. 3 Conclusions

We have presented the design and synthesis of a new triazolophane-based anion pair receptor for the binding of linear guest like the bifluoride ion HF_2^-. The purity of the macrocycle **10** limited the interpretation of the data on a qualitative level. ^{1}H and ^{19}F NMR experiments show the possibility of including the bifluoride ion HF_2^- inside the cavity of **10** by establishing hydrogen bonds with the inner CH protons of the receptor and corroborate the modeling studies carried out on the parent triazolophane. Speciation curves generated by using HySS software suggest that the association constant for the binding of $TBAHF_2$ by **10** to form the 1:1 complex $TBAHF_2$@**10** is > 10^5 M^{-1}.

4. 4 Experimental Section

General information and instrumentation

All syntheses were carried out using chemicals as purchased from commercial sources unless otherwise noted. ^{1}H NMR spectra were recorded on a Varian (400 and 500 MHz for ^{1}H NMR) ultrashield spectrometer.

Synthesis

Azide building block synthesis. **3,5-diazide benzoic acid (2-a** in Scheme 4. 1). To an ice-cooled, vented solution of 3,5-diaminobenzoic acid (5.0 g, 32.8 mmol) in 1M glacial acetic acid (200 mL) t-butyl nitrite (17g, 170 mmol) is carefully syringed dropwise and stirred at 0°C for 1 hour. The solution assumes a dark densy aspect. A solution of sodium azide (16 g, 246 mmol) in distilled H_2O (75 mL) is added dropwise to the reaction and stirred for 5 hours at 0°C. The reaction is poured into ice-water and extracted with ethyl-acetate (4 x 200 mL). The organic layer is washed extensively with 0.5 M HCl (3 x 200 mL), saturated NH_4Cl (2 x 100 mL) and brine (2 x 100 mL). The combined organic fractions are dried with $MgSO_4$ and concentrated under vacuum. The crude product (about 3 g) is purified by column chromatography (2:1 AcOEt:Hexane). Two fractions were collected and checked by ^{1}H-NMR. Both presented the desired product and additional byproducts. Further purification using a 1:1 mixture of EthylAcetate:Hexane gave the desired product in low yields (3%). **3,5-diazide benzoic acid (2-b** in Scheme 4. 1). To an ice-cooled, vented solution of 3,5-diaminobenzoic acid (5.0 g, 32.8 mmol) in H_2SO_4 (aq) : ACN (200 mL of total solution: 28 ml of acid with 112 mL of water and 60 mL of acetonitrile) is carefully syringed sodium nitrite (previously dissolved in 50 mL of water) dropwise and stirred at 0°C for 30 minutes. The solution assumes a dark densy aspect. A solution of sodium azide (16 g, 246 mmol) in distilled H_2O (50 mL) was added dropwise to the reaction and stirred for 2 hours at 0°C. The addition of azide produced bubbling into solution with a change in colour. The crude was extracted with AcOEt, washed with brine and the organic solvent evaporated. By ^{1}H-NMR the product appeared clean and the yield quantitave. **3,5-diazido-N,N-**

dicyclohexylbenzamide (4 in Scheme 4. 1)**.** Carboxilic acid **2** (0.5 g, 2.5 mmol) was dissolved in dry THF (15 mL), cooled to 0°C and 3-4 drops of DMF were added. $SOCl_2$ (0.5 mL) was added and the solution was warmed at 50°C for 2hrs. The solvent was removed under vacuum and the crude dissolved in chloroform (10 mL). Dicyclohexyl amine was dissolved (2 mL, 2.21 g) in chloroform (15mL) and added to previous solution. Triethylamine (2mL) was then added and the resulting solution was stirred for 24 hrs at r.t. The day after, the solution was diluted with $CHCl_3$, washed with Na_2CO_3(aq), dried over $MgSO_4$ and concentrated. The crude was purified by chromatography (Hexane:AcOEt from 100:0 to 90:10). Acetylene building block synthesis. **2,6-diiodo-4-*tert*-butyl aniline (6** in Scheme 4. 1). 4-(tert-butyl)aniline (3 g, 20.1 mmol) was dissolved in ethanol (100 mL) and iodine (10 g, 40.2 mmol) and silver sulphate (13 g, 40.2 mmol) were added. The mixture was stirred vigorously for 1 h at room temperature. Insoluble salts were removed by filtration. After concentration, the residue was taken up in DCM (100 mL). The solution was sequentially washed with 5% NaOH aqueous solution (100 mL x 2) and water (100 mL x 2), dried over anhydrous $MgSO_4$ and the solvent removed under vacuum. The residue was purified by column chromatography (silica gel, DCM:hexane 1:3) to give an oily liquid.

2,6-diiodo-4-*tert*-butyl benzene (**7-a** in Scheme 4. 1). The starting aniline (0.5 g, 1.25 mmol) were dissolved in EtOH (7 mL) and H_2SO_4 (0.140 mL) was added dropwise at 0°C. $NaNO_2$ (0.170 g, 2.5 mmol) were added quickly to the solution at r.t. The solution was refluxed for 1 day. EtOH was evaporated and neutralized with NaOH 2N. The water solution was extracted with chloroform and the organic phase was washed with water and dried over MgSO4. The crude was purified by chromatography (Hexane:AcOEt 100:0 to 99:1). **2,6-diiodo-4-*tert*-butyl benzene** (**7-b** in Scheme 4. 1). The starting aniline (0.2 g, 0.5 mmol) was dissolved in THF (10 mL) and H_2SO_4 (0.532 mL) was added dropwise at 0°C. $NaNO_2$ (0.103 g, 1.5 mmol) and H_2O_2 (0.015 mL) were added quickly to the solution at r.t. The solution was left reacting at r.t. for 2 hours. The solvent was removed under vacuum and the crude was washed with water, extracted with chloroform and dried over $MgSO_4$. **1,3-diacetylene-5-*tert*-butyl benzene** (**8** in Scheme 4. 1). 3,5-diiodo-1-tert-butylbenzene (0.7 g, 1.8 mmol) was dissolved in THF (20 mL) and the solution

degassed for 15 minutes. *Bis*-triphenylphosphine dichloropalladium (0.13 g, 0.18 mmol) and CuI (0.035 g, 0.18 mmol) were added and the solution was purged under Ar for additional 10 minutes. TMS (0.5 g, 5.52 mmol) and *i*-Pr_2NH (1.3 mL) were added and the solution stirred under Ar atmosphere. After 1hr, the suspension was filtered and the solvent removed. The dark oil obtained was dissolved in water, extracted in DCM and dried over $MgSO_4$. The crude was then filtrated through a short silica gel column using hexane as eluant and used for the following reaction. The oil obtained from the previous reaction was dissolved in THF (30 mL) and a saturated solution of K_2CO_3 in MeOH (30 mL) was added. The solution was left reacting for 2 hrs. The solvent was evaporated and the crude was washed with water, extracted with DCM, dried over $MgSO_4$ and purified by cromatography over silica using hexane as eluant.

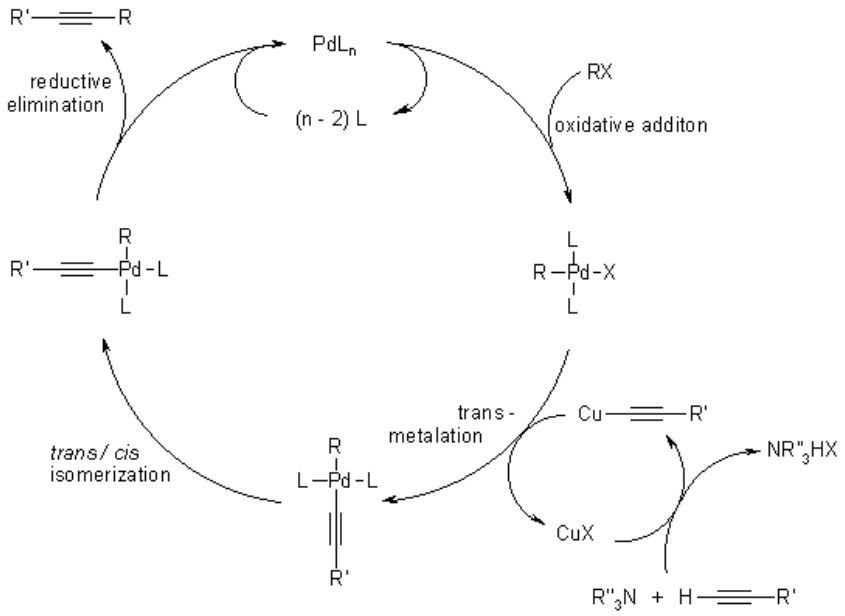

Figure 4. 8 Mechanism of the Sonogashira reaction.

Precursor 9. 3,5-diazido-N,N-dicyclohexylbenzamide (0.2 g, 0.54 mmol) and 1-(tert-butyl)-3,5-diethynylbenzene (0.9 g, 5.44 mmol) were dissolved in toluene (100 mL) previously purged with Ar for 10 minutes. The solution was purged for additional 10 minutes, then CuI (0.03 g, 0.16 mmol) and DBU (0.4 mL) were added and the solution was kept at 60° C for 1 hr. The product was purified by cromatography (DCM:MeOH from 100:0 to 98:2). Triazolophane **10**. In a two-necked flask the DBU (0.83 g, 5.5mmol) was dissolved in toluene (200 mL) and

purged for 30' under Ar. The solution was warmed to 70°C and CuI (0.02 g, 0.08 mmol) was added. The 3,5-diazido-N,N-dicyclohexylbenzamide **4** (0.1g, 0.27 mmol) and the diethylene precursor **9** (0.1 g, 0.27 mmol) were dissolved in toluene (50 mL), purged for 15 minutes with Ar and added to the DBU solution slowly overnight through an addition funnel. The reaction crude was evaporated and purified by chromatography (DCM:MeOH from 100:0 to 98:2). A further purification was performed using a mixture of DCM:Acetone (from 100:0 to 90:10) as eluent.

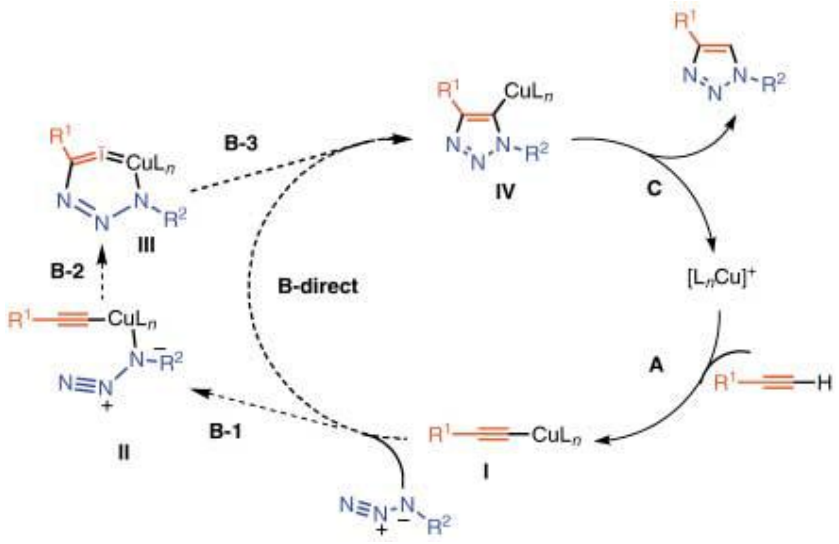

Figure 4. 9 Mechanism of the click reaction proposed by Sharpless.[23]

Binding Studies

<u>^{1}H NMR binding experiment of **10** with $TBAHF_2$ in DCM solution.</u> The complexation behaviour of **10** toward $TBAHF_2$ was studied by ^{1}H and ^{19}F NMR, at 298 K. The titration experiments were carried out by adding aliquots of a 40 mM solution of $TBAHF_2$ in CD_2Cl_2 into the NMR tube containing a 0.5 mM solution of **10** in the same solvent. A second experiment was performed using a 5 mM solution of **10** in order to record ^{19}F NMR spectra.

4. 5 References and Notes

[1] Li, Y. J.; Flood, A. H. *Angew. Chem., Int. Ed.* **2008**, *47*, 2649.
[2] Li, Y. L.; Flood, A. H. *J. Am. Chem. Soc.* **2008**, *130*, 12111.
[3] Li, Y. J.; Griend, D. A. V.; Flood, A. H. *Supramol. Chem.* **2009**, *21*, 111.
[4] Zahran, E. M.; Hua, Y. R.; Li, Y. J.; Flood, A. H.; Bachas, L. G. *Anal. Chem.* **2010**, *82*, 368.
[5] Hua, Y. R.; Flood, A. H. *Chem. Soc. Rev.* **2010**, *39*, 1262.
[6] Hua, Y. R.; Ramabhadran, R. O.; Uduehi, E. O.; Karty, J. A.; Raghavachari, K.; Flood, A. H. *Chem.--Eur. J.* **2011**, *17*, 312.
[7] Zahran, E. M.; Hua, Y. R.; Lee, S.; Flood, A. H.; Bachas, L. G. *Anal. Chem.* **2011**, *83*, 3455.
[8] McDonald, K. P.; Hua, Y. R.; Lee, S.; Flood, A. H. *Chem. Commun.* **2012**, *48*, 5065.
[9] Ibid.
[10] Lee, S.; Hua, Y. R.; Park, H.; Flood, A. H. *Org. Lett.* **2010**, *12*, 2100.
[11] Juwarker, H.; Lenhardt, J. M.; Pham, D. M.; Craig, S. L. *Angew. Chem., Int. Ed.* **2008**, *47*, 3740.
[12] McDonald, K. P.; Ramabhadran, R. O.; Lee, S.; Raghavachari, K.; Flood, A. H. *Org. Lett.* **2011**, *13*, 6260.
[13] Ramabhadran, R. O.; Hua, Y. R.; Li, Y. J.; Flood, A. H.; Raghavachari, K. *Chem.--Eur. J.* **2011**, *17*, 9123.
[14] Kang, S. O.; Day, V. W.; Bowman-James, K. *Inorg. Chem.* **2010**, *49*, 8629.
[15] Kang, S. O.; Powell, D.; Day, V. W.; Bowman-James, K. *Angew. Chem., Int. Ed.* **2006**, *45*, 1921.
[16] Motekaitis, R. J.; Martell, A. E.; Murase, I.; Lehn, J. M.; Hosseini, M. W. *Inorg. Chem.* **1988**, *27*, 3630.
[17] Motekaitis, R. J.; Martell, A. E.; Murase, I. *Inorg. Chem.* **1986**, *25*, 938.
[18] Cametti, M.; Rissanen, K. *Chem. Commun.* **2009**, 2809.
[19] Goursaud, M.; De Bernardin, P.; Dalla Cort, A.; Bartik, K.; Bruylants, G. *Eur. J. Org. Chem.* **2012,** *19*, 3570
[20] Sun, H. R.; DiMagno, S. G. *J. Am. Chem. Soc.* **2005**, *127*, 2050.
[21] Sharma, R. K.; Fry, J. L. *J. Org. Chem.* **1983**, *48*, 2112.
[22] Patent, Reference: 2481922; 2563037
[23] Rostovtsev, V. V.; Green, L. G.; Fokin, V. V.; Sharpless, K. B. *Angew. Chem., Int. Ed.* **2002**, *41*, 2596.
[24] Landini, D.; Molinari, H.; Penso, M.; Rampoldi, A. *Synthesis-Stuttgart* **1988**, 953.
[25] Alderighi, L.; Gans, P.; Ienco, A.; Peters, D.; Sabatini, A.; Vacca, A. *Coord. Chem. Rev.* **1999**, *184*, 311.
[26] Fujiwara, F. Y.; Martin, J. S. *J. Am. Chem. Soc.* **1974**, *96*, 7625.
[27] Martin, J. S.; Fujiwara, F. Y. *J. Am. Chem. Soc.* **1974**, *96*, 7632.
[28] Experiments performed cooling down the temperature of a 0.4 M solution of $TBAHF_2$ in dichloromethane revealed by ^{19}F a clear doublet instead of a broad singlet for the bifluoride ion, es expected.

CHAPTER V

Selective inclusion of the high-energy conformer of N-methyl morpholine N-oxide within aryl-extended Calix[4]pyrroles

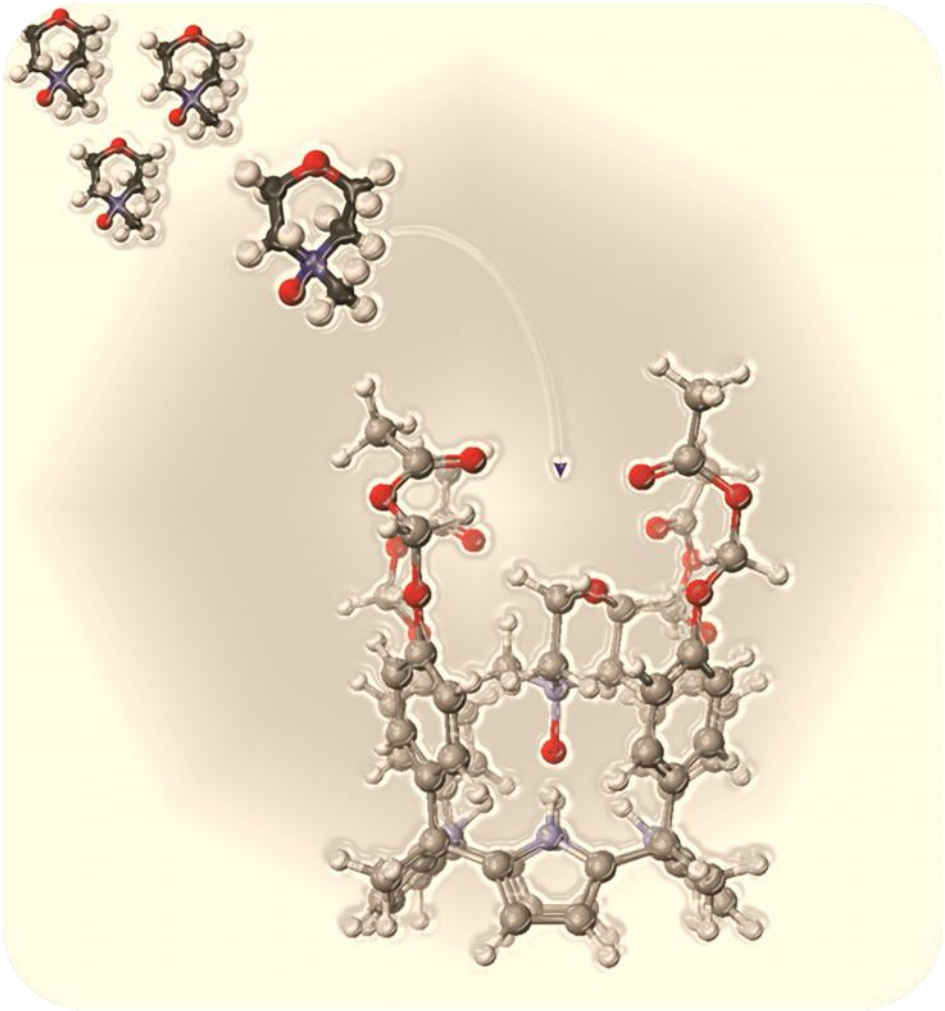

5. 1 Introduction

It is widely known that aryl-extended calix[4]pyrroles are ideal receptors for the binding of anionic guests (*Chapter 2 and 3*). On the contrary, few examples are reported in literature regarding their ability in the recognition and inclusion of neutral molecules with electron rich groups capable of acting as hydrogen-bond acceptors. *N*-oxides,[1,2,3,4] are known for their numerous applications in synthetic organic chemistry[5,6] and for their biological activity[7]. They are also known to be very good hydrogen bonding acceptors.[8,9,10] We present here an example of selective inclusion of the high energy conformer of *N*-methyl morpholine *N*-oxide (NMMO) in a calix[4]pyrrole substituted in the *meso* position by four aromatic rings. This *N*-oxide (Figure 5. 1) is commonly used at industrial scale as cellulose solvent in fiber making[11] or at lab scale as co-catalyst in the oxidation of alcohols to carbonyl groups in presence of tetrapropylammonium perruthenate as catalyst.[12] The *N*-methyl morpholine *N*-oxide can be synthesized by oxidation of the starting *N*-methylmorpholine with hydrogen peroxide[13] (30% aq), although the one we used in our experiments was purchased. NMMO can exist in two chair conformations, being the one with the oxygen atom in axial position energetically favored by 2 kcal/mol based on simple molecular mechanism calculations. A similar conclusion is reached when the cyclohexane A values for methyl (1.74) and hydroxyl (0.8) groups are taken in consideration.[14]

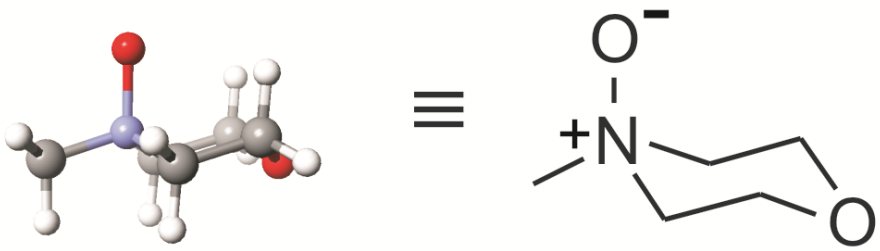

Figure 5. 1 Minimized structure of the low energy conformer of *N*-methylmorpholine-*N*-oxide (NMMO).

5. 2 Results and Discussion

N-methyl morpholine N-oxide (NMMO)

In inclusion complexes, the exchange between complexed and free guest species is usually fast on the human time scale but slow on the ^{1}H NMR time scale (< 10 sec^{-1}). The possibility of including reactive species in molecular containers produces a twofold effect (*Chapter 1, General introduction*). On the one hand, the inclusion process protects the reactive species from external reagents. On the other hand, it can also prevent its thermal decomposition. As mentioned above, NMMO is used as co-oxidant in the liquid-phase in the catalytic oxidation of alcohols to carbonyl groups by tetrapropylammonium perruthenate (TPAP). We describe here a supramolecular inclusion effect. We found that the included NMMO, aside of having adopted the high energy conformation, possesses chemical properties different from those in the bulk solution. Inside the cavitand NMMO is stable for longer time than in solution. Moreover, NMMO in combination with a catalytic amount of TPAP oxidizes primary and secondary alcohols to aldehydes and ketones, respectively. The reaction takes places at room temperature at millimolar concentration in high yields in a reduced amount of time that goes from minutes to hours depending on the substrate. In contrast, the oxidation reaction does not progress to a considerable extent when NMMO is inside the cavitand **1** and the TPAP outside. The inclusion of NMMO within the cavity of the aryl-extended calix[4]pyrrole represents a fascinating possibility of manipulating the properties (conformational preference and reactivity) of small molecules by confinement in small space.[15] In order to understand the dynamics and thermodynamics of the inclusion process occurring between the high energy conformer of N-methyl morpholine *N*-oxide (NMMO) and the aryl-extended calix[4]pyrrole **1**, we first fully characterized the ^{1}H NMR spectrum of NMMO in the bulk acetonitrile solution.

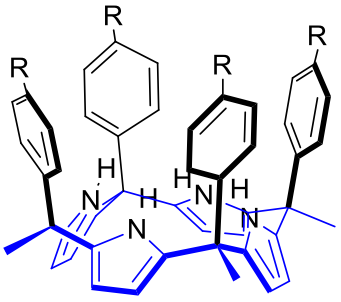

1

Figure 5. 2. Structure of the α,α,α,α-isomer of aryl-extended calix[4]pyrrole **1**

In solution, NMMO predominantely adopts the conformation in which the methyl group on the nitrogen atom is oriented in an equatorial position (Figure 5. 3 a).[16] This conformer is energetically favoured due to reduction in the steric strain caused by the 1,3-diaxial interactions between the methyl group and the axial protons $H\beta'_{ax}$ on the C_1 and C_5 carbons exhibited in the alternative chair conformer.[17] The cychohexane A value (steric size) for the hydroxyl group is considerably smaller than for the methyl group providing clear preference for the equatorial orientation in the latter.

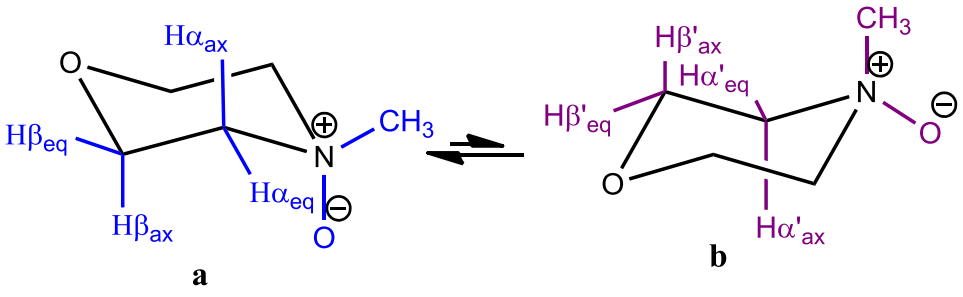

Figure 5. 3. Conformational equilibrium between the two cyclohexane chairs of *N*-methyl morpholine *N*-oxide (NMMO).

We performed the complete assignment of the proton signals observed in the ^1H NMR spectrum of NMMO in acetonitrile solution (Figure 5. 4) by means of 2D experiments. The equatorial protons in α position with respect to the nitrogen atom in conformer ***a***, $H\alpha_{eq}$, resonate at δ = 2.85 ppm and appear as a multiplet (d,d,d) because of multiple scalar coupling with the geminal proton nucleus $H\alpha_{ax}$

($^2J_{gem}$ = 11.5 Hz) and the adjacent proton nuclei Hβ$_{ax}$ ($^3J_{cis}$ = 2.3 Hz) and Hβ$_{eq}$ ($^3J_{trans}$ = 1.1 Hz). The signal at δ = 3.37 ppm corresponds to the Hα$_{ax}$ and appears as multiplet (d,d,d) due to the coupling with the geminal Hα$_{eq}$ ($^2J_{gem}$ = 11.5 Hz), and the vicinal Hβ$_{ax}$ and Hβ$_{eq}$ protons ($^3J_{trans}$ = 10.7 Hz and $^3J_{trans}$ = 3.3 Hz, respectively). Likewise, the Hβ$_{eq}$ protons resonating at δ = 3.47 ppm and the Hβ$_{ax}$ centered at δ = 4.23 ppm show a similar coupling pattern. The singlet sharp singlet corresponding to the protons of the methyl group on the nitrogen atom resonates at δ = 3.09 ppm.

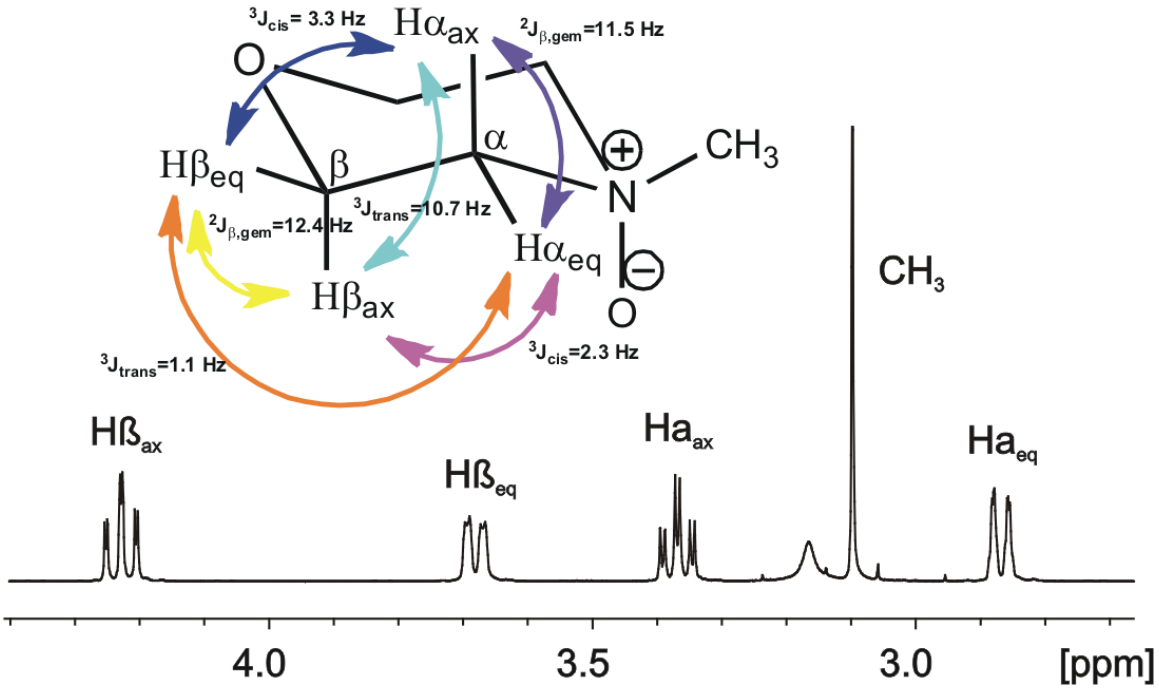

Figure 5. 4. ^{1}H NMR spectrum of *N*-methyl morpholine *N*-oxide (NMMO) in acetonitrile-d$_3$.

2D NOESY and 2D DQF COSY NMR experiment resulted helpful to confirm the existence of NMMO as only one conformer in solution. Given the lack of NOEs signals between the protons of the methyl group and the rest of proton signals, the placement of the methyl in equatorial position seems to be fully justified.

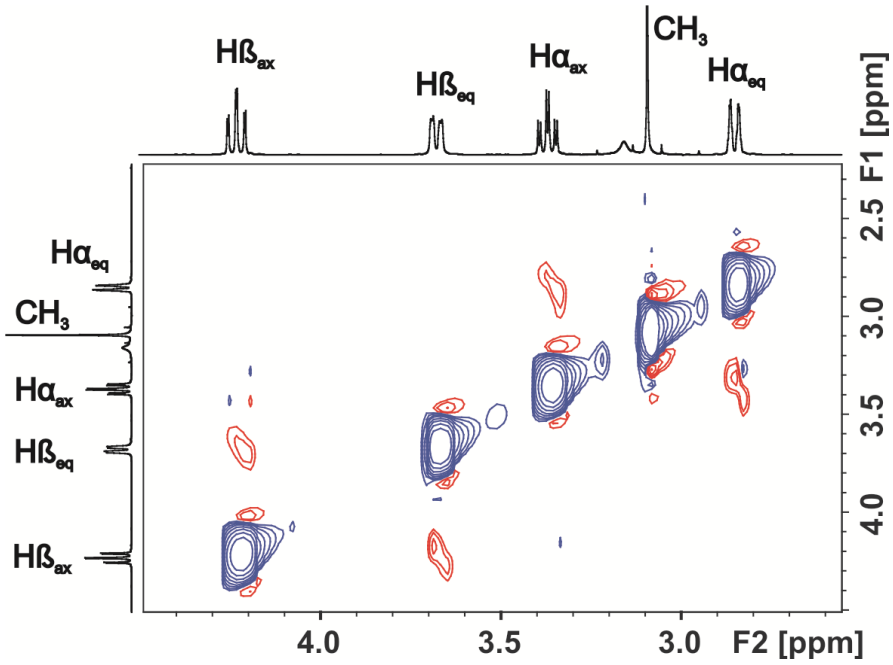

Figure 5. 5. 2D NOESY spectrum of *N*-methyl morpholine *N*-oxide (NMMO) recorded in acetonitrile-d_3

A 2D DQF COSY NMR experiment was also helpful in identifying the conformer **a** of the *N*-oxide as the exclusive specie in solution. The DQF COSY spectrum (Figure 5. 6) shows cross peaks between J-coupled protons. The intensity of the cross peak is proportional to the value of the coupling constants between them. For example, a strong cross peak is easily detected between the Hα_{eq} and Hα_{ax} protons (δ = 2.85 ppm and 3.37 ppm, respectively) as a consequence of the geminal coupling ($^2J_{gem}$ = 11.5 Hz). While weak or almost negligible cross peaks are observed between the Hα_{eq} at δ = 2.85 ppm, Hβ_{eq} at δ = 3.47 ppm and Hβ_{ax} at δ = 4.23 ppm since the coupling constants between them are smaller ($^3J_{trans}$ = 1.1 Hz and $^3J_{cis}$ = 2.3 Hz, respectively). As expected for a DQF experiment, the diagonal peak of the methyl group is not observed. [18]

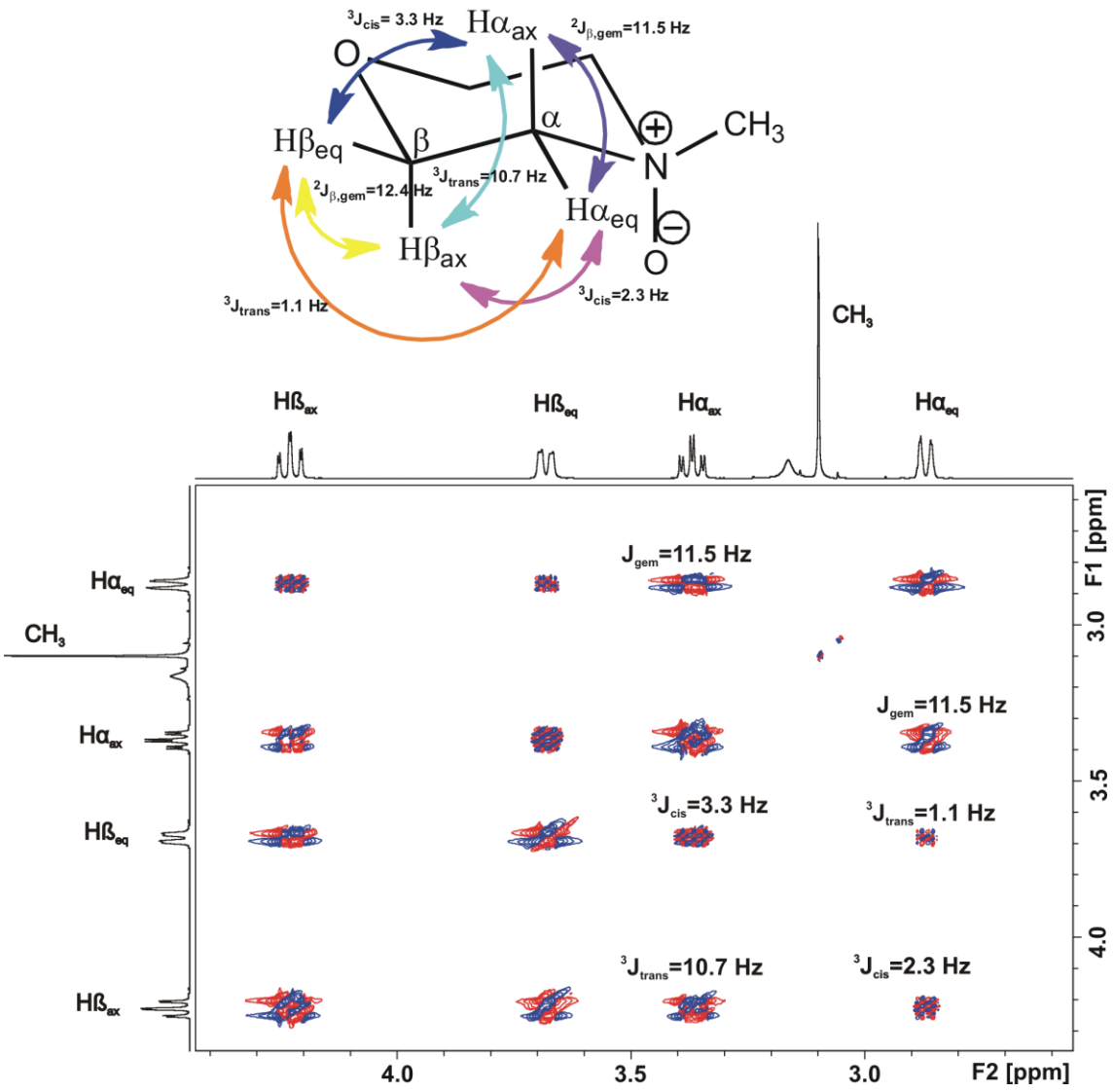

Figure 5. 6. 2D DQF COSY NMR spectrum of *N*-methyl morpholine *N*-oxide (NMMO) recorded in acetonitrile-d_3.

N-methyl morpholine N-oxide (NMMO): Inclusion Studies

^{1}H NMR titration experiments of NMMO with calix[4]pyrrole **1** established the formation of a 1:1 complex having an association constant value $K_{ass} > 10^4$ M^{-1}. The inclusion of the guest in the deep aromatic cavity of the host is confirmed by a significant downfield shift experienced by the NH protons of calix[4]pyrrole **1**, resonating at δ =10.71 ppm (Δδ = 2.5 ppm). This shift is due to the establishment of hydrogen bonding interactions between the NH protons of **1** and the oxygen atom of NMMO.

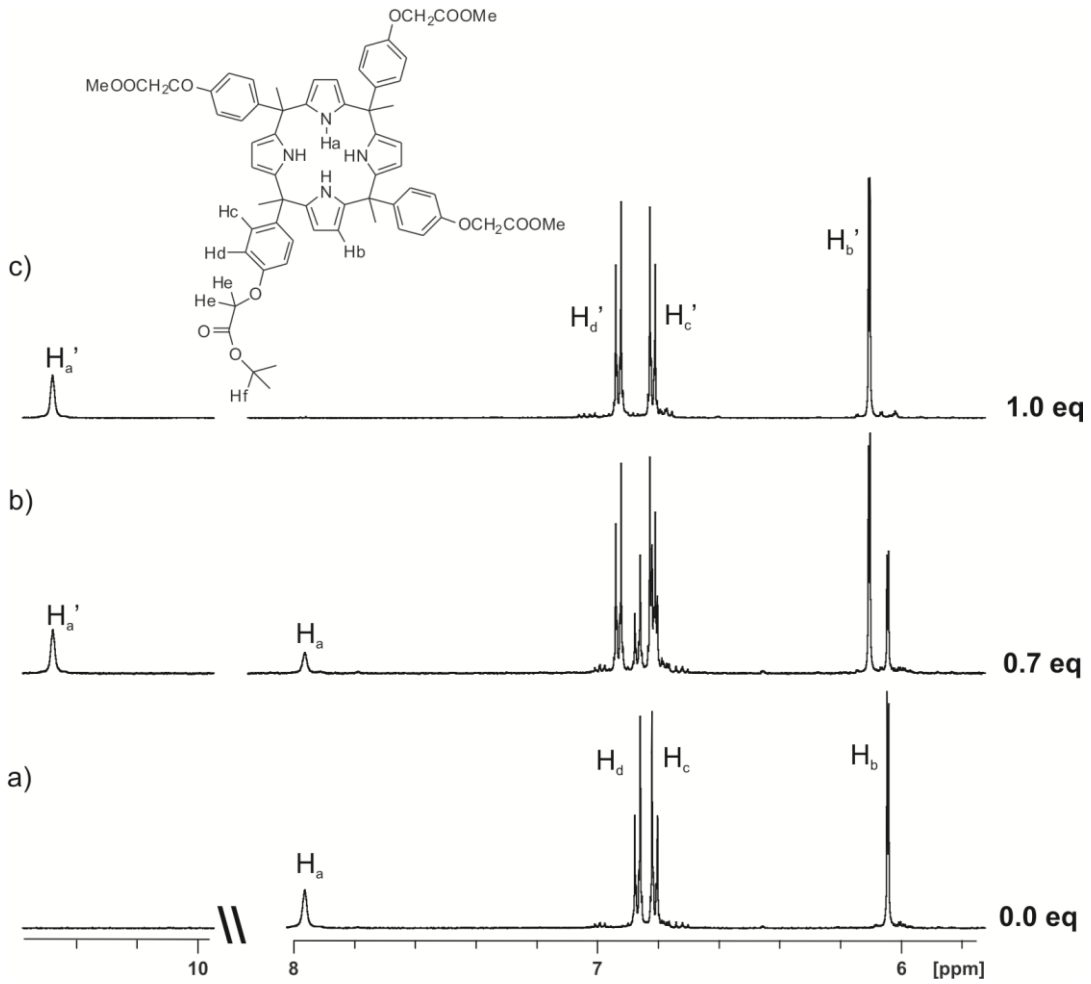

Figure 5. 7. Selected downfield region of the ^{1}H NMR spectrum acquired in acetonitrile-d_3 during the titration of the aryl-extended calix[4]pyrrole **1** with NMMO: a) 0 equivalents; b) 0.7 equivalents; c) 1 equivalent of NMMO added to a 1 mM solution of **1**.

After addition of 0.7 equivalent of NMMO, separate proton signals for the free and bound receptor are detected. This observation indicates that the host is involved in a chemical exchange process that is slow on the ^{1}H NMR timescale. The protons signals of the included NMMO appear upfield shifted due to the shielding effect exerted by the *meso* aromatic rings of the calix[4]pyrrole host. We assign the **Hα'$_{eq}$** protons to the signal resonating at δ = 0.80 ppm while the **Hα'$_{ax}$** protons appear at δ = 1.06 ppm (Figure 5. 8). The chemical shift values for the axial and equatorial **Hβ'** protons are δ = 3.11 ppm and δ = 3.27 ppm, respectively. The protons of the methyl group in the included NMMO resonate at δ = 1.23 ppm. After the addition of more than 1 equivalent of NMMO, new signals appear in the ^{1}H NMR spectrum of the mixture that correspond to the protons of free NMMO. The proton signals for the free receptor are no longer detected indicating that the receptor is 100%

complexed in agreement with a stability constant value for the 1:1 complex higher than 10^4 M^{-1}.

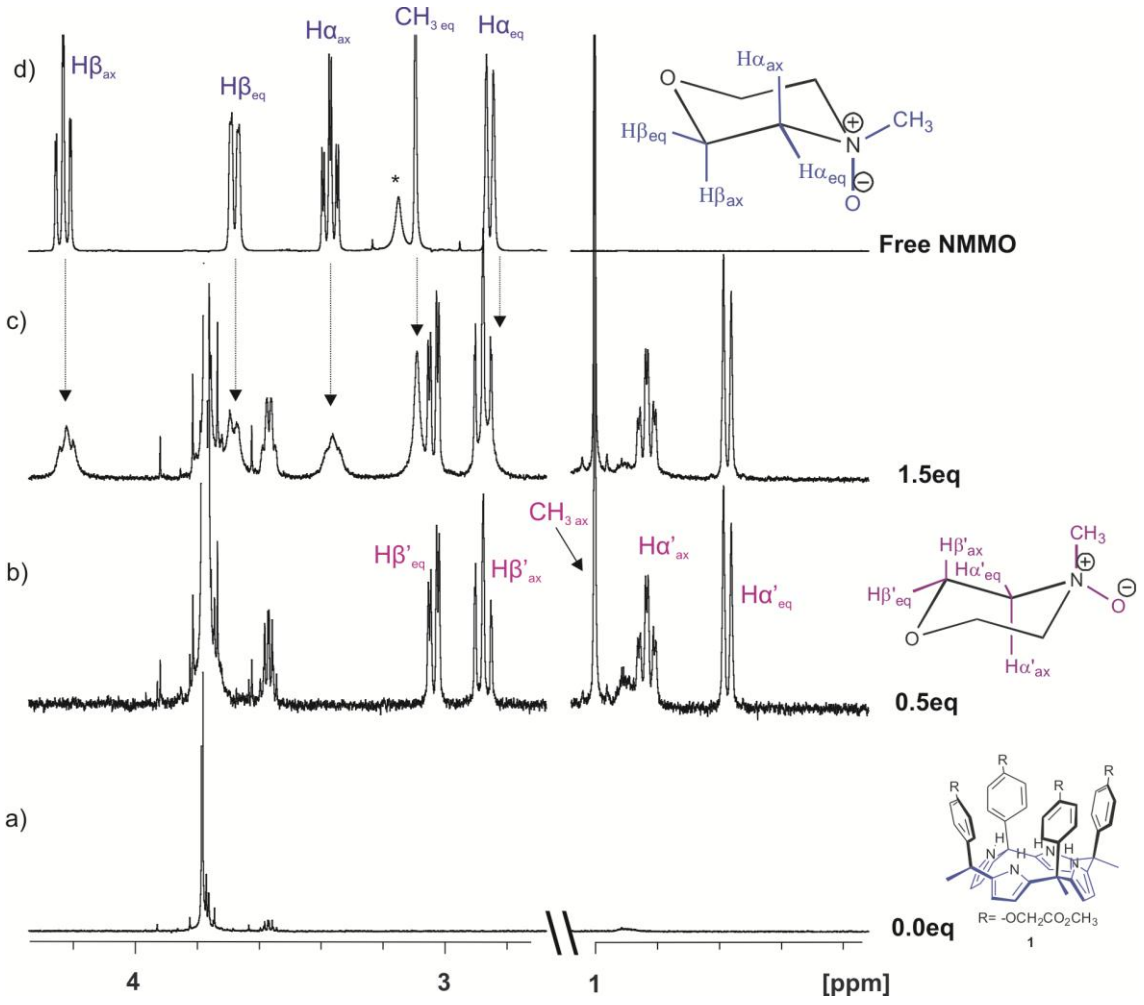

Figure 5. 8. Selected upfield region of the ^{1}H NMR spectrum acquired during the titration of the aryl-extended calix[4]pyrrole **1** with NMMO in acetonitrile-d_3 solution: a) 0 equivalents; b) 0.5 equivalents; c) 1.5 equivalent added; d) free NMMO. The broad signal at ~ 3.2 ppm indicated with an asterisk corresponds to water.

Although the ^{1}H NMR experiments described above support the inclusion process of the NMMO in the deep aromatic cavity of **1** producing a highly stable complex, both kinetically and thermodynamically, they did not give direct information on the conformer of NMMO involved in the NMMO@**1** complex in solution. We expected a deep inclusion of the *N*-oxide group into the aromatic cavity of **1** and the formation of hydrogen bonds with the NH protons. Molecular modelling studies suggested the potential existence of a conformational switch for the NMMO guest upon binding. If the NMMO guest adopts the conformation in which the oxygen atom is placed in an equatorial conformation the steric clashes that exist

between the aromatic walls of **1** and the hydrogen bonded guest are noticeably reduced (Figure 5. 9 - a). On the contrary, in the case of Figure 5. 9 - b, the aryl extended walls of the calix[4]pyrrole **1** are forced to adopt a more open conformation in order to create a bigger inner space and let the NMMO be included.

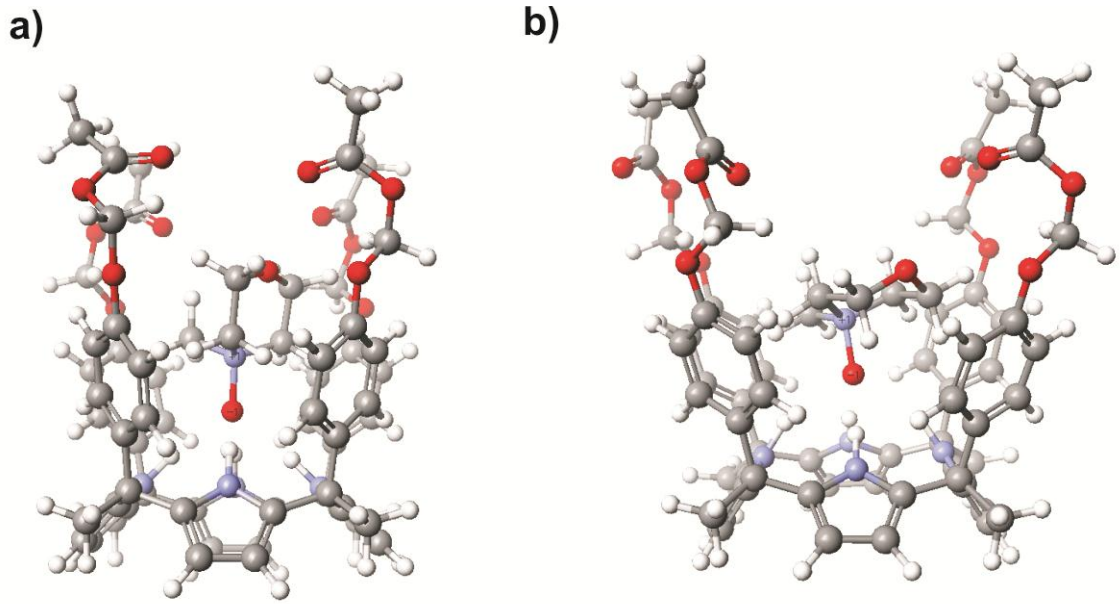

Figure 5. 9 CAChe minimized structures of the high (a) and low (b) energy conformer of *N*-methylmorpholine-*N*-oxide (NMMO) in the aryl-extended calix[4]pyrrole **1**.

We performed 2D ROESY and DQF COSY NMR experiments, in order to investigate the conformation adopted by the *N*-methyl morpholine *N*-oxide when bound in the NMMO@**1** complex. The observation of a single set of proton signals for the bound NMMO suggested that a single conformer has been included.

Figure 5. 10 depicts the 2D NOESY spectrum of NMMO@**1.** We detected NOE cross peaks between the protons of the included guest and the host, in agreement with the proposed inclusion nature of the complex. However, we focus our attention on the cross peaks resulting from NOEs (close spatial proximity) that exist between the singlet of the methyl protons of the bound NMMO and its equatorial Hα' and axial Hβ' protons. The presence of these contacts is the first indication of the trapping of the NMMO inside the receptor in a different conformation to the one exhibited for the guest in the bulk solution. Moreover, the multiplicity of the proton signals of the included guest and the chemical exchange pattern that exist

between the protons of the free NMMO suggested that the included guest adopted the high energy conformation assigned for the six membered chair in solution. For this reason, the protons $H\alpha_{ax}$ and $H\beta_{ax}$ in axial position in the conformer ***a*** adopt the equatorial position in conformer ***b*** ($H\alpha'_{eq}$ and $H\beta'_{eq}$, respectively). In the same way, the equatorial protons $H\alpha_{eq}$ and $H\beta_{eq}$ switch to $H\alpha'_{ax}$ and $H\beta'_{ax}$ in axial position.

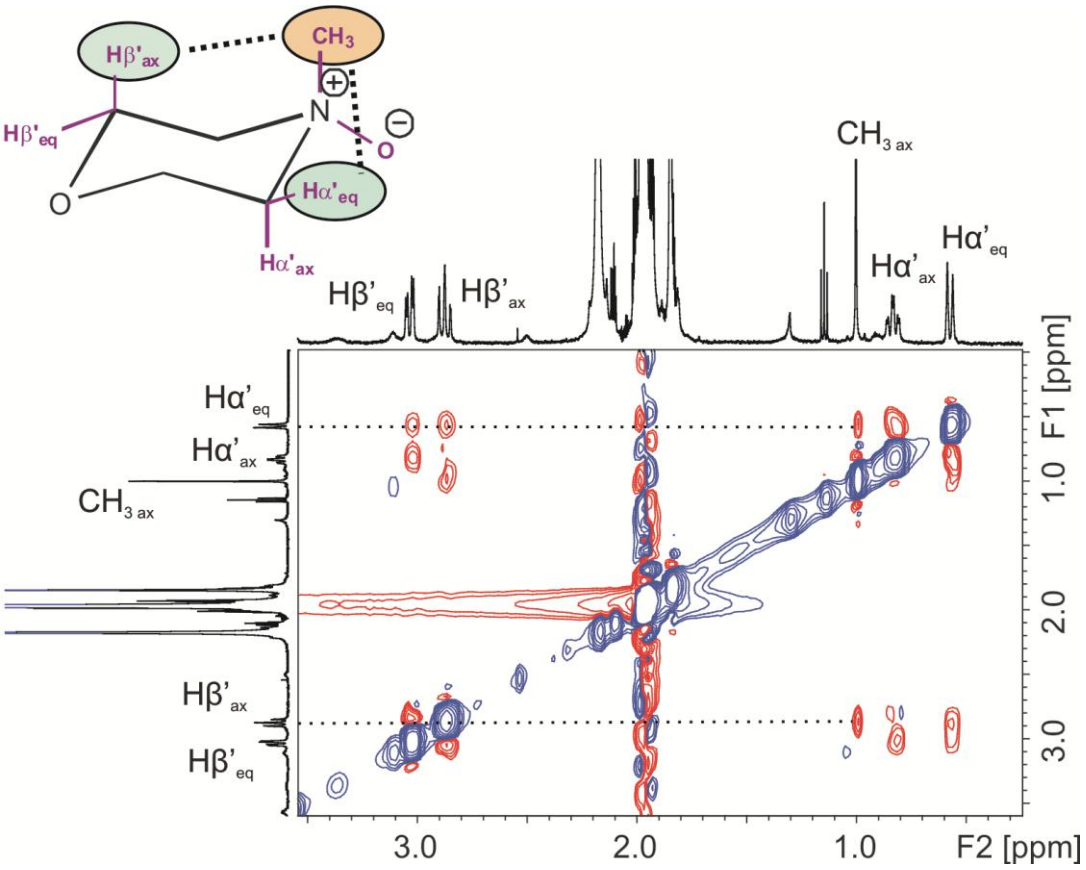

Figure 5. 10. Selected region of the 2D NOESY of *N*-methyl morpholine *N*-oxide included in **1**.

In agreement with the results of the NOESY experiment, the 2D DQF COSY NMR experiment validates our assignement for the protons of the included NMMO.

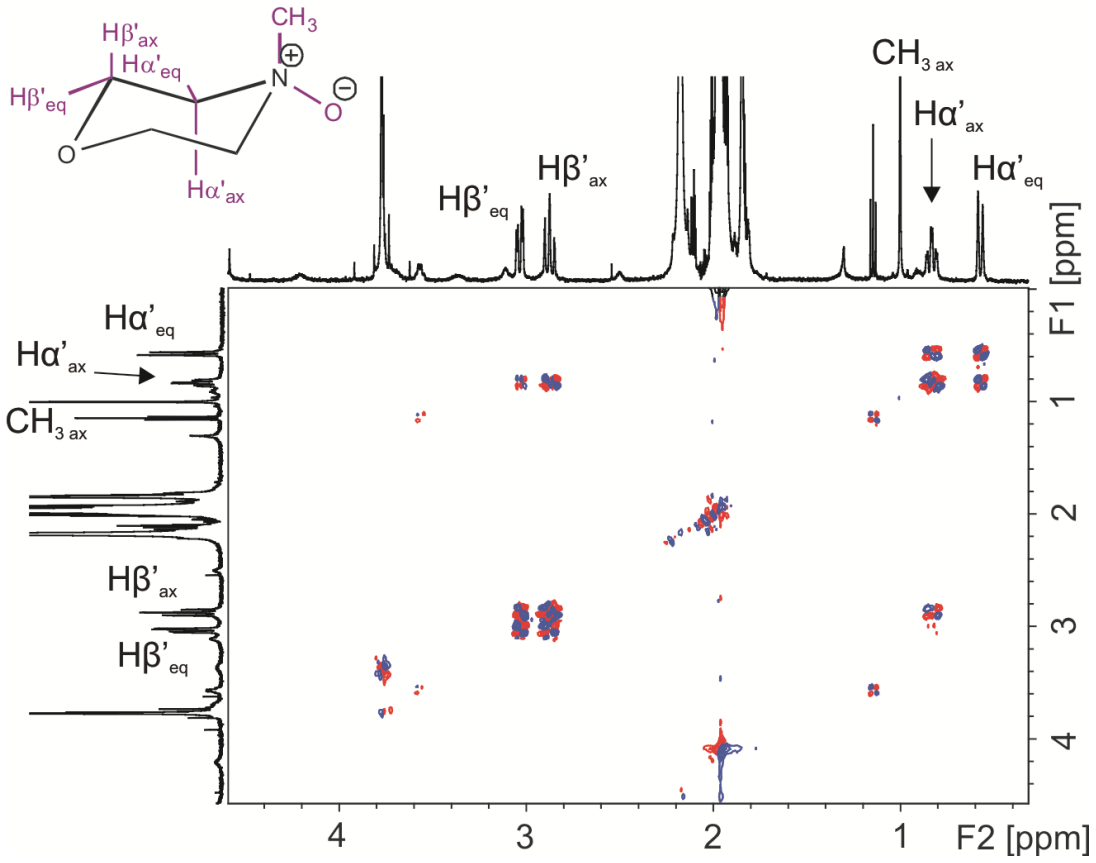

Figure 5. 11. 2D DQF COSY NMR of *N*-methyl morpholine *N*-oxide (NMMO) included in the aryl-extended calix[4]pyrrole **1**.

Luckily, we grew single crystals of the NMMO@**1** complex suitable for X-ray diffraction from acetonitrile solution. The solution of the diffraction pattern demonstrated that in the solid state the NMMO is included in the chair high energy conformation of the six membered cycle supporting the results obtained in solution and molecular modelling studies (Figure 5. 12).

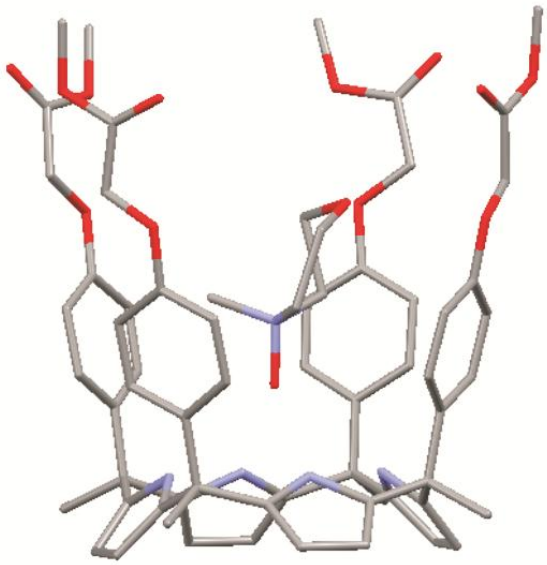

Figure 5. 12. Solid state structure of NMMO@**1** complex in which the NMMO adopts the high energy chair conformation of the six membered cycle. Hydrogen atoms and solvent molecules have been omitted for clarity.

To characterize the kinetic stability of the complex, we performed a 2D EXSY experiment at 298 K in presence of an excess of guest (1.5 equivalents of NMMO). By integration of the diagonal and the cross peaks of free and bound guest involved in chemical exchange (protons H_β axial and H_β' equatorial), we calculated with the help of D2DNMR software the exchange rate constant value for the guest exiting the host, as k_{out} = 9.1 s^{-1}. Thus the free energy barrier for the dissociation process was quantified as ΔG_{diss}= 18 Kcal/mol^{-1}. The high energy barrier associated with the dissociation to the guest hints to the existence of a required conformational exchange in the structure of the bound cavitand, from cone to 1,3-alternate, prior to the substitution of the guest by another guest or solvent molecules. The required change of conformation for the bound host as a prerequisite to guest exchange has also been postulated in *Chapters 2* and *3* for the binding of anions (Figure 5. 13).

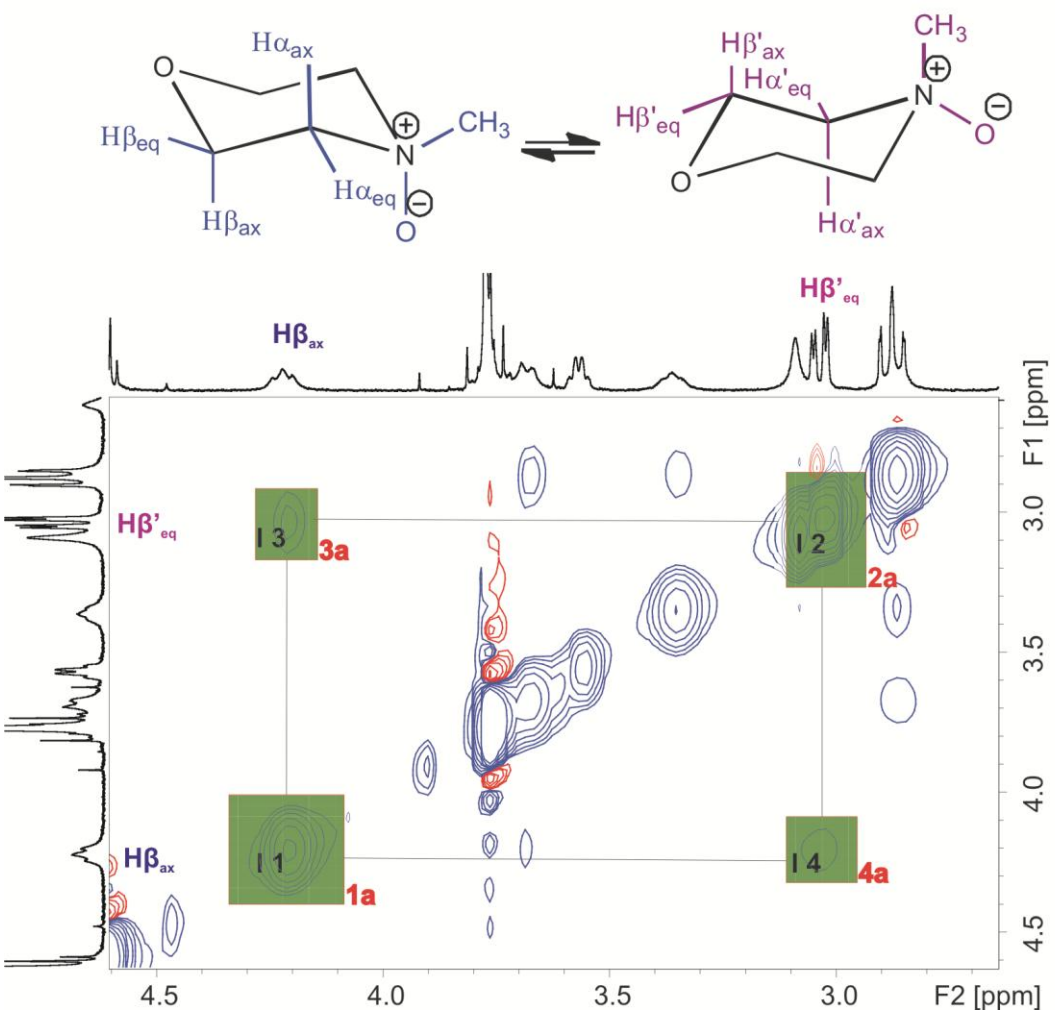

Figure 5. 13. EXSY ^{1}H NMR spectrum of **1** containing 1.5 equivalents of NMMO in acetonitrile-d_3 at 298 K.

*Reactivity of N-methyl morpholine N-oxide (NMMO) included in aryl-extended calix[4]pyrrole **1***

As mentioned before, the NMMO is commonly used as co-oxidant in the catalytic oxidation of alcohols to carbonyl groups using tetrapropylammonium perruthenate (TPAP). The TPAP reagent in fact can be rendered catalytic only if suitable *N*-oxides are added to the reaction mixture and the NMMO has been proved to be one of the most effective and easily to prepare.[19] The reaction of oxidation is strongly autocatalytic. This means that the rate of the reaction is initially slow but accelerates as the concentration of the product increases, while decreases near the end of the reaction because of a reduction in the concentration of the reactants.[20] It has been suggested that colloidal RuO_2, formed when

perruthenate is reduced by organic reductants, is responsible for the autocatalytic nature of these reactions.[21] Although the precise nature of the catalytic reaction is not exactly defined, it seems that the perruthenate RuO_4^- coordinates with the colloidal RuO_2 particles.[22]

$$[RuO_4]^- + nRuO_2 \longrightarrow [RuO_4 \cdot nRuO_2]^-$$

The presence of water can retard the catalytic turnovers since water molecules can be bound to the RuO_2 particles and reduce the sites available for the RuO_4^-. Thus, molecular sieves are usually added to the reaction mixture in order to remove the water of crystallization of the NMMO and the one formed during the reaction. On the contrary, reactions carried out in acetonitrile instead of dichloromethane leads to greatly improved systems.[23]

We were interested in evaluating the effect that the inclusion of the NMMO by calix[4]pyrrole **1** (supramolecular inclusion effect) could produce in the outcome of reactions like the oxidation of primary and secondary alcohols to carbonyl groups. The chemical reactivity of NMMO was first monitored by performing "control experiments". To a 0.5 M solution of benzyl alcohol in acetonitrile 1.5 equivalents of NMMO were added at r.t. and the reaction was monitored by ^1H NMR before and, every 15 minutes, after the addition of TPAP catalyst. Molecular sieves were also added to the reaction mixture in order to remove the water produced during the reaction since it could affect negatively the catalytic turnover number.[12] The ^1H NMR spectrum of the reaction mixture before the addition of TPAP is shown in Figure 5. 14 - a. The signals corresponding to the protons of the NMMO in the low-energy chair conformation of the six membered cycle, as well as the signals of the benzyl alcohol are easily distinguishable. Once the catalyst is added (Figure 5. 14 - b), a new singlet appear in the downfield region of the spectra corresponding to the aldehyde proton of the benzaldehyde product. The proton signals of the starting benzyl alcohol are no longer detected in the mixture. We consider the disappearing of the methylene protons H_5 of the benzyl alcohol at δ = 4.6 ppm and the appearance of the aldehyde-H_4 proton at δ = 10.0 ppm as unquestionable signs of the quantitative oxidation of the primary alcohol to the

aldehyde. In the aliphatic region of the spectrum, the signals of the protons of the tetrapropylammonium cation are also distinguishable. The ^{1}H NMR spectra of the reaction crude recorded after 15 (Figure 5. 14 - c) and 30 minutes (Figure 5. 14 - d) do not show any significant changes, indicating that the reaction is complete after the first couple minutes.

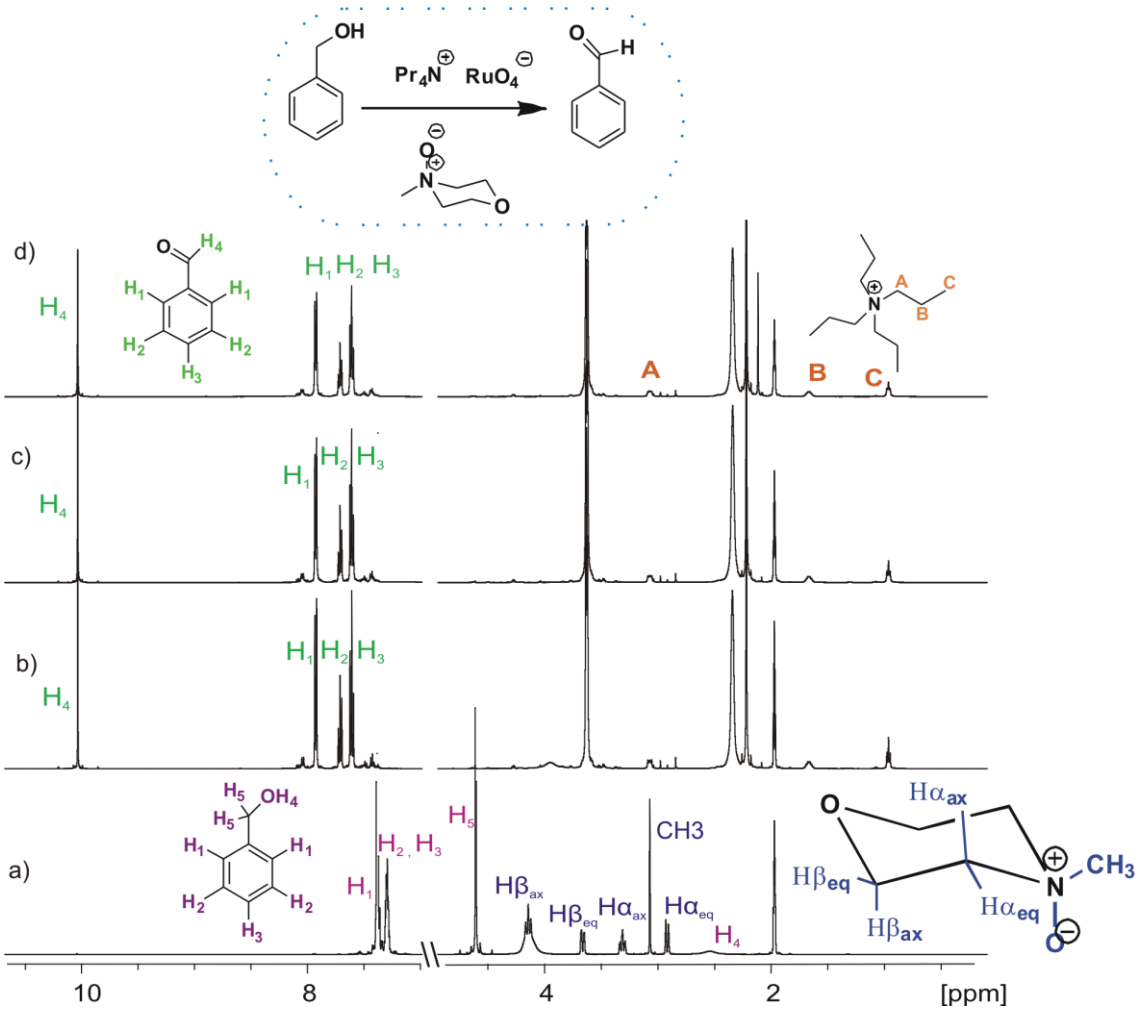

Figure 5. 14. ^{1}H NMR spectra acquired for a 0.5 M solution of benzyl alcohol and 1.5 equivalents of NMMO in ACN-d_3 (2 mL/mmol, 10 mL), r.t. and with 4Å molecular sieves (500 mg/mmol) before (a) and after addition of 1 equivalent of TPAP at ~ 5 minutes (b). The spectra (c) and (d) were recorded after 15 and 30 minutes, respectively.

The reaction was then repeated under the same conditions but adding to the solution a slight excess of calix[4]pyrrole **1** respect to the NMMO, in order to be sure that the *N*-oxide would be fully included in the receptor. The ^{1}H NMR spectrum of the second reaction crude containing the benzyl alcohol, the TPAP and the NMMO@**1** is reported in Figure 5. 15. The formation of the NMMO@**1** complex is confirmed by the signal resonating at δ = 10.47 ppm corresponding to the

pyrrole NHs of the bound host. The characteristic proton signals for the protons of the included NMMO in the high energy conformation are also detected. The spectrum shows a proton signal with low intensity at 10.0 ppm corresponding to the aldehyde H_4 proton of the benzylaldehyde, indicating that a reduced amount of product is formed under these conditions. Probably, all the moles of TPAP catalyst added have been consumed in the oxidation of the alcohol. However, most of the starting alcohol remains intact, as confirmed by the intense signals of the methylene H_5 protons of the benzyl alcohol resonating at δ = 4.6 ppm. After one hour of reaction, no changes are observed in the ^{1}H NMR spectrum of the mixture.

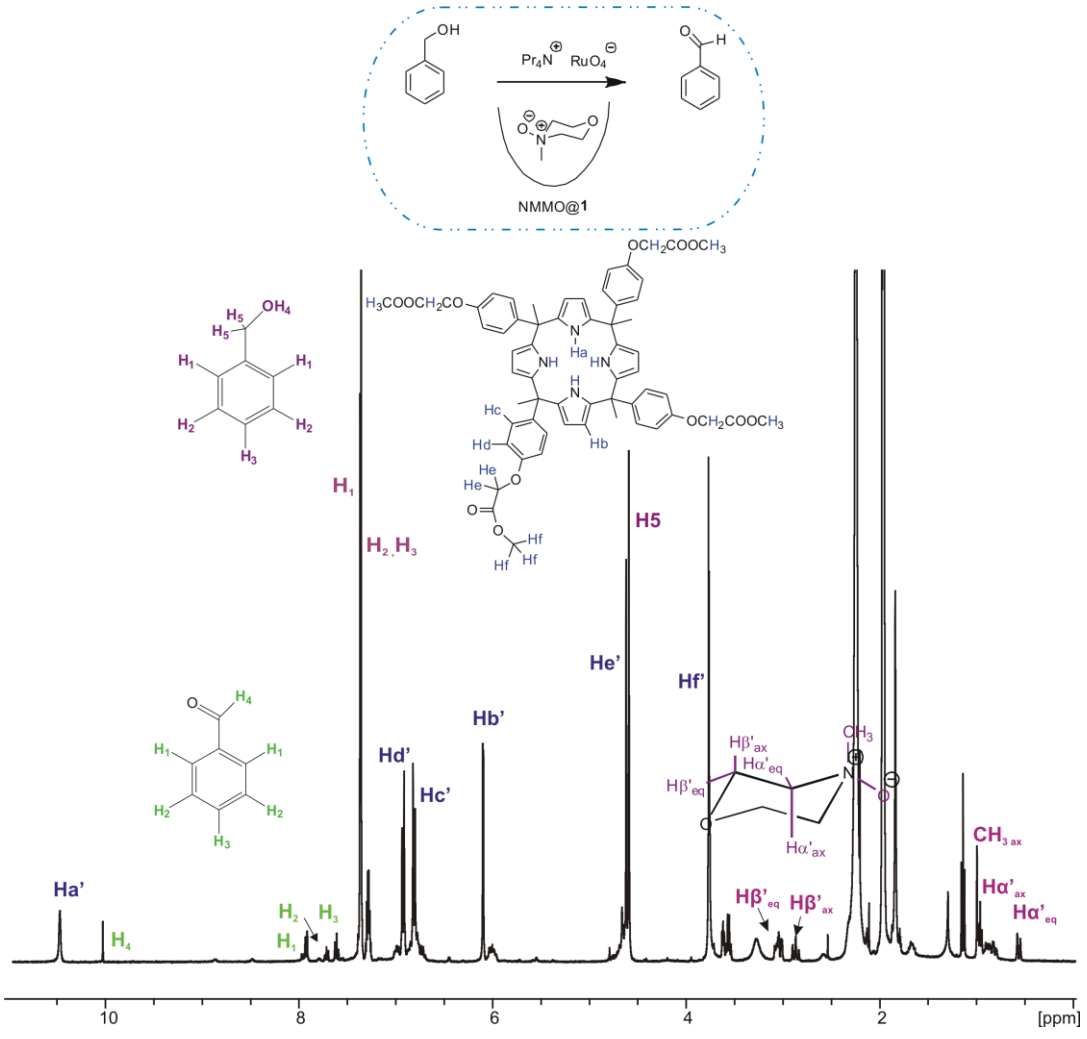

Figure 5. 15. ^{1}H NMR spectrum of the reaction crude of a solution of benzyl alcohol, NMMO and calix[4]pyrroles **1** in acetonitrile-d_3 and after addition of TPAP.

This experiment indicates that the reoxidation of the catalyst does not occur when the NMMO is included in the calixpyrrole **1**. The included NMMO can be realeased

within seconds by the addition of an excess of the highly competitive trimethylamine *N*-oxide.

The use of a secondary alcohol like the phenethyl alcohol corroborated our previous experimental findings. The oxidation of phenethyl alcohol was monitored using ^{1}H NMR spectroscopy (Figure 5. 16 - a). The rate of the oxidation reaction for the secondary alcohol was significantly slower than the oxidation of the primary alcohol. Inside the calix[4]pyrrole **1** the NMMO was not effective in the reoxidation of the TPAP catalyst. Consequently, only traces of acetophenone were observed in the reaction mixture (Figure 5. 16 – b).

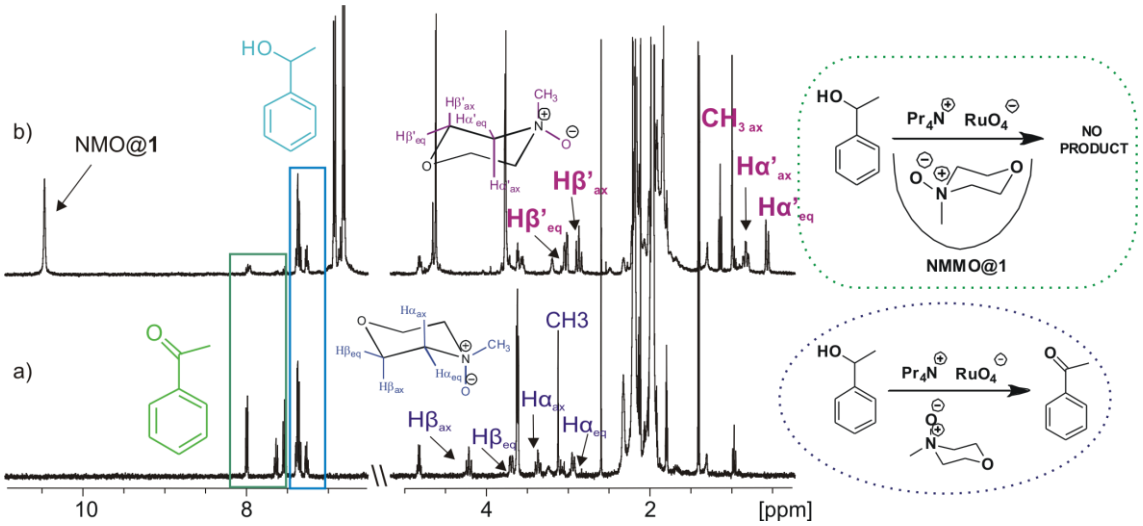

Figure 5. 16. Selected regions of the ^{1}H NMR spectra of solutions in acetonitrile-d_3 of: a) phenethyl alcohol, NMMO, TPAP and acetophenone; b) phenethyl alcohol, NMMO, TPAP and calix[4]pyrroles **1** in acetonitrile-d_3.

The catalytic oxidation of the phenethyl alcohol with TPAP was also monitored using gas-cromatography. Two reactions were carried out in parallel, one in presence of free NMMO and another with the NMMO@**1** inclusion complex. We also performed a calibration curve for the phenethyl alcohol in a range of concentrations between 2 mM and 5 mM, which allowed the quantification of the concentration of the alcohol in the two reactions. The reaction performed in the presence of free NMMO in solution showed a decrease in the initial concentration of phenethyl alcohol from 5 mM to 2 mM only after 5 minutes. After 10 minutes the concentration of the alcohol was 0.2 mM and it was not detected in the reaction mixture after 15 minutes. Moreover, a new chromatographic peak appeared with a

retention time of 3.95 minutes in addition to the peak of the phenethyl alcohol eluting at 3.9 minutes. The area of the first peak increased at the expenses of the area of the phenethyl alcohol during the first 15 minutes of the reaction and remained constant in aliquots taken from the reaction mixture during 2 hours. We assigned the peak with retention time of 3.95 minutes to the acetophenone formed in the oxidation reaction. On the contrary, the chromatograms corresponding to the analyses of the reaction crude performed by incorporating the calix[4]pyrrole **1** showed exclusively the existence of the chromatographic peak corresponding to the starting phenethyl alcohol, even after 2 hours of reaction.

5. 3 Conclusions

We have reported an example of inclusion of high energy conformers of *N*-oxides in aryl-extended calix[4]pyrroles. In particular, we have demonstrated the possibility of stabilizing the high energy conformer of *N*-methyl morpholine *N*-oxide (NMMO) within **1** with high association constants and high stability, both thermodynamic and kinetic. The interesting trapping has been studied through a combination of 2D NMR experiments, molecular modeling and X-ray diffraction technique. We have also evaluated the effect that the inclusion has in modifying the normal chemical reactivity of the NMMO by studying the outcome of reactions in which the *N*-oxide is commonly used as sacrificial oxidant (e.g. oxidation of primary and secondary alcohol to carbonyl derivatives with tetrapropylammonium perruthenate as catalyst). The progress of the oxidation reactions has been monitored by ^{1}H NMR spectroscopy and gas chromatography analysis, in the presence of free *N*-methylmorpholine *N*-oxide or as inclusion complex with the aryl-extended calix[4]pyrrole **1** (NMMO@**1**). In all the cases, the free NMMO resulted fundamental for the positive outcome of the reactions and its complexation by **1** did not allowed the appearance of the desired aldehyde/ketone derivatives in the reaction mixtures but only of the starting alcohols.

5. 4 Experimental Section

General information and instrumentation

All syntheses were carried out using chemicals as purchased from commercial sources unless otherwise noted. ^{1}H NMR spectra were recorded on a Bruker Avance 400 (400.1 MHz for ^{1}H NMR) and Bruker Avance 500 (500.1 MHz for ^{1}H NMR) ultrashield spectrometer; Gas-Chromatography experiments were carried out on Agilent GS (Model 6890N).

Synthesis

meso-Tetramethyltetrakis(hydroxyphenyl) calix[4]pyrrole 1: see Chapter 2.

NMMO Reactivity Studies

Oxydation of benzyl alcohol. Solid TPAP (5 mmol) is added in one portion to a stirred mixture of benzyl alcohol (5 mmol, 0.52 mL), NMMO (7.50 mmol) and 4Å molecular sieves (500 mg/mmol) in deuterated acetonitrile (2 mL/mmol, 10 mL) at r.t. under Ar. ^{1}H-NMR spectra were recorded from the reaction mixture every 15 minutes.

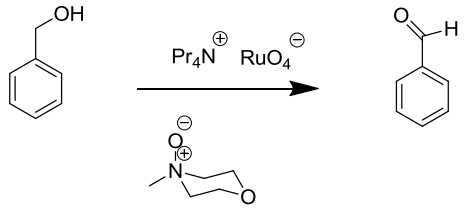

Oxydation of benzyl alcohol in presence of aryl-extended calix[4]pyrroles **1**. Solid TPAP (2.27 μmol) is added in one portion to a stirred mixture of benzyl alcohol (4.8 mmol, 0.5 mL), NMMO (7.24 mmol), aryl-extended calixpyrrole **1** (72 mmol) and 4Å molecular sieves (500mg/mmol) in deuterated acetonitrile (4 mL) at r.t. under Ar. The volume of solvent used for the reaction was higher than 2 mL/mmol, in order to solubilize the aryl-extended calixpyrrole **1** added to the reaction mixture**.** ^{1}H-NMR spectra were recorded after 5 minutes and one hour.

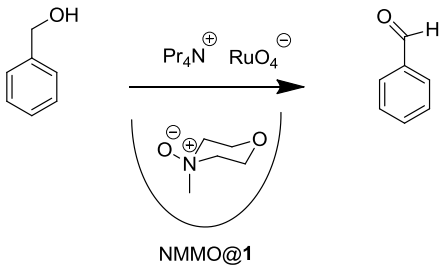

Oxydation of phenethyl alcohol with NMMO and with NMMO@1- **NMR studies**. The reactions were carried out in parallel in two separated NMR tubes, by preparing stock solution of NMMO (2.26 mg, 19.29 mM), TPAP (5.08 mg, 14.4 mM) and phenethyl alcohol (10 µL, 82.6 mM).

Oxidation of phenethyl alcohol: Solid TPAP (4.5 µL) was added to a solution of phenethyl alcohol (1.29 µmol, 15.7 µL) and NMMO (1.94 µmol, 100.7 µL) in 0.5 mL of acetonitrile. The reaction was monitored for 24 hours (~ 50% of product formed).

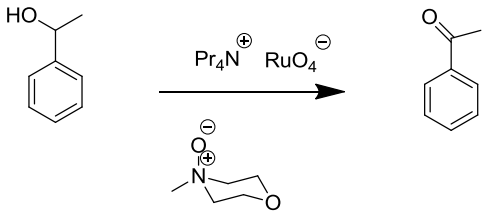

Oxidation of phenethyl alcohol with NMMO@**1**: Solid TPAP (4.5 µL) was added to a solution of phenethyl alcohol (1.29 µmol, 15.7 µL), NMMO (1.94 µmol, 100.7 µL) and calix[4]pyrroles **1** (2 µmol) in 0.5 mL of acetonitrile. The reaction was monitored for 24 hours and no product was observed by ^{1}H NMR.

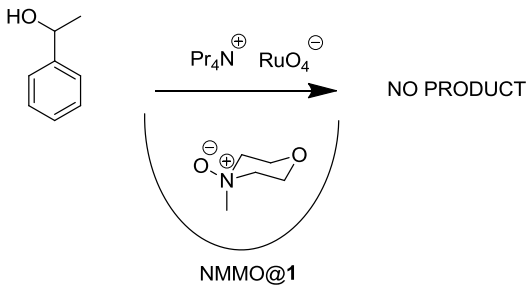

Oxydation of phenethyl alcohol with NMMO and NMMO@1 - **Gas chromatography** studies.

Monitoring of the concentration of starting alcohol during the reaction was performed with the aid of a calibration curve in the range of 2 mM to 5 mM. Stock solutions of phenethyl alcohol were prepared in 20 mL of acetonitrile. Aliquots of 2.5 mL of each stock solution were transferred in vials and analyzed by injecting 0.2 µl of each solution three times under the same conditions. The method used in the experiment consisted in increasing the temperature of 20°C each 5 minutes from 30 to 300°C. The peak of the phenethyl alcohol has retention time of 3.9 minutes. The calibration curve reported in Figure 5. 17 is obtained by plotting the value of the area of the phenethyl alcohol peak for each concentration (2.0 mM, 2.5mM, 3.0 mM, 3.5 mM, 4.0 mM, 4.5 mM, 5 mM). The value of the area reported for each concentration is calculated as average of the three injections.

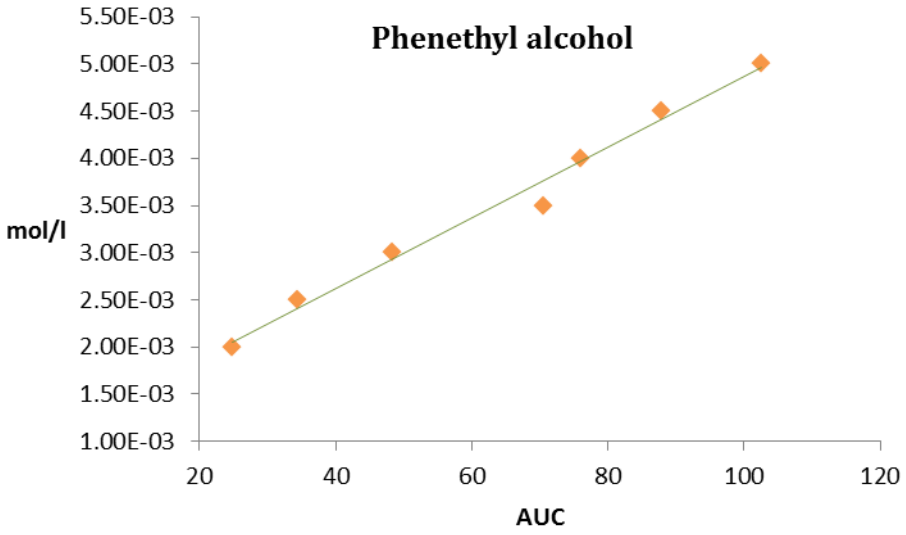

Figure 5. 17. Calibration curve plot determined by gas chromatography for the AUC of the phenethyl alcohol peak at different concentrations (2.0 mM, 2.5mM, 3.0 mM, 3.5 mM, 4.0 mM, 4.5 mM, 5 mM).

Oxydation of phenethyl alcohol with NMMO. Solid TPAP (5 µmol) was added in one portion to a stirred mixture of phenethyl alcohol (5 µmol, 12µL), NMMO (149 µmol) and solided 4Å molecular sieves (50 mg) in acetonitrile (20 mL) at r.t. under Ar. Aliquots of 0.5 mL of solution were collected, filtered to remove the catalyst and analysed after 5 minutes, 10 minutes, 15 minutes, 30 minutes, 1 hour and 2 hours using the same method reported for the determination of the calibration curve. The reaction was complete after 15 minutes.

N-oxide Inclusion

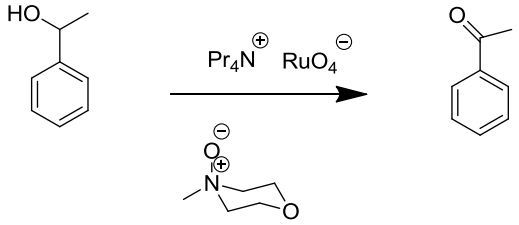

Oxydation of phenethyl alcohol with NMMO@**1**. Solid TPAP (5 µmol) was added in one portion to a stirred mixture of phenethyl alcohol (5 µmol, 12µL), NMMO (149 µmol) and solided 4Å molecular sieves (50 mg) in acetonitrile (20 mL) at r.t. under Ar. Aliquots of 0.5 mL of solution were collected, filtered to remove the catalyst and analysed after 5 minutes, 10 minutes, 15 minutes, 30 minutes, 1 hour and 2hours using the same method reported for the determination of the calibration curve. No product was observed in the reaction mixture.

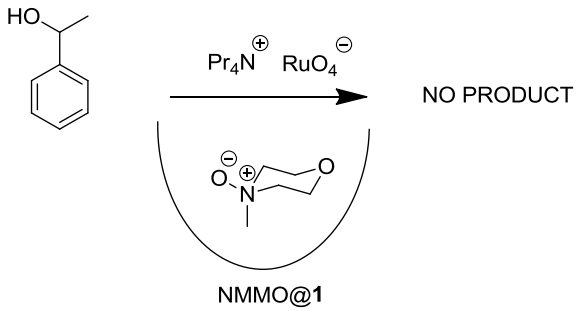

5. 5 References and Notes

[1] Chas, M.; Gil-Ramirez, G.; Escudero-Adan, E. C.; Benet-Buchholz, J.; Ballester, P. *Org. Lett.* **2010**, *12*, 1740.
[2] Gil-Ramirez, G.; Chas, M.; Ballester, P. *J. Am. Chem. Soc.* **2010**, *132*, 2520.
[3] Ballester, P.; Gil-Ramirez, G. *Proc. Natl. Acad. Sci. U. S. A.* **2009**, *106*, 10455.
[4] Verdejo, B.; Gil-Ramirez, G.; Ballester, P. *J. Am. Chem. Soc.* **2009**, *131*, 3178.
[5] Albini, A. *Heterocycles* **1992**, *34*, 1973.
[6] Jacobsen, E. N.; Marko, I.; Mungall, W. S.; Schroder, G.; Sharpless, K. B. *J. Am. Chem. Soc.* **1988**, *110*, 1968.
[7] Stevens, M.; Pannecouque, C.; De Clercq, E.; Balzarini, J. *Biochem. Pharmacol.* **2006**, *71*, 1122.
[8] Hancock, L. M.; Beer, P. D., *Chem. Commun.*, **2011**, *47*, 6012-6014.
[9] Chen, M. J.; Han, S. J.; Jiang, L. S.; Zhou, S. G.; Jiang, F.; Xu, Z. K.; Liang, J. D.; Zhang, S. H., *Chem. Commun.*, **2010**, *46*, 3932-3934.
[10] Atwood, J. L.; Dalgarno, S. J.; Hardie, M. J.; Raston, C. L. *New J. Chem.* **2004**, *28*, 326.
[11] Rosenau, T.; Potthast, A.; Sixta, H.; Kosma, P. *Prog. Polym. Sci.* **2001**, *26*, 1763.
[12] Ley, S. V.; Norman, J.; Griffith, W. P.; Marsden, S. P. *Synthesis-Stuttgart* **1994**, 639.
[13] Hoh, G. L. K.; Barlow, D. O.; Chadwick, A. F.; Lake, D. B.; Sheeran, S. R. *J. Am. Oil Chem. Soc.* **1963**, *40*, 268.
[14] Anslyn, Eric V.; Dougherty, Dennis A., *Modern Physical Organic Chemistry*, Sausalito, 2006.
[15] Porel, M.; Jayaraj, N.; Raghothama, S.; Ramamurthy, V. *Org. Lett.* **2010**, *12*, 4544.
[16] Opietnik, M.; Potthast, A.; Kitaoka, T.; Rosenau, T., *J. Label Compd. Radiopharm*, **2010**, *53*, 78-80.
[17] Jerry March, *Advanced Organic Chemistry, 4th Edition,* WILEY-VCH Verlag GmbH & Co, 1992.
[18] Berger, S.; Braun S.; *200 and More NMR Experiments,* WILEY-VCH Verlag GmbH & Co. KgaA, 1998.
[19] Luzzio, F. A.; Guziec, F. S. *Org. Prep. Proced. Int.* **1988**, *20*, 533.
[20] Lee, D. G.; Wang, Z.; Chandler, W. D. *J. Org. Chem.* **1992**, *57*, 3276.
[21] Lee, D. G.; Congson, L. N. *Can. J. Chem.* **1990**, *68*, 1774.
[22] Lee, D. G.; Perezbenito, J. F. *J. Org. Chem.* **1988**, *53*, 5725.
[23] Ashby, E. C.; Goel, A. B. *J. Org. Chem.* **1981**, *46*, 3936.

CHAPTER VI

Design and Synthesis of Resorcin[4]arene Derivatives as Potential Ligands for Supramolecular Catalysis

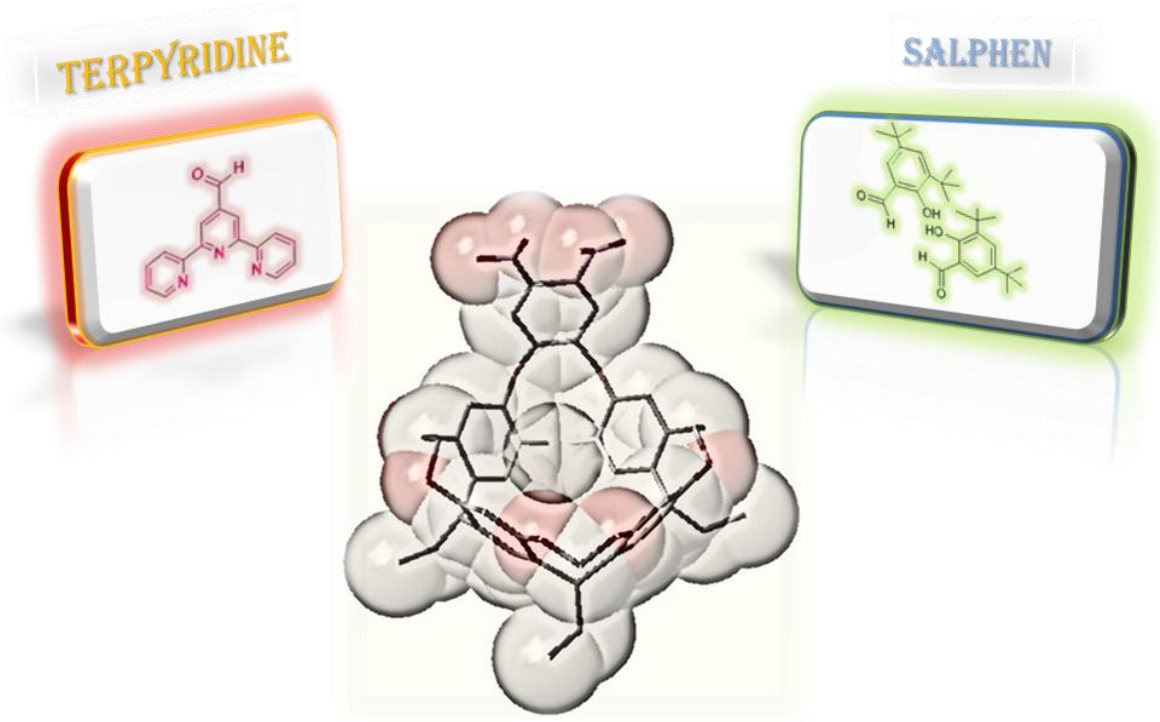

6. 1 Introduction

Many examples of synthetic receptors derived from resorcin[4]arenes (Figure 6. 1) have been introduced and studied by Cram and co-workers.[1] Resorcinarenes were originally thought to form a folded structure in organic solvents adopting a bowl-shape cavity in which it was possible to trap numerous molecules.[2] MacGillivray and Atwood[3] demonstrated that the same resorcinarenes self-assemble forming large hexameric capsules[4] as well as dimeric structures.[5] The elaboration of the upper rim of resorcin[4]arenes by bridging the aromatic phenol substituents affords cavitands. The bridging strategy not only provides an increase in the shielding of the bound guest but also preorganizes and prevents the cavity from collapsing on itself. Cavitands posses significantly larger binding affinities for organic molecules in solution than resorcina[4]arenes. An example of a cavitand host is supplied by pyrazine-bridged resorcinarenes. These compounds having flexible walls at their upper rim are able to adopt C_{4v} vase or C_{2v} kite conformations in function of the external temperature or pH.[6,7] Self-folding cavitands are resorcin[4]arenes derivatives with eight amido groups at its upper rim. They form an array of intramolecular hydrogen bonds that stabilizes the cavitand in the vase-conformation.[8,9] Moreover, head-to-tail linked amide groups within self-folding cavitands can adopt either a clockwise or counterwise orientation giving rise to conformational enantiomers that interconvert in solution.[10] In general, resorcin[4]arenes constitute a privileged scaffold for the preparation of a wide variety of elaborated cavitands into which molecular recognition binding sites and coordination sites for catalytic metals can be installed and combined, as already explained in the *General Introduction* (Chapter 1) of this thesis. These types of macrocyclic receptors can bind a wide range of aromatic molecules predominantly in a 1:1 stoichiometry forming complexes generally stabilized by a range of weak interactions, such as hydrogen bonds, C–H ••• π, cation-π, etc. On the contrary, there is very little evidence for a significant binding of neutral molecules with simple resorcin[4]arenes in organic solvents. Water-solubilizing groups, such as sulfonates, can be appended to the rim of the bowl cavity, thereby increasing the affinity for neutral organic guests in water as a consequence of hydrophobic

interactions. Resorcinarenes have been also used as hosts for cations in basic media. Phenolate resorcinares in fact are efficient hosts for the molecular recognition of organic ammonium ions in protic solvents.[11,12] The affinity of the mentioned receptors for the ammonium ions is high (10^3 - 10^6 M^{-1}) and relies on the simultaneous charge-charge and cation-π interactions.[13] These receptors have been used in the development of promising binary systems for the recognition of biologically important ammonium cations like choline, acetylcholine and carnitine.[14,15] Unfortunately, the main drawback of the resorcin[4]arene receptors that are effective in protic media is the low selectivity exhibited for the alkyltrimethylammonium motif, present in choline and carnitine derivatives, compared to bulkier tetraalkylammonium ions.[16] This low selectivity is due to the reduced concavity of these receptors that only surrounds a small fraction of the ammonium ion. In fact, only neutral or anionic cavitands have been shown to possess the ability of binding inside their cavities alkylammonium hosts with high size-selectivity.[17,18]

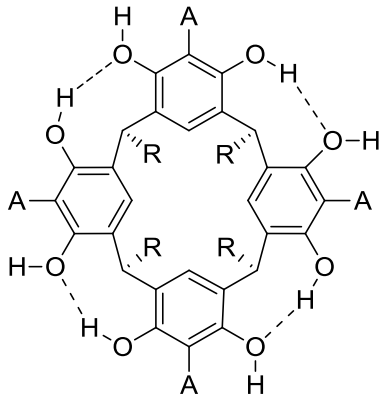

1
R = Et
A = H

Figure 6. 1 Resorcin[4]arene structure. In the nomenclature used for the macrocycle, [4] indicates the number of resorcinol units that form the receptor.

The overarching theme of the research presented in this chapter is the design of molecules and supramolecules featuring an aromatic cavity or cleft capable of including neutral and ionic species and with potential applications as efficient supramolecular catalysts. For this purpose we wanted to create resorcin[4]arene

derivative receptors with one substituent at their upper rim capable to act as catalytic centre. Our supramolecular strategy to catalysis implies the design criteria of placing a catalytic site close to the binding site. A lot of efforts have been dedicated to the synthesis of the trimethylene-bridged resorcinarene scaffold **2.** This receptor features a dinitrophenyl unit as extended aromatic wall for further elaboration at the upper rim and alkyl (i.e. ethyl) chains at the lower rim for solubility purposes (Figure 6. 2).

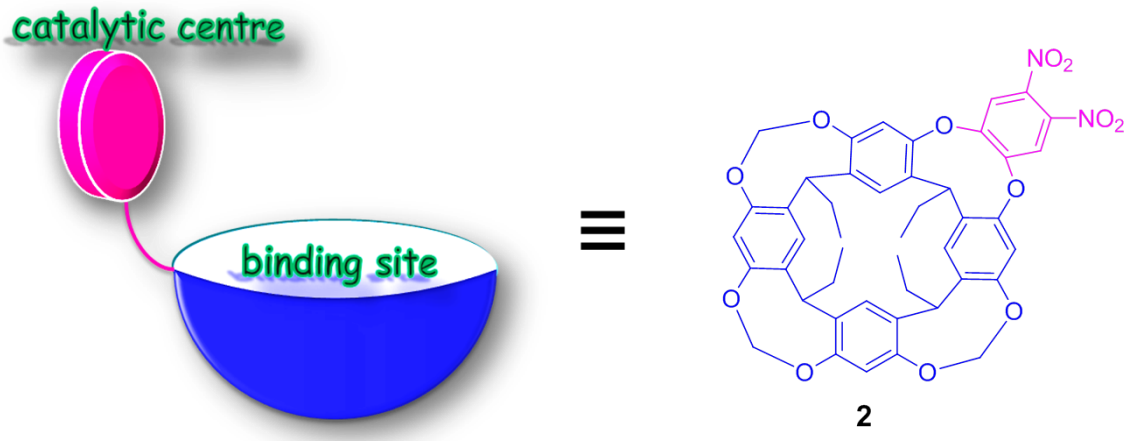

Figure 6. 2 Trimethylene-bridged resorcin[4]arene 2 (blue) with a dinitrophenyl wall (pink), for the inclusion of positively charged unsaturated substrate or biologically active molecule (e.g. choline) by cation-π interactions.

One of our aims was to study how the simple structure of **2** affected the binding selectivity toward different ions compared to the more elaborated resorcin[4]arene – derivatives with four aromatic bridges. We were also interested in the evaluation of the single aromatic wall cavitands that we prepared as building blocks of supramolecular catalyst precursors. With this purpose in our mind, we synthesized the *Salphen – Resorcin[4]arene* **5** and the *Terpyridine – Resorcin[4]arene* **7** as potential ligands for supramolecular catalysis. The synthesis of these compounds is depicted in the general Scheme 6. 1.

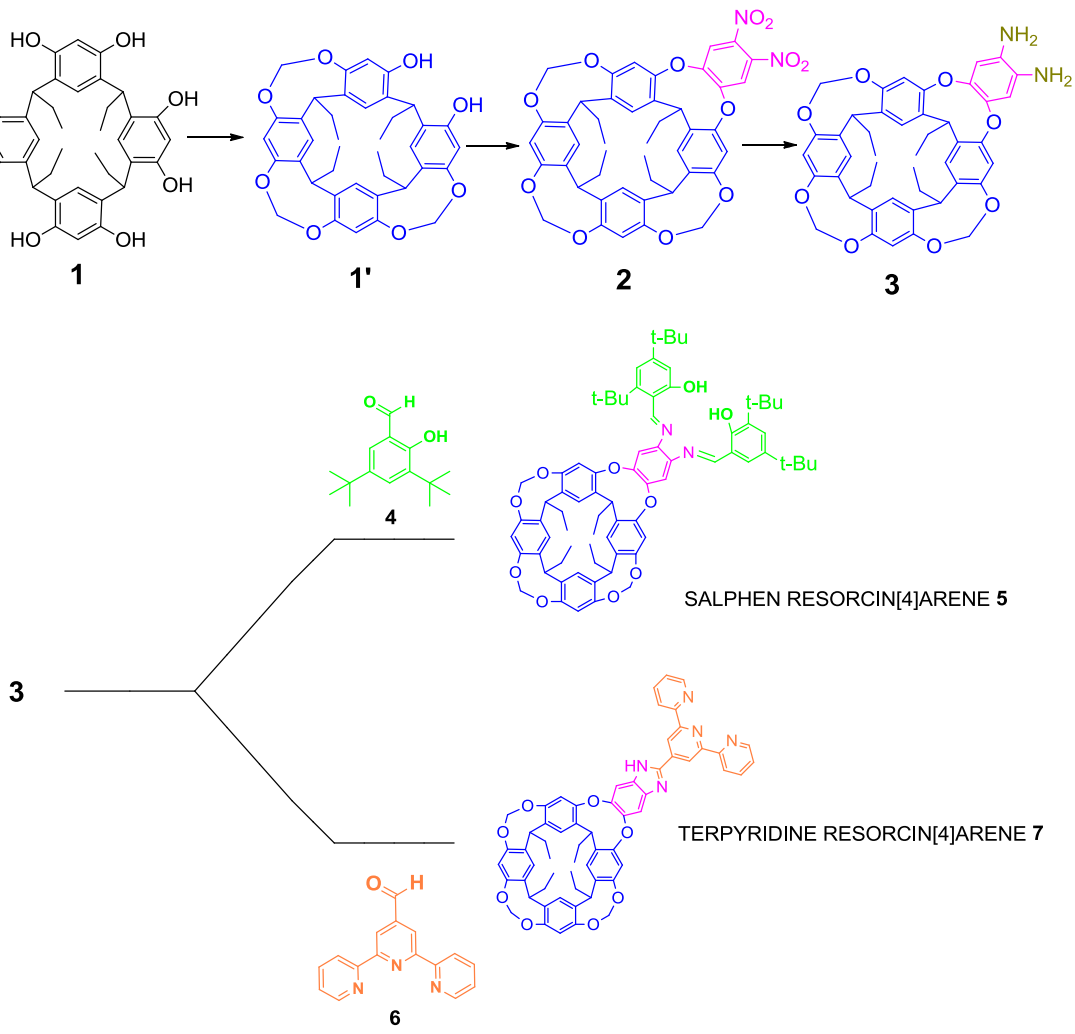

Scheme 6. 1. General synthetic scheme for the preparation of the resorcin[4]arene - derivatives **5** and **7.**

The *Salphen – Resorcin[4]arene* **5** (Figure 6. 3) was synthesized by reacting the diamino groups in the aromatic wall of **3** with an excess of benzyl aldehyde **4.**

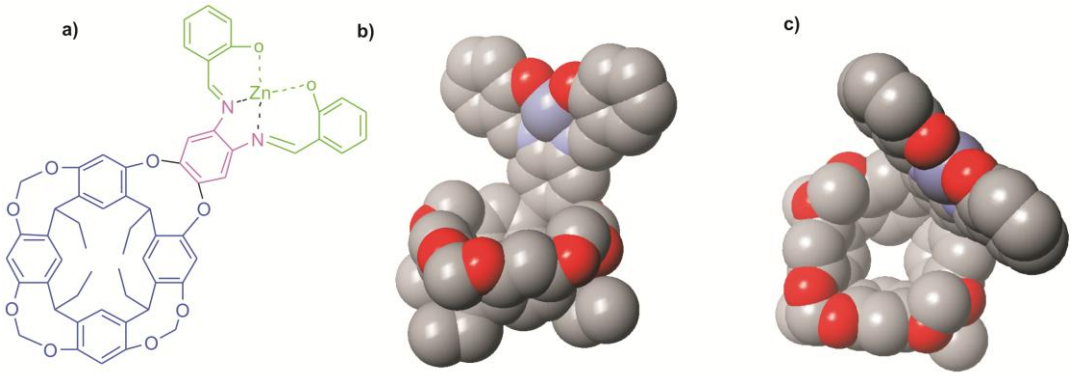

Figure 6. 3 Line drawing structure (a) and CAChe energy minimized structure (b = front view, c = top view) of the Zn-Salphen Resorcin[4]arene **5.** For clarity, hydrogen atoms are omitted.

The main interest in the synthesis of Zn-salphen resorcin[4]arene complexes lies in the possibility of using them as catalyst in the acylation reaction of choline using acetyl imidazole as reactant (Scheme 6. 2). We believe that both substrates can be simultaneously bound to the Salphen trimethylene bridged cavitand. In particular, choline molecules can be included within the aromatic cavity of cavitand **5** through cation-π interactions while the imidazole can be coordinated to the Zn^{+2} metal that also acts as a Lewis acid catalyst for the reaction.

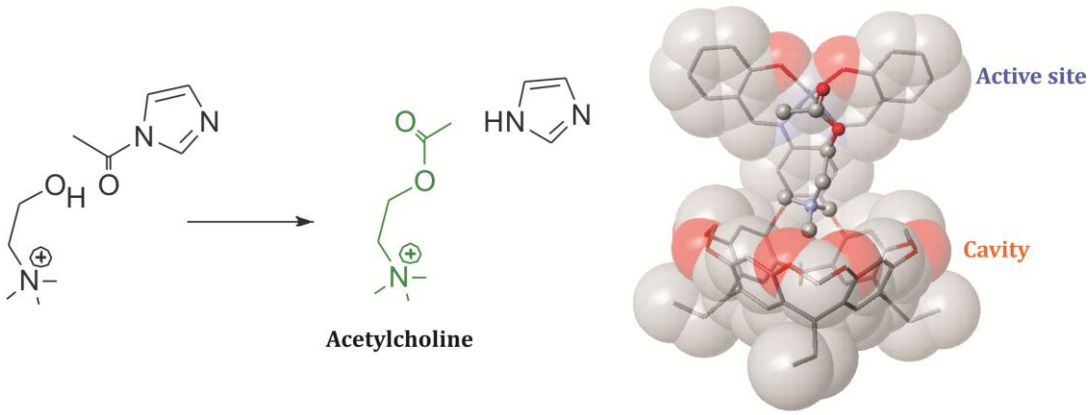

Scheme 6. 2 Acylation reaction of choline using acetyl imidazole as reactant. Energy minimized structure of the complex formed by the Salphen derivative and acetylcholine.

Terpyridine – Resorcin[4]arene **7** presents an extended aromatic wall formed by the terpyridine moiety covalently linked to the mono-wall cavitand **3** throught an imidazolyl spacer (Figure 6. 4).

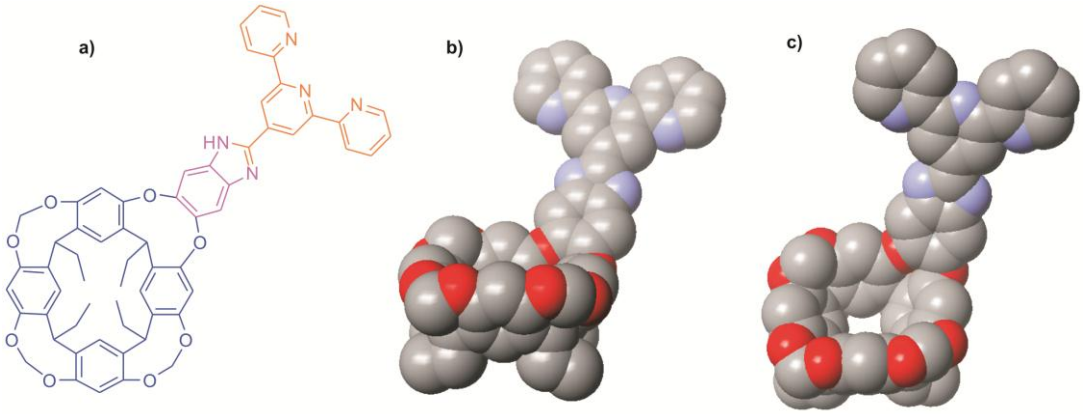

Figure 6. 4 Line drawing structure (a) and CAChe energy minimized structure (b = front view, c = top view) of the Terpyridine – Resorcin[4]arene **7**. For clarity, hydrogen atoms are omitted.

The main goal of the synthesis of Terpyridine derivative **7** resided in their further applications as Ruthenium - complexes for the catalytic epoxidation of unsaturated substrates with an alkylammonium terminal chain (Scheme 6. 3). Considering the proposed design, we believe that the substrate is likely to be included in the cavity of the resorcinarene-derivative through its trimethylalkylammonium terminal through cation – π interactions, while the double bond can be adequately disposed in front of the Ru^{IV}=O active site of the receptor to undergo an epoxidation reaction.

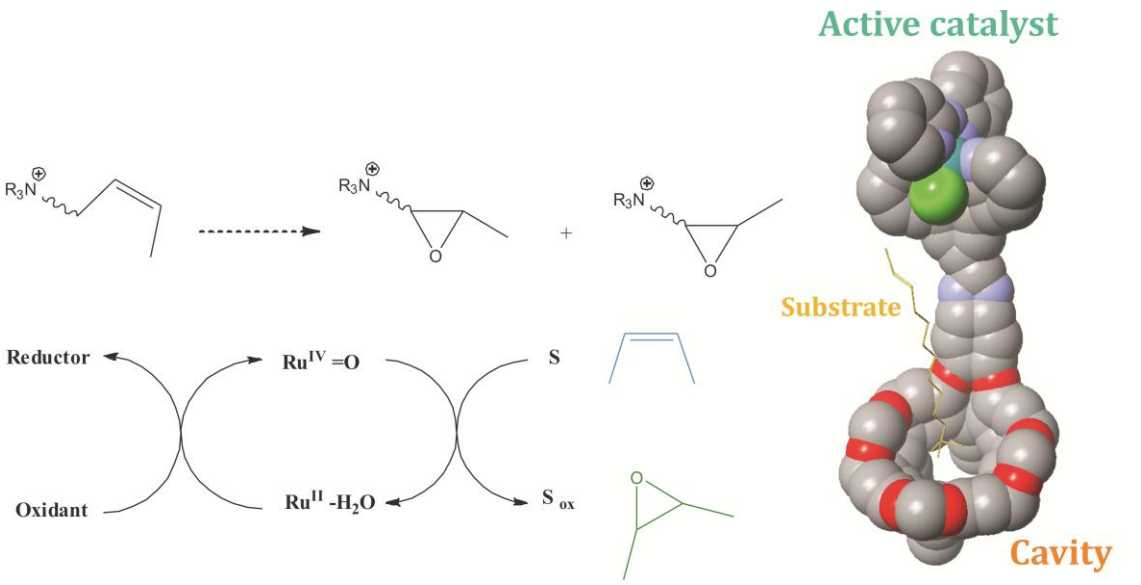

Scheme 6. 3 Schematic representation of the catalytic epoxidation reaction of an unsaturated substrate (S) by Ruthenium metal centre. Energy minimized structure of the Terpyridine receptor **7** to be used as potential supramolecular catalyst.

6. 2 Results and discussion

6.2. 1 Synthesis of cavitand 2

Resorcin[4]arenes are easily obtained in large scale from the acid catalyzed condensation of acetaldehyde and resorcinol.[19] Based on the relative configuration of the substituents at the methylene bridges of the resorcin[4]arene, four different configurational isomers exist[20]: the all-*cis* (*ccc*), the *cis-cis-trans* (*cct*), the *cis-trans-trans* (*ctt*) and *trans-cis-trans* (*tct*) (Figure 6. 5).

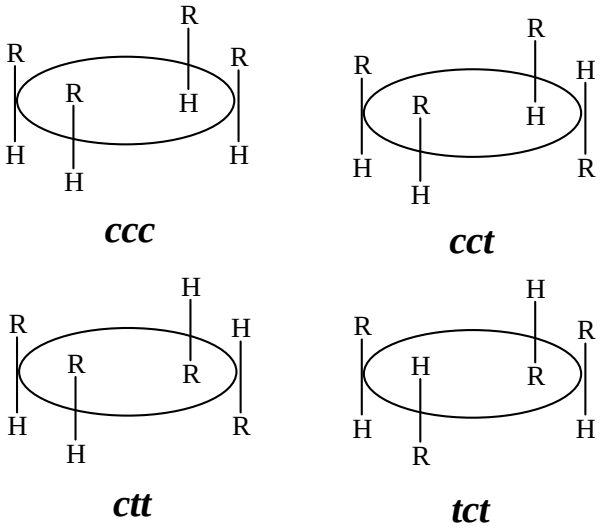

Figure 6. 5 Resorcinarene's configurational isomers.

In the reaction crudes of the acid condensation reactions only two of the four possible stereoisomers are usually detected (Figure 6. 6): the R-*cis*-*cis*-*cis* with C_{4v} symmetry and the R-*cis*-*trans*-*trans* with C_{2v} symmetry. The stereoisomer **1** (C_{4v}) of the cyclic tetramer is usually obtained as almost the exclusive reaction product.

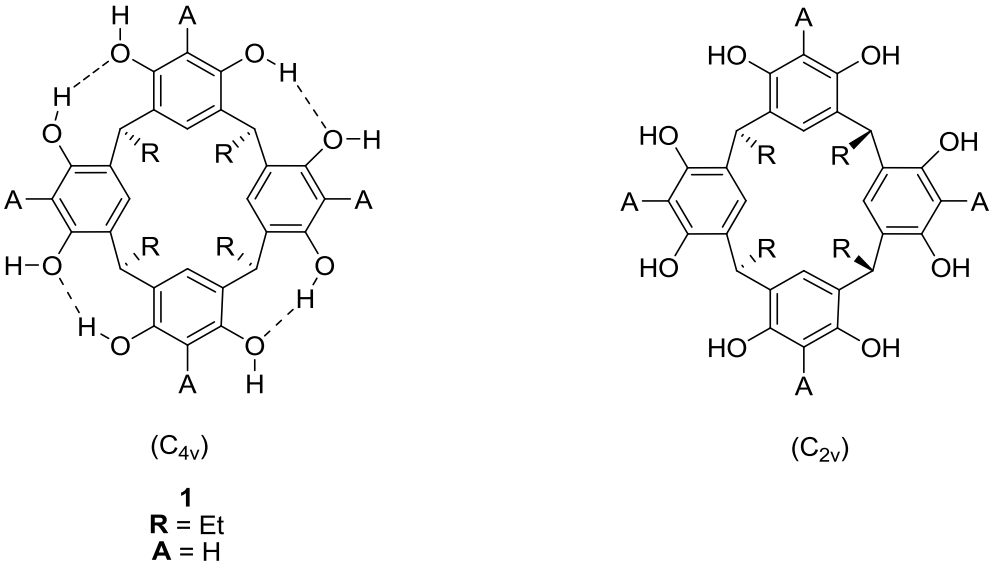

Figure 6. 6 Molecular structures of the two configurational stereoisomers of Resorcin[4]arenes obtained from the acid condensation reaction of resorcinol and aliphatic aldehydes.

The flexible and three dimensional structure of the resorcin[4]arenes allows the existence of the single configurational isomer R-cis-cis-cis in different

conformations: crown (C_{4v}, **a**), chair (C_{2h}, **b**), boat (C_{2v}, **c**) and saddle (D_{2d}, **d**) as shown in Figure 6. 7.

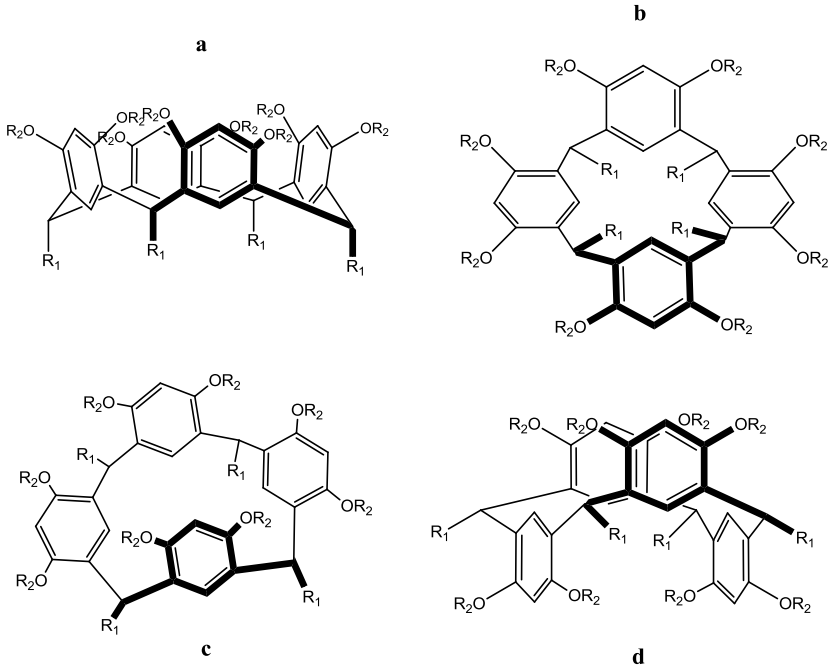

Figure 6. 7 Possible conformations of the R- cis, cis, cis configurational isomer.

The all-cis crown isomer of **1** is isolated as the main macrocyclic product in the condensation reaction of resorcinol and propionaldehyde. The precipitation of the least soluble isomers serves as themodynamic sink. The ^{1}H-NMR spectrum of **1** indicates an effective C_{4v} symmetry in solution. Most likely, the formation of a seam of hydrogen bonds in the upper rim of the compound is possible only when the molecule adopts this conformation for the energetic advantage.

The standard procedure for the cyclotetramerization reaction was employed by reacting the resorcinol with 1.5 equivalents of propionic aldehyde in ethanol/water solution containing concentrated aqueous HCl (2:2:1 volumetric ratio) at 75°C for 2 hours and by continuous stirring at room temperature for one week (Scheme 6. 4).

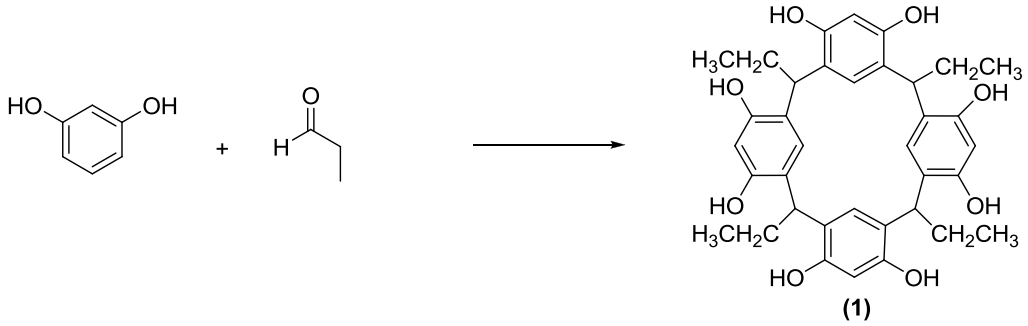

Scheme 6. 4 Synthesis of resorcin[4]arene **1**. Conditions: resorcinol, propionaldehyde (1.5 equivalents), EtOH/H_2O/HCl (2:2:1), 75 °C, 2 hrs, then r.t. 7 days (yield: 67%).

The product that precipitated from the reaction mixture was recrystallized from EtOH/water (1:1). As indicated above, when using aliphatic aldehydes only the C_{4v} isomers are isolated. The acid-catalyzed condensation of resorcinol with aldehydes is interpreted in terms of cationic intermediates and electrophilic aromatic substitution reactions (Scheme 6. 5).[21] Weinelt and Schneider undertook kinetic and molecular modeling studies on the mechanism of the acid-catalyzed condensation reaction between resorcinol and acetaldehyde and concluded that a) the ring closure is as fast as the chain propagation process, b) the macrocyclic products are the thermodynamic sink of the reactions and c) linear oligomers longer then four aryl units depolymerize fast in comparison with ring opening, promoting the formation of the cyclic tetramer.[22]

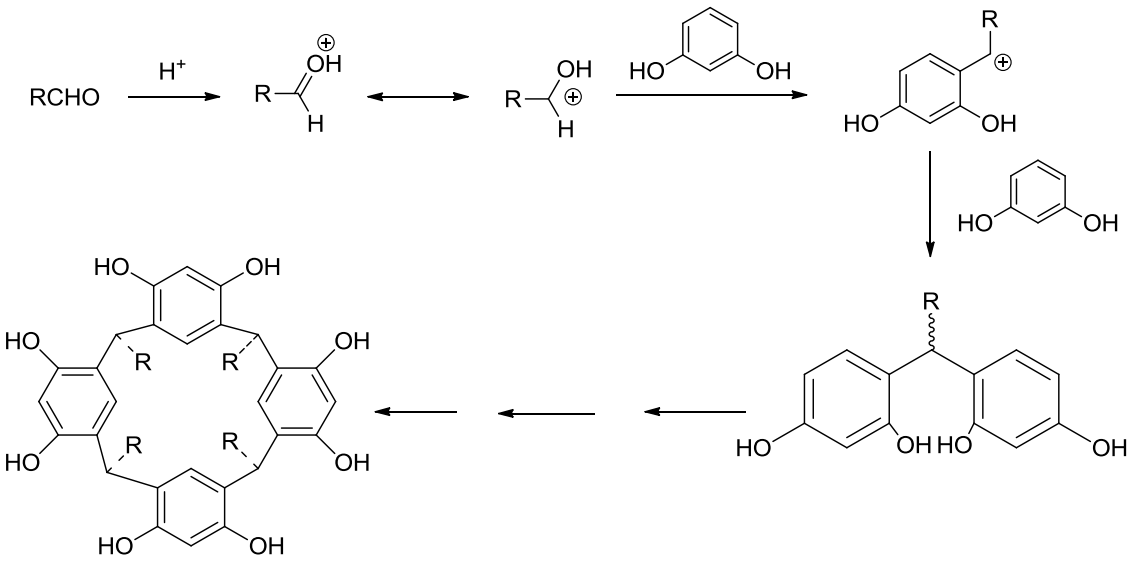

Scheme 6. 5 Pathway for the acid-catalized condensation of resorcinols and aldehydes.

The synthesis of the hybrid trimethylene-bridged dinitrophenyl resorcinarene **2** was achieved by building first the trimethylene-bridged resorcinarene scaffold and by introducing in a second step the dinitrobenzene moiety through the two remaining adjacent phenol oxygens (Scheme 6. 6).

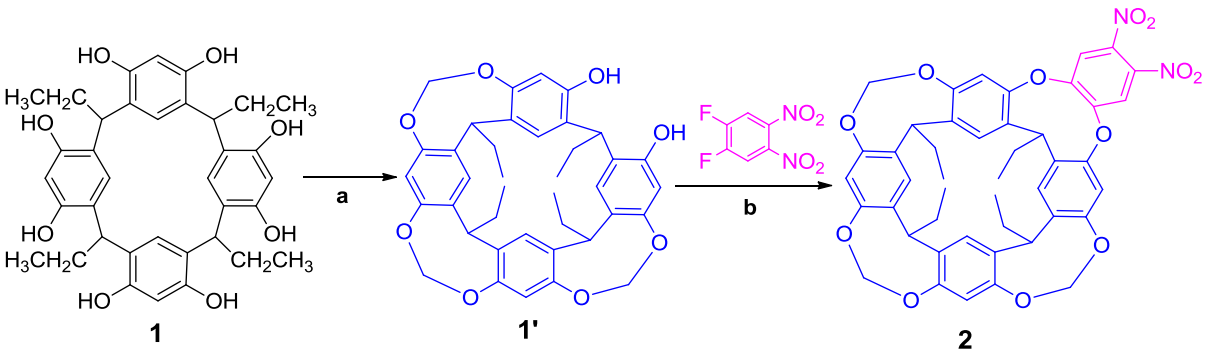

Scheme 6. 6 Synthesis of the hybrid bridged resorcinarene **2** starting from resorcinarene **1**. Conditions: a) K_2CO_3 (8 equivalents), CH_2Br_2 (2.2 equivalents), DMSO, 85 °C, 3 hrs (yield 18%). b) 1,2-difluoro-4,5-dinitrobenzene (1.1 equivalents), DMF, NEt_3 (2 equivalents), 80 °C, 2 hrs (yield 46%).

The trimethylene-bridged diol resorcinarene **1'** was prepared by reacting **1** with 8 equivalents of K_2CO_3 and 2.2 equivalents of CH_2Br_2 in dry DMSO, at 85 °C for 3 hours and purified by flash chromatography using a mixture of dichloromethane:ethyl acetate (from 100:0 to 95:5) with 18% yield.[23] The ^1H NMR spectrum of **1'** shows two doublets for the diastereotopic protons of the methylene

bridges, with geminal coupling $^2J_{H\text{-}H} \sim 7$ Hz. In accordance with the C_2 symmetry of the molecule, two chemically non-equivalent methylene groups can be distinguished. We assigned the **H_i** signals to the protons oriented towards the cavity and belonging to the two methylene bridges in α position respect to the diol. These protons resonate at δ = 4.5 ppm. The inwardly directed **H_r** proton of the remaining methylene group resonates at δ = 4.4 ppm. The protons outwardly oriented **H_o** and **H_q** are downfield shifted with respect to the germinal ones that are inwardly oriented and resonate at δ = 5.77 and δ = 5.74 ppm, respectively.

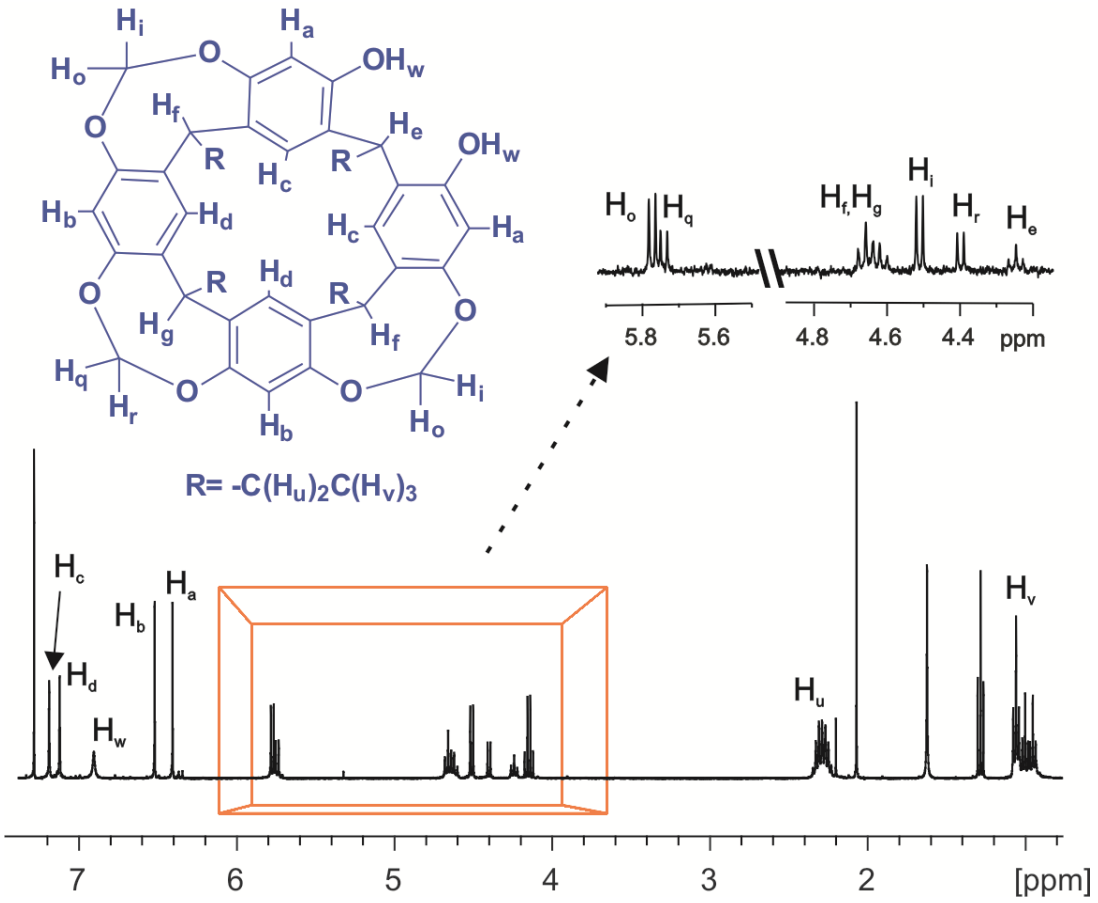

Figure 6. 8. ^{1}H-NMR spectrum of the trimethylene-bridged diol resorcinarene **1'** in chloroform-*d* solution.

The hybrid trimethylene-bridged dinitrophenyl resorcinarene **2** was prepared by reacting the trimethylene-bridged diol resorcinarene **1'** with 1.1 equivalents of 1,2-difluoro-4,5-dinitrobenzene using NEt_3 as base, in dry DMF at 80 °C for 2 hours. The installation of the aryl wall was confirmed by the appearance in the ^{1}H NMR spectrum of **2** of a singlet at δ = 7.96 ppm corresponding to the **H_m** protons of the

dinitrophenyl group, as well as by the downfield shift of the **H_e** peak at δ = 5.59 ppm (Δδ = 1.35 ppm), as consequence of the different magnetic environment experienced by **H_e** (Figure 6. 9).

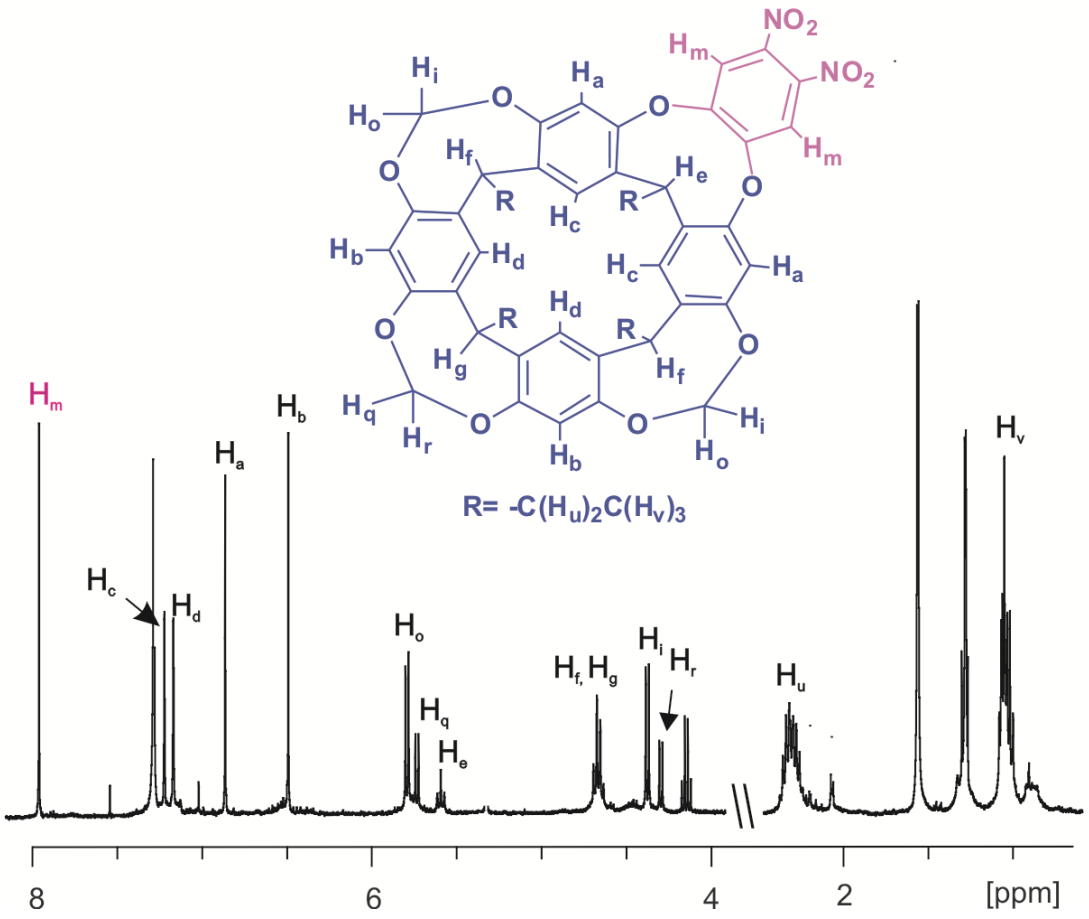

Figure 6. 9 ^{1}H-NMR spectrum of the trimethylene-bridged dinitrophenyl resorcinarene **2** in chloroform-*d* solution.

All the signals in the ^{1}H-NMR of **2** were assigned to the corresponding protons by means of 2D NMR experiments. In particular, 2D NOESY experiment was very useful (Figure 6. 10). The NOEs cross peaks observed between the H_c and H_d protons assigned to the signals at δ = 7.22 ppm and δ = 7.17 ppm and the H_u and H_v protons of the ethyl chain indicate that these protons are directed toward the lower rim of **2**. Likewise, the methine protons H_f and H_g (δ = 4.66 ppm) displayed similar NOEs. On the contrary, the peak assigned to H_a (δ = 6.86 ppm) gives NOE with the vicinal H_m protons (δ = 7.96 ppm) of the extended phenyl wall while H_b (δ = 6.49 ppm) shows NOE with the inwardly oriented protons H_i and H_r of the methylene bridges (δ = 4.37 ppm and δ = 4.29 ppm). Taken together, these results

indicated that H_a and H_b correspond to the aromatic protons in the upper rim of the cavitand.

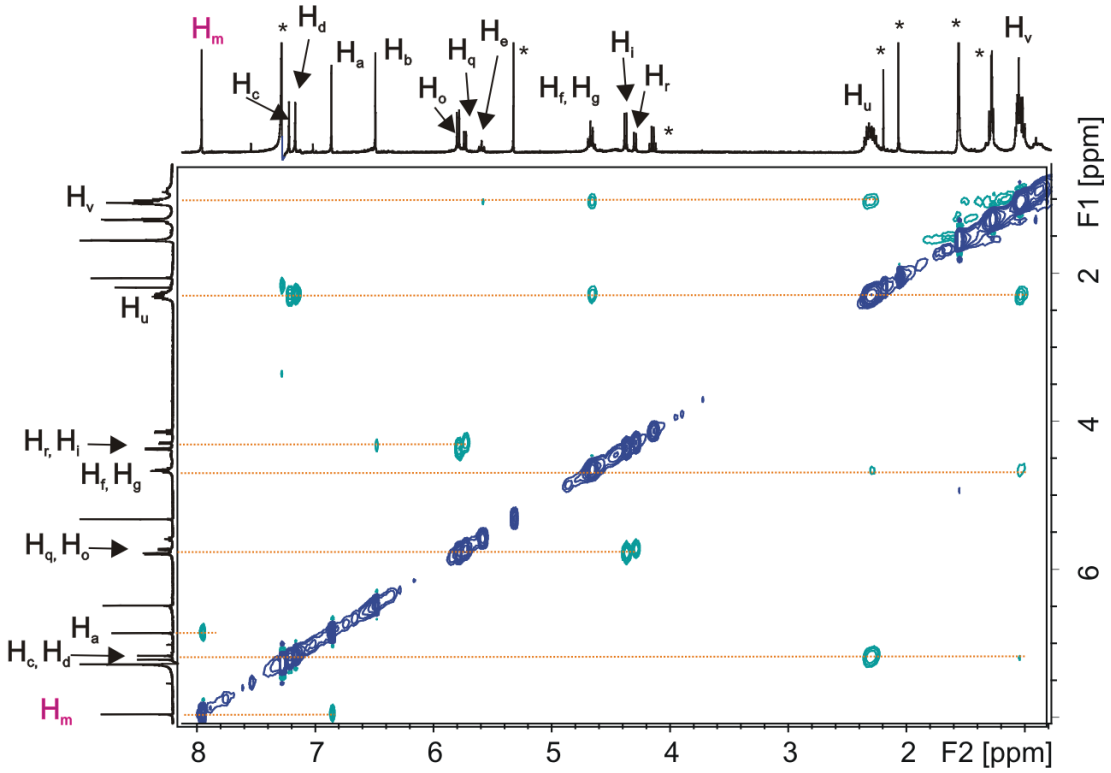

Figure 6. 10. 2D NOESY NMR spectrum of the hybrid trimethylenebridged dinitrophenyl resorcinarene **2**. The asterisk * indicates residual proton signals of the solvent.

In order to install the Salphen or the Terpyridine arms as ligands for the catalytic centre into the cavitand scaffold, we reduced the dinitro groups of **2,** affording the diamino derivative **3** (Scheme 6. 7). The reduction was achieved under mild conditions and in quantitative yields, by adding a catalytic amount of Ni/Raney to a THF solution containing **2** and stirring the resulting suspension under H_2 atmosphere at room temperature overnight.

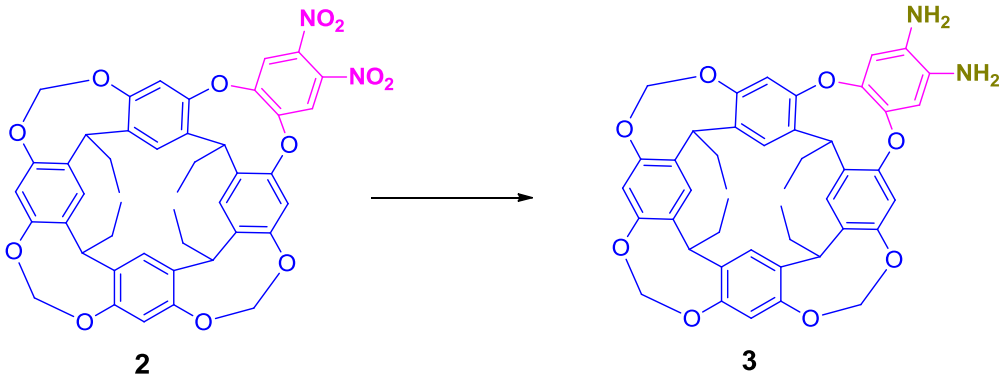

Scheme 6. 7 Synthesis of the trimethylene bridged diaminophenyl resorcinarene **3** starting from trimethylene bridged dinitrophenyl resorcinarene **2**. Conditions: H_2, Ni/Raney, THF, r.t, overnight (yield 100%).

The reduction of the nitro groups (-NO_2) to amines (-NH_2) was confirmed by the upfield shift experienced by the H_m protons to δ = 6.48 ppm and the concomitant appearance of a new broad signal at δ = 3.36 ppm corresponding to the four protons of the two -NH_2 functional groups.

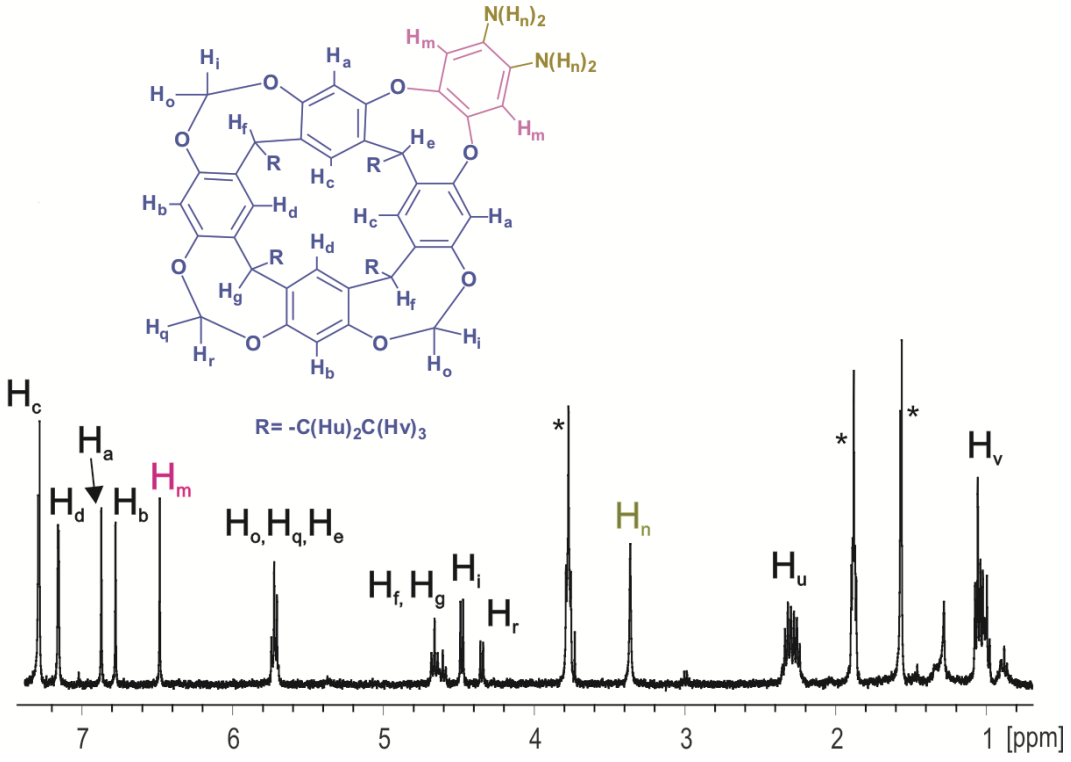

Figure 6. 11 ^{1}H-NMR spectrum of the trimethylene-bridged diamine phenyl resorcinarene **3** in chloroform-*d* solution. The asterisk * indicates residual proton signals of the THF solvent.

6.2. 2 Synthesis of the Salphen Resorcin[4]arene 5

Due to the reduced stability of the diamine **3**, we immediately reacted **3** with the corresponding aldehyde **4** or **6.** In particular, the *Salphen – Resorcin[4]arene* **5** was synthesized by reacting **3** with an excess of 3,5-di-*tert*-butyl-2-hydroxybenzaldehyde[24] **4** under reflux of toluene for 24 hours[25]. The Salphen compound **5** was purified by chromatography using a mixture of Hexane:AcOEt (from 100:0 to 95:5) to remove the excess of **4** (Scheme 6. 8).

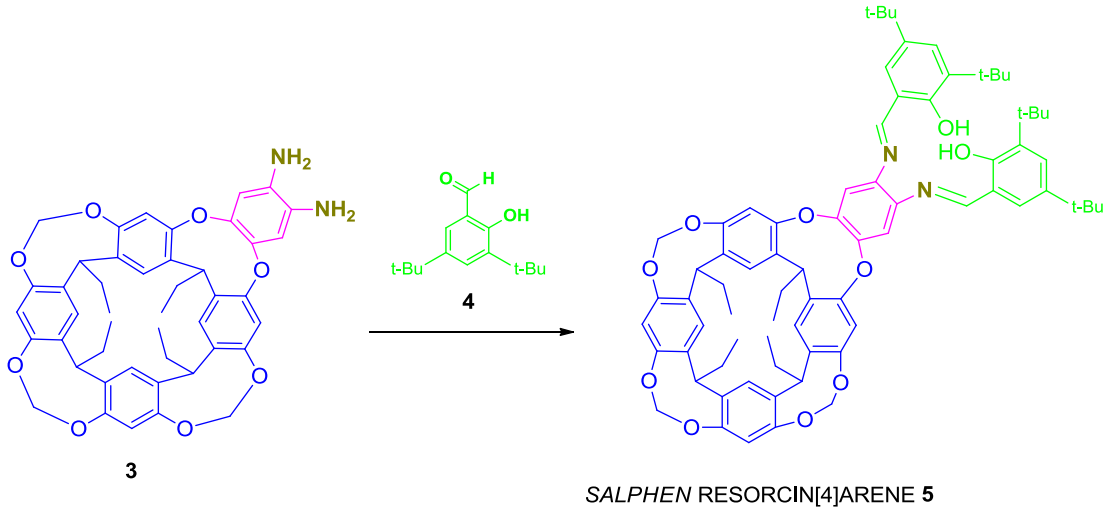

Scheme 6. 8 Synthesis of the Salphen Resorcinarene **5** from the trimethylene bridged diaminophenyl resorcinarene **3** and 3,5-di-tert-butyl-2-hydroxybenzaldehyde **4**. Conditions: toluene, reflux, 24 hrs (yield 52%).

By means of 2D NMR experiments, we were able to assign all the signals of the ^{1}H NMR spectrum to the corresponding protons in ligand **5** (Figure 6. 12). The formation of the imine linkages between the diamine cavitand **3** and the benzaldehyde **4** was confirmed by the observation of the signals corresponding to both the protons of the *Salphen* moiety at low field (green colour) and to the cavitand (blue and pink colours). Diagnostic signals were those of the protons $\mathbf{H_t}$ resonating at δ = 8.64 ppm that corresponded to the imine groups.

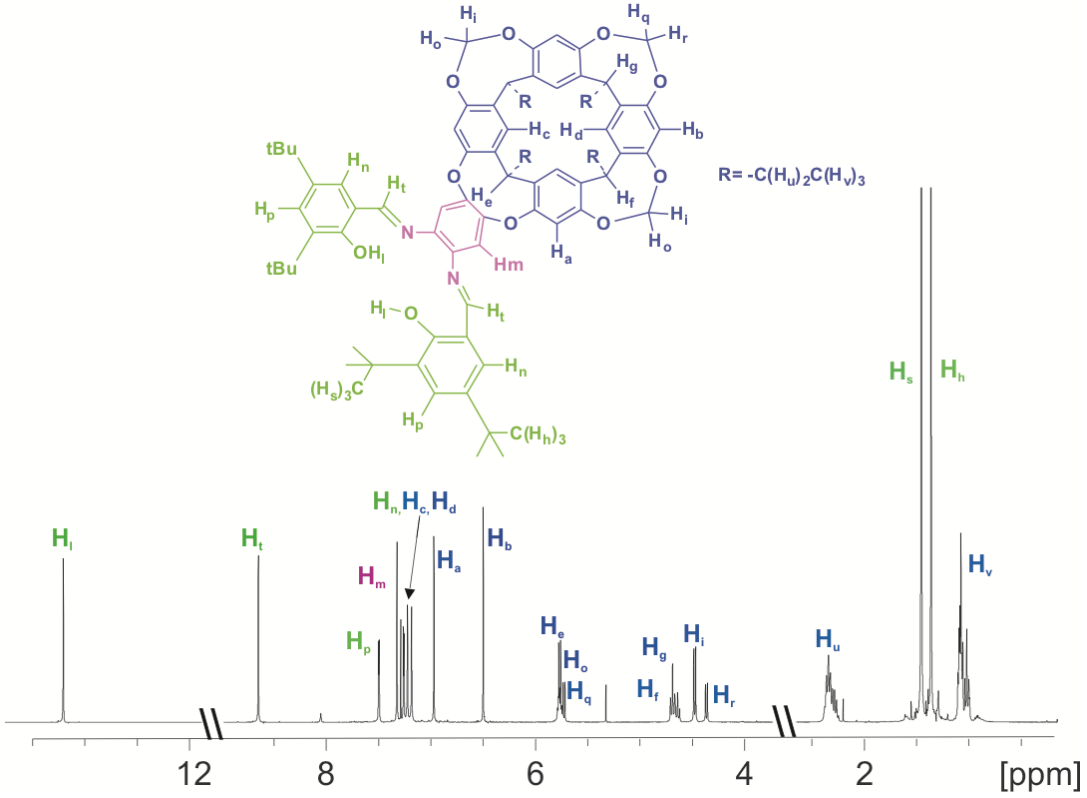

Figure 6. 12 ^{1}H-NMR spectrum of the Salphen Resorcinarene **5** in chloroform-*d* solution.

6.2. 3 Synthesis of Terpyridine 6

As explained before, the synthesis of the terpyridine unit **6** that contains an aldehyde group was performed in order to covalently attach it to the diamine resorcin[4]arene receptor **3** obtained from the reduction of the dinitro compound **2** through the formation of an imidazol spacer. Since terpyridines are interesting ligands for a wide range of transition metals[26,27,28,29,30,31,32,33], we plan to use this substituent for the catalytic application of the cavitands developed in this work.

The synthesis[34] starts from 2,6-dibromopyridine-4-carboxilic acid **9**. The diacid is converted into the bromide-derivative **10** by reaction with tribromide phosphorous oxide at 175 °C in an autoclave system. Next, the carboxylic function was esterified to give **11** under Fisher conditions and reduced to alcohol by treatment with sodium borohydride. The obtained alcohol **12** was converted into the aldehyde **13** by Swern oxidation. The final step involved a cross-coupling aromatic reaction. Modern palladium (0)-catalyzed coupling reactions combine the desired efficiency and simplicity with controllable substitution possibilities.[35]

Suzuki, Negishi and Stille couplings are all based on a Pd^0/Pd^{II} catalytic cycle. The Stille cross-coupling, in particular, has become a popular terpyridine preparation route, due to its universal building-block principle, its multigram product accessibility and the well-directed functionalization at almost every desired position of the terpyridine rings. Terpyridines can be obtained by reaction of appropriate 2,6-dibromopyridines, the central building blocks, with freshly distilled 2-(tributylstannyl)pyridine catalyzed by palladium (0) in toluene for 16 hours (Scheme 6. 9).

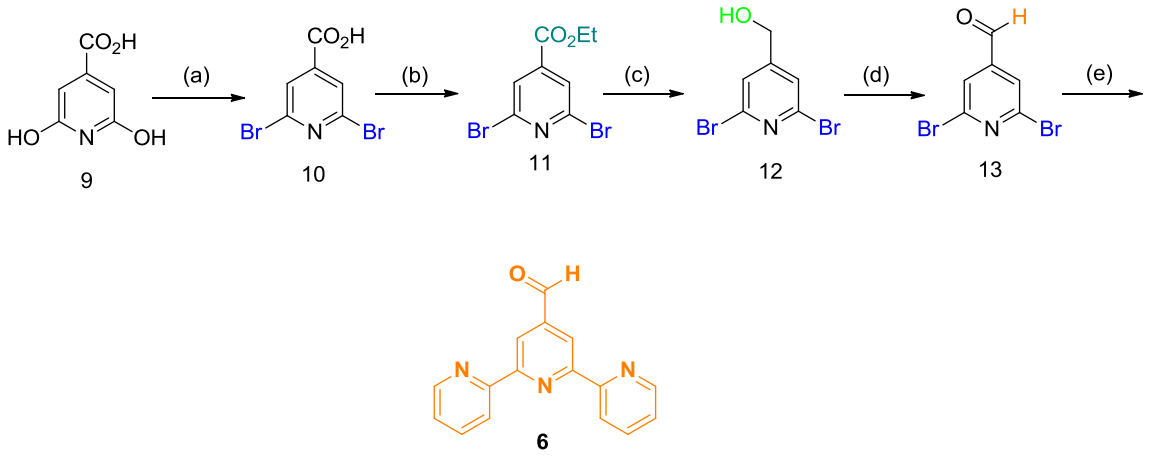

Scheme 6. 9 Synthesis of terpyridine aldehyde **6**. Conditions: (a) 1.5 equiv of $POBr_3$, 175° C in autoclave (56%); (b) 1 equiv sulphuric acid 96%, 1 equiv EtOH, 78° C, 4 hrs 30 min, (96%); (c) 4.9 equiv of $NaBH_4$, EtOH, 3 hrs (86%); (d) 1.1 equiv of oxalyl chloride, 1.4 ml of DMSO, CH_2Cl_2, -78° C, Et_3N (74%); (e) 2 equiv of stannylpyridine, 0.02 equiv of $Pd(PPh_3)_4$, toluene, 16 hrs (77%).

6.2. 4 Synthesis of the Terpyridine Resorcin[4]arene 7

The synthesis of the *Terpyridine* Resorcin[4]arene **7** was achieved by adding dropwise a defect of Terpyridine **6** (~ 0.8 equivalents) to a solution of **3** in dioxane while bubbling with air. The solution was heated up to 100° C and left reacting for 3 hours at the same temperature. The pure ligand **7** was isolated in 77% yield from the reaction mixture by crystallization from MeOH (Scheme 6. 10).

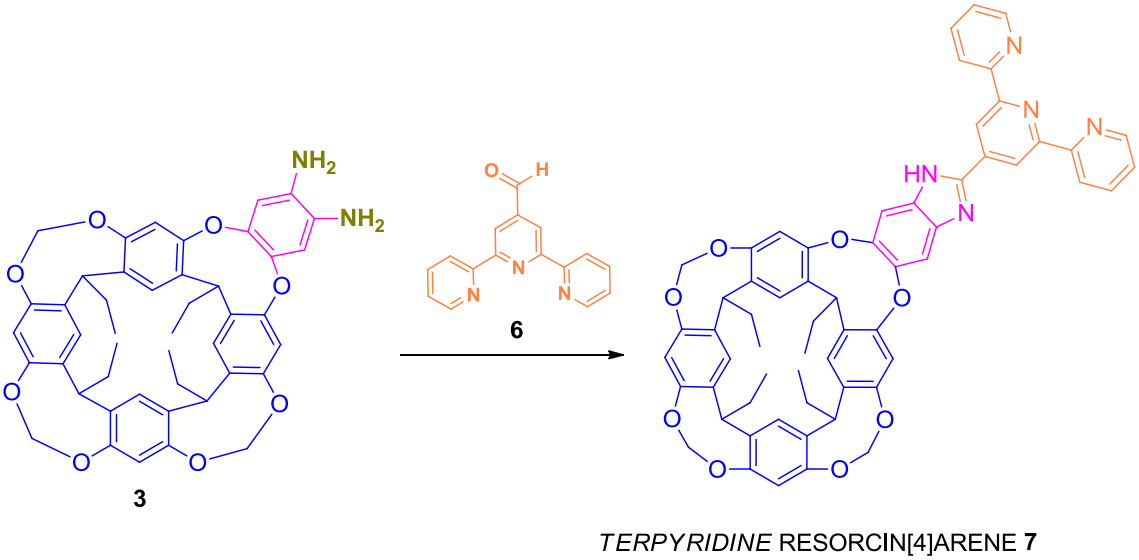

Scheme 6. 10 Synthesis of the Terpyridine Resorcinarene **7** from the trimethylene bridged diaminophenyl resorcinarene **3** and terpyridine **6** (0.8 equivalents). Conditions: dioxane, 100° C, 3 hrs (yield 77%).

The ^{1}H NMR spectrum of **7** in chloroform confirms the successful coupling of the terpyridine ligand with the cavitand component through the formation of the imidazole spacer. In chloroform solution, the tautomeric equilibrium of the benzimidazolyl substituent is slow on the NMR timescale, having as consequence the observation of different signals for the aromatic protons[36] (H_s and $H_{s'}$ in Figure 6. 13). The symmetry reduction imparted in the molecule by the presence of this spacer generates a high number of proton signals than originally expected. Neverthless, we assigned the observed signals to all the protons in the receptor by performing 2D NMR experiments. In addition to the peaks belonging to the cavitand (indicated with blue colour), the spectrum shows the expected five sets of protons of the terpyridine moiety (Figure 6. 13 - a, orange colour). We assigned the proton H_t of the imidazole NH group to the signal resonating at δ = 8.74 ppm and the signals at δ = 6.87 ppm and at δ = 6.49 ppm to the H_s and $H_{s'}$ protons in the aromatic ring of the benzymidazolyl spacer.

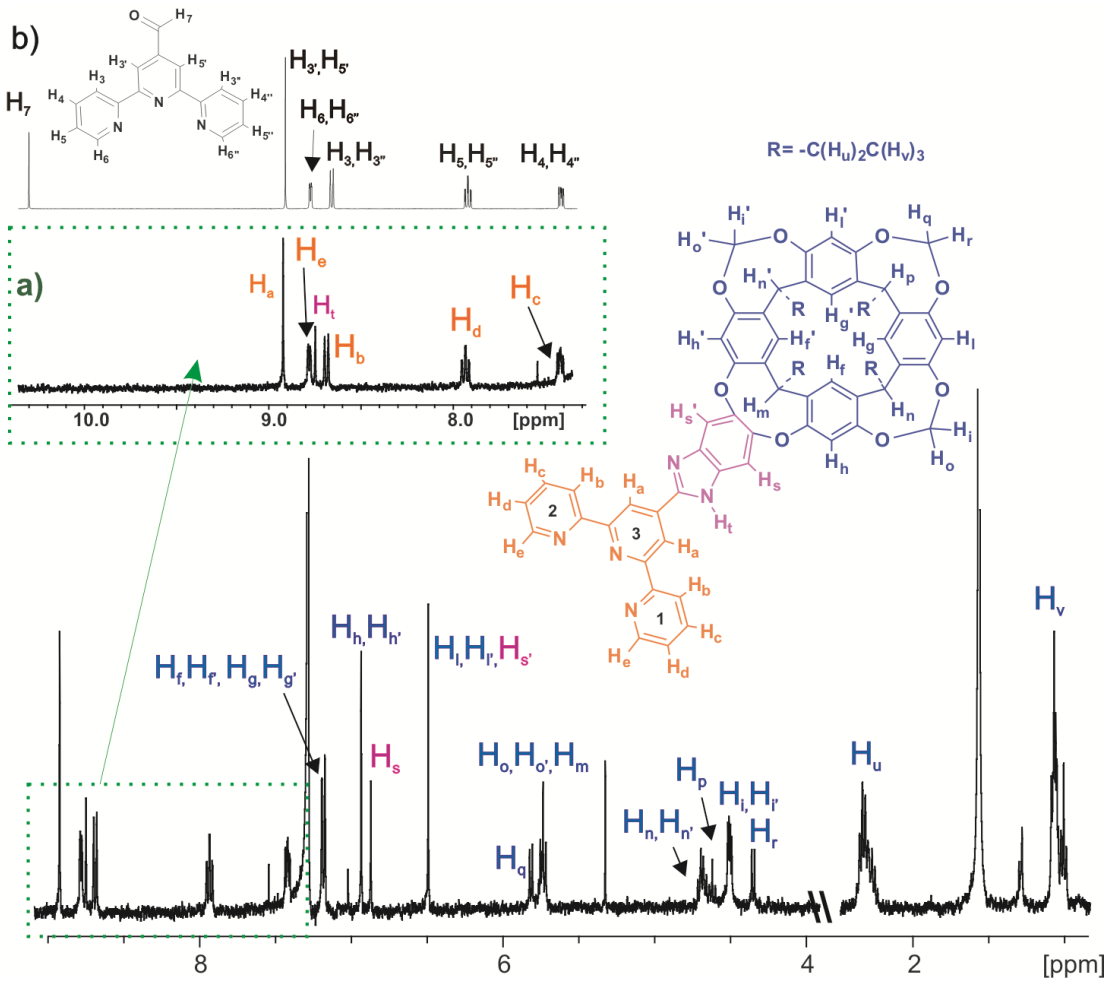

Figure 6. 13 ^{1}H-NMR spectrum of the Terpyridine Resorcinarene **7** in chloroform-d solution with expansion of the aromatic region corresponding to the terpyridine moiety linked to the cavitand through the imidazolyl spacer (a) and the free terpyridine aldehyde **6** (b). The numbering of the free terpyridine has been maden following the one reported in literature.

It is worth noting that in THF the tautomerization equilibrium of the imidazolyl group was also slow on the NMR time.[37] Also in this case, the asymmetry of the cavitand provokes the observation of some protons as diastereotopic pairs.

We observed that when performing the same reaction with > 0.9 equivalents of Terpyridine **5** the overall yield drops down due to the concomitant formation of the *bis*-terpyridine resorcin[4]arene **8** (Figure 6. 14).

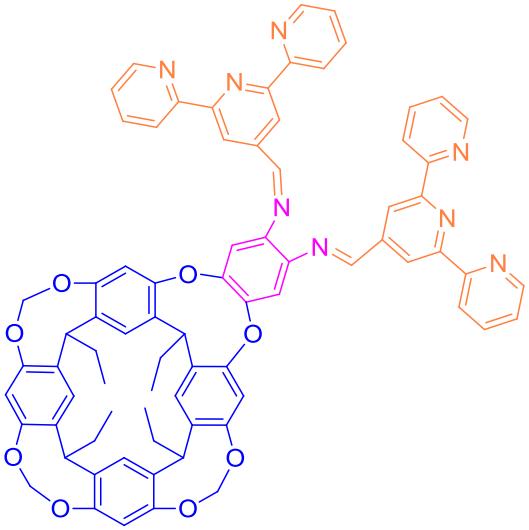

8

Figure 6. 14 Bis-terpyridine resorcin[4]arene derivative **8** formed in the reaction mixture in addition to the desired ligand **7** when > 0.9 equivalents of Terpyridine **5** are used as reactant.

We also tried to purify the *Terpyridine* Resorcin[4]arene **7** from the reaction mixture by HPLC or flash chromatography in reverse phase, using a mixture of THF:H_2O (60:40) or THF:$H_2$0:TFA (60:40:0.1). However, all our efforts resulted useless, due to the instability of **7** in C18 silica columns.

6. 3 Conclusions

The milestone of this work has been the synthesis of cavitand receptors decorated with substituents that can be used as ligands for catalytic metal centers. In particular, we have prepared the hybrid trimethylene-bridge dinitrophenyl resorcinarene **2.** This compound is expected to be able to include guests with a trimethylalkylammonium terminal knob by means of cation-π interactions. We have also installed in this functionalized cavitand two flexible arms (Salphen or Terpydine). These arms are located close to the binding site and will be used as ligands for the binding of catalytic metal centres. We plan to explore the properties of these molecules featuring a binding site in close proximity with a catalytic site for the following selective and catalytic reactions: acylation of choline with acetyl imidazole, in the case of the ligand **5**, and epoxidation of unsaturated saubstrates using ligand **7.**

6. 4 Experimental Section

General information and instrumentation

All syntheses were carried out using chemicals as purchased from commercial sources unless otherwise noted. ^{1}H NMR spectra were recorded on a Bruker Avance 400 (400.1 MHz for ^{1}H NMR) and Bruker Avance 500 (500.1 MHz for ^{1}H NMR) ultrashield spectrometer.

Synthesis

Resorcin[4]arene **1** (67%).[38] In 1 L two-necked round bottomed flask equipped with a magnetic stirrer, resorcinol (66 g, 600mmol) was dissolved in EtOH (300 mL) and water (300 mL) and *cc* HCl (150 mL) were added. Propionaldehyde (36 mL) was added dropwise and the system was left reacting first at 75 °C for 2hrs, then at r.t. for 6 days. A yellow precipitates appeared after only 30 minutes of reaction that was filtered off and rinsed with EtOH/water (1:1). The solid was collected and dried under vacuum over P_2O_5 before any further use.

Trimethylene-bridged resorcin[4]arene diol **1'** (18%). K_2CO_3 (38 g, 274 mmol) and CH_2Br_2 (5.3 mL, 75 mmol) were added, under nitrogen, to a solution of resorcinarene **1** (20.5 g, 34.1 mmol) in dry DMSO (10 mL). The purple mixture was stirred at 85°C for 3 hrs. The reaction was quenched by addition of HClaq (10%, 30 mL), and the resulting mixture was extracted with CH_2Cl_2 (3 x 30 mL). The organic layers were collected, washed with water (5 x 15 mL), dried over Na_2SO_4 and the solvent was evaporated under reduced pressure. The crude was purified by flash using a DCM:AcOEt mixture (from 100:0 to 90:10). The product appears as white foam. ^{1}H-NMR (400 MHz, $CDCl_3$) δ (ppm) 7.18 (s, 2H), 7.12 (s, 2H), 6.9 (bs, 2H), 7.33 (s, 2H), 6.51 (s, 2H), 6.40 (s, 2H), 5.77 (d, 2H, $^2J_{H-H}$ =7.02 Hz), 5.74 (d, 1H, $^2J_{H-H}$ =7.02 Hz), 4.65 (t, 2H, $^3J_{H-H}$ =8.05 Hz), 4.62 (t, 1H, $^3J_{H-H}$ =8.05 Hz), 4.5 (d, 2H, $^2J_{H-H}$ =7.02 Hz), 4.39 (d, 1H, $^2J_{H-H}$ =7.02 Hz), 4.24 (t, 1H, $^3J_{H-H}$ =8.05 Hz), 2.28 (m, 8H), 1.05 (t, 6H, $^3J_{H-H}$ =7.43 Hz), 1.0 (t, 3H, $^3J_{H-H}$ =7.43 Hz), 0.95 (t, 3H, $^3J_{H-H}$ =7.43 Hz).

Trimethylene-bridged dinitrophenyl resorcinarene **2** (46%). Trimethylene-bridged resorcin[4]arene diol **1'** (4 g, 6.28 mmol) and 1,2 difluoro-4,5-dinitrobenzene (1.4 g, 6.9 mmol) were dissolved in dry DMF (50 mL) under nitrogen. Triethylamine (1.7 mL, 11.94 mmol) was added dropwise and the reaction mixture was stirred at 80°C for 2 hrs. The DMF was evaporated under reduced pressure and the residue was dissolved in DCM (20 mL), washed with HCl 10% (20 mL), washed with brine and the solvent removed under vacuum. The desired product **2** was purified by Combiflash using a mixture of Hex:AcOEt (from 90:10 to 0:100). ^{1}H-NMR (500 MHz, $CDCl_3$) δ (ppm) 7.96 (s, 2H), 7.22 (s, 2H), 7.17 (s, 2H), 6.86 (s, 2H), 6.49 (s, 2H), 5.79 (d, 2H, $^{2}J_{H-H}$ =7.02 Hz), 5.73 (d, 1H, $^{2}J_{H-H}$ =7.02 Hz), 5.59 (t, 1H, $^{3}J_{H-H}$ =8.05 Hz), 4.66 (m, 3H), 4.37 (d, 2H, $^{2}J_{H-H}$ =7.02 Hz), 4.29 (d, 1H, $^{2}J_{H-H}$ =7.02 Hz), 2.3 (m, 8H), 1.04 (m, 12 H).

Trimethylene-bridged diamine phenyl resorcinarene **3** (100%). A suspension of catalytic amount of Ni/Raney in THF (3 mL) was added into a round bottom flask containing the resorcinarene **2** (5 g, 0.62 mmol) and protected from light. The apparatus was purged with H_2 and the mixture was stirred at r.t. overnight. The catalyst was removed by using a Teflon filter and the solvent evaporated under vacuum and at r.t. ^{1}H-NMR (400 MHz, $CDCl_3$) δ (ppm) 7.915 (s, 2H), 7.15 (s, 2H), 6.86 (s, 2H), 6.77 (s, 2H), 6.48 (s, 2H), 5.72 (m, 4H:1H, 2H, 1H), 4.65 (t, 2H, $^{3}J_{H-H}$ =8.05 Hz), 4.60 (t, 1H, $^{3}J_{H-H}$ =8.05 Hz), 4.48 (d, 2H, $^{2}J_{H-H}$ =7.02 Hz), 4.36 (d, 1H, $^{2}J_{H-H}$ =7.02 Hz), 3.36 (bs, 4H), 2.28 (m, 8H), 1.02 (m, 12 H).

Salphen Resorcinarene **5** (52%). To a solution of diaminoresorcinarene **3** in toluene (50 mL), 3,5-di-*tert*-butyl-2-hydroxybenzaldehyde **4** in toluene (10 mL) was added under argon atmosphere and the mixture was left reacting under reflux for 24 hrs. The solvent was removed under reduced pressure and the crude was purified on silica using a mixture of Hexane:AcOEt (from 100:0 to 95:5). ^{1}H-NMR (500 MHz, $CDCl_3$) δ (ppm) 13.22 (s, 2H), 8.66 (s, 2H), 7.50 (d, 2H, $^{4}J_{H-H}$=2.3 Hz), 7.33 (s, 2H), 7.26 (d, 2H, $^{4}J_{H-H}$=2.3 Hz), 7.23 (s, 2H), 7.19 (s, 2H), 6.98 (s, 2H), 6.50 (s, 2H), 5.77 (d, 2H, $^{2}J_{H-H}$ =7.02 Hz), 5.77 (t, 1H, $^{3}J_{H-H}$ =8.05 Hz), 5.73 (d, 1H, $^{2}J_{H-H}$ =7.02 Hz), 4.69 (t, 2H, $^{3}J_{H-H}$ =8.05 Hz), 4.65 (t, 1H, $^{3}J_{H-H}$ =8.05 Hz), 4.48 (d, 2H, $^{2}J_{H-H}$ =7.02 Hz), 4.37 (d, 1H, $^{2}J_{H-H}$ =7.02 Hz), 2.32 (m, 8H), 1.46 (s, 18H), 1.36 (s, 18H),

1.08 (t, 9H, $^{3}J_{H-H}$ =7.16 Hz), 1.02 (t, 3H, $^{3}J_{H-H}$ =7.16 Hz). ^{13}C-NMR (500 MHz, $CDCl_3$) δ (ppm) 12.30-12.35-12.48 (CH_v), 29.41 (CH_s), 31.44 (CH_r), 22.68-23.13-23.24-24.69 (CH_u), 35.59 (CH_e), 38.16-38.34 (CH_f, CH_g), 99.48-99.62 (CH_i+ CH_o, CH_q, CH_r), 115.9 (CH_a), 116.2 (CH_m), 116.6 (CH_b), 120.25-122.68 (CH_d, CH_c), 127 (CH_n), 128.88 (CH_p), 34.23, 35.2, 118.15, 135.67, 137.34, 137.62, 138.21, 138.53, 140.43, 140.78, 151.47, 154.55, 154.80, 155.14, 155.32, 158.52, 165.37 (CH_t). HR MALDI m/z calculated for $C_{75}H_{84}N_2O_{10}$ 1172.6, found 1172.6. Elementar analysis calculated for $C_{75}H_{84}N_2O_{10}$ + 2(AcOEt): C, 73.86; H, 7.47; N, 2.08; found C, 73.96; H, 7.12; N, 2.63.

Terpyridine Resorcin[4]arene **7** (77%). In an Ace Glass Tube, diaminoresorcinarene **3** was dissolved in dioxane (2 mL) and a solution terpyridine **6** (0.118g, 0.45 mmol) in dioxane (2 mL) was added dropwise while purging the diamine solution with air. The system was closed and the mixture, which turned from pale yellow to strong orange, was left reacting at 100°C for 3hrs. The solvent was removed under vacuum and the crude crystalized in MeOH. ^{1}H-NMR (400 MHz, THF-d_8) δ (ppm) 9.04 (s, 2H), 8.96 (s, 1H), 8.73 (m, 4H), 7.95 (m, 2H), 7.61 (s, 1H), 7.42 (m, 2H), 7.34 (m, 2H), 7.33 (s, 1H), 7.31(s, 1H), 7.16 (s, 1H), 6.99 (s, 1H), 6.91 (s, 1H), 6.42 (s, 1H), 6.39 (s, 1H), 5.79 (t, 1H, $^{3}J_{H-H}$ =8.05 Hz), 5.67 (d, 1H, $^{2}J_{H-H}$ =7.02 Hz), 5.67 (d, 1H, $^{2}J_{H-H}$ =7.02 Hz), 5.56 (d, 1H$^{2}J_{H-H}$ =7.02 Hz), 4.66 (m, 3H, $^{3}J_{H-H}$ =8.05 Hz), 4.41 (d, 1H, $^{2}J_{H-H}$ =7.02 Hz), 4.38 (d, 1H, $^{2}J_{H-H}$ =7.02 Hz), 4.35 (d, 1H, $^{2}J_{H-H}$ =7.02 Hz), 2.38 (m, 8H), 1.04 (m, 12H). ^{13}C-NMR (500 MHz, THF) δ (ppm) 11.73(CH_v), 11.82(CH_v), 11.86(CH_v), 11.94(CH_v), 22.83 (CH_u), 22.90(CH_u), 22.93(CH_u), 22.93(CH_u), 35.39(CH_m), 38.17(CH_p), 38.36(CH_n), 38.37($CH_{n'}$), 99.18-99.23-99.26(CH_o+$CH_{o'}$, CH_i+$CH_{i'}$, CH_q+CH_r), 110.12(CH_h), 112.92(CH_s), 115.98-116.24-116.56-116.67(CH_l, $CH_{l'}$, $CH_{h'}$, $CH_{s'}$), 119.18 (CH_a), 120.20(CH_f, $CH_{f'}$), 120.70-149.09(CH_e, $CH_{e'}$, CH_b, $CH_{b'}$), 122.11-122.24(CH_g, $CH_{g'}$), 123.87 (CH_c, $CH_{c'}$), 131.74, 133.58, 135.51, 135.94, 136.59(CH_d, $CH_{d'}$), 137.50, 137.62, 137.75, 137.91, 137.96, 138.0, 143.41, 143.79, 145.67, 153.28, 154.85, 154.87, 154.95, 155.18, 155.19, 155.45, 155.67, 155.73, 155.83, 156.24; HR MALDI m/z calculated for $C_{61}H_{51}N_5O_8$ 981.37, found 982.37 $[M+H]^+$.

Terpyridine Synthesis

2,6-dibromopyridine-4-carboxilic acid **10** (56%). Citrazinic acid (4 g, 25.01 mmol) and $POBr_3$ (11.19 g, 39.02 mmol) were heated at 152°C for an hour (pression ~ 10 bar), then at 175°C for further 7 hours (pressure ~ 20 bar). Finally, the temperature was reduced to 110°C and left reacting overnight. The day after, the reaction was cooled down to 30°C and a black solid was obtained, which was arrastred with water. The suspension was filtered off to obtained a black solid which was dissolved in CH_2Cl_2 and extracted with water and a brown aqueous phase that was extracted with CH_2Cl_2. The resulting organic phases were collected, dried over $MgSO_4$ and the solvent was removed under vacuum.

2,6-dibromopyridine-4-ethyl ester **11**(96%). A mixture of the carboxylic acid (2.7 g, 9.61 mmol) and 96% H_2SO_4 (0.7 mL) in ethanol (21.5 ml) was heated under reflux at 78°C for 4 hrs and 30 min. Ethanol was removed under vacuum and the residue was washed with water. The aqueous phase was extracted with CH_2Cl_2 (25 mL x 3) and the combined organic phases was dried over $MgSO_4$, filtered and the solvent evaporated. The crude (3.04 g) was purified by flash cromatography using a mixture of Hexane:CH_2Cl_2 (1:1).

2,6-dibromo-4-hydroxymethylpyridine **12** (86%). NaBH4 (0.9 g, 4.94 mmol) was added in portions to a solution of carboxilate **11**(1.5 g, 4.85 mmol) in EtOH (90 ml) at 0°C and the mixture was refluxed for 3 hrs. EtOH was removed under vacuum and H_2O was added (60 mL). The excess of $NaBH_4$ was destroyed by addition of 1N HCl (5ml) and the solution was neutralised with Na_2CO_3 aqueous solution. Tha aqueous phase was extracted with CH_2Cl_2 (30 mL x 3) and the combined organic phases were dried over $MgSO_4$. The solvent was removed under vacuum affording **12** in 84% yield.

2,6-dibromopyridine-4-carbaldehyde **13** (74%). To a solution of oxalyl chloride (4.54 ml, 9.09 mmol) in CH_2Cl_2 (58.5 ml) at -78°C was added under N_2 atmosphere a solution of DMSO (1.4 ml, 19.83 mmol) in CH_2Cl_2 (9.75ml). After 10 min, a solution of the alcohol (2.2 g, 8.26 mmol) in 29 ml of CH_2Cl_2 was added. The mixture was stirred for 15 minutes and Et_3N (5.8 ml, 41 mmol) was added. The cooling bath was removed and H_2O was added at r.t. The aqueous phase was extracted with CH_2Cl_2 (30 mL x 3) and the combined organic phases were dried

over $MgSO_4$. Evaporation of the solvent under vacuum and purification by flash chromatography using a mixture of CH_2Cl_2:Hexane (2:3) gave **13** in 74% yield (Scheme 6. 11).

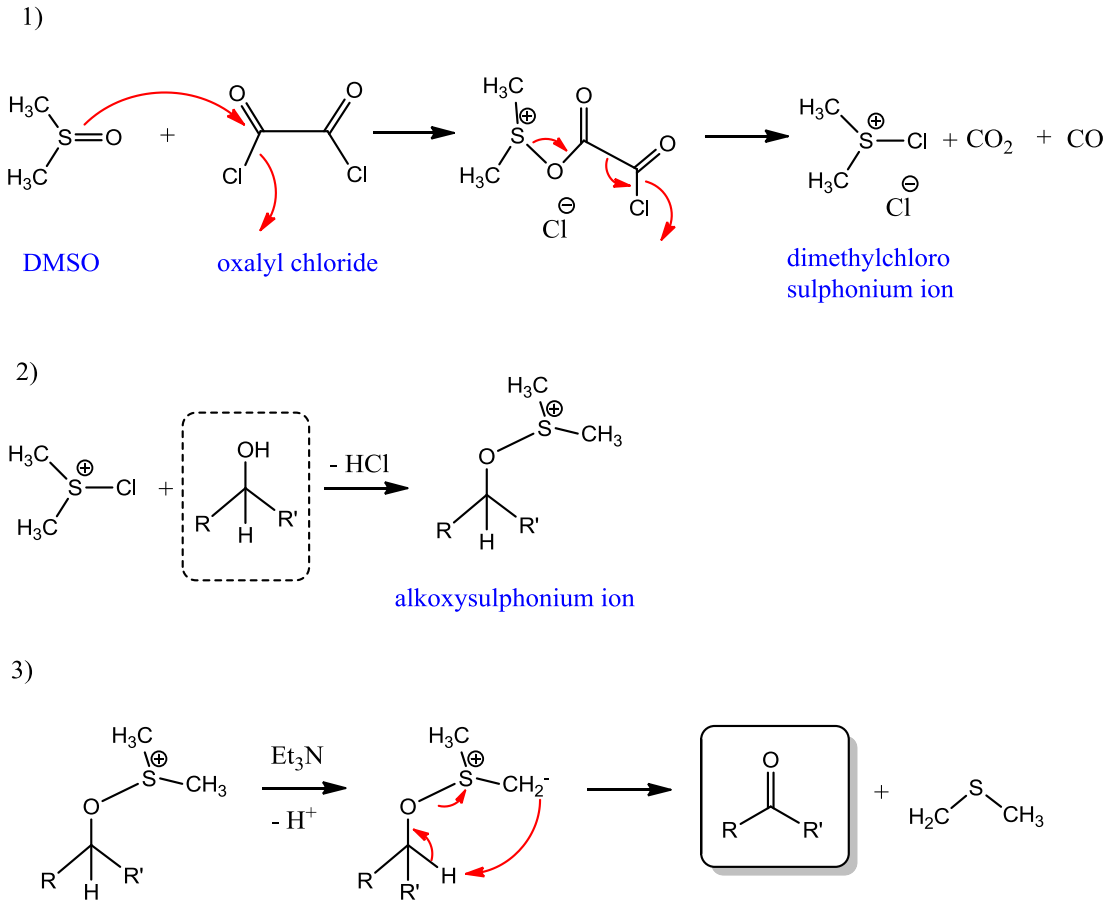

Scheme 6. 11 Mechanism of the Swern oxidation, where primary or secondary alcohols are oxidized to aldehydes or ketones, respectively, by treating them with dimethyl sulfoxide (DMSO) activated by oxalyl chloride at low temperatures (-78 °C to -60 °C) and then with an organic base like triethyl amine. The Swern oxidation is the best alternative to the use of carcinogenic chromium based oxidizing agents. The reaction must be performed below -60 °C to avoid the formation of side products like mixed thioacetals. However, the use of trifluoroacetic anhydride instead of oxalyl chloride allows the reaction to be warmed up to -30 °C.[39]

Terpyridine **5** (77%). Preparation of the 2-(tributylstannyl)pyridine: To a degassed three-necked round-bottom flask equipped with a magnetic stirrer, 2-bromopyridine (2.56 mL, 26.90 mmol) was added under an argon atmosphere. Distilled diethylether (DEE, 50 mL) was added stepwipe. The system was cooled to -80°C followed by the dropwise addition of *n*-BuLi (1.6 M solution in *n*-hexane, 21 mL, 33.60 mmol). The reaction mixture was kept at the same temperature for 3 hrs. Afterwards, tributyl zinc chloride (9 mL, 33.60 mmol) was added and the reaction mixture was stirred first at -80°C for 3hrs, then at r.t. for 12 hrs. All the

solvents were evaporated under vacuum and 60 mL of distilled DEE was added. The mixture was filtrated to remove any solid impurities and the filtrate was evaporated under reduced pressure. The resulting 2-(tributylstannyl)pyridine was used in the following reaction without any further treatment. The ^{1}H-NMR and ^{119}Sn-NMR spectra of the product resulted comparable with the commercial one. However, in both cases the product was not totally pure. For this reason, it was further purified by performing a distillation by Kugelrohr at 149°C and 0.13 mbar. The 2-(tributylstannyl)pyridine was stored in the freezer used for the synthesis of **5** reaction the same day in which the reaction was carried out.

To a solution of 2,6-dibromopyridine-4-carbaldehyde **13** (0.96 mg, 3.64 mmol) in toluene (50 mL), $Pd(PPh_3)_4$ (0.084 g, 0.073 mmol) and freshly distilled 2-(tributylstannyl)pyridine (2.67g, 7.27 mmol) were added and the mixture was left reacting overnight at 130°C (Scheme 6. 12). After 16 hours the solvent was evaporated under reduced pressure and the crude was washed with distilled[40] CH_2Cl_2 (50 mL). The suspension was filtrated on celite and the solvent was removed under vacuum. The crude was purified by Combiflash using a mixture DCM:AcOEt (from 100:0 to 95:5) and the terpyridine **5** was recrystallized by MeOH (30 mL).

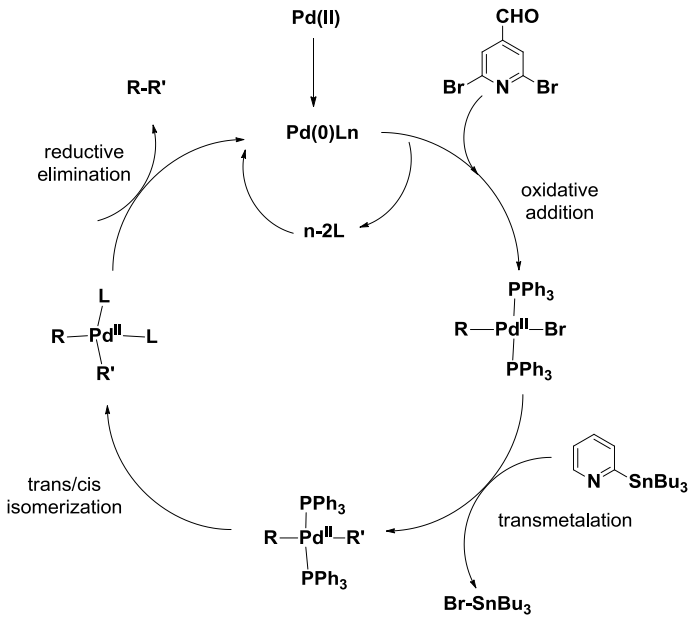

Scheme 6. 12 Mechanism of the Still cross coupling reaction[41] to give **5**.

6. 5 References and Notes

[1] Moran, J. R.; Karbach, S.; Cram, D. J. *J. Am. Chem. Soc.* **1982**, *104*, 5826.
[2] Kikuchi, Y.; Kato, Y.; Tanaka, Y.; Toi, H.; Aoyama, Y. *J. Am. Chem. Soc.* **1991**, *113*, 1349.
[3] MacGillivray, L. R.; Atwood, J. L. *Nature* **1997**, *389*, 469.
[4] Palmer, L. C.; Shivanyuk, A.; Yamanaka, M.; Rebek, J. *Chem. Commun.* **2005**, 857.
[5] Cram, D. J.; Choi, H. J.; Bryant, J. A.; Knobler, C. B. *J. Am. Chem. Soc.* **1992**, *114*, 7748.
[6] Moran, J. R.; Ericson, J. L.; Dalcanale, E.; Bryant, J. A.; Knobler, C. B.; Cram, D. J. *J. Am. Chem. Soc.* **1991**, *113*, 5707.
[7] Roncucci, P.; Pirondini, L.; Paderni, G.; Massera, C.; Dalcanale, E.; Azov, V. A.; Diederich, F. *Chem.--Eur. J.* **2006**, *12*, 4775.
[8] Rudkevich, D. M.; Hilmersson, G.; Rebek, J. *J. Am. Chem. Soc.* **1998**, *120*, 12216.
[9] Rudkevich, D. M.; Hilmersson, G.; Rebek, J. *J. Am. Chem. Soc.* **1997**, *119*, 9911.
[10] Hooley, R. J.; Shenoy, S. R.; Rebek, J. *Org. Lett.* **2008**, *10*, 5397.
[11] Schneider, H. J.; Kramer, R.; Simova, S.; Schneider, U. *J. Am. Chem. Soc.* **1988**, *110*, 6442.
[12] Schneider, H. J.; Guttes, D.; Schneider, U. *J. Am. Chem. Soc.* **1988**, *110*, 6449.
[13] Ma, J. C.; Mecozzi, S.; Dougherty, D. A. *Abstr. Pap. Am. Chem. Soc.* **1997**, *214*, 350.
[14] Inouye, M.; Hashimoto, K.; Isagawa, K. *J. Am. Chem. Soc.* **1994**, *116*, 5517.
[15] Koh, K. N.; Araki, K.; Ikeda, A.; Otsuka, H.; Shinkai, S. *J. Am. Chem. Soc.* **1996**, *118*, 755.
[16] Bonal, C.; Israeli, Y.; Morel, J. P.; Morel-Desrosiers, N. *J. Chem. Soc., Perkin Trans. 2* **2001**, 1075.
[17] Hof, F.; Trembleau, L.; Ullrich, E. C.; Rebek, J. *Angew. Chem., Int. Ed.* **2003**, *42*, 3150.
[18] Ballester, P.; Shivanyuk, A.; Far, A. R.; Rebek, J. *J. Am. Chem. Soc.* **2002**, *124*, 14014.
[19] A. G. S. Högberg, *J. Org. Chem.*, **1980**, *45*, 4498.
[20] A. G. S. Högberg, *J. Am. Chem. Soc.* **1980**, *102*, 6046.
[21] C. D. Gutsche, *Calixarenes*, 2nd Edition, RSC, 2008
[22] Weinelt, F.; Schneider, H. J. *J. Org. Chem.* **1991**, *56*, 5527.
[23] Menozzi, E.; Busi, M.; Ramingo, R.; Campagnolo, M.; Geremia, S.; Dalcanale, E. *Chem.--Eur. J.* **2005**, *11*, 3136.
[24] An equimolar solution of **3** and **5** would give a resorcinarene derivative with the benzaldehyde **5** linked to **3** by an imidazolyl spacer.
[25] The reaction was left reacting also for 48 hours; however a decreasing in the yield was observed (32%), probably because of the instability of **5** in solution.
[26] Arduini, A.; Bussolati, R.; Masseroni, D.; Royal, G.; Secchi, A. *Eur. J. Org. Chem.* **2012**, 1033.
[27] Kamata, K.; Suzuki, A.; Nakai, Y.; Nakazawa, H. *Organometallics* **2012**, *31*, 3825.
[28] Kotova, O.; Daly, R.; dos Santos, C. M. G.; Boese, M.; Kruger, P. E.; Boland, J. J.; Gunnlaugsson, T. *Angew. Chem., Int. Ed.* **2012**, *51*, 7208.
[29] Suntharalingam, K.; White, A. J. P.; Vilar, R. *Inorg. Chem.* **2010**, *49*, 8371.
[30] Akcakayiran, D.; Mauder, D.; Hess, C.; Sievers, T. K.; Kurth, D. G.; Shenderovich, I.; Limbach, H. H.; Findenegg, G. H. *J. Phys. Chem. B* **2008**, *112*, 14637.
[31] Haensch, C.; Chiper, M.; Ulbricht, C.; Winter, A.; Hoeppener, S.; Schubert, U. S. *Langmuir* **2008**, *24*, 12981.
[32] Lombard, J.; Lepretre, J. C.; Chauvin, J.; Collomb, M. N.; Deronzier, A. *Dalton Trans.* **2008**, 658.
[33] Barigelletti, F.; Flamigni, L.; Balzani, V.; Collin, J. P.; Sauvage, J. P.; Sour, A.; Constable, E. C.; Thompson, A. M. W. C. *Coord. Chem. Rev.* **1994**, *132*, 209.
[34] Fallahpour, R. A. *Synthesis-Stuttgart* **2000**, 1665.
[35] Ulrich S. Shubert, Harald Hofmeier and George R. Newkome, *Modern Terpyridine Chemistry*, WYLEY-VCH Verlag GmbH & Co. KGaA, Weinheim, 2006.
[36] Ceniceros-Gomez, A. E.; Ramos-Organillo, A.; Hernandez-Diaz, J.; Nieto-Martinez, J.; Contreras, R.; Castillo-Blum, S. E. *Heteroat. Chem.* **2000**, *11*, 392.
[37] Nagy, P. I.; Tejada, F. R.; Messer, W. S. *J. Phys. Chem. B* **2005**, *109*, 22588.
[38] Tunstad, L. M.; Tucker, J. A.; Dalcanale, E.; Weiser, J.; Bryant, J. A.; Sherman, J. C.; Helgeson, R. C.; Knobler, C. B.; Cram, D. J. *J. Org. Chem.* **1989**, *54*, 1305.
[39] Kobayashi, T.; Kobayashi, S. *Molecules* **2000**, *5*, 1062.
[40] The use of distilled dichloromethane resulted necessary in order to avoid the metallation of **5** by Fe-traces present in the dichloromethane, as confirmed by the pink colour of the solution containing **5**.

[41] Stille, J. K. *Angew. Chem., Int. Ed. Engl.* **1986**, *25*, 508.

CHAPTER VII

General Conclusions and Future Perspectives

This thesis focused on the design of *Supramolecular Hosts*.

We have designed and synthesized unprecedented calix[4]pyrrole cavitands with two and four phosphonate groups. The receptors differ by the relative spatial orientation of the phosphonate groups installed in the upper rim of the common aryl-extended calix[4]pyrrole scaffold. We have evaluated the binding properties of the *bis* and *tetra* phosphonate receptors with tetraalkylammonium chloride salts and primary alkylammonium chloride in DCM and ACN solutions. In DCM solution, the diastereomeric hosts form thermodynamically ($K_a > 10^4$ M^{-1}) and kinetically highly stable 1:1 ion-paired complexes with quaternary trimethylphosphonium/ammonium chloride salts like TMPCl. In solution, the relative orientation of the P=O groups with respect to the aromatic cavity has a strong impact on the binding properties of the receptor and in the geometry of its ion-paired complex. The design of heterotopic receptors for the binding of ion pairs represents an emerging field in Supramolecular Chemistry due to the potential applications of these molecules as salt solubilizers, extracting agents and membrane transportes and makes these systems an interesting topic for further investigation in the future. In particular, the exclusive preparation of calix[4]pyrroles with only inwardly oriented phosphonate groups by using a specific template represents a promising design of receptors for the transport of biological molecule through membrane. Likewise, we have presented the design and synthesis of a new triazolophane-based anion pair receptor for the binding of linear guest like the bifluoride ion HF_2^-.

We also prepared aryl-extended calix[4]pyrroles for the selective inclusion of *N*-oxides typically used as sacrificial agents in oxidation reactions. In particular, we have demonstrated the possibility of stabilizing the high energy conformer of *N*-methyl morpholine *N*-oxide (NMMO) within aryl-extended calix[4]pyrroles with high association constants and high stability, both thermodynamic and kinetic. We have evaluated the effect that the inclusion has in modifying the normal chemical

reactivity of the NMMO by studying the outcome of reactions in which the *N*-oxide is commonly used as sacrificial oxidant (e.g. oxidation of primary and secondary alcohol to carbonyl derivatives with tetrapropylammonium perruthenate as catalyst).

Finally, we have synthesized cavitand receptors decorated with substituents that can be used as ligands for catalytic metal centers. In particular, we have prepared a hybrid trimethylene-bridge dinitrophenyl Resorcinarene and we have installed in this functionalized cavitand two flexible arms (Salphen or Terpydine). These arms are located close to the binding site and will be used as ligands for the binding of catalytic metal centres. We plan to test these molecules for the acylation of choline with acetyl imidazole, in the case of the Salphen ligand, and for the epoxidation of unsaturated substrates using the Terpyridine ligand.